

NOTE TO USERS

The original manuscript received by UMI contains pages with indistinct and/or slanted print. Pages were microfilmed as received.

This reproduction is the best copy available

UMI

**LAKE AND LAND BREEZES IN SOUTHWESTERN ONTARIO:
OBSERVATIONS, ANALYSES AND NUMERICAL MODELLING**

DAVID MICHAEL LESLIE SILLS

**A thesis submitted to the Faculty of Graduate Studies
in partial fulfilment of the requirements
for the degree of**

Doctorate of Philosophy

**Graduate Programme in Earth and Space Science
York University
Toronto, Ontario**

September 1998



**National Library
of Canada**

**Acquisitions and
Bibliographic Services**

**395 Wellington Street
Ottawa ON K1A 0N4
Canada**

**Bibliothèque nationale
du Canada**

**Acquisitions et
services bibliographiques**

**395, rue Wellington
Ottawa ON K1A 0N4
Canada**

Your file Votre référence

Our file Notre référence

The author has granted a non-exclusive licence allowing the National Library of Canada to reproduce, loan, distribute or sell copies of this thesis in microform, paper or electronic formats.

The author retains ownership of the copyright in this thesis. Neither the thesis nor substantial extracts from it may be printed or otherwise reproduced without the author's permission.

L'auteur a accordé une licence non exclusive permettant à la Bibliothèque nationale du Canada de reproduire, prêter, distribuer ou vendre des copies de cette thèse sous la forme de microfiche/film, de reproduction sur papier ou sur format électronique.

L'auteur conserve la propriété du droit d'auteur qui protège cette thèse. Ni la thèse ni des extraits substantiels de celle-ci ne doivent être imprimés ou autrement reproduits sans son autorisation.

0-612-33550-X

Lake and Land Breezes in Southwestern Ontario:
Observations, Analyses and Numerical Modelling

by DAVID MICHAEL LESLIE SILLS

a dissertation submitted to the Faculty of Graduate Studies of
York University in partial fulfillment of the requirements for the
degree of

DOCTOR OF PHILOSOPHY

© (1998)

Permission has been granted to the LIBRARY OF YORK
UNIVERSITY to lend or sell copies of this dissertation, to the
NATIONAL LIBRARY OF CANADA to microfilm this dissertation
and to lend or sell copies of the film, and to UNIVERSITY
MICROFILMS to publish an abstract of this dissertation.

The author reserves other publication rights, and neither the
dissertation nor extensive extracts from it may be printed or
otherwise reproduced without the author's written permission.

ABSTRACT

Southwestern Ontario is a region bordered on three sides by lakes. Thermally-induced pressure gradients at the shores of these lakes can give rise to mesoscale circulations known as 'lake breezes' and 'land breezes'. This study is a broad investigation of the character of lake and land breezes in this region and their effects on summer severe weather and the local and regional transport of air pollutants such as ozone. Data from the SOMOS field project (summer 1993) and the ELBOW field project (summer 1997) provide the observational basis for this study. These data include high-density surface meteorological measurements, satellite and radar data, upper-air soundings and air chemistry data including ground-level ozone measurements. SOMOS data are used to identify occurrences of lake and land breezes and produce a preliminary lake and land breeze climatology for the region. It is found that lake and land breezes each occurred in this region on roughly 50% of study days and are capable of affecting all parts of the region. In addition, strong relationships between lake breezes and the incidence of both summer severe weather and high ozone events are suggested. These relationships are explored in detail through case studies of selected SOMOS and ELBOW days. 'Classic' lake and land breezes occurred during August 14-15, 1993, accompanied by severe weather and high ozone. 'Highly-perturbed' lake breezes were observed to occur in association with severe weather on July 14, 1997. A non-hydrostatic, fully-compressible mesoscale model (MC2) was employed to simulate conditions on these case study days.

The field observations were used to subjectively evaluate the model while model simulation data provided four-dimensional insight on the mesoscale processes that were observed. When using 5 km horizontal grid spacing, the model predicts lake breezes with reasonable accuracy (not so with land breezes) and helps to elucidate the role of the lake breeze front in the initiation of severe thunderstorms and the local transport of ozone. Experiments with passive tracers within the model suggest that high ozone may be delivered to the surface from a layer aloft by complex, three-dimensional motions at the lake breeze front.

ACKNOWLEDGEMENTS

At the top of this long list is a big thank-you to my supervisor, Dr. Peter Taylor. I feel privileged to have benefited from his caring guidance and words of wisdom over the years. Helpful guidance has also been provided by Dr. Donald Hastie and Dr. Gary Klaassen. I have benefited immensely from collaborations with Patrick King of AES Downsview. Part of this work has been carried out at the King City Weather Radar Research Facility and I am grateful for the use of the facilities there and the assistance received from Norman Donaldson, Paul Joe, Norbert Driedger, Peter Rodriguez and Robert Nissen. The MC2 Group at RPN (Michele Desgagné, Robert Benoit and Yves Chartier) provided invaluable assistance with the operation of the MC2 model. The MC2+C group at York (Jack McConnell, David Plummer, Jacek Kaminski and Lori Neary) has also provided useful information regarding MC2. The following people helped greatly with obtaining data and background material for this study: Jim Salmon, Paul Stalker, Mike Leduc, Duncan Fraser, David Yap, Neville Reid, Craig Fitzner, George Wolff, Tom Monosmith, and Stephen Lamming. Mesonet data plotting software was developed at York University and Zephyr North and RAOB rawinsonde plotting software was developed by Environmental Research Services in Pennsylvania. I would also like to thank the following people for useful conversations and/or inspiring words: Bill Moroz, Douw Steyn, Xin Qiu, Keith Ayotte, Phil Chadwick, Ron Stewart, Mar-Jean Olson and Apollo Tang. Additional inspiration was provided by: John, Paul, George and Ringo,

Alex, Geddy and Neil, the Rheostatics, the Tea Party, Edvard Munch, Lawren Harris and Windsor thunderstorms. The members of Peter Taylor's research group have been good listeners over the years and presentations have benefitted from their comments. For assistance above and beyond the call of duty, I extend thanks to Sally Marshall, Karen Cunningham and Vladka Soltesz.

Finally, for loving support and encouragement, I thank my wife Heather, my Family and Friends.

Dedicated with love to Heather Kepran



In memory of Jean Patterson

TABLE OF CONTENTS

Abstract	iv
Acknowledgements	vi
Table of Contents	ix
List of Tables	xii
List of Figures	xiii
Chapter One - Introduction	1
1.1 Thesis Background	1
1.1.1 Thesis Motivation and Objectives	1
1.1.2 Methodology	2
1.1.3 Research Context	3
1.2 Sea Breezes, Lake Breezes and Land Breezes	4
1.3 Lake Breeze and Land Breeze Characteristics	5
1.3.1 General Features	5
1.3.2 Lake and Land Breeze Fronts	12
1.3.3 Synoptic Environments	14
1.3.4 Effects on Coastal Climatology	16
1.4 Roles in Severe Summer Weather	18
1.5 Air Pollution Effects	23
Chapter One Figures	26
Chapter Two - Observations and Analysis	29
2.1 Introduction	29
2.2 The SOMOS Project	30
2.2.1 Project Background	30
2.2.2 The Field Campaign	31
2.2.3 Supporting Measurements	32
2.2.4 Analysis of the Consolidated Dataset	35
2.2.4.1 Representativeness of the Data	36
2.2.4.2 Identification of Lake Breeze Occurrences in the Dataset	39
2.2.4.3 Identification of Land Breeze Occurrences in the Dataset	43
2.2.4.4 Summertime Lake and Land Breeze Climatologies	45
2.2.4.5 Lake Breezes and Ground-level Ozone	54
2.2.4.6 Lake Breezes and Severe Summer Weather	57

2.3 The ELBOW Project	62
2.3.1 Project Background	62
2.3.2 The Field Campaign	63
2.3.3 Supporting Measurements	65
2.3.4 Observations of Lake Breeze Storm Initiation	66
2.4 Summary	68
Chapter Two Tables	70
Chapter Two Figures	73
Chapter Three - Numerical Modelling and Discussion	103
3.1 A Brief History of Lake and Land Breeze Modelling	103
3.2 Mesoscale Numerical Modelling with MC2	107
3.2.1 MC2 Model Description	108
3.2.2 Spatial and Temporal Modelling Considerations	109
3.2.3 Vertical Level Definitions	110
3.2.4 Horizontal Dimensions and Nesting Strategy	111
3.2.5 MC2 Settings	114
3.2.6 Initialization and Boundary Condition Data	116
3.2.7 Model Modifications	118
3.2.7.1 Implementing Passive Tracers	118
3.2.7.2 Modification to Shallow Convection	120
3.2.8 Discussion of General Results	120
3.3 Sensitivity Studies	122
3.3.1 Surface Albedo	124
3.3.2 Surface Roughness Length	124
3.3.3 Soil Moisture Availability	125
3.3.4 Deep Soil Temperature	126
3.3.5 Lake Surface Temperatures	127
3.3.6 Sensitivity Test Conclusions	128
Chapter Three Tables	130
Chapter Three Figures	132
Chapter Four - Case Studies	139
4.1 Introduction	139
4.2 'Classic' Lake and Land Breezes during SOMOS: August 14 - 15, 1993 ..	141
4.2.1 Overview	141
4.2.2 Synoptic Conditions	142
4.2.3 Mesoscale Observations, Model Results and Comparisons	144
4.2.3.1 August 14 Lake Breezes	145
4.2.3.2 August 14 - 15 Land Breezes	155
4.2.3.3 August 15 Lake Breezes	158

4.2.4	Evaluation of Model Performance	162
4.2.5	Severe Weather	163
4.2.5.1	Synoptic-Scale Dynamics	164
4.2.5.2	Mesoscale Analysis	166
4.2.6	Ozone Transport	174
4.2.6.1	August 14 Lake Breezes	174
4.2.6.2	August 14 - 15 Land Breezes	183
4.2.6.3	August 15 Lake Breezes	184
4.3	'Highly-Perturbed' Lake Breezes during ELBOW: July 14, 1997	185
4.3.1	Overview	185
4.3.2	Synoptic Conditions	186
4.3.3	Mesoscale Observations, Model Results and Comparisons	188
4.3.4	Evaluation of Model Performance	199
4.3.5	Thunderstorms and Severe Weather	200
4.3.5.1	Synoptic Conditions	200
4.3.5.2	Mesoscale Conditions and Analysis	203
4.3.5.3	Mechanism for Storm Initiation and Maintenance	208
4.3.5.4	Frequency of Occurrence of the July 14 Lake Breeze Pattern	210
4.4	Summary	211
	Chapter Four Figures	213
Chapter Five - Discussion and Conclusions		293
5.1	Introduction	293
5.2	Regional Lake and Land Breeze Characteristics	293
5.2.1	The SOMOS Study	293
5.2.2	The ELBOW Study	297
5.3	The Role of Lake Breezes in Summer Severe Weather	298
5.4	The Role of Lake and Land Breezes in High Ozone Concentrations	300
5.5	Skill and Utility of the MC2 Model	302
5.6	Directions for Future Research	304
References		307
Appendix A - Lake and Land Breeze Occurrence Records		A-1
Appendix B - Chronology of MC2 Model Revisions		B-1
Appendix C - Surface Divergence Calculation Method		C-1
Appendix D - Interviews with Tupperville and Tilbury Tornado Witnesses		D-1

LIST OF TABLES

Table 2.1. Mean maximum and minimum air temperatures over land and mean Lake Huron and Lake Erie surface temperatures for April, July and October	70
Table 2.2. July, August and September 1993 departures from 29-year mean values and selected climate records at (a) Windsor and (b) London	71
Table 2.3. Lake and land breeze occurrence statistics for individual shores and combinations of shores based on data from 63 days and 62 nights	72
Table 2.4. Observed temporal characteristics of lake and land breezes during SOMOS	72
Table 3.1. Vertical thermodynamic and momentum level heights (m) used for all MC2 runs	130
Table 3.2. Settings selected for 100 km, 25 km, and 5 km grid MC2 model runs	131

LIST OF FIGURES

Figure 1.1. Schematic diagram describing the initiation process for lake breezes	26
Figure 1.2. Idealized illustration of a typical lake breeze circulation and its associated front based on the literature referred to in the thesis	27
Figure 1.3. Idealized illustration of a typical land breeze circulation and its associated front based on the literature referred to in the thesis	28
Figure 2.1. Map of the Windsor-Quebec City corridor	73
Figure 2.2. Map showing the SOMOS study region and its topography	74
Figure 2.3. Map showing the locations of the SOMOS mesonet stations	75
Figure 2.4 . Map showing the locations of AES, OMEE, NWS and SEMOS surface meteorological stations	76
Figure 2.5. Map showing the locations of ground-level ozone monitoring stations in the study region	77
Figure 2.6. Plot of surface station data at 15 LST on August 8, 1993 showing onshore lake breeze flow on the shores of each lake	78
Figure 2.7. Plot of time series data from the Morpeth station on August 8, 1993	79
Figure 2.8. Wind hodograph showing the clockwise diurnal rotation at the Morpeth station on August 8, 1993	80
Figure 2.9. Remapped GOES-7 visible satellite image valid at 1502 LST (2002 UTC) on August 8, 1993	81
Figure 2.10. Remapped GOES-7 visible satellite image valid at 09 LST (1400 UTC) on September 5, 1993	82
Figure 2.11. Plot of surface station data on August 26, 1993 at 05 LST showing offshore flow on the shores of each of the lakes	83

- Figure 2.12. Wind rose plots showing mean wind speed and direction frequencies between the hours of 12 LST and 18 LST for days with lake breezes on all lakeshores (a), lake breezes on no lakeshores (b) and all study days (c) 84
- Figure 2.13. Wind rose plots showing average wind speed (in knots) and direction frequencies between the hours of 00 LST and 06 LST for days with land breezes on all lakeshores (a), land breezes on no lakeshores (b) and all study days (c) 87
- Figure 2.14. Bar graph showing the frequency of different gradient wind regimes and lake and land breeze occurrences (breeze on any shore) associated with each regime . . 90
- Figure 2.15. Bar graph showing lake and land breeze episode characteristics 90
- Figure 2.16. Maps showing the occurrence frequencies of the Lake Erie lake breeze (a), the Lake Huron lake breeze (b), and the Lake St. Clair lake breeze (c) 91
- Figure 2.17. Map showing the occurrence frequency of lake breezes from any lake at stations in the study region 94
- Figure 2.18. Map showing the number of hours of hourly-averaged ground-level ozone exceedances of the Canadian federal one-hour ozone criterion 95
- Figure 2.19. Map showing the maximum observed hourly-averaged ground-level ozone concentration during the study period at each station in the study region 96
- Figure 2.20. Map showing the number of hours of hourly-averaged ground-level ozone exceedances of the Ontario provincial one-hour ozone criterion during the SOMOS study period 97
- Figure 2.21. Map showing annually-averaged lightning day count for southern Ontario 98
- Figure 2.22. Map showing the ten year return period, one-hour rainfall over southern Ontario 99
- Figure 2.23. Map of average annual tornado incidence per 100² km² 100
- Figure 2.24. Map of the ELBOW study region and its topography 101
- Figure 2.25. Map showing the locations of the ELBOW special surface stations and surface stations operated by AES and Ontario Hydro 102

Figure 3.1. Diagram illustrating the nesting strategy used for MC2 runs	132
Figure 3.2. MC2 domains for the 100 km (a), 25 km (b) and 5 km (c) grid model runs showing the geographical area of the domain and the grid mesh	133
Figure 3.3. 10 m winds from the 5 km grid model run valid at 2200 UTC on August 8, 1993 for increased (a), baseline (b) and decreased (c) lake surface temperatures	136
Figure 4.1. Divergence values calculated from observed five-minute, 10 m wind data between 0000 LST on August 11 and 0000 LST on August 16	213
Figure 4.2. Map showing the locations of triangles A and B and their vertices used for the divergence calculations	214
Figure 4.3a-c. CMC objectively analyzed sea level pressure for 1200 UTC on August 14 (a) and 0000 UTC (b) and 1200 UTC (c) on August 15	215
Figure 4.4. As in Figure 4.3, except that sea level pressure values are those predicted by the 100 km MC2 model run	216
Figure 4.5. Regional operational surface analysis valid at 1800 UTC on August 14. .	217
Figure 4.6. As in Figure 4.5, except valid for 0600 UTC on August 15	218
Figure 4.7. As in Figure 4.6, except valid for 1800 UTC on August 15	219
Figure 4.8a-c. Sea level pressure patterns as computed by the MC2 model on the 25 km grid valid for 1800 UTC on August 14 (a) and 0600 UTC (b) and 1800 UTC (c) on August 15	220
Figure 4.9a-b. Winds at the 850 hPa level as predicted by the MC2 model on the 25 km grid for 2000 UTC on August 14 (a) and 1700 UTC on August 15 (b)	221
Figure 4.10. Lake surface temperatures as measured by a satellite-borne infrared sensor	222
Figure 4.11a-d. A sequence of mesonet station plots for August 14 at 0900 LST (a), 1200 LST (b), 1500 LST (c) and 1900 LST (d)	223

Figure 4.12a-d. Modelled 10 m winds for August 14 at 1400 UTC (a), 1700 UTC (b) and 2000 UTC (c) on August 14 and 0000 UTC (d) on August 15	225
Figure 4.13a-d. Modelled 1.5 m temperatures for August 14 at 1400 UTC (a), 1700 UTC (b) and 2000 UTC (c) on August 14 and 0000 UTC (d) on August 15	227
Figure 4.14. As in Figure 4.13, except values are 1.5 m dew point temperatures	229
Figure 4.15. Map showing the inland penetration distance of the Lake Huron, Lake Erie and Lake St. Clair lake breezes over time	231
Figure 4.16. As in Figure 4.15, except that inland penetration distances are inferred from MC2 modelled winds and divergence values	232
Figure 4.17. Time series plots for locations at the Cedar Point station on the shore of Lake Huron and the inland Walnut station	233
Figure 4.18. As in Figure 4.17, except that observed and modelled time series values are for the Morpeth station location on the shore of Lake Erie	234
Figure 4.19. Divergence at the 10 m level at 1800 UTC on August 14 as predicted by the MC2 5km grid model run	235
Figure 4.20. Time series data from the Stoney Point mesonet station on the south shore of Lake St. Clair	236
Figure 4.21. As in Figure 4.20, except that time series values are for the Cedar Point station on the shore of Lake Huron	237
Figure 4.22a-c. A sequence of mesonet station plots for 2100 LST (a) on August 14, and 0400 LST (b) and 0700 LST (c) on August 15	238
Figure 4.23a-c. Modelled 10 m winds for 0200 UTC (a), 0900 UTC (b) and 1200 UTC (c) on August 15	239
Figure 4.24a-c. Modelled 1.5 m temperatures for 0200 UTC (a), 0900 UTC (b) and 1200 UTC (c) on August 15	240
Figure 4.25. As in Figure 4.24, except values are 1.5 m dew point temperatures	241

Figure 4.26a-c. A sequence of mesonet station plots for 0900 LST (a), 1200 LST (b) and 1500 LST (c) on August 15	242
Figure 4.27a-c. Modelled 10 m winds for 1400 UTC (a), 1700 UTC (b) and 2000 UTC (c) on August 15	243
Figure 4.28a-c. Modelled 1.5 m temperatures for 1400 UTC (a), 1700 UTC (b) and 2000 UTC (c) on August 15	244
Figure 4.29. As in Figure 4.28, except values are 1.5 m dew point temperatures	245
Figure 4.30a-b. Analyzed 250 hPa charts valid for 1200 UTC on August 14 (a) and August 15 (b)	246
Figure 4.31a-b. Analyzed 500 hPa charts for 1200 UTC on August 14 (a) and August 15 (b) showing geopotential heights on the 500 hPa surface with the 500-1000 hPa thickness pattern superimposed	247
Figure 4.32a-c. Analyzed 850 hPa charts for August 14 at 1200 UTC (a) and August 15 at 0000 UTC (b) and 1200 UTC (c)	248
Figure 4.33a-c. Analyzed 850 hPa winds for August 14 at 1200 UTC (a) and August 15 at 0000 UTC (b) and 1200 UTC (c)	249
Figure 4.34a-b. Radiosonde data from Flint, Michigan at 1200 UTC on August 14 (a) and August 15 (b) plotted on a skew-T diagram using RAOB software	250
Figure 4.35. Visible GOES-7 satellite image valid at 2000 UTC on August 14 over an area including the study region	252
Figure 4.36. Plot of mesonet station winds and temperatures at 1500 LST (2000 UTC) on August 14 using the standard synoptic plotting format	252
Figure 4.37a-b. A vertical cross-section (a) through the combined horizontal and vertical modelled wind fields at 2000 UTC on August 14	253
Figure 4.38. A vertical cross-section through the potential temperature field at 2000 UTC	254
Figure 4.39. Modelled wind, temperature and dew point profiles at 2000 UTC on August 14 plotted on a skew-T diagram using RAOB software	255

Figure 4.40a-c. Composite maximum reflectivity radar data in the study region for 1745 UTC (a), 1930 UTC (b) and 2015 UTC (c) on August 15	256
Figure 4.41. Vertical cross-section through the combined horizontal and vertical modelled wind fields at 1830 UTC on August 15	257
Figure 4.42. Vertical cross-section through the combined horizontal and vertical modelled wind fields at 2000 UTC on August 15	257
Figure 4.43. Modelled wind, temperature and dew point profiles at 1800 UTC on August 15 plotted on a skew-T diagram using RAOB software	258
Figure 4.44. Map showing maximum one-hour average ozone concentrations on August 14 recorded at sites in the study region	259
Figure 4.45a-b. Times series of wind direction and ozone concentration data at Sarnia (a) and Port Huron (b)	260
Figure 4.46. Map showing station winds, the estimated lake breeze penetration distances and observed surface ozone concentrations (ppb) at 1300 LST on August 14	261
Figure 4.47. Idealized schematic diagram illustrating the 'ozone aloft' hypothesis ...	262
Figure 4.48a-d. Plan views of surface tracer concentrations at 1200 UTC (a), 1600 UTC (b) and 2000 UTC (c) from the 5 km grid MC2 model run for August 14 .	263
Figure 4.49a-f. Vertical cross-sections through the tracer field at 1600 UTC (a), 1800 UTC (b), 2000 UTC (c) and 2200 UTC (d) on August 14 and 0000 UTC (e) on August 15	265
Figure 4.50a-b. CMC objectively analyzed sea level pressure for 1200 UTC on July 14 (a) and sea level pressure predicted by the 100 km MC2 model run for 1200 UTC on July 14	267
Figure 4.51a-b. Analyzed 850 hPa geopotential and temperature contours (a) and winds (b) at 1200 UTC on July 14	268
Figure 4.52. Sea level pressure at 2100 UTC on July 14 as predicted by the 25 km grid MC2 model run	269

Figure 4.53. Radiosonde data from the DTX station northwest of Detroit at 1200 UTC on July 14	270
Figure 4.54. Lake surface temperatures as measured by a satellite-borne infrared sensor	271
Figure 4.55a-d. GOES-8 visible satellite images valid at 1532 UTC (a), 1732 UTC (b), 1902 UTC (c) and 2015 UTC (d)	272
Figure 4.56. Visible GOES-8 satellite image valid at 1545 LST showing lake-induced cloud lines	274
Figure 4.57. Close-up view of the visible satellite image at 1545 LST with station data at times with data available nearest 1545 LST	274
Figure 4.58a-b. Radiosonde data from the Exeter base station at 2011 UTC on July 14 (a) and MC2 data from the 5 km grid model run for the same location at 2000 UTC on July 14 (b)	275
Figure 4.59. Vertical motion at 500 m and the 10 m wind field valid at 1600 LST on July 14 as output by the MC2 model on the 5 km grid	277
Figure 4.60. Vertical cross-sections through the combined horizontal and vertical wind fields and the air temperature field at 1600 LST	277
Figure 4.61. Map showing the suggested arrangement of lake breeze fronts and frictional and topographical convergence zones at 1545 LST on July 14	278
Figure 4.62a-c. Modelled 10 m winds for 1500 UTC (a), 1800 UTC (b) and 2100 UTC (c) on July 14	279
Figure 4.63a-c. Modelled 1.5 m temperatures for 1500 UTC (a), 1800 UTC (b) and 2100 UTC (c) on July 14	280
Figure 4.64a-c. As in Figure 4.63, except values are 1.5 m dew point temperatures ..	281
Figure 4.65a-c. A sequence of mesonet station plots for 1000 LST (a), 1300 LST (b) and 1600 LST (c) on July 14	282
Figure 4.66. Analyzed 250 hPa chart valid for 1200 UTC on July 14	283

Figure 4.67. Analyzed 500 hPa chart for 1200 UTC on July 14	283
Figure 4.68a-d. GOES-8 visible satellite images valid at 2045 UTC (a), 2132 UTC (b), 2202 UTC (c) and 2315 UTC (d) showing the development of a severe thunderstorm on July 14	284
Figure 4.69a-d. Constant altitude (1.5 km) radar data from the King City radar at 2050 UTC (a), 2130 UTC (b), 2200 UTC (c) and 2320 UTC (d) on July 14	285
Figure 4.70. Map of the ELBOW study area showing station winds and sea level pressures , a subjective isobaric analysis, and the estimated boundary of the thunderstorm outflow at 1900 LST on July 14	286
Figure 4.71. Map showing precipitation accumulation in the Great Lakes region between 1200 UTC on July 14 and 1200 UTC on July 15 as estimated by NEXRAD Doppler radars in the United States	287
Figure 4.72. Map showing the locations of triangles A, B and C and their vertices used for divergence calculations	288
Figure 4.73. Divergence time series from triangle A, B and C calculated using one-hour, 10 m wind data between 0000 LDT on July 14 and 0000 LDT on July 15 ..	289
Figure 4.74. Schematic diagram showing the estimated positions of lake breeze fronts relative to the estimated position of the storm outflow boundary	290
Figure 4.75a-b. Constant altitude (1.5 km) radar data (a) from the King City radar at 0310 UTC on July 15	291
Figure 4.76. Plots of the modelled 625 m positive vertical motion field at 2000 UTC on 14 July 1997 (a), 2 July 1997 (b) and 15 August 1993 (c)	292

CHAPTER ONE - INTRODUCTION

1.1 Thesis Background

1.1.1 Thesis Motivation and Objectives

Southwestern Ontario (defined for this study as the land area in Ontario enclosed by 83.5°W on the west, 81.0°W on the east, 41.5°N on the south and 43.5°N on the north) is a region bounded largely by rivers and lakes, including two Great Lakes. These lakes have a dominant influence on the climate of the region (Brown *et al.*, 1980). Lake and land breezes that can occur in association with these lakes may dominate flow in the lowest few kilometres of the troposphere and result in complex wind fields at the mesoscale and at finer scales. Knowledge of these circulations is important for weather forecasting and air pollution management as well as for agricultural, marine and aviation interests. However, the effects of these circulations on regional climatology, daily weather and air quality are not fully known. The extent to which these circulations affect inland areas of the region is also not well known.

The object of this study is to develop a better understanding of lake and land breezes as they occur in southwestern Ontario and nearby areas of southeastern Michigan and to assess their effects on the occurrence and location of severe summer weather and the transport of pollutants such as ozone in the lower troposphere. The observational basis for this study is provided by data from the SOMOS field study carried out during summer

1993 and data from the ELBOW field study carried out during the summer of 1997.

Mesoscale numerical modelling of selected cases is also conducted using the Canadian MC2 model to further investigate lake and land breezes and their influences in this region. A secondary objective of this study is to evaluate the performance of the MC2 model under lake and land breeze conditions.

1.1.2 Methodology

Lake and land breeze characteristics in the southwestern Ontario region are found by analyzing meteorological data from the SOMOS field study. The main component of this dataset is surface meteorological data from a mesoscale network of 11 stations with a five minute time interval. Data from operational stations at one hour intervals, when added to the mesonet data, give a 30 station network from which to analyze lake and land breezes.

A second field study, the ELBOW project, focussed on the collection of a greater variety of meteorological data over a larger region of southern Ontario. Three special meteorological stations were installed giving surface observations at five minute intervals. With the addition of operational stations, data from a network of 27 stations are available from which to analyze lake breezes.

A mesoscale numerical model, the Canadian MC2 model, is used to simulate atmospheric conditions for case studies during SOMOS and ELBOW. This model has not been

thoroughly tested with thermally-induced mesoscale circulations and an evaluation of the model under these conditions should provide useful knowledge for the MC2 modelling community and perhaps the mesoscale modelling community in general. Model results are compared to SOMOS and ELBOW observations to facilitate this evaluation.

Much of the existing lake and sea breeze modelling literature consists of idealized numerical simulations, mainly in two dimensions. A much smaller number of simulations have been performed using realistic initial and boundary conditions with a three-dimensional model. This is likely due to the lack of computer power in the past to perform such complex simulations and to the increased control over factors affecting the circulations afforded by idealized simulations. Also, case study model simulations of lake and land breezes in three dimensions can provide significant insight into the evolution and dynamics of the observed circulations. It is for these reasons that three-dimensional case study simulations are conducted here rather than modelling of idealized conditions.

1.1.3 Research Context

To provide context for this research, an attempt was made to collect and review the existing literature regarding sea, lake and land breezes. Though workers in this area of research have contributed hundreds of papers on the subject, it is believed that the most significant and relevant papers were found. Published research has also addressed the associations between these circulations, severe summer weather and air pollution effects,

and many of these papers were also reviewed. The following sections are meant to serve as a general overview from the known literature in the each of the above research areas.

1.2 Sea Breezes, Lake Breezes and Land Breezes

The onshore surface winds of the sea breeze and the nocturnal offshore surface winds of its counterpart, the land breeze, have been studied since ancient times. Aristotle pondered the origin of sea breeze winds over two thousand years ago (see Simpson, 1994).

Believing the wind to be a 'dry exhalation', he found the generation of the sea breeze difficult to explain since such an exhalation could not be expected to originate over the moist sea. Much nearer to modern times, the arrival and inland penetration of the sea breeze were investigated near Boston in 1890 by a group from Harvard College Observatory (Davis *et al.*, 1890). Using a team of over 100 people, they tracked the progress of sea breezes as far inland as 30 km. In the last century, hundreds of papers have been written on the topic, describing observed characteristics, proposing theoretical models and, with the advent of computers, performing numerical simulations.

Though recognized in work dating as far back as 1799 (Ellicott, 1799), breezes produced by the Great Lakes of North America have been thoroughly investigated in only the last several decades. The shore of Lake Michigan was the site for several pioneering field studies of lake breezes including those of Moroz (1967) and Lyons (1972). Early lake breeze investigations were also conducted on the shores of Lake Erie (Biggs and Graves,

1962), Lake Huron (Munn and Richards, 1964), and Lake Ontario (Estoque *et al.*, 1976). Lake and land breezes near lakes appear to have the same initiation processes as sea and land breezes near oceans. However, as will be discussed later, the evolutions of these circulations through the day can be very different. Since the ocean and lake circulations share many similar characteristics, they shall be referred to interchangeably in the text of this thesis. The exceptions will be in instances when the character of the ocean and lake circulations diverge.

1.3 Lake Breeze and Land Breeze Characteristics

1.3.1 General Features

Contemporary textbooks, such as *Meso-Scale Atmospheric Circulations* (Atkinson, 1981), *Mesoscale Meteorological Modeling* (Pielke, 1984) and *Sea Breeze and Local Wind* (Simpson, 1994), offer detailed though oversimplified explanations of the formation of lake or sea breezes. Each shows that during clear, calm conditions along a straight coastline, daytime insolation heats a land surface more rapidly than a water surface due to differences in the thermal properties of common soils and water.

Atkinson writes that air over land expands more rapidly than air over water due to the warmer underlying surface during the day. The vertical pressure gradient over land must then decrease under hydrostatic conditions. Assuming that surface pressures over land and water are initially the same, this results in higher pressure over land than over water

at constant heights above the surface causing air above the surface to flow offshore towards lower pressure during the day. This flow aloft induces a flow opposite in direction at the surface known as the 'sea breeze' or 'lake breeze'.

Pielke describes a process very similar to that of Atkinson. However, Pielke explains the formation of the pressure gradient aloft in terms of mass mixing rather than the expansion of air. That is, he states that the pressure gradient aloft forms in response to enhanced upward mass flux over land caused by turbulent mixing in the unstably stratified boundary layer.

Simpson's description involves the expansion of air over land being limited vertically by a capping stable layer. It is, therefore, the sideways expansion of air over land that results in a low pressure region near the surface. The resulting land-water pressure difference gives rise to onshore flow near the surface and a weak return flow is induced aloft to balance the system.

A more complete description of the lake breeze initiation process, modified from a 'textbook definition' suggested by Pearce (1955), is offered below with the aid of diagrams in Figure 1.1 (note that tables and figures appear at the end of each chapter). It is assumed that the day is clear and calm, the shoreline is straight, and constant pressure surfaces over land and water are initially horizontal. After sunrise, the land surface begins

to warm more rapidly than the water surface. This causes air over land to warm more rapidly than the air over water and thus the expansion of the air over land occurs at a relatively higher rate. This expansion causes the constant pressure surfaces over land to be forced upward through the depth of the atmosphere. The resulting pressure differences across the shoreline result in a weak, lakeward tidal motion (Figure 1.1a). Pearce estimated that lakeward velocities would be on the order of 1 km h^{-1} . This adjustment occurs rapidly and the pressure surfaces aloft quickly become horizontal once more. Near the surface, however, hydrostatic conditions result in lower pressure over land since the air over land is warmer than that over water from the surface to a level several hundred metres above the ground. This pressure gradient causes a flow from lake to land near the surface known as the 'lake breeze' (Figure 1.1b). Near the surface, convergence occurs over land and divergence occurs over water due to this onshore flow. This induces an upward motion over land while a downward motion is induced over the water. These motions again shift the constant pressure surfaces in the vertical so that a lake-land pressure gradient is achieved aloft. The resulting flow from land to lake aloft is called the 'return layer flow' (Figure 1.1c) and completes the circulation. These steps occur nearly simultaneously and the entire process occurs continuously with the addition of heat to the surface.

The intensity of the lake breeze circulation, as with all circulations that are thermally forced at the surface, is directly proportional to the magnitude of the horizontal

temperature gradient and the depth of the temperature perturbation in the atmosphere.

This fundamental concept is shown mathematically by Pielke and Segal (1986). Thus, in the case of lake breezes, a greater temperature contrast between air over land and over water results in a more intense circulation. Conversely, a stably-stratified lower atmosphere will tend to vertically restrict the land-water air temperature perturbation resulting in a less intense circulation. The maximum intensity and depth of the lake breeze has also been found to decrease with decreasing lake size though lake breezes may still develop on lakes only a few kilometres in width (Segal *et al.*, 1997).

Along a straight coastline in flat terrain, the lake breeze initially blows perpendicular to the shore, then may approach geostrophic balance (flow parallel to the shore) after a period of time due to the Coriolis acceleration if the circulation is long lived (Lyons, 1972). This period of time is dependent upon the latitude of the location but is on the order of several hours for the Great Lakes region. The onshore wind may exhibit significantly more complicated behaviour in the presence of complex coastal topography and/or an irregular shoreline (Simpson, 1994). Lakes breezes, especially on the Great Lakes, become nearly as well-developed as their oceanic counterparts having a typical maximum inflow wind speed of 4-7 m s⁻¹ and a slightly weaker typical maximum return current of 2-5 m s⁻¹ aloft (Moroz, 1967; Lyons, 1972; Lyons and Olsson, 1973; Keen and Lyons, 1978). The maximum depth of a typical lake breeze inflow layer is between 500 m and 1000 m with the return current extending to 1000-2000 m above the inflow layer

(Moroz, 1967; Lyons, 1972; Lyons and Olsson, 1973; Keen and Lyons, 1978). A typical lake breeze, based on observations from the literature cited here, is illustrated in Figure 1.2.

Sea breezes have been observed to penetrate inland between 40 km and over 300 km depending largely on latitude while typical penetration distances for the Great Lakes region have been found to be near 30 km (Atkinson, 1981). These circulations also extend offshore but knowledge of this aspect is minimal due to the sparsity of data over water. To the author's knowledge, no detailed measurements of the lakeward extent of lake breezes have been made though a few studies have examined this aspect of the sea breeze. For example, Finkele *et al.* (1995) sampled a sea breeze circulation cell with an aircraft over the southern coast of Australia and found that the over-sea extent was several times larger than the inland penetration distance.

Physick (1976) found by numerical simulation that, for gulfs and lakes roughly the size of the Great Lakes or smaller, circulations on each shore should not occur independently but interact to form a mesoscale high pressure area with associated subsidence over the water. This result has been confirmed by Estoque (1981) and Comer and McKendry (1993), among others and probably represents the most significant difference between the dynamics of lake and sea breezes. Moroz and Hewson (1966) postulated that the return flow aloft associated with a lake breeze may be much more pronounced than that which is

observed along ocean coastlines due to this effect.

The lake breeze circulation usually dissipates as changes in air temperature over land and over the lake eliminate the horizontal pressure gradient. This typically occurs near sunset.

Lake breezes have also been observed to retreat to the shoreline due to an increase in cloud cover or increase in the offshore gradient wind (Ryznar and Touma, 1981).

Simpson (1977) suggests that in the evening when dissipative processes such as convective turbulence near the surface subside, the lake breeze frontal vortex may detach from the evanescent circulation and continue to penetrate inland. Simpson further postulates that deeply penetrating lake breeze fronts exist in most cases in the form of such a cut-off vortex.

Though lake breezes can occur any time of year as long as conditions for its development are met, they are most frequently observed in the spring and summer months. This is due to large lake-land temperature differences that typically occur in the spring and the prevalence of synoptic conditions conducive to lake breeze development during the mid-summer months. Ryznar and Touma (1981), using data collected over a period of six years, found that the occurrence of lake breezes on the eastern shore of Lake Michigan reached a maximum in August though lake breezes were recorded as late as November. Biggs and Graves (1962) found a maximum occurrence on the western shore of Lake Erie in June and July over three years of spring and summer observations. Lastly, Lyons

(1972) reported the highest frequency of lake breeze occurrence in the late spring and summer months on the eastern and western shores of Lake Michigan over 10 warm-season months. Occurrences earlier and later in the year were fairly common and were recorded even in January and February.

The land breeze forms after sunset when radiational surface cooling commences. Since land surfaces cool more rapidly than water surfaces, air over land becomes cooler than air over water and begins to contract. The constant pressure surfaces over land shift downward through the depth of the atmosphere in response and the initiation process described for the lake breeze occurs, but in reverse. Thus, an offshore flow is generated near the surface while an onshore flow is induced aloft. However, radiational cooling also stabilizes the nocturnal boundary layer so that the land breeze circulation is inhibited vertically. Maximum velocities within the circulation are significantly lower than that for lake breezes due to this restriction (Pielke and Segal, 1986). Air trajectories are rarely of sufficient length for the Coriolis force to become important (Munn and Richards, 1964). Thus, the land breeze usually blows perpendicular to the coast in the presence of flat terrain and a straight coastline. As with lake breezes, complex coastal topography and/or irregularly shaped coastlines may result in a significantly different offshore wind. Currently, the spatial extent of these breezes is less well-known than that of lake breezes. This is due to the difficulties inherent in measuring these weak winds over land, the lack of measurements over water, and perhaps also due to lack of motivation since summer

land breezes are regarded as relatively innocuous. The author knows of no detailed studies of the spatial characteristics of land breezes associated with lakes. Keen and Lyons (1978), however, included a diagram summarizing the structure of the land breeze according to 'the recent literature'. Additionally, at least two studies have documented the spatial characteristics of land breezes associated with an ocean or sea. Wexler (1946) briefly mentions a study that found the average outflow depth of the land breeze on the Black Sea to be 180 m. Land breezes on two successive days at Wallop's Island in the northeastern United States were investigated by Meyer (1971) using ultra-sensitive radar. It was found that the maximum depth of the land breeze outflow was near 90 m with a return flow extending to 800 m above the outflow layer. A typical land breeze, based on observations from the literature cited here, is illustrated in Figure 1.3.

As with lake breezes, land breezes can occur any time of year that suitable meteorological conditions exist. However, a detailed study of land breeze occurrence frequency has yet to be undertaken.

1.3.2 Lake and Land Breeze Fronts

After the initial development of a lake breeze circulation, the leading edge of the lake breeze may begin to show many similarities in temperature, humidity, pressure and wind changes to a scaled-down synoptic-scale cold front. This occurs primarily by the tightening of horizontal gradients at the lake breeze convergence zone. There can be a

sharp decrease in temperature, increase in moisture content and change in wind velocity as the front passes . However, these changes may not always be observed due to inland modification of air mass properties such as temperature and humidity, or an onshore gradient wind that reduces gradients of these properties at the leading edge of the circulation. Lyons (1972) found that shifts in wind direction are the best markers for inland lake breeze tracking. The rate of inland advance is highly dependent upon the gradient wind. However, lake breeze winds behind the front are usually greater than the propagation speed of the front. Thus, upward vertical motion occurs at the frontal convergence zone. Lyons and Olsson (1973) observed that the Lake Michigan lake breeze front was 1-2 km wide and calculated maximum vertical velocities of over 1 m s^{-1} and peak convergence values greater than $200 \times 10^{-5} \text{ s}^{-1}$ using a two-dimensional form of the continuity equation. Simpson (1977) has pointed out various similarities between lake breeze fronts and laboratory gravity currents including the presence of a 'head' at the leading edge. These characteristics have also been observed with thunderstorm outflow boundaries (Simpson, 1977). A typical lake breeze front, based on observations from the literature cited here, is illustrated in Figure 1.2.

Since a land breeze front moves out over the lake, it is rarely observed. However, many characteristics similar to the lake breeze front can be assumed. Since the land breeze circulation is weaker than that of the lake breeze, the land breeze front will likely possess less intense gradients of temperature, moisture and wind. Meyer's radar study of the land

breeze near Wallop's Island found that the land breeze front penetrated up to 25 km seaward (Meyer, 1971) with a propagation speed of about 1 m s^{-1} . A typical land breeze front, based on observations from the literature cited here, is illustrated in Figure 1.3.

1.3.3 Synoptic Environments

In order for local thermal forcing to predominate over synoptic-scale dynamics, the synoptic-scale pressure gradients must be relatively weak in the coastal region and clear to partly clear skies must be present so that insolation may heat the land surface. By definition, the air over the land surface must be warmer than air over the lake. Sensitivity tests conducted by Arritt (1987) show that details of the water surface temperature have little effect on the simulated lake breeze as long as the water surface is cool enough to stably stratify the atmosphere over the lake. However, several studies have shown that a greater land-water temperature difference is required for the development of a lake breeze as the gradient wind increases (Watts, 1955; Biggs and Graves, 1962).

The gradient wind plays a very important role in the evolution of sea and lake breezes. This role has been investigated through numerical simulations conducted by Estoque (1962), Savijärvi and Alestalo (1988), Bechtold *et al.* (1991), Arritt (1993), and Comer and McKendry (1993), among others. In a calm or very light gradient wind, there is little to hinder the development of lake breezes which may exist along the entire perimeter of the lake. An offshore gradient wind can result in a strong lake breeze front due to

increased convergence at the lake breeze boundary but can overpower a lake breeze if it is strong enough to overcome thermally-forced flow (typically $7-10 \text{ m s}^{-1}$, Atkinson, 1981). Estoque (1962) found that a gradient wind parallel to the shore can either strengthen or weaken the lake breeze depending on the direction it blows along the shore. With a gradient wind that blows parallel to the shore with the lake to the left (in the northern hemisphere), offshore flow near the surface induced by friction differences between land and lake strengthens the pressure gradient and thus the lake breeze circulation. In the opposite case of a gradient wind blowing parallel to the shore with the lake on the right (in the northern hemisphere), frictional differences result in an onshore flow near the surface that weakens the lake breeze circulation. Similar behaviour is noted by Bechtold *et al.* (1991) though they show that changes in circulation intensity due to these frictional differences are small. Light onshore gradient winds reduce the gradients between air over the land and that over the lake and result in weaker lake breeze circulations. In this case, the lake breeze front may form some distance inland. However, an onshore flow of more than a few metres per second may suppress development of the lake breeze.

Land breezes have requirements for their formation similar to those for lake breezes: light winds associated with a weak pressure gradient, clear to partly clear skies, and a lake-land temperature gradient. To the author's knowledge, no detailed study of the effect of the gradient wind on the land breeze circulation has been conducted though Bechtold *et al.* (1991) included several land breeze hours in their numerical simulations of sea breezes.

The effect of the gradient wind is likely to be opposite to that found with lake breezes. That is, for a given gradient wind speed, onshore winds should tend to increase the strength of the land breeze circulation while offshore winds result in a weak or absent circulation. Winds parallel to the shore would likely have less effect on circulation strength. This appears to be supported by Bechtold *et al.* (1991) though they show that the land breeze is suppressed in the northern hemisphere when the gradient wind is coast-parallel with land to the left due to frictional drag causing an onshore deviation of the coast-parallel wind. Generally, land breeze circulations are weaker than those of lake breezes and are thus expected to have lower thresholds of suppression by the gradient wind.

1.3.4 Effects on Coastal Climatology

Onshore lake breeze winds near the surface deliver cool, moist marine air to locations at and near the coast. In the spring and summer months when lake breezes are most active, these locations have lower mean daily maximum temperatures than locations farther inland (Brown *et al.*, 1980). Moisture content in the air remains relatively high through the day behind the lake breeze front. Wind speed may increase or decrease behind the lake breeze front depending on the synoptic conditions. Also, stable stratification of air over water and subsidence that caps the lake breeze inflow layer serve to restrict convection over lakes and coastal regions resulting in decreased cloudiness and increased insolation. Conversely, enhanced upward vertical motion at the lake breeze front very

often results in a band of cumulus clouds parallel to the shore and can even initiate deep moist convection (defined here as convective activity resulting in precipitation at the surface) including showers and thunderstorms. This process has been studied extensively over the Florida peninsula (Byers and Rodebush, 1948; Pielke, 1974; Blanchard and Lopez, 1985; Wilson and Megenhardt, 1997) and, to a far lesser extent, in the vicinity of Lake Michigan (Moroz and Hewson, 1966; Chandik and Lyons, 1971) (the relationship between lake breezes and thunderstorms is discussed in more detail in a later section). Coastal regions with high lake breeze frequencies will have a local climatology more strongly influenced by the above effects than those with lower frequencies.

The effects of land breezes on coastal climatology are less well-known than those for lake breezes. Shallow offshore winds near the surface can be expected to deliver land-cooled air over the lake. However, over land, these winds enhance mechanical mixing. Thus, the surface air temperature should be warmer and the relative humidity lower at land locations within the land breeze circulation when compared to those stations farther inland under strong stable stratification. Indeed, mean daily minimum temperatures at coastal locations in southern Ontario have been found to be slightly higher than those at locations farther inland during the spring and summer months (Brown *et al.*, 1980). The increased minimum temperatures during land breezes and the decreased maximum temperatures during lake breezes result in a reduced diurnal temperature range at coastal locations. This is important for some types of agriculture (Brown *et al.*, 1980). The

general effect on wind speed is not clearly known. The land breeze front is capable of producing cumulus clouds and even initiating deep moist convection (Neumann, 1951). As with lake breezes, coastal regions with higher land breeze frequencies will have a local climatology more greatly influenced by the above effects than those with lower frequencies.

1.4 Roles in Summer Severe Weather

Lake breezes can affect the occurrence of summer severe weather in several ways. First, as was mentioned previously, stable stratification of air over water disables the convective boundary layer while the convective boundary layer is greatly limited by subsidence that caps the lake breeze inflow layer over land. Also, desiccation due to this subsidence increases the height of the lifting condensation level. Thus, the requirement that the lifting condensation level be less than or equal to the convective boundary layer depth for cumulus cloud development may not be met (Segal *et al.*, 1997). Indeed, on many lake breeze days, the sky over the lake and areas inland behind the lake breeze front are completely cloud-free. This convective suppression results in reduced frequencies of thunderstorms over lakes such as the Great Lakes (see Kendall and Petrie, 1962). It is likely then that severe weather elements such as large hail, damaging winds and tornadoes are also less frequent over lakes and nearby shore areas. Indeed, Newark (1984) found that tornado occurrence appeared to be inhibited in land areas adjacent to the Great Lakes.

Second, lake breeze circulations can aid in the development and maintenance of severe convective storms. Three ingredients are necessary for the development of severe thunderstorms and associated severe weather elements including some or all of damaging winds, heavy rain, large hail and frequent lightning. The required ingredients are large quantities of low-level moisture, deep layers of conditional instability and significant upward vertical motion. The synoptic-scale environment can usually provide the first two ingredients. However, the third ingredient is not always available on the synoptic scale. Occasionally, the lake breeze is the only forcing mechanism available to provide the lift required to initiate development. In other cases, the lake breeze front may serve to enhance lift in a column caused by synoptic-scale dynamics. Enhanced upward vertical motion can also result from the collision of two lake breeze fronts (Simpson, 1994). Outflow boundaries emanating from beneath subsequent showers and thunderstorms can interact with lake breeze fronts or other outflow boundaries to initiate even more intense thunderstorms. Deep moist convection occurring along a lake breeze front can evolve into a quasi-stationary storm with intense lightning and high potential for flash flooding. Several studies (Clodman and Chisholm, 1994; Murphy, 1991) have investigated cases when very high to extreme rainfall accumulations occurred with a quasi-stationary thunderstorm on a lake breeze front. Clodman and Chisholm found that these storms typically have the following features: an area of about 200 km², duration of about two hours, slow movement in any direction, and the frequent occurrence of two or more storms of varying intensity separated by clear areas. They suggest that the lake breeze is

able to provide the required strong, moist, low-level inflow required for the development of these severe storms. Low-level, vertical wind shear produced by the lake breeze circulation might also play a role in sustaining a strong thunderstorm updraft.

Lastly, Wakimoto and Wilson (1989) have shown that vertical vorticity produced by shearing (Helmholtz) instability in the horizontal shear zone of a surface boundary such as a lake breeze front can contribute to tornadogenesis. It has been thought that a mesocyclone at the mid-levels of a thunderstorm is required to produce a tornado at the surface (Wakimoto and Wilson, 1989). However, a new class of tornadoes has recently been identified (Bluestein, 1985; Brady and Szoke, 1989; Wakimoto and Wilson, 1989) that is forced by mesoscale boundary-layer interactions and generally develop in benign environments with low to moderate instability and relatively weak shear. These weak, small and short-lived (about twenty minutes maximum) tornadoes are surface-based and occasionally extend to the base of the parent cloud. The tornado is the result of intensification of a low-level vertical vortex at a mesoscale boundary such as a lake breeze front. When the pre-existing vortex becomes co-located with the updraft of a parent cloud experiencing rapid development, it undergoes vortex tube stretching, intensifying the vorticity to tornadic levels. This type of tornado shows waterspout-type characteristics and thus has been called a 'landspout'. Recent high-resolution numerical modelling work done by Lee and Wilhelmson (1997) suggests that there is less chance involved in the co-location of the updraft and the low-level vortex (which they call a

'misocyclone' after Fujita, 1981) than previously thought. Their simulations show that misocyclones forming along surface boundaries due to shearing instability can act to initiate updrafts and deep convection on their own. Tornadoes of this type may account for a significant percentage of those ranking F0 and F1 on the Fujita scale of tornado intensity (Fujita, 1981) and have been also observed to reach F2 and even F3 intensities. Tornadoes with surface-based or 'landspout' characteristics have been recorded in Ontario on several occasions:

- An F0 tornado touched down in Albuna, Ontario southeast of Windsor in the late afternoon of May 31, 1991 (Murphy, 1991). The tornado occurred when the parent thunderstorm was in the developing stage with tops at only 6.7 km and had a track of only a few kilometres. The parent thunderstorm was initiated at the intersection of a weak surface front and a Lake Erie lake breeze front.
- On August 14, 1984 in western North York, an F1 tornado was observed to move slowly from northeast to southwest along a track 2.8 km long (Bertolone, 1984). Though the author does not mention lake breezes as a possible factor, time series of wind, temperature and dew point temperature data included with the report strongly suggest that the tornado occurred near the Lake Ontario lake breeze front.
- On August 28, 1992, an F1 tornado in Newcastle, Ontario near the north shore of

Lake Ontario was observed on King City Doppler radar (Joe *et al.*, 1995). The tornado lasted less than ten minutes and could only be seen by using the radar's lowest elevation angle (0.5°) suggesting a surface-based phenomenon.

- In Etobicoke, Ontario, just northeast of Pearson International Airport, a short-lived F0 tornado was spawned from a low-topped, weak reflectivity thunderstorm in the late afternoon of September 17, 1988 (Hogue *et al.*, 1989). The tornado occurred as the parent cumulonimbus was experiencing rapid growth. Low-level convergence at a weak surface trough was thought to be the principal contributing factor supporting the event.

In the first two cases, the tornadic storms apparently occurred in association with a lake breeze convergence zone. Lake breezes are not explicitly implicated with the latter two cases, though in both cases tornadoes occurred within 15 km of the Lake Ontario shoreline. Many more tornadoes of weak to moderate strength that have occurred in southern Ontario may well have been initiated on boundaries such as a lake breeze front.

There is recent evidence that even the initiation process for violent (F4-F5) tornadoes may not be directly related to mesocyclones at mid-levels in the parent thunderstorm (Fujita and Wakimoto, 1982; Wakimoto and Wilson, 1989). An emerging concept is that all tornadogenesis occurs in the planetary boundary layer by the processes described

above but a violent tornado is possible if the parent thunderstorm possesses a mesocyclone. The link between the tornado at the surface and the mesocyclone aloft has yet to be understood. If this is the case, then one might be tempted to speculate that a large number of tornadoes may be influenced by lake breeze activity in regions such as the Great Lakes region and other regions with large lakes such as southern Manitoba.

1.5 Air Pollution Effects

Many studies have demonstrated the exacerbation of air pollution problems in coastal areas. Some of these effects are the result of the onshore flow of relatively cool marine air in either the absence or presence of a lake breeze. Other effects are related specifically to mesoscale circulations such as lake and land breezes. One of the generally occurring effects of the onshore flow of marine air is fumigation of pollutants downwind of the shoreline. Effluent from a smokestack at the shore blown inland by onshore winds may be confined to a plume in the stably stratified marine air. However, as this plume intersects the convective boundary layer inland, pollutants can be mixed down to the surface resulting in fumigation (Lyons and Cole, 1973).

Another commonly occurring effect in coastal areas is plume trapping. Stably stratified marine air moving onshore can have a mean mixing depth that is 10% of that existing away from the influence of the lake (Lyons and Cole, 1973). Thus, effluent that is ejected into this layer is effectively trapped and high concentrations of pollutants can

subsequently reach the surface.

Fumigation and plume trapping commonly occur in association with lake breezes.

However, lake and land breezes can introduce unique problems. The first is the ability of lake and land breezes to transport pollutants in three dimensions. Lake and land breezes are quasi-closed circulations and pollutants emitted into them can be recirculated several times over the near-shore area (Lyons, 1972). That is, pollutants emitted into the inflow layer get lofted in the frontal regions and disperse into the return flow aloft. A fraction of these pollutants are forced into the inflow layer again by the descending branch of the circulation. Remaining pollutants reside in an elevated layer aloft. Lyons and Olsson (1973) observed a helical trajectory within a lake breeze circulation and suggested that the motion of pollutants might include an along-coast component in addition to the cross-coast components. Lyons *et al.* (1995) have successfully simulated this three-dimensional behaviour using a numerical model. Also, during periods of stagnant synoptic conditions, lake and land breezes can occur nearly continuously, effectively confining pollutants to coastal regions and causing the accumulation of pollutants over periods of several days (Simpson, 1994; Lu and Turco, 1995). Despite apparently adequate ventilation with onshore winds, rapidly deteriorating air quality can result.

Another effect on air pollution peculiar to lake breezes involves the enhanced production of ground-level ozone or 'photochemical smog'. The ingredients for enhanced ground-

level ozone concentrations include: a plentiful supply of reactive hydrocarbons (RHC) and nitrogen oxides (NO_x), strong insolation, relatively high air temperatures, light wind speeds and limited mixing depths (Lyons and Cole, 1976). Three of these ingredients - strong insolation, high temperatures and light winds - are also conditions conducive to the development of lake breezes. When a lake breeze occurs, enhanced insolation is common over the lake and at inland locations affected by the circulation and can result in increased ozone production there.

Thus, the occurrence of high concentrations of pollutants, especially ground-level ozone, in coastal regions is highly correlated with the occurrence of lake and sea breezes and, to a lesser extent, land breezes. Examples of major coastal cities suffering from the above air quality problems include Los Angeles, Athens, Chicago, Tokyo and, in Canada, Vancouver and Toronto.

CHAPTER ONE FIGURES

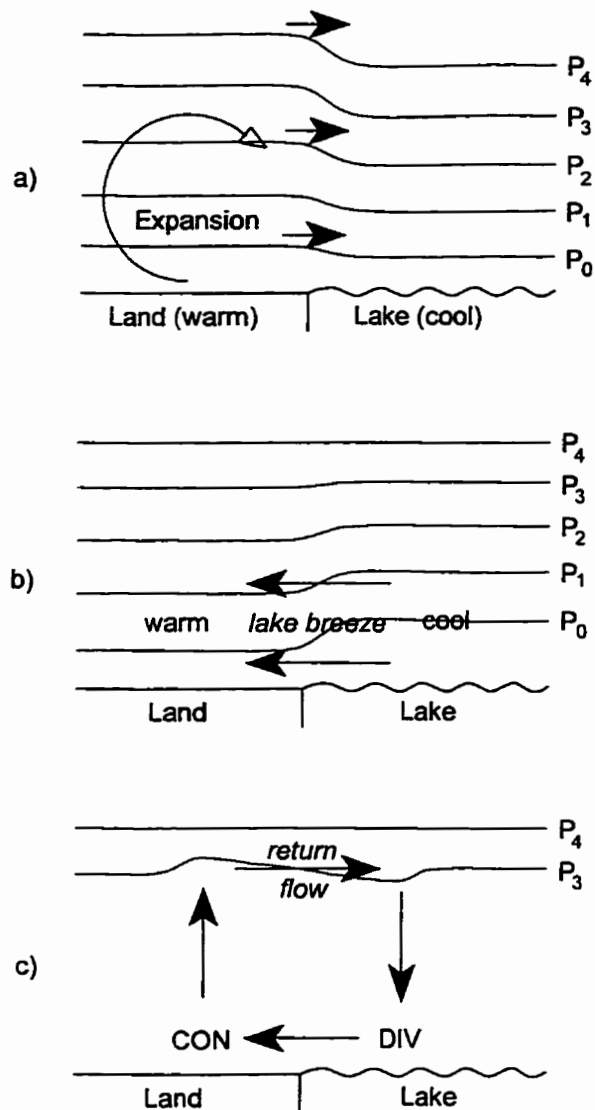


Figure 1.1. Schematic diagram describing the initiation process for lake breezes. The process includes three stages (a-c) that occur nearly simultaneously. In the diagrams, $P_n > P_{n+1}$. See the text for the full discussion of these diagrams.

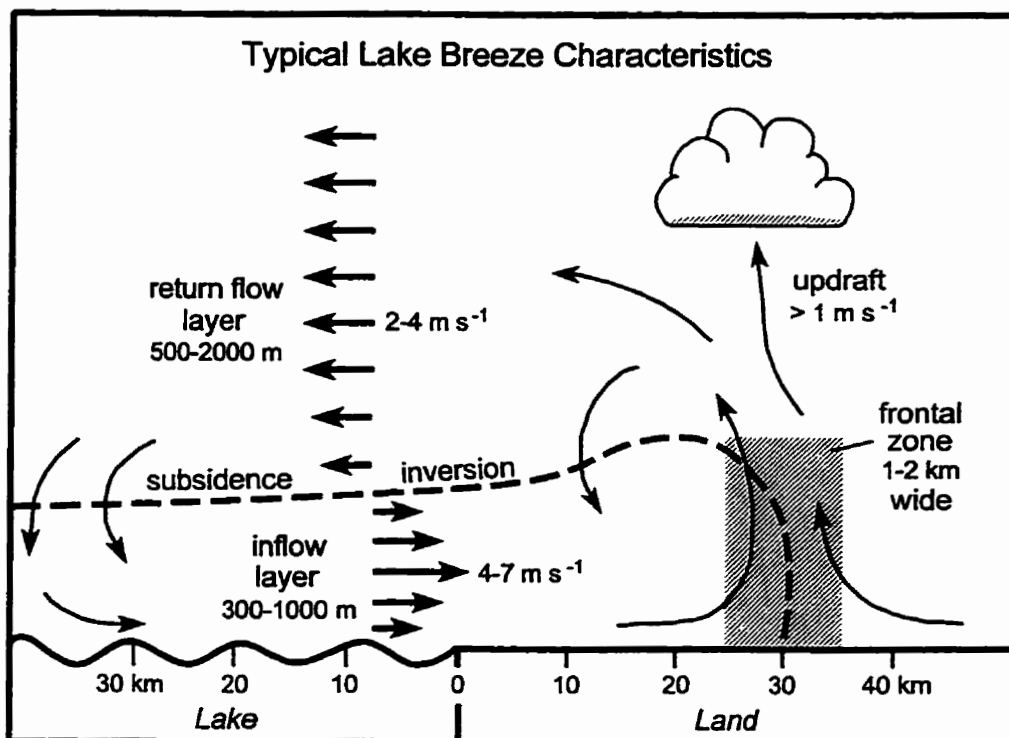


Figure 1.2. Idealized illustration of a typical lake breeze circulation and its associated front based on the literature referred to in the thesis. Common features are labelled. The dashed line represents the outer boundary of the inflow layer. The frontal zone is not shown to scale.

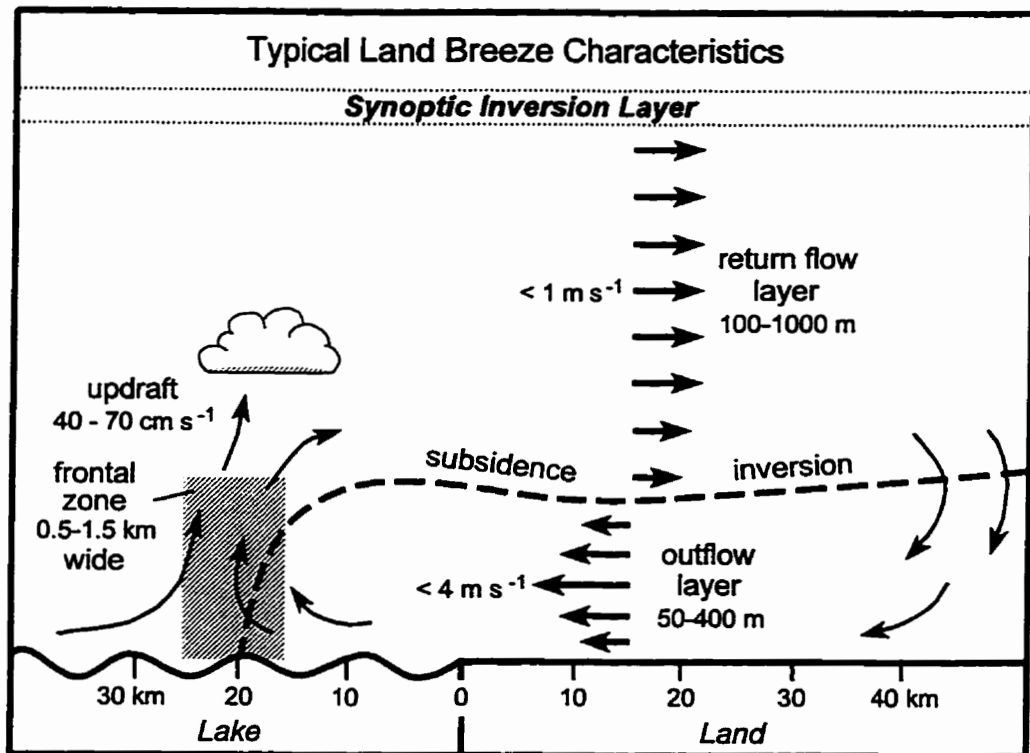


Figure 1.3. Idealized illustration of a typical land breeze circulation and its associated front based on the literature referred to in the thesis. Common features are labelled. The dashed line represents the outer boundary of the outflow layer. The frontal zone is not shown to scale.

CHAPTER TWO - OBSERVATIONS AND ANALYSIS

2.1 Introduction

Observations for this study were collected during two separate field projects: the Southern Ontario Oxidant Study (SONTOS) - Meteorological Measurements project (SOMOS) and the Effect of Lake Breezes on Weather project (ELBOW). These projects are described in greater detail in the following sections. Neither dataset is of sufficient length for the development of a truly representative regional lake or land breeze climatology (data over several years would likely be required in this region due the strong synoptic-scale influence). However, the SOMOS dataset features continuous observations from closely-spaced stations over a period of more than sixty summer days and is used here to conduct a limited investigation of the character of lake and land breezes in southwestern Ontario (defined here to be the land area in Ontario enclosed by 83.5°W, 81.0°W, 41.5°N and 43.5°N). The available data also allow investigations of lake and land breezes and their effects on a case study basis. A greater variety of meteorological data were collected for the ELBOW project but the focus was on data collection during a few intensive periods of observation of several days in length. Thus, the ELBOW dataset is used only on a case study basis. In addition, the observational data gathered during both of these projects are sufficient for the evaluation of mesoscale numerical modelling results since modelling of this type can only be carried out on a short-term basis.

2.2 The SOMOS Project

2.2.1 Project Background

A layer of ozone gas (O₃) at high altitudes in the atmosphere protects Earth's inhabitants by absorbing much of the Sun's harmful ultra-violet radiation. Near ground level, however, this gas is a well-known respiratory irritant and can cause damage to several types of agricultural crops (Mukammal *et al.*, 1982; Yap *et al.*, 1988). Frequent high concentrations of ground-level ozone in many parts of eastern North America during the summer of 1988 led to intensified efforts to identify the sources of the precursors of this pollutant and to address issues of emissions abatement. The Canadian Council of Ministers of the Environment (CCME) identified the Windsor-Quebec City corridor (WQC) as the area in Canada where higher than acceptable concentrations of ground-level ozone occur most often and for the longest periods (CCME, 1990). Research aiding the development of a management plan to control ozone precursors was undertaken by the Canadian Institute for Research in Atmospheric Chemistry (CIRAC). Participants in the development of the Canadian Federal / Provincial NO_x/VOC Management Plan under the CIRAC umbrella included York University, Ontario Hydro, Unisearch Associates, the Ontario Ministry of Environment and Energy (OMEE) and the Atmospheric Environment Service (AES) of Environment Canada. Field studies including intensive atmospheric chemistry and meteorological measurements were carried out during the summers of 1992 and 1993 by SONTOS researchers (Reid, 1996). In 1992, a station was commissioned at a rural site approximately 140 km northeast of Toronto near Hastings,

Ontario, for the measurement of ozone and its precursors as well as basic meteorological variables. The location of Hastings within the WQC is shown in Figure 2.1. In 1993, the observation program at Hastings was conducted simultaneously with a similar program in adjacent southeastern Michigan (SEMOS - Southeast Michigan Ozone Study) (Wolff and Korsog, 1996) and was further augmented by a high-quality surface mesoscale meteorological observation program in southwestern Ontario. The latter field project, called the Southern Ontario Oxidant Study - Meteorological Measurements (acronym SOMOS rather than the awkward SOOSMM), was carried out by Dr. Peter Taylor and David Sills (the author) of the Department of Earth and Atmospheric Sciences at York University and Dr. James Salmon of Zephyr North and is described briefly below.

2.2.2 The Field Campaign

A mesoscale network (mesonet) of meteorological stations was installed in southwestern Ontario roughly between London and Windsor. Land use in this region is predominantly agricultural with flat to gently rolling terrain. The topography of the region is shown in Figure 2.2. Eleven sites were selected to provide coverage in areas not already serviced by existing weather stations. Seven of the sites were located within one kilometre of a lake shoreline while the remainder were located between roughly 10 km and 35 km inland. Figure 2.3 shows the locations of the eleven mesonet stations. Data were collected over a period of 63 days, between July 15 and September 15, 1993, using a 10 m ATMOS (Automated Transportable Meteorological Observing Station) tower at each site in the

mesonet. The towers were loaned to the project from AES and Ontario Hydro. On each tower, 10 m winds, 1.5 m temperature and relative humidity, and the temperature difference between 9.5 m and 1.5 m levels were measured at one second intervals. The estimated errors associated with measurements of wind speed and direction, temperature, humidity and delta temperature were $\pm 0.1 \text{ m s}^{-1}$, $\pm 5^\circ$, $\pm 0.3^\circ\text{C}$, $\pm 5\%$, and $\pm 0.1^\circ\text{C}$, respectively. These parameters, and derived quantities such as maximum scalar wind speed and standard deviations of wind speed and wind direction, were recorded as five minute averages with a datalogger. Three stages of quality control were applied to the data. First, an automatic check was performed on each data value to assure that it fell within reasonable limits for its parameter. Next, a temporal integrity check was performed to ensure that data from all stations were properly synchronized. Finally, data were examined visually for anomalous values using custom computer software. Any rejected data were flagged in the database. Though several minor technical problems were encountered in the field, no station had a data recovery rate of less than 94% and the overall data recovery rate was greater than 98%. Sills *et al.* (1994) provide additional details regarding the field program.

2.2.3 Supporting Measurements

Additional data from several sources were obtained to aid in the analyses. Hourly surface observations from existing meteorological stations in southwestern Ontario were obtained from the Atmospheric Environment Service (AES) of Environment Canada and the

Ontario Ministry of Environment and Energy (OMEE). Data from Lake Erie buoys were provided by the Great Lakes CoastWatch program of the NOAA Great Lakes Environmental Research Laboratory (GLERL) in Michigan. SEMOS researchers provided hourly data from special SEMOS surface stations and several existing National Weather Service (NWS) surface stations in southeastern Michigan. OMEE and SEMOS stations recorded wind data and, at a few stations, air temperature data. Figure 2.4 shows the locations of the AES, OMEE, SEMOS, NWS stations and buoys.

Overall, surface stations were evenly distributed throughout southwestern Ontario and southeastern Michigan except in the northwestern portion of the study region where no surface station data were available. It should be noted that wind, temperature and dew point temperature measurement heights were non-standard at several stations. AES, NWS and SEMOS station measurements conformed to the World Meteorological Organization (WMO) standard of 10 m for wind and 1.5 m for temperatures with the exception of AES auto-stations that recorded temperatures at 5 m. OMEE stations recorded both wind and temperatures at 10 m with the exception of the Merlin station which recorded only wind at 9 m. Buoy measurements of wind and temperatures were made at 4 m.

Rawinsonde data from Flint, Michigan, roughly 90 km northwest of Detroit, were obtained for selected days in the study period. SEMOS researchers also provided rawinsonde data from several special sites in the vicinity of Detroit on intensive

observation days. Boundary-layer temperature measurements with an instrumented aircraft were made by SEMOS on several of these days.

Remapped visible satellite images from the GOES-7 satellite were obtained from AES for most of the days in the study period. These high resolution (2-3 km) images, valid on the half hour, can reveal the positions of lake breeze fronts and other important mesoscale features such as thunderstorms and associated outflow boundaries in addition to synoptic-scale phenomenon. Occasionally, cumuli along land breeze fronts are also identifiable over a lake in the first few visible satellite images of the morning.

Maximum reflectivity radar composites with data from several US radar sites including Detroit, Michigan, Cleveland, Ohio and Erie, Pennsylvania were obtained from Weather Services International (WSI). These radar images were available on the quarter hour. Data from the Exeter radar in southwestern Ontario operated by Environment Canada were not available since no archive was maintained at that time.

Daily lake surface temperature data were provided by GLERL. These images show lake surface temperature as detected by a satellite-borne infrared sensor averaged over a period of several days. The Lake Erie buoys also measured lake surface temperature on an hourly basis. Generally, when buoy-derived temperatures are greater than 4°C, the mean difference between satellite-derived and buoy-derived temperatures is 0.4°C with a

standard deviation of 1.0°C (Irbe, 1992).

Hourly-averaged ground-level ozone concentrations from monitoring stations in southwestern Ontario were obtained from OMEE. Surface measurements of nitrogen oxides, sulphur dioxide and carbon monoxide were also made at a few of these sites. Similar data were obtained for southeastern Michigan through SEMOS. Figure 2.5 shows the locations of all 19 ground-level ozone monitoring stations in the study region. Aircraft measurements of ozone, nitrogen oxides and temperature for several intensive days were also made available by SEMOS.

2.2.4 Analysis of the Consolidated Dataset

Preliminary analysis of the SOMOS surface mesonet data indicated that lake and land breezes had occurred in the region on more than 50% of study days (Sills *et al.*, 1994). In addition, several periods with high ground-level ozone concentrations were found to be accompanied by well-developed lake and land breezes. It was also recognized in the preliminary study that deep, moist convection appeared to develop preferentially in the 'convergence zones' between the lakes on some lake breeze days. These interesting preliminary results led to a broadened investigation of the character of lake and land breezes in southwestern Ontario and their effects on ground-level ozone concentrations and summer severe weather using the SOMOS consolidated dataset. The results of this investigation are presented below.

2.2.4.1 Representativeness of the Data

The driving force behind lake and land breezes is the temperature difference between air over land and air over the lake. This difference varies markedly through the year due mainly to the large thermal capacity of water. Climatological values of mean maximum and minimum 1.5 m air temperatures for an area near the centre of the SOMOS study region are given for the months of April, July and October in Table 2.1. Mean air temperature data over Lakes Huron and Erie were unavailable but the climatological values of mean surface temperatures provide an estimate of air temperatures at 1.5 m. The table shows that the mean maximum daytime land-lake temperature difference is greatest for April then gradually decreases through the year as the lakes warm. Conversely, the mean maximum nighttime lake-land temperature difference increases gradually from April to October. These difference values suggest that lake breezes should be most active in the spring months and that land breezes should be most active in the fall months. However, the incidence of lake and land breezes are also controlled to a great extent by synoptic-scale conditions. Thus, while the temperature difference in the summer months is not at its maximum, synoptic conditions in the Great Lakes region are typically more conducive to lake breezes than in spring months. Thus, lake breezes in the Great Lakes region typically occur most frequently in the summer months, as was discussed in Chapter One. The same might be true for land breezes since these summer synoptic conditions are also conducive to land breezes. However, there are no data to support this

argument. Since the SOMOS study was conducted mainly in the summer months, it is likely then that a significant fraction of the lake breezes (and possibly land breezes) that occurred during 1993 were observed. Conditions during the months of the SOMOS study will next be compared to climatologically normal values to assess the representativeness of the observed data.

The summer of 1993 was characterized by a persistent upper-level trough over western North America and an equally persistent high pressure ridge over the Great Lakes Basin. This pattern resulted in southwest winds over much of central North America that ushered in large amounts of tropical moisture. Devastating floods occurred over the Central Plains and Midwest States of the U.S. and double the normal rainfall fell over parts of the Canadian Prairies. However, high pressure ridging over southeastern Canada over the same period pushed the storm track to the north and west of the Great Lakes Basin (Climate Change Detection Division, 1993). This pattern quickly broke down in September as several low pressure systems moved through the area during the last two weeks of the study period. July, August and September 1993 temperature, precipitation and sunshine departures from normal values were calculated from climate records for Windsor (AES, 1994a) and London (AES, 1994b) and are shown in Table 2.2 along with the mean wind direction and the numbers of precipitation and thunderstorm days.

Considering departures for both locations, July had near normal temperatures,

precipitation and sunshine. However, in August, both stations observed mean temperatures warmer than normal by more than 1 °C, half of the normal precipitation and below normal sunshine hours. In September, both stations had mean maximum temperatures around 3 °C colder than normal, about double the normal precipitation and 28% less hours of sunshine than normal. SEMOS researchers found that temperatures in southeastern Michigan during 1993 were also near or slightly above normal (Wolff and Korsog, 1996). These statistics suggest that conditions conducive to lake breeze formation (clear skies and warm air temperatures over land) were average during July, greater than normal in August, and less than normal in September. Overall, recognizing that half of study days were in the month of August, lake breeze activity during the entire study period was likely slightly greater than normal in southwestern Ontario and southeastern Michigan.

Thus, though the lake and land breezes that have occurred in this small sample (63 summer days, 62 nights) may not be entirely representative of characteristics over a much longer period of time, analyses of these observations should provide a good first-order description of these circulations in southwestern Ontario and southeastern Michigan. It is recognized, however, that synoptic-scale patterns can vary markedly from year to year and that these patterns can have a significant impact on the characteristics of these circulations. Spring and autumn lake and land breezes may also have different mean characteristics.

2.2.4.2 Identification of Lake Breeze Occurrences in the Dataset

Since ancient times, one of the most widely recorded features of sea and land breezes has been the diurnal reversal of the wind near the shore (Pielke and Segal, 1986; Steyn and Kallos, 1992; Simpson, 1994). Several climatological studies of the sea breeze have used this as a main criterion when identifying this circulation. Recent examples are investigations by Steyn and Faulkner (1986) and Banfield (1991). However, lake breeze identification in the Great Lakes region has focussed more closely on the detection of rapid changes in surface parameters that accompany the passage of a lake breeze front (Moroz, 1967; Lyons, 1972; Estoque *et al.*, 1976; Ryznar and Touma, 1981). The reasons for this are not clearly stated but are likely due in part to the increased frequency of synoptic-scale disturbances in the Great Lakes region as compared to the more benign environments of the tropics and some oceanic coastlines. These disturbances tend to disrupt the typical diurnal wind behaviour. Examination of the inland penetration of the lake breeze in these studies also likely required detection of the lake breeze front, as had been done for the sea breeze by Simpson (1977). When considering the occurrence of lake breezes at inland locations, it must be recognized that though lake breeze circulations may reach well inland, weaker land breeze circulations are more likely to occur closer to the shore. Thus, a diurnal reversal of wind does not necessarily occur at inland locations affected by the lake breeze.

Lyons (1972) established three criteria for identifying lake breeze occurrences. First, a

lake breeze has to be a mesoscale circulation distinct from synoptic-scale fronts. Second, the presence of a return flow aloft is required to distinguish a lake breeze from an onshore gradient wind extending to great heights. Third, there must be a definable convergence zone between over-land and over-lake airstreams, usually called the 'lake breeze front' or the 'wind-shift line'. All but the second criteria can be determined using the SOMOS consolidated dataset. Since no vertical profiles of wind were measured at any of the stations in the study region, a return layer aloft cannot be confirmed. Thus, a modified identification process involving several stages was used.

Mesoscale meteorological analyses were conducted for each day in the study and lake breeze occurrences were catalogued for each land station in the study region (lake breezes not reaching the shore in the study region were not considered). First, sequences of surface station plots of all station data were inspected visually and, in many cases, the leading edge of a lake breeze was indicated by sharp changes in wind speed and direction, temperature and dew point that gradually progressed inland. The moderately dense nature of the mesonet enhanced the detectability of this leading edge. A surface station plot at a single time frame is shown in Figure 2.6. Though the arrival of the lake breeze front usually resulted in a decrease in temperature and an increase in dew point, these signals were not always detectable inland most likely owing to modification of the marine air mass. In these cases, and for stations without temperature and dew point data, a rapid shift to onshore winds revealed the leading edge of the lake breeze. In fact, Lyons (1972)

states that the detection of the wind shift line is best for identifying the lake breeze front using surface data. The surface station plots also revealed divergent flow patterns over and inland from the lakes. Buoy and AES station data over Lake Erie were particularly helpful in this regard since, in some cases, they showed opposing and divergent winds over the lake.

Time series of station data (see Figure 2.7) were next examined visually for rapid changes in surface parameters associated with the passage of a lake breeze front. In most cases, this choice of data display made the arrival of the lake breeze easier to detect, especially for mesonet stations with five minute data. Wind hodographs were also examined and analyzed for diurnal wind rotation / reversal (Figure 2.8) though, as mentioned previously, this method works best near the shore where land breezes are most likely to occur.

For further confirmation, animations of visible satellite images were analyzed for evidence of lake breezes circulations. A single satellite image on a day with well-developed lake breezes on all lakes is shown in Figure 2.9. The inland extent of the lake breeze could usually be determined by finding the boundary between cloud-free skies over the lake and scattered cumuli inland. Typically, onshore flow at a lakeshore in the absence of a lake breeze circulation was depicted as a clear area downwind of the lake with scattered cumuli gradually growing in size further downwind, indicating the

presence of a gradually growing convective boundary layer. In the presence of a lake breeze circulation, however, the transition from clear skies to scattered cumuli was significantly more abrupt. In many cases, enhanced cumulus development was evident at the lake breeze front. In addition, the cloud edge could often be seen progressing gradually inland through the day.

Care was taken when inferring the positions of lake breeze fronts using satellite imagery since with offshore gradient winds, cumuli occasionally continue lakeward for several kilometres before dissipating. Also, the satellite viewing angle at the latitude of the SOMOS study area is nearly 45° . Thus, the top of a cloud 5 km in height would be shown on a remapped satellite image about 5 km north of its actual location. Fortunately, most fair weather cumuli occur at lower levels so that the viewing angle error is within a few kilometres. There were some days when convective clouds were partially or totally absent, or there was a layer of thin cirrus preventing full view of the underlying convective clouds. In these cases, satellite imagery was far less useful in detecting lake breezes.

As a final check, AES and NWS surface synoptic charts were examined for each day to ensure that sharp air mass changes attributed to lake breeze fronts were not the result of synoptic-scale frontal passages. In addition, both satellite and radar imagery were used to ensure that frontal signatures in the surface data were not associated with outflow from

shower or thunderstorm downdrafts.

The lake breeze identification process described above is quite labour intensive and intrinsically subjective. However, it is felt that its use here resulted in more accurate estimates of lake breeze frequency than could be obtained using the more stringent (and objective) criteria used in other studies of Great Lakes lake breezes (see discussion in section 2.2.4.4). In addition, it is felt that these results are replicable given substantial knowledge of and experience with meteorological data analysis. Lake breezes were most easily detectable in light wind situations. The most difficult cases were those with moderate onshore flow, usually from the southwest, since no upper air observations were available in the area to confirm a return flow. Satellite imagery and data from over Lake Erie helped greatly on these days. However, if the occurrence of a lake breeze could not be confirmed with confidence, no lake breeze was assumed to have occurred. Thus, resulting lake breeze frequency values are expected to have a 1-2 day (2-3%) maximum error of the conservative kind. The lake breeze occurrence record, grouped by lakeshore and by station, is provided in Appendix A.

2.2.4.3 Identification of Land Breeze Occurrences in the Dataset

Occurrences of nocturnal land breezes were much more difficult to detect from the surface network since they typically did not produce a front over land. Also, infrared satellite imagery could not be used in the same manner as visible satellite imagery for

lake breeze detection since image resolution is too coarse. As mentioned previously, some well-developed land breezes produced a long-lived line of clouds at a convergence zone over the lake which could be detected by visible satellite images at the beginning of the following day (Figure 2.10). For the most part, however, land breeze occurrences were identified by visual inspection of surface station plots of all station data (Figure 2.11) and wind hodographs (Figure 2.8). The surface station plots revealed organized offshore flow along a lakeshore and, in some cases, divergent or diffluent patterns over land. In a few cases, data over Lake Erie allowed the identification of a land breeze convergence zone over the lake. The wind hodographs were used to identify diurnally reversing flow mainly at stations along the shore. This analysis was most useful when an offshore gradient flow made the identification of a land breeze using surface station plots inconclusive. However, as with lake breezes, frequent synoptic disturbances tended to disrupt the typical diurnal pattern.

Due to the limited amount of data for identification of land breezes, confidence when identifying land breezes was lower than that for lake breezes. For this reason, land breeze occurrences are grouped by lakeshore only and individual station occurrence records were not attempted. Several marginal cases were not designated as land breezes. Thus, resulting land breeze frequency values are expected to have a 2-3 day (3-5%) maximum error of the conservative kind. The land breeze occurrence record with land breezes grouped by lakeshore is provided in Appendix A.

2.2.4.4 Summertime Lake and Land Breeze Climatologies

Through analysis of the consolidated dataset, it was found that lake and land breezes had a considerable influence on surface wind flow in the study region. Table 2.3 shows lake and land breeze occurrence frequencies grouped by lakeshore for the 63 days and 62 nights of the study. Note that the lakeshores as defined here consist only of the lakeshore segments that are located within the study region and that a lake / land breeze was considered to have occurred on a lakeshore if a lake / land breeze was identified at one or more stations on that lakeshore. Occurrences of lake / land breezes at a single station were, however, rare. Lake breezes were identified in the study region on 57% of study days while land breezes were identified on 58% of study nights. The Lake Erie shore had the most lake and land breeze activity (54%, 56%) followed by Lake Huron (51%, 50%) then Lake St. Clair (46%, 40%). This result was unexpected in the lake breeze case since Lake Erie is the warmest of the three Lakes during the summer months. On 43% of days, lake breezes developed on all shores in the study region while land breezes developed on all shores on 40% of nights.

The author knows of no other studies of land breeze frequency in the Great Lakes region. However, the lake breeze frequencies found here for individual shorelines are significantly higher than that found by other researchers: 25-45% for Lake Michigan (Lyons, 1972), 30% for Lake Ontario (Comer and McKendry, 1993), and less than 25% for Lake Erie (Biggs and Graves, 1962). To check if this difference is due to these studies

having examined frequencies over a greater number of months in the year including months with lower frequencies, lake breeze occurrence values for the month of August from the SOMOS data and from data in the literature are compared. In August 1993, Lake Erie lake breezes were the most frequent (21 days) followed by Lake Huron (18) then Lake St. Clair (17) lake breezes. August lake breezes on the eastern shore of Lake Michigan were found by Ryznar and Touma (1981) to occur on an average of 7 days. Lyons (1972) found that Chicago lake breezes occurred on an average of 11 August days. Finally, Biggs and Graves (1962) recorded lake breezes on the western shore of Lake Erie on an average of 5 August days. Clearly, the occurrence values calculated using the SOMOS data are much higher than those from other studies in the Great Lakes region. One possible reason is that the criteria used for some of these studies were too stringent. For instance, Ryznar and Touma only considered 'true' lake breezes occurring with an offshore gradient wind. Biggs and Graves' criteria are also overly stringent and likely eliminated a significant fraction of lake breeze occurrences. Another possibility is that conditions during August 1993 were unusually conducive to lake breeze development. Indeed, as was shown earlier, conditions in the SOMOS study region during August 1993 were warmer and drier than normal.

On several days, multiple lake breeze passages were recorded at individual stations (see Appendix A). This occurred mainly on days when the Lake Huron lake breeze penetrated inland past the Lake Erie shore. Thus, a station on the north shore of Lake Erie would

experience a Lake Erie lake breeze frontal passage early in the day then a Lake Huron lake breeze frontal passage later in the afternoon or the evening.

Wind rose plots for the period between 10 LST and 16 LST are shown for days with lake breezes on all lakes (Figure 2.12a), days with no lake breezes (Figure 2.12b) and all days (Figure 2.12c). It can be seen that, on days with lake breezes on all shores (43% of days), onshore winds were most frequent at nearly every station in the study region. Stations as far inland from Lake Huron as London (approximately 60 km) show a surprising amount of lake breeze influence. Some patterns emerge such as divergent winds over Lake Huron, Lake Erie and eastern Lake St. Clair. The frequencies of calms at stations over western Lake Erie are significantly higher than for other stations. This is likely due to mesoscale high pressure that is typically present over the lake when lake breezes occur. Comparing the three diagrams, it appears that onshore lake breeze winds have a considerable influence on the prevailing flow during the study period, even at inland stations. Average wind speeds during lake breezes ranged from 3-7 knots or 2-4 m s⁻¹. This corresponds well with the average surface winds speeds of 5 m s⁻¹ or less found with the Lake Ontario breeze (Comer and McKendry, 1993). Winds speeds are significantly higher in the no-lake-breeze case and this is likely part of the reason that lake breezes did not develop on these days.

Wind rose plots for the period between 0000 LST and 0600 LST are shown for nights

with land breezes on all shores (Figure 2.13a), nights with no land breezes (Figure 2.13b) and all nights (Figure 2.13c). The greatest land breeze influence seems to be in the eastern half of the study region where even inland stations show a land breeze influence. Stations in the southwestern portion of the study region show less influence though a diffluent pattern is suggested. At least part of this difference can be attributed to the topography of the region (see Figure 2.2). The southwestern third of the study region is quite flat with elevations (above mean sea level) between about 180 m at the lakeshores and 200 m inland. East of this region, the elevation increases gradually towards the northeast to a maximum elevation within the study region of about 300 m. Elevations at stations along the shores of Lake Huron and Lake Erie decrease to near 180 m. Thus, land breezes may be enhanced at night by the downslope flow of land-cooled air towards the lakes.

A relatively high incidence of calms is reported mainly at the operational stations such as Windsor and London. These values may be partially due to the reduced sensitivity of the operational wind instruments at these stations. The no-land-breeze case shows wind rose frequencies similar to those of the no-lake-breeze case. Wind speeds in land breezes at the coasts range from 3-7 knots or 2-4 m s⁻¹. Values at inland stations showing a land breeze influence have lighter winds of 1-2 knots or around 1 m s⁻¹. These values also compare well with values of 1-5 m s⁻¹ obtained for Lake Ontario land breezes (Comer and McKendry, 1993). Note that data from NWS stations were not obtained for all study days and have been omitted from the wind rose analyses.

Table 2.4 shows the temporal characteristics of the lake and land breezes observed during SOMOS. These averaged values combine observations from all of the three lakeshores. Thus, on a day with lake breezes on all shores, for example, the start time would indicate the time at which lake breezes were in evidence on all shores. There are often differences in start and end times for each lake but an analysis of this type was not undertaken. Thus, values presented here serve only as a general guide. The average lake breeze start time was 11 LST and the average end time was 19 LST. The start time is two hours later than the most frequent start time found by Lyons (1972) on the western Lake Michigan shore. This difference may be attributed to the 'bulk approach' taken to start and end time identification as described above. The average land breeze start time was 22 LST and the average end time was 07 LST. Average land breeze duration was about one hour longer than the average lake breeze duration of eight hours.

During the study period, the most common gradient wind regimes were southwesterly, light and variable, and northwesterly (Figure 2.14). Most lake breezes and land breezes occurred in conjunction with light and variable winds. The development of lake or land breezes was often prevented in southwesterly and northwesterly wind regimes. It was also found that lake and land breezes tend to occur in episodes. The majority of lake breeze days (land breeze nights) occurred within episodes of four or more days (nights) in length (Figure 2.15). One lake breeze episode had a duration of eight days. There is also a

tendency for lake and land breezes to occur contiguously for periods of up to five days. This behaviour has serious consequences for the dispersion of air pollutants (see discussion in Chapter One). The occurrence of lake breeze, land breeze and contiguous lake-land breeze episodes is strongly correlated with the light and variable gradient wind regime. Interestingly, periods when lake breeze and land breezes were inactive were usually quite short. For example, the longest period without lake or land breezes in August was only two days.

As mentioned previously, a lake breeze occurrence record was established for each of the 30 stations in the study region. However, data from NWS stations were not obtained for all study days and are left out of this analysis. Subjectively contoured plots of lake breeze occurrence values are shown for Lake Erie (Figures 2.16a), Lake Huron (Figure 2.16b) and Lake St. Clair (Figure 2.16c). Frequency values represent the percent frequency of days with a lake breeze frontal passage from the specified lake during the 63 days of the study. Several 'virtual stations' were added to help resolve the patterns of contours in data-sparse regions. Since no *in situ* meteorological observations were available at these points, percentage frequency values were estimated using only satellite imagery and observations at nearby stations. Note also that slight increases in the size of number symbols indicate an increasing degree of confidence due to increased temporal resolution of data at the SOMOS stations or a greater number of available station parameters.

There is a tight gradient in lake breeze frequency along the north shore of Lake Erie. The Lake Erie lake breeze reached stations in the northern part of the study region on only one day. Conversely, Lake Huron is shown to have had influence over the entire study region with stations on the north shore of Lake Erie reporting lake breeze frontal passages on 11% of study days. The plot for Lake St. Clair shows a more even distribution around the Lake.

It appears that lake characteristics such as shape, size and warm season surface temperature may have a large influence on the extent of inland penetration. Lake Erie is the warmest of the three lakes. Its major axis runs along a WSW-ENE line nearly parallel to the Lakes's northern shore in the southern portion of the study region. Lake breeze penetration was mainly restricted to a distance 40 km or less from the shore. The plot for Lake St. Clair, by far the smallest of the three lakes with a quasi-circular shape and surface temperatures usually between that of Lake Erie and southern Lake Huron, has very closely-spaced, quasi-concentric contours around the lake. Lake Huron is the largest and coldest of the three lakes and its major axis arcs along a northwest to south curve nearly perpendicular to the lake's southern shore in the northern part of the study region. The Lake Huron lake breeze penetration pattern appears to follow an extrapolation of this axis reaching over 100 km inland. It is likely that the longer residence time of air parcels travelling along the lake's major axis results in greater cooling efficiency. Also, an analysis of the seven cases in which the Lake Huron lake breeze penetrated over 100 km

southward reveals that light, onshore (having a dominant northerly component) gradient flow was present in each case. The onshore flow appears to aid the southerly inland penetration of the lake breeze. In most of these cases, stations near the Lake Huron shore showed calm or offshore winds late in the day even as the lake breeze appeared to be continuing to penetrate southward. In effect, the lake breeze vortex had become detached from the subsiding circulation, as described in Chapter One. This supports the hypothesis that most deeply penetrating lake breezes exist in the form of a cut-off vortex (Simpson, 1977). Thus, the combination of the colder lake surface temperature, the size of the lake and its shape appears to explain the greater degree of penetration for the Lake Huron lake breeze in this region.

Figure 2.17 shows a subjectively contoured map of lake breeze occurrence frequencies at each station using all station data. The format used for this map is the same as that used in Figure 2.16 with the additional proviso that if a station reported lake breeze frontal passages from more than one individual lake in a single day, it was still counted as only one lake breeze day. The highest observed frequency of lake breeze days, 51%, during the 63 days of the study occurred at both the Dashwood station on the southeastern Lake Huron shore and the Erieau station on the Lake Erie shore. Frequencies greater than 50% are also implied by the contouring in a few other locations along the shores of Lake Huron and Lake Erie. The maximum observed frequency on the Lake St. Clair shore is 43% though the contouring implies a maximum greater than 45% on the northeastern

shore. Elongated minima were observed in areas between the Lakes with the most pronounced minimum between Lakes Huron and Erie. Clearly, all parts of southwestern Ontario and nearby portions of southeastern Michigan were affected by lake breeze circulations.

Some thought was given to extending the investigation of lake and land breeze frequency in this region beyond the study period using only operational surface meteorological data. However, a study of this type was not undertaken for several reasons. First, data would not be available at less than one hour intervals reducing confidence when identifying lake breeze fronts. Also, the locations of operational stations, mainly clustered around Windsor-Detroit and Sarnia-Port Huron, leave large segments of coastline unrepresented. Due to these restrictions, a different identification process, most likely requiring a diurnal wind reversal criterion, would be necessary. The difficulty in using this criterion for the Great Lakes region has already been discussed. Second, as mentioned previously, observations over a period of several years would likely be required for accurate lake and land breeze occurrence frequency values in this region. Thus, large volumes of surface meteorological observations, surface analyses and satellite images would have been required from several different organizations. Though a more accurate understanding of lake breeze occurrence in the region is desirable, it was felt that such an investigation was beyond the scope of the present study.

2.2.4.5 Lake Breezes and Ground-level Ozone

The Windsor-Quebec Corridor from southwestern Ontario to southern Quebec has been identified by the CCME (1990) as the region in Canada most frequently and seriously affected by high ozone concentrations. Maximum hourly averaged ozone concentrations in this region often reach 150 ppb during the late-spring and summer months and have been observed to reach values near 200 ppb on occasion (Fuentes and Dann, 1994).

Within this corridor, rural southwestern Ontario has been singled out as having the most frequent and persistent ozone exceedances (Fuentes and Dann, 1994). Observations made by Kelly *et al.* (1986) show that more frequent occurrences of even higher concentrations can be expected in areas of southeastern Michigan. Ozone 'episode-days', defined in Ontario as days with widespread ozone levels greater than 80 ppb (Ontario one-hour criterion) at more than eight stations simultaneously, usually occur on the backsides of slow-moving anti-cyclonic systems or in the warm sector of cyclonic systems (Yap *et al.*, 1988). Meteorological conditions in these synoptic regimes usually consist of clear to partly clear skies, warm temperatures and gradient flow with a significant southerly component. Episodes in southern Ontario have been observed to last from one to eight days (Yap *et al.*, 1988). Though significant sources of ozone precursors exist in southwestern Ontario and southeastern Michigan, more than half of the ozone measured there is attributed to long-range transport over several days from areas in the United States to the south and west (Yap *et al.*, 1988; Kelly *et al.*, 1986). In order for transport to occur over a period of days, ozone must remain in high concentrations overnight (Wolff

et al., 1977). Aircraft observations south of the Great Lakes region have confirmed that a residual mixed layer can exist aloft with only small decreases in concentration overnight (Clarke and Ching, 1983). Such a layer of ozone aloft can be mixed down to the surface once the nocturnal inversion breaks up causing rapid increases in surface concentration during the day (McKendry *et al.*, 1997; Neu *et al.*, 1994).

Localities near the shores of Lakes Huron and Erie experience the highest concentrations of ozone in southwestern Ontario (Mukammal *et al.*, 1982) and have the greatest number of hours and days exceeding the Canadian federal 82 ppb one-hour ozone criterion (Fuentes and Dann, 1994). Figure 2.18 shows that the number of exceedance hours decreases with distance inland from the shores of these lakes. It is thought that this effect is most likely due to ozone being delivered to the surface by lake breeze circulations (Chung, 1977; Mukammal *et al.*, 1982). This hypothesis is supported when comparing Figures 2.17 and 2.18, noting that the exceedance pattern closely matches the lake breeze frequency pattern in the eastern portions of the study region. Additional similarities over extreme southwestern Ontario may have been revealed had a decreased contour interval been used between 50 and 80 hours. The hypothesis is also supported since, as discussed in Chapter One, the occurrence of high ozone concentrations in coastal regions is highly correlated with the occurrence of lake breezes.

Maximum ground-level ozone concentrations in both the Ontario and Michigan portions

of the study region reached values greater than 80 ppb (the Ontario one-hour ozone criterion) on 20 out of the 63 days of the study period. Lakes breezes occurred in the study region on 16 or 80% of these days. If only the Ontario portion of the study region is considered, 12 out of 63 days had maximum ozone concentrations greater than 80 ppb and lake breezes occurred on nine or 75% of these days. This appears to confirm a strong correlation between lake breezes and high ozone events in southwestern Ontario and southeastern Michigan. Of the 20 days during the study period with maximum ozone concentrations over 80 ppb, six occurred in July and one occurred in September, with the majority occurring in August. Two periods of high ground-level ozone concentrations (though not officially ozone episodes) occurred in August. The first six-day period stretched from August 11 to August 16. This period occurred within an eight-day lake breeze episode. Also, contiguous lake and land breezes occurred from August 11 to August 15. Lake and land breezes during this period were quite vigorous. Maximum one-hour ozone concentrations ranged from 83 ppb on the 16th to 147 ppb on the 14th. The second period of high ground-level ozone concentrations consisted of three days between August 25 and August 27. This period occurred within a four day lake breeze episode. Land breezes were active only on August 24 and 25. Maximum one-hour ozone concentrations ranged from 90 ppb to 94 ppb, relatively low considering the potential that existed due to the very hot and sunny conditions.

Figure 2.19 shows the maximum observed hourly ozone concentrations during the study

period. The highest maximum value, 147 ppb, was recorded at the Port Huron site on August 14. In fact, seven of the maximum values between Windsor and Sarnia occurred on August 14. These values were among the highest recorded in Ontario and Michigan during 1993. Lake breezes were very well-developed on this day and relationships between the lake breezes and the high ozone observations are examined in Chapter Four (Case Studies). A map showing the number of hours with ozone concentrations recorded above 80 ppb in the study region is shown in Figure 2.20. The pattern that emerges from these maps is that the highest ozone concentrations and most frequent exceedances occurred in the vicinity and downwind of the Windsor - Detroit and Sarnia - Port Huron industrial and urban centres. Though the highest one-hour ozone concentrations were associated with the Sarnia - Port Huron area, the Windsor - Detroit ozone problem was considerably more persistent. This pattern suggests that local sources are major contributors to the ozone problem in this region.

2.2.4.6 Lake Breezes and Severe Summer Weather

Southwestern Ontario is the most thunderstorm-prone region in Canada with up to 36 thunderstorms per year on average (Kendall and Petrie, 1962; Sajecki, 1988). This region also has the highest annual tornado incidence in Canada (Newark, 1984). Using lightning flash detection data over three warm seasons, Clodman and Chisholm (1996) found that the average number of days with lightning in southern Ontario reaches a maximum in a WSW to ENE band inland from each of the lakes in the region (Figure 2.21). An average

of more than 30 days per year with lightning was observed in this band decreasing to near 25 days per year along the lake shores and to less than 20 lightning days per year east of Lake Simcoe. Although Clodman and Chisholm attribute this elongated maximum to the superimposition of several different physical effects, lake breeze activity is thought to be an important factor in the portion of the maximum from eastern Lake St. Clair to London while orographic effects (see Figure 2.2) are thought to be important in the portion of the maximum extending farther to the northeast. They also show that the lightning flash count in southwestern Ontario has a strong diurnal variation with a pronounced late-afternoon maximum.

Annually-averaged extreme rainfall statistics for southern Ontario prepared by Hogg and Carr (1985) show that ten year return period, one-hour rainfall has a local maximum in a similar elongated WSW to ENE band from Lake St. Clair to London (Figure 2.22). A maximum value of 49 mm is located within this band while values decrease to less than 40 mm towards the lakeshores. A secondary, quasi-circular maximum area is located to the northeast with a maximum value of 48 mm to the northwest of Lake Ontario. As with the lightning flash data, this secondary maximum area is most likely associated with orographic effects.

Average annual tornado incidence values calculated using Canadian tornado data from 1950 to 1979 (Newark, 1984) show a maximum over southwestern Ontario inland from

the shores of Lakes Huron and Erie (Figure 2.23). Newark states that the occurrence of tornadoes appears to be inhibited by cool marine air affecting land areas adjacent to the Great Lakes. He also finds that tornadoes in Canada generally have their peak activity between 1500 and 1700 local time. The elongated maxima in lightning flash, extreme rainfall, and tornado incidence data appear to be inversely correlated with the elongated minimum in lake breeze frequency shown in Figure 2.17 though the lake breeze frequency minimum is located slightly closer to the Lake Erie shore (this difference may reflect the small sample size used to determine the lake breeze frequency pattern).

These relationships may be better understood by considering both the lake breeze frequency values and the known effects of lake breezes on the development of deep, moist convection. Stations that show the highest occurrences of lake breeze frontal passages are likely to have the lowest probabilities of observing convective storms on lake breeze days due to restrictions to convection behind the front that often occur in the region. Stations between two lakes that show a minimum occurrence of lake breeze frontal passages are likely to experience maximum convective storm activity on lake breeze days since there is a minimum of convective restriction and the possibility of enhanced lift near the lake breeze front. Minima between two lakes should also be the average locations for collisions between the two lake breeze fronts. Collision events can result in even greater lift. While the most pronounced lake breeze frequency minimum between Lakes Huron and Erie correlates well with the lightning flash and extreme

rainfall maxima, the secondary minima between Lakes Erie and St. Clair and between Lakes Huron and St. Clair appear not be as well represented. Late afternoon maxima for lightning flash count and tornado occurrence in southwestern Ontario correlate well with the time of peak intensity and penetration distance of lake breezes.

Summer severe weather in Ontario is defined by AES (Chadwick, 1994) to include:

- tornadoes,
- thunderstorm wind gusts greater than 90 km h^{-1} ,
- hailstones with diameters of 20 mm or greater, and
- rainfall rates greater than 50 mm in one hour or 75 mm in three hours.

Near-severe weather is defined to include:

- funnel clouds or waterspouts,
- hailstones with diameters less than 20 mm,
- thunderstorm wind gusts greater than 70 km h^{-1} .

Severe or near-severe weather occurred in the study region on eight days during the study period: July 28, August 3, 14, 15, 24, 27, 31 and September 5 (Chadwick, 1994). Events included weak tornadoes, funnel clouds, damaging wind gusts, large hail and heavy rainfall. With the exception of storms occurring during the early morning hours of August 24 and August 31, all severe or near-severe weather occurred between 12 LST and

20 LST. Considering only these days when severe or near-severe weather occurred during daylight hours, lake breezes were found to be occurring in the study region previous to the event on five out of the six days. On the sixth day, lake breezes highly perturbed by the gradient wind are suspected but cannot be confirmed with confidence. It is believed that on at least four of these five days, August 14, 15, 27, and September 5, enhanced convergence and lift at lake breeze fronts initiated the deep, moist convection that resulted in the severe or near-severe weather event.

On August 14, a thunderstorm that formed in the vicinity of the Lake Huron and Lake St. Clair lake breeze fronts produced a probable weak tornado. On August 15, a thunderstorm with at least one weak tornado appeared to be initiated at the merger point between the Lake Erie and Lake St. Clair lake breeze fronts. Quasi-stationary thunderstorms producing heavy rain also occurred in the vicinity of the Lake Erie lake breeze front on this day (more detailed analyses of the August 14 and 15 events are given in Chapter Four). On August 27, a storm that developed near the Lake Huron lake breeze front produced damaging wind gusts and large hail. Finally, on September 5, a funnel cloud was observed beneath a bank of cumulus clouds in the vicinity of the Lake Erie lake breeze front. No thunderstorm appeared to be associated with the near-severe weather in this case. In each of the cases with tornadoes or funnel clouds, morning wind profiles from Flint, Michigan indicated low values of storm-relative helicity and parent thunderstorms, if present, appeared not to be supercellular in nature. That is, the vortices

appear to be non-mesocyclone, or 'landspout', type vortices (see discussion in Chapter One). Clearly, lake breezes and the occurrence of severe and near-severe weather are closely related in this region. Interestingly, one-hour ground-level ozone values reached over 80 ppb on several of the severe and near-severe weather days.

2.3 The ELBOW Project

2.3.1 Project Background

A field project was conducted in the summer of 1997 to observe lake breeze fronts in southwestern Ontario and determine their role(s) in initiating deep moist convection, including severe storms. Of special interest were days when lake breezes were highly perturbed by the gradient wind. Lake breezes in this situation appear to be frequently associated with severe thunderstorm development when the gradient wind is out of the southwest (King, 1996). However, these circulations were difficult to identify with confidence in the SOMOS dataset and other databases since lake breeze signals in the resulting surface wind and temperature patterns were ambiguous.

The experiment was led by Patrick King of the Meteorological Research Branch (MRB) of Environment Canada and David Sills (the author) of the Centre for Research in Earth and Space Science (CRESS) at York University. The University of Western Ontario cooperated by allowing the use of facilities at its agricultural research station approximately 10 km northwest of London. The ELBOW project will be described below.

Additional project information is provided by King *et al.* (1998).

2.3.2 The Field Campaign

The ELBOW experiment was conducted in southwestern Ontario in the flat to gently rolling countryside between Lakes Erie and Huron though the area of interest shifted somewhat farther northeast than that for the SOMOS project (Figure 2.24). Originally, two intensive observations periods (IOPs) were planned: one in May to coincide with near maximum land-water temperature differences and a second in July when deep moist convection is typically more frequent but land-water temperature differences are less. The May IOP was aborted due to unseasonably cold and windy weather. It was partially replaced by a short IOP from June 24 to June 25. The July IOP proceeded largely as planned from July 8 to July 18. The AES operational radar site at Exeter served as the base of operations. This site offered access via an internet connection to current meteorological data and was located within an hour's drive of both lakes.

A 10 m portable meteorological tower was installed at the Exeter radar site at the start of the May IOP. Similar towers were installed at the start of the July IOP at sites near St. Thomas and Port Stanley. These towers measured 10 m winds, 1.5 m temperature and relative humidity, and the temperature difference between 9.5 m and 1.5 m levels at one second intervals. These instruments and their measurement accuracies were very similar to those discussed previously for the SOMOS field project. Precipitation accumulation

was also measured at the Exeter site. These parameters, and derived quantities such as maximum scalar wind speed and standard deviations of wind speed and wind direction, were recorded as five minute averages with a datalogger. The Exeter site was located about 20 km inland from Lake Huron while the St. Thomas site was located about 8 km inland from Lake Erie. The Port Stanley site was situated about 300 m from the Lake Erie shore near a 30 m bluff.

Rawinsonde data were collected on most of the IOP days using a NCAR 'CLASS' type ground station, Vaisala sondes and helium-filled balloons. Launches were usually made in the afternoon either from the Exeter radar site or the UWO research station site. Most flights produced data to heights of 20 km or greater. The amount of helium used was reduced to obtain a lower ascent rate and more data in the lowest levels of the troposphere.

Mobile spotter teams were also used to supplement the fixed network of stations by taking spot measurements in the vicinity of lake breeze fronts. The spotters also took observations and photographs in the event of developing showers or thunderstorms.

A Vaisala sonde was flown on a kite on most days relaying data to a ground station at the Exeter radar site. Flight duration was limited by the sonde battery life to about two hours. Kite measurements, including serial ascents / descents, were made up to an altitude of

approximately 800 m.

2.3.3 Supporting Measurements

As had been done with the SOMOS field data, the special measurements made during the investigation were combined with standard surface and upper-air observations, satellite imagery and radar data. The resulting consolidated dataset was found sufficient for a limited study of the role of lake breezes in the initiation of deep, moist convection.

Surface observations from existing meteorological stations in southern Ontario were obtained from AES and Ontario Hydro. AES data were available at hourly intervals while Ontario Hydro data were available every 15 minutes. Hourly data from Lake Erie and Lake Huron buoys were obtained from the U.S. National Climatic Data Center (NCDC). Figure 2.25 shows the locations of ELBOW, AES and Ontario Hydro stations as well as the buoy locations within the ELBOW study region. Note that some of these stations made measurements at non-standard heights. For instance, the buoy over Lake Huron made all atmospheric measurements at 2.4 m. Rawinsonde data from Flint, Michigan, roughly 90 km northwest of Detroit, were obtained for selected IOP days. Remapped visible satellite images from the GOES-8 satellite were obtained from AES for selected IOP days. These very high resolution (1-2 km) images were available every 15 minutes except when the satellite was in 'rapid-scan' or 'ultra-scan' mode which produces images every 1-5 minutes. Conventional radar data were obtained from the Exeter and King City

radar facilities. Various types of radar images are available at 10 minute intervals.

Doppler radar data at 10 minute intervals were also obtained from the King City radar facility. The effective Doppler range included the far eastern portions of the ELBOW study region.

Daily lake surface temperature data were provided by the Great Lakes CoastWatch program of the NOAA Great Lakes Environmental Research Laboratory (GLERL) in Michigan. These images show lake surface temperatures as detected by a satellite-borne infrared sensor and averaged over a period of several days. The buoys also measured lake surface temperature at hourly intervals.

2.3.4 Observations of Lake Breeze Storm Initiation

Lake breezes occurred on various days within the ELBOW IOPs. On four of these days, June 24, June 25, July 14 and July 18, lake breezes were observed to have a controlling influence on the occurrence and location of thunderstorms and, in some cases, severe weather.

On June 24, lake breezes developed but were perturbed by a moderate westerly gradient flow. Thunderstorms, including a severe storm, were initiated along cloud lines extending inland from shore segments of Lakes Huron and St. Clair that were parallel with the wind, as seen on visible satellite imagery (not shown). Another cloud line was visible inland

from the north shore of Lake Erie. It is believed that these lines were fronts associated with the perturbed lake breeze circulations. The severe storm appeared to be initiated where these lines merged just west of London near 1500 LST. The thunderstorm complex, a 'multicell cluster', continually redeveloped on its northwestern flank nearly cancelling the southeast storm motion. The storm produced heavy rains with localized flooding, wind gusts that downed trees and power lines, and small hail. There were also unconfirmed reports of large hail, microbursts and a funnel cloud with this storm.

On the following day, June 25, the position of the Lake Erie lake breeze front inland from the north shore of Lake Erie was revealed by special and spot observations indicating a wind shift line and by visible satellite imagery showing a slow-moving line of clouds (not shown). A line of strong thunderstorms developed along this front near 1600 LST as a cold front was approaching from the northwest. The storms produced brief heavy rain, gusty outflow winds and small hail. No reports of weather exceeding severe thresholds were received for any of these storms.

On July 14, a moderate westerly gradient flow resulted in highly-perturbed lake breezes in the study region. Lake Huron and Lake Erie lake breeze fronts extended well inland and appeared to merge. A severe thunderstorm developed explosively at the apparent point of merger near Stratford, Ontario around 1600 LST. This storm developed into a quasi-stationary multicell complex. Over 200 mm of rain were reported from this storm over a

period of several hours resulting in localized flooding. Severe wind gusts, possibly due to microbursts, downed trees and flipped airplanes at a local airport. There were also unconfirmed reports of large hail.

The last event of this type occurred on July 18. Mesonet observations and visible satellite imagery (not shown) indicate that strong thunderstorms developed along the Lake Erie lake breeze front near 1200 LST as a cold front was approaching from the northwest. These storms moved rapidly to the southeast producing brief heavy rain. No reports of severe weather were received with these storms.

2.4 Summary

Field observations and supporting data from the SOMOS study were used in this chapter to develop a preliminary summertime lake and land breeze climatology for southwestern Ontario and nearby areas of southeastern Michigan. Meteorological and air chemistry data from this study will be used in Chapter Four (Case Studies) to investigate the relationships between lake breezes and severe weather and between lake / land breezes and high ground-level ozone for the period from August 14 to August 15. ELBOW field observations and supporting data for the July 14 case will be used in Chapter Four to investigate the relationship between highly-perturbed lake breezes and the generation of severe weather. For both case studies, a mesoscale numerical model will be used to simulate lake (and land) breeze conditions. The observational data will be used to

evaluate the performance of the model. It is also expected that the model results will provide additional insight into the complex, fine-scale processes associated with the lake and land breezes.

CHAPTER TWO TABLES

Table 2.1. Mean maximum and minimum air temperatures over land and mean Lake Huron and Lake Erie surface temperatures for the months of April, July and October. Mean maximum daytime and nighttime temperature difference across the shore of each lake are also given (source: Brown *et al.*, 1980).

Month	April	July	October
Mean Maximum Inland Air Temperature (°C)	13	27	16
Mean Minimum Inland Air Temperature (°C)	2	15	5
Mean Lake Huron Surface Temperature (°C)	1 - 2	16 - 18	11 - 13
Mean Lake Erie Surface Temperature (°C)	2 - 4	19 - 21	14 - 16
Mean Maximum Daytime Land-Lake Huron Temperature Difference (°C)	11 - 12	9 - 11	3 - 5
Mean Maximum Daytime Land-Lake Erie Temperature Difference (°C)	9 - 11	6 - 8	0 - 2
Mean Maximum Nighttime Lake Huron-Land Temperature Difference (°C)	-1 - 0	1 - 3	6 - 8
Mean Maximum Nighttime Lake Erie-Land Temperature Difference (°C)	0 - 2	4 - 6	9 - 11

Table 2.2. July, August and September 1993 departures from 29-year mean values and selected climate records at (a) Windsor and (b) London. The mean wind direction and the numbers of precipitation and thunderstorm days are also included.

<i>(a) WINDSOR</i>	July		August		September	
Mean Max. Temp. (C)	1		1.1		-3.3	
Mean Min. Temp. (C)	1.9		1		-1.3	
Precipitation (mm / %)	-29.3	-34%	-43.3	-51%	39.7	46%
Sunshine (hours / %)	3.7	1%	-29.1	-11%	-53.5	-28%
Mean Wind Direction	SSW		N		SSW	
Precipitation Days	14		15		17	
Thunderstorm Days	8		5		4	

<i>(b) LONDON</i>	July		August		September	
Mean Max. Temp. (C)	-0.3		1.3		-2.9	
Mean Min. Temp. (C)	1.6		1.1		-1.3	
Precipitation (mm / %)	14.3	19%	-47.2	-53%	49.6	58%
Sunshine (hours / %)	-19.4	-7%	-12.5	-5%	-45.2	-28%
Mean Wind Direction	WNW		W		W	
Precipitation Days	15		18		18	
Thunderstorm Days	7		6		3	

Table 2.3. Lake and land breeze occurrence statistics for individual shores and combinations of shores based on data from 63 days and 62 nights. Values are presented by day / night and by percentage of study days / nights.

	Lake breeze		Land breeze	
	Days	%	Nights	%
Lake Huron shore	32	51	31	50
Lake Erie shore	34	54	35	56
Lake St. Clair shore	29	46	25	40
All three shores	27	43	25	40
Any of the three shores	36	57	36	58

Table 2.4. Observed temporal characteristics of lake and land breezes during SOMOS.

	Lake Breeze	Land Breeze
Average start time (LST)	11	22
Range (LST)	08 - 14	19 - 03
Average end time (LST)	19	07
Range (LST)	12 - 21	01 - 10
Average duration (hours)	8	9
Range (hours)	03 - 12	3 - 14

CHAPTER TWO FIGURES

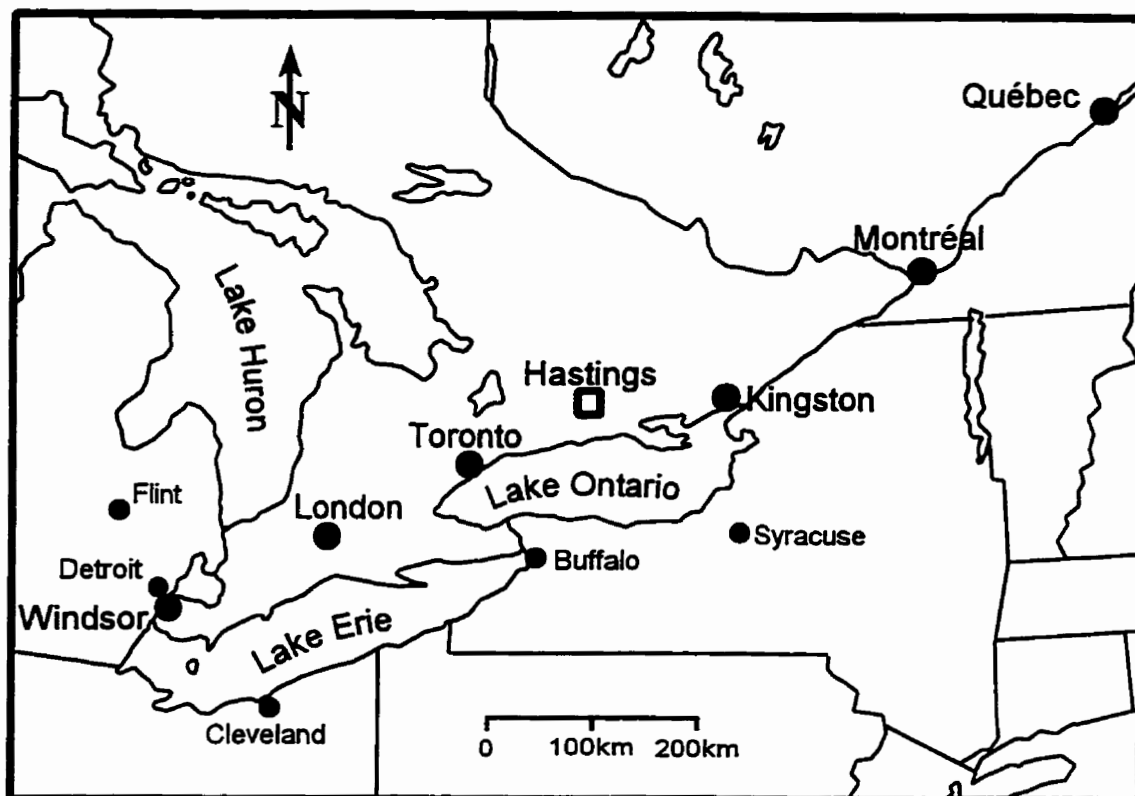


Figure 2.1. Map of the Windsor-Quebec City corridor illustrating the location of the Hastings site and the shorelines of the eastern Great Lakes. Major Canadian and U.S. cities are also labelled and provincial and state boundaries are marked.

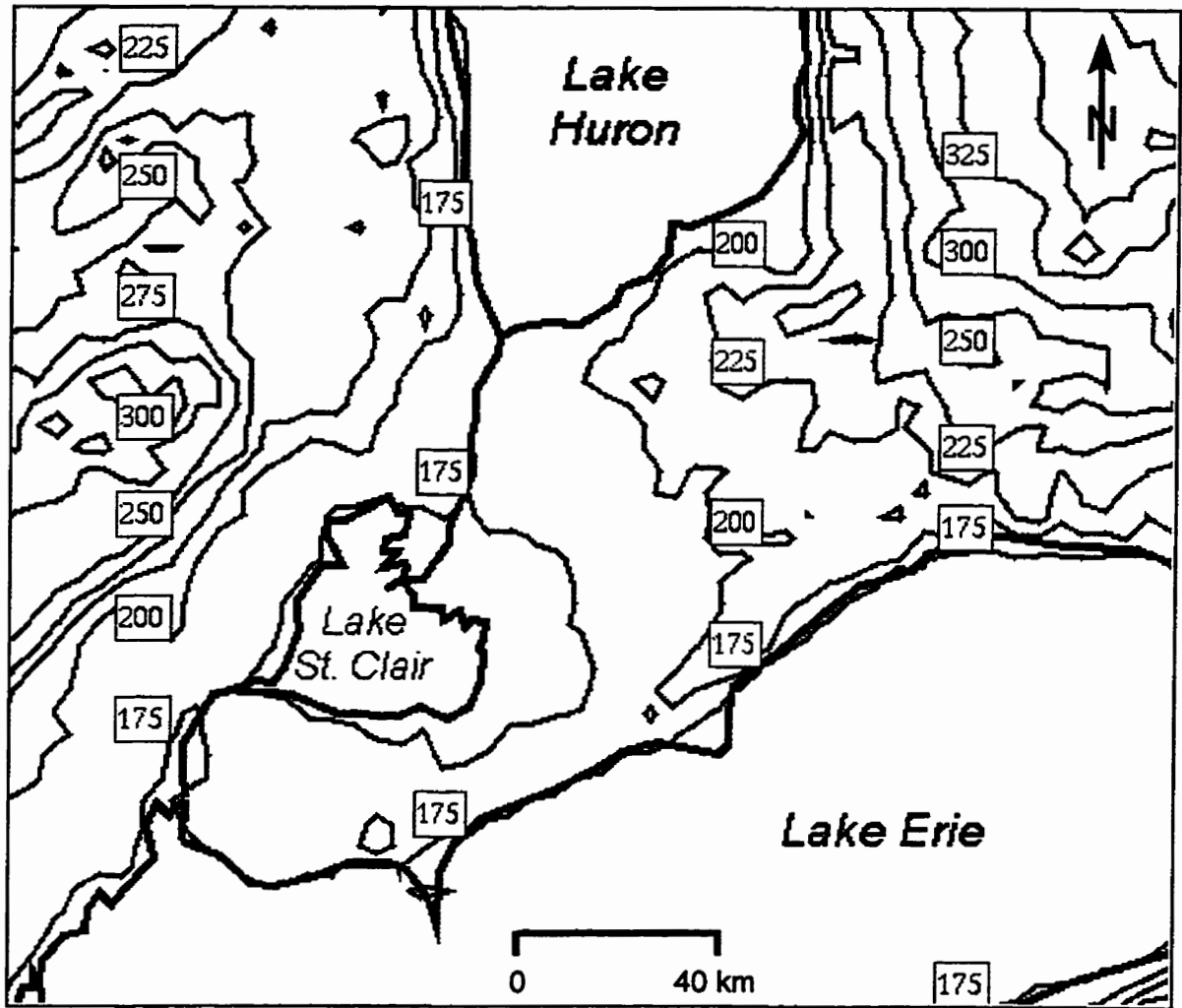


Figure 2.2. Map showing the SOMOS study region and its topography. Elevations above mean sea level are in metres and the contour interval is 25 m.

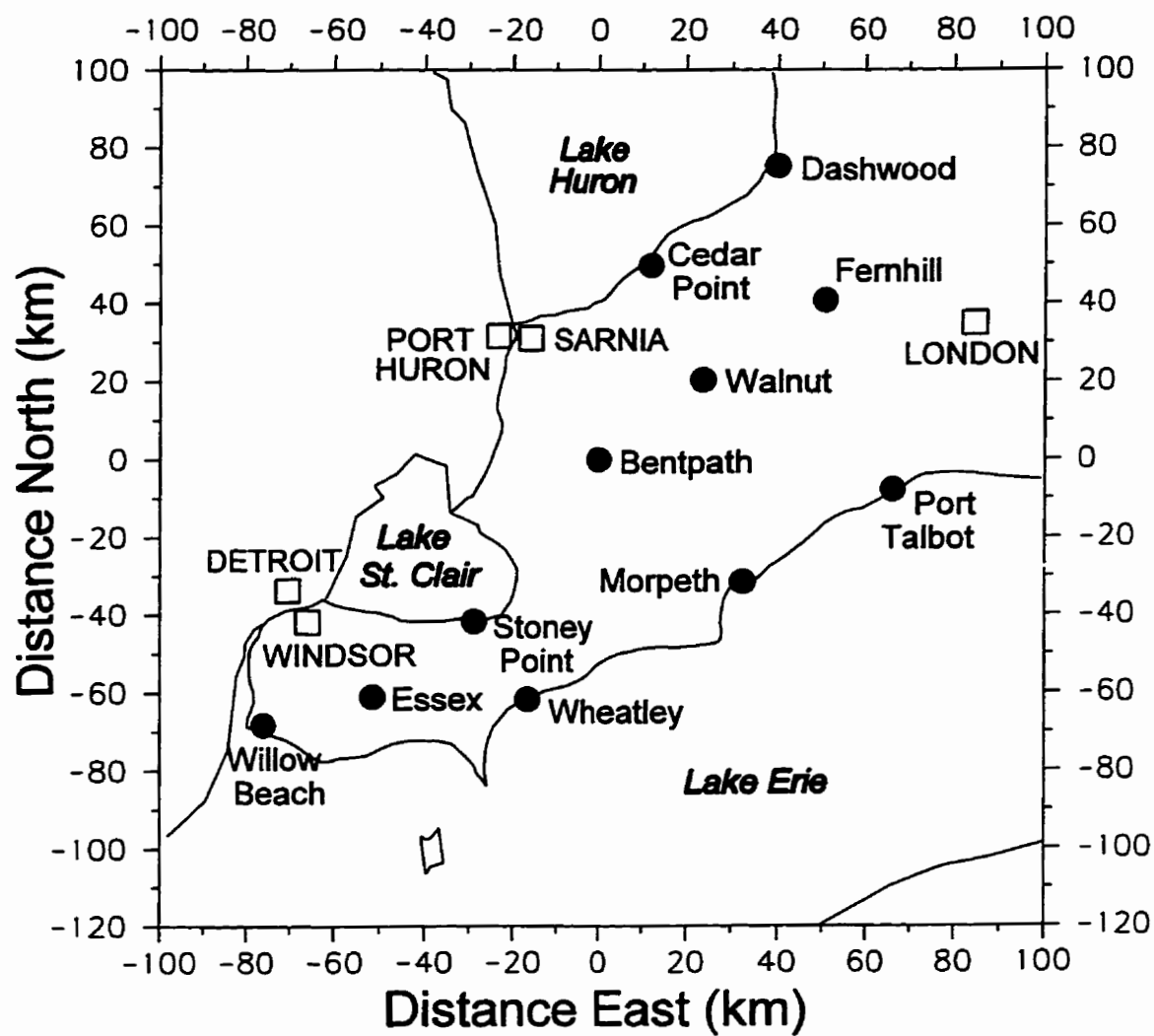


Figure 2.3. Map showing the locations of the SOMOS mesonet stations within the study region. Major Ontario and Michigan cities are also shown.

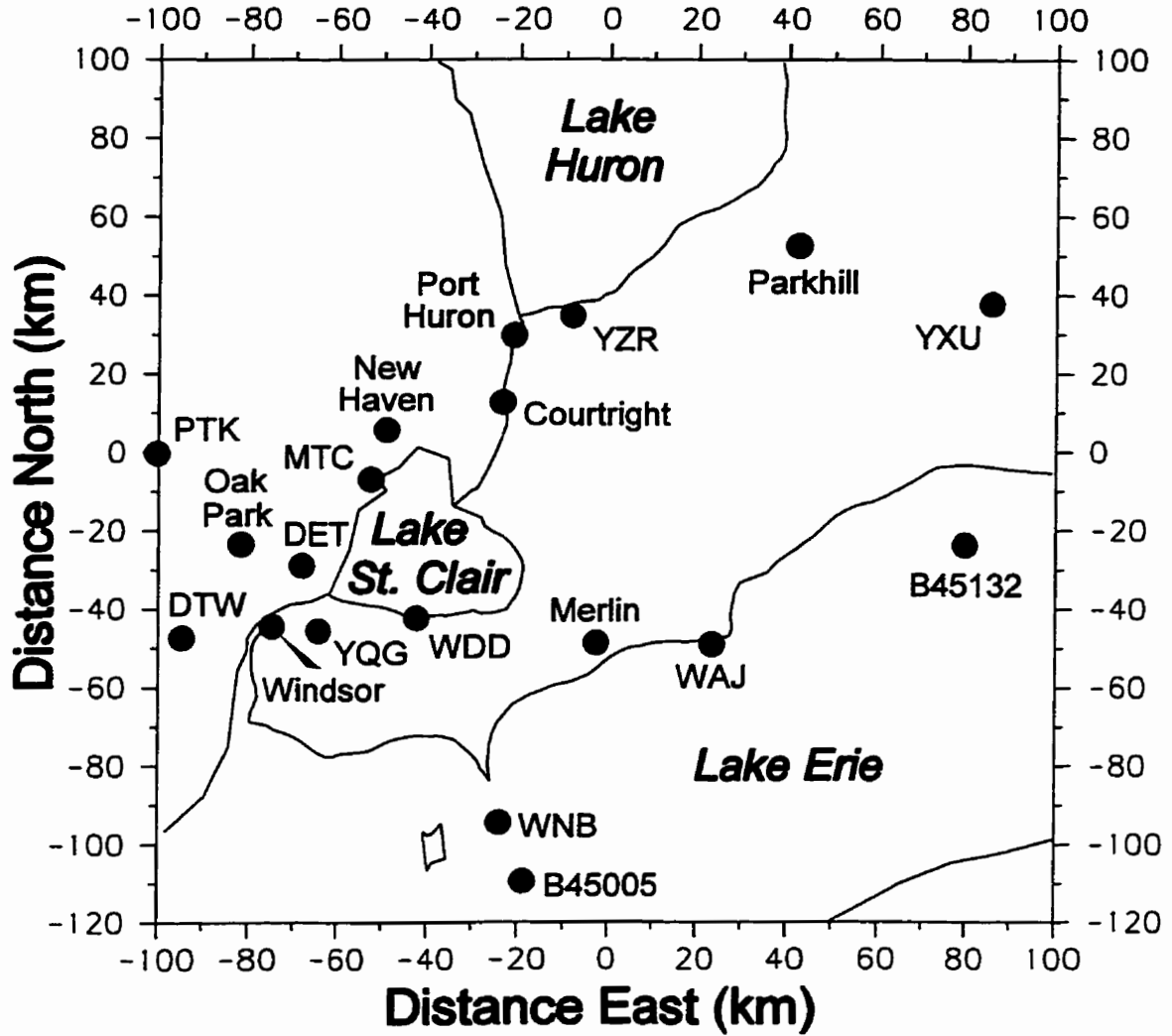


Figure 2.4. Map showing the locations of AES, OMEE, NWS and SEMOS surface meteorological stations. AES and NWS stations are labelled with their three-letter identifiers. Lake Erie buoys are also shown and are labelled with a 'B' plus their buoy number.

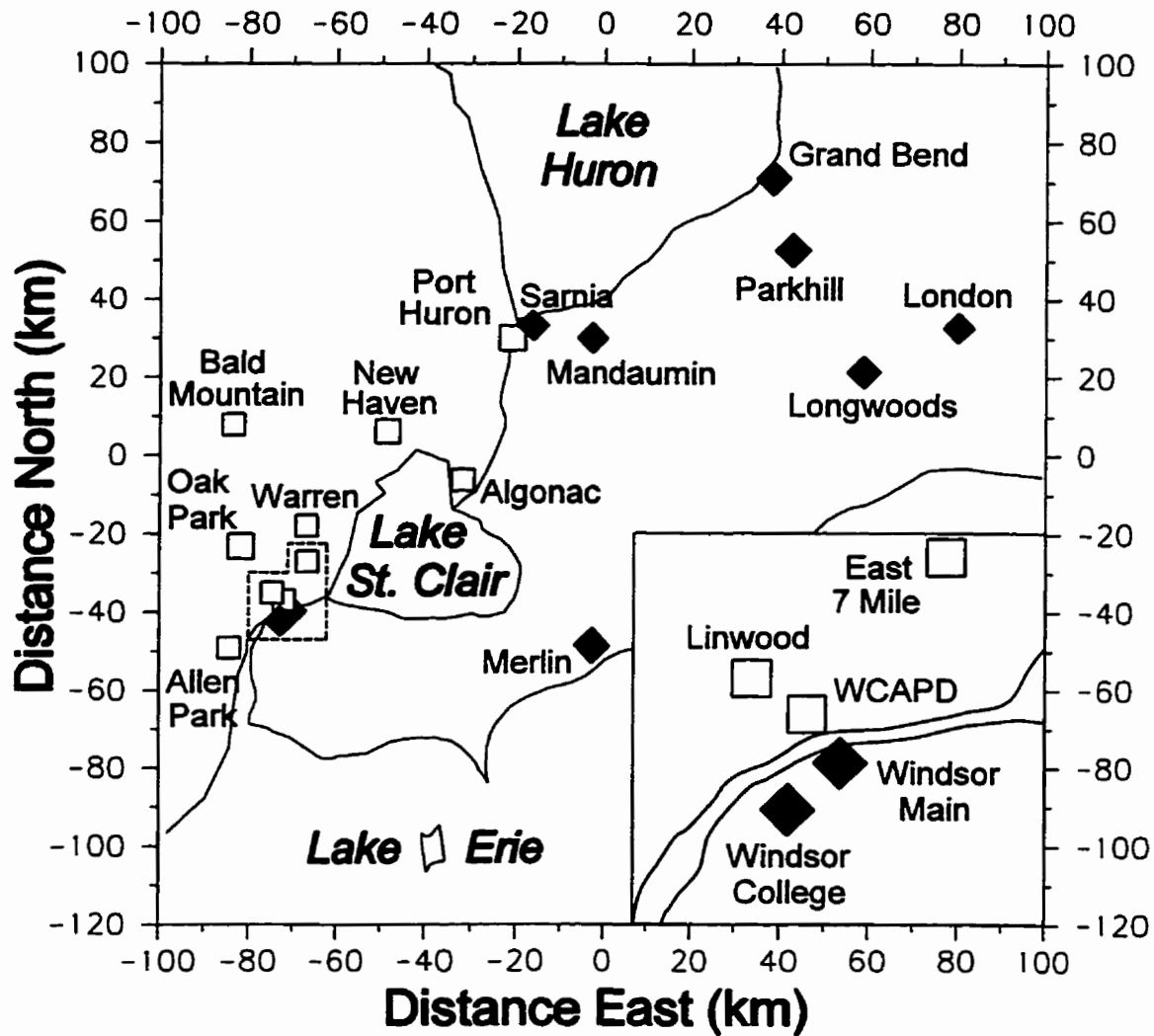


Figure 2.5. Map showing the locations of ground-level ozone monitoring stations in the study region. Inset shows stations in the Windsor-Detroit area.

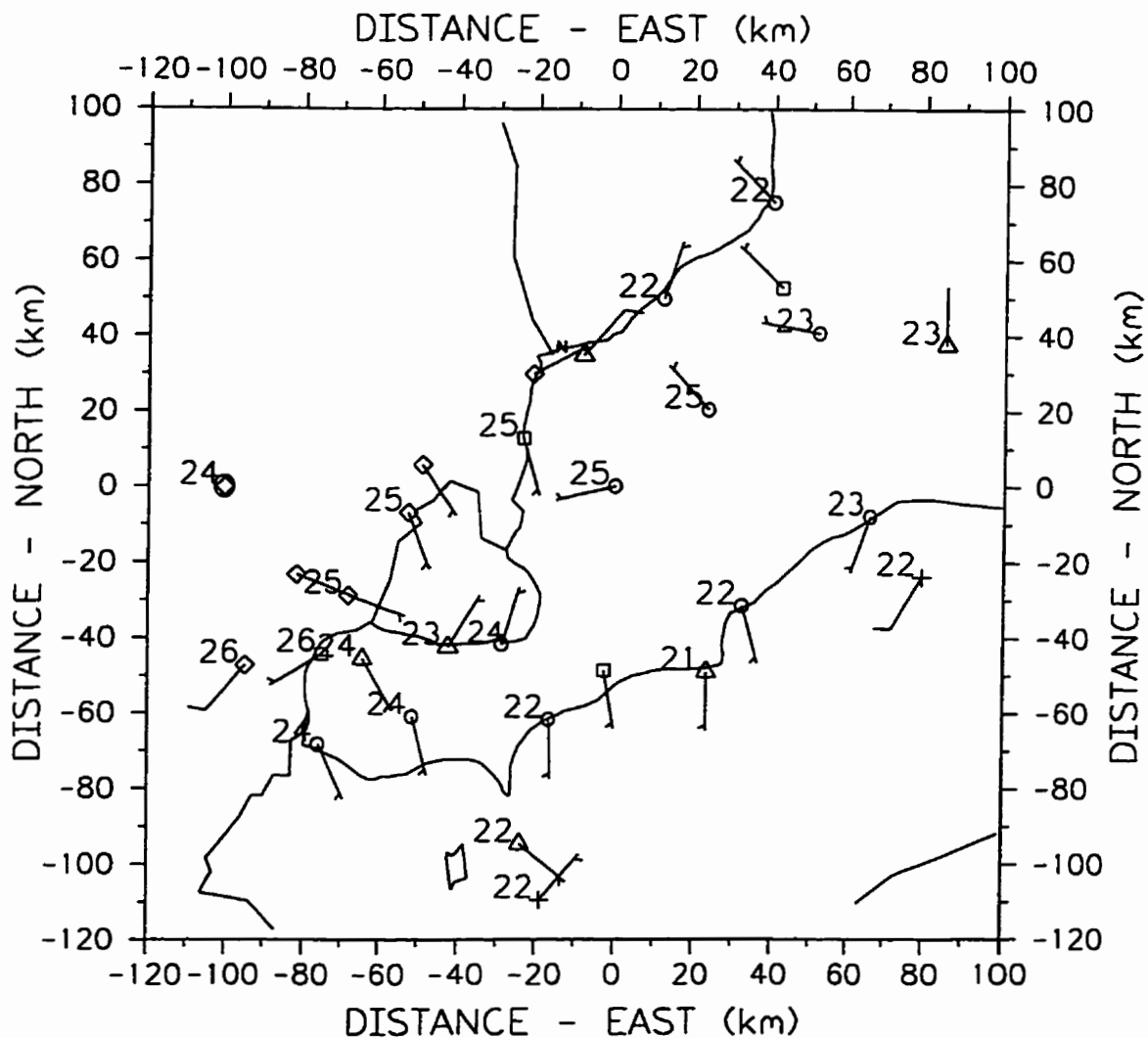


Figure 2.6. Plot of surface station data at 15 LST on August 8, 1993 showing onshore lake breeze flow on the shores of each lake and extending inland southeast of Lake Huron and northeast of Lake St. Clair. Only temperatures ($^{\circ}\text{C}$) and winds (knots) are shown for clarity. Short bars represent 3-7 knots and long bars represent 8-12 knots. The absence of a barb indicates a wind speed between calm and 3 knots. Calms are denoted by a circle around the station marker.

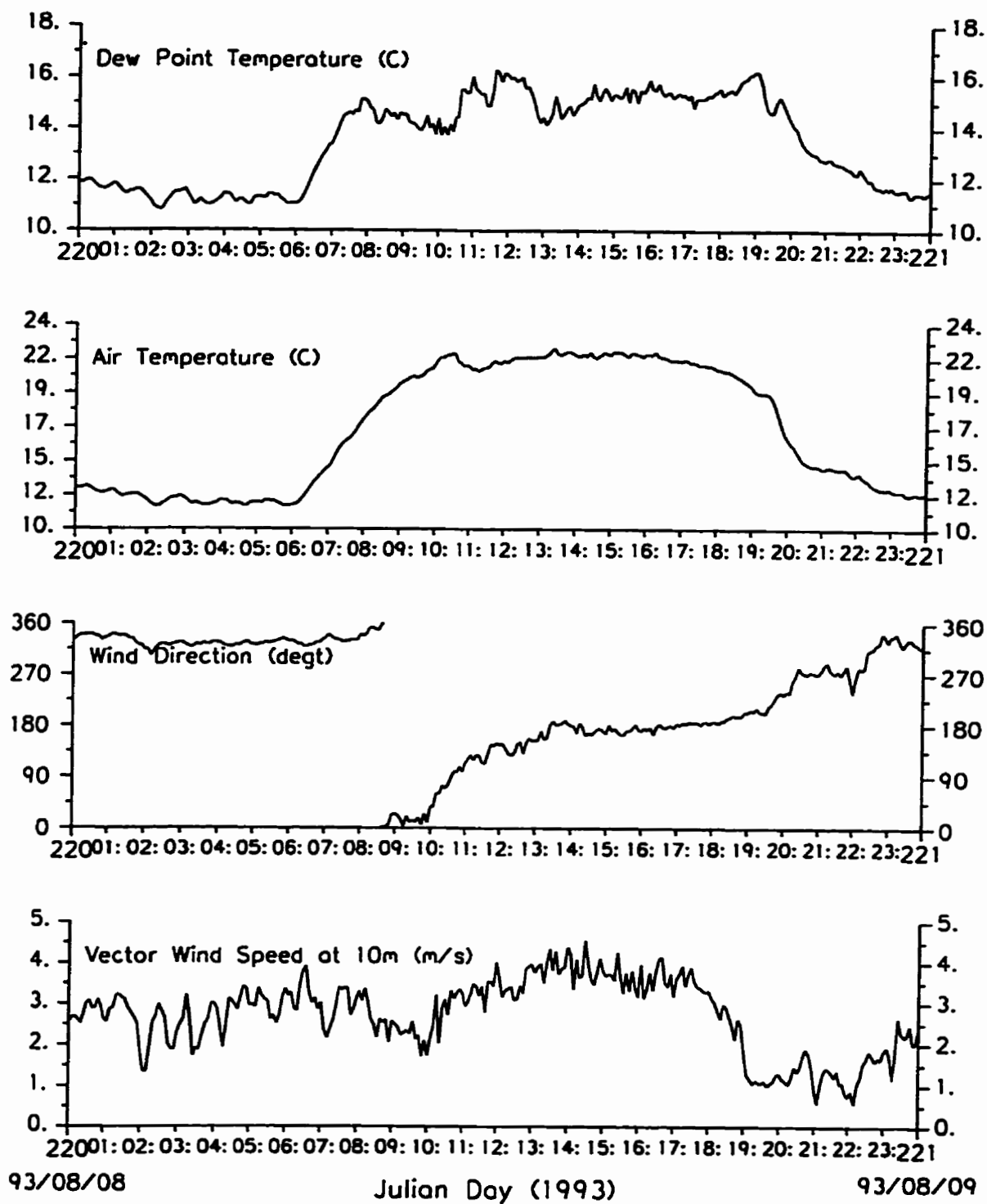


Figure 2.7. Plot of time series data from the Morpeth station on August 8, 1993. The arrival of the Lake Erie lake breeze is evident between 10 LST and 11 LST.

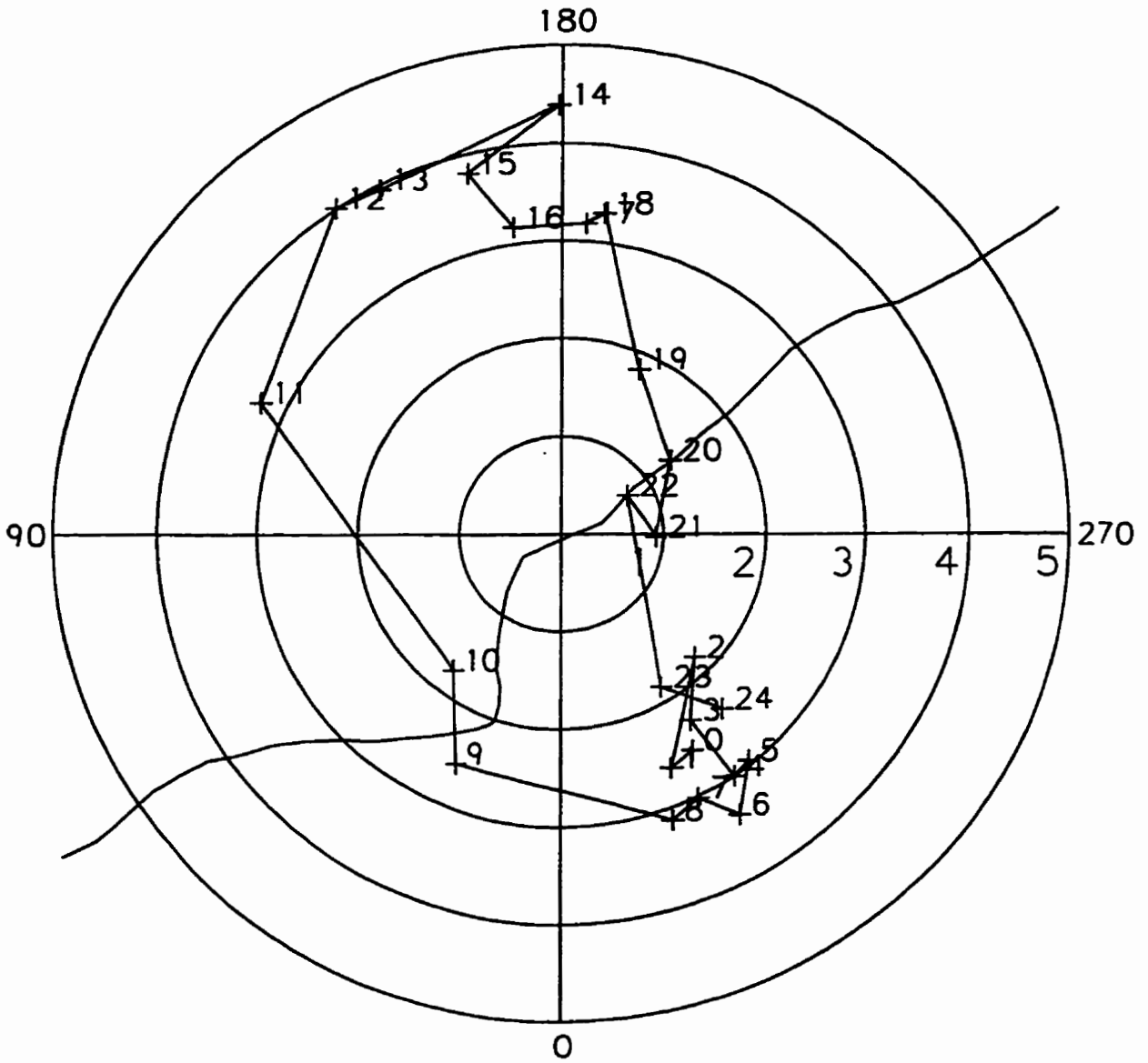


Figure 2.8. Wind hodograph showing the clockwise diurnal rotation at the Morpeth station on August 8, 1993. Wind contours are at intervals of 1 knot, wind directions are labelled along the outside of the hodograph and points are labelled with the time in LST.

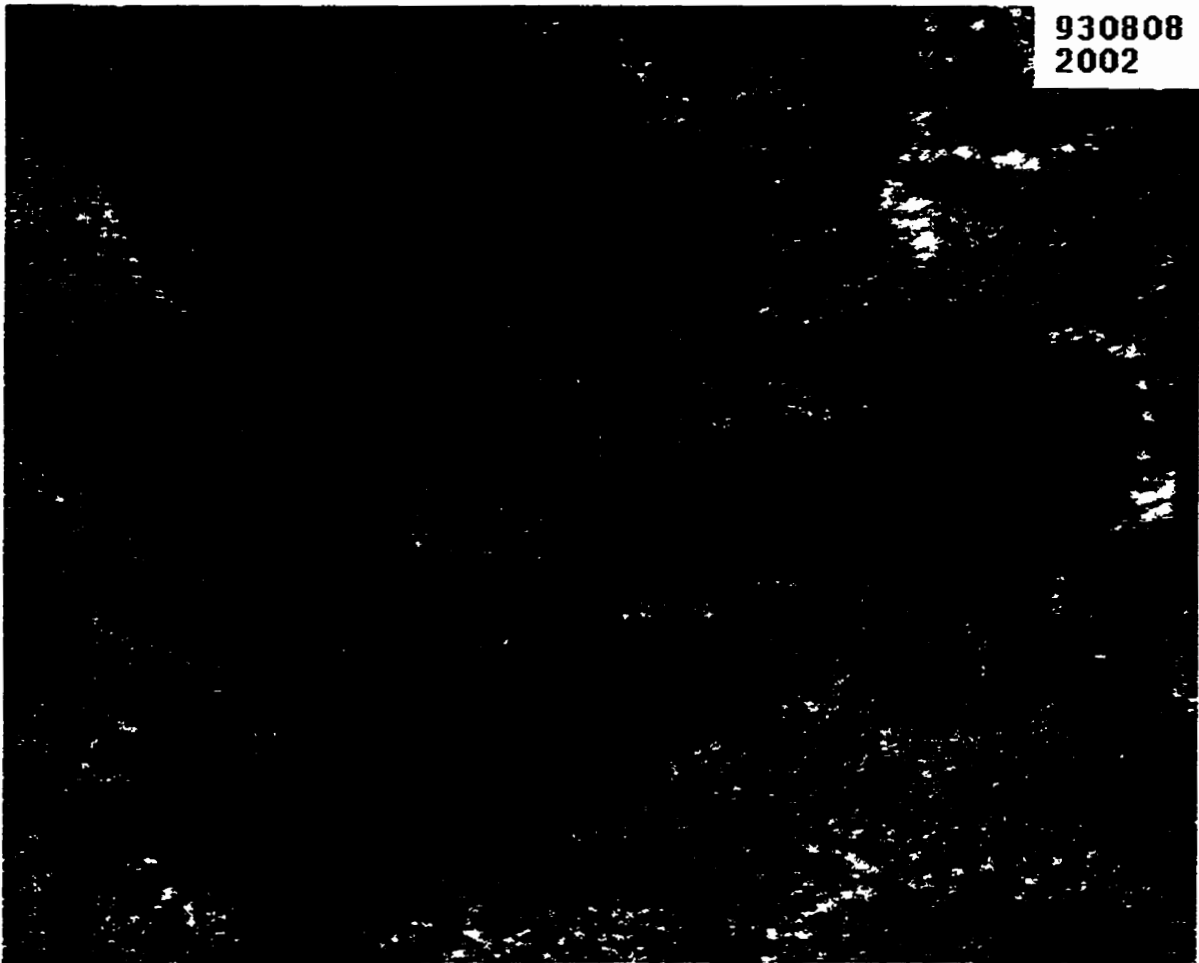


Figure 2.9. Remapped GOES-7 visible satellite image valid at 15:02 LST on August 8, 1993. The approximate positions of the lake breeze fronts are delineated by the boundaries between clear skies and cumuliform clouds. Larger cumuli are present along fronts in several areas.

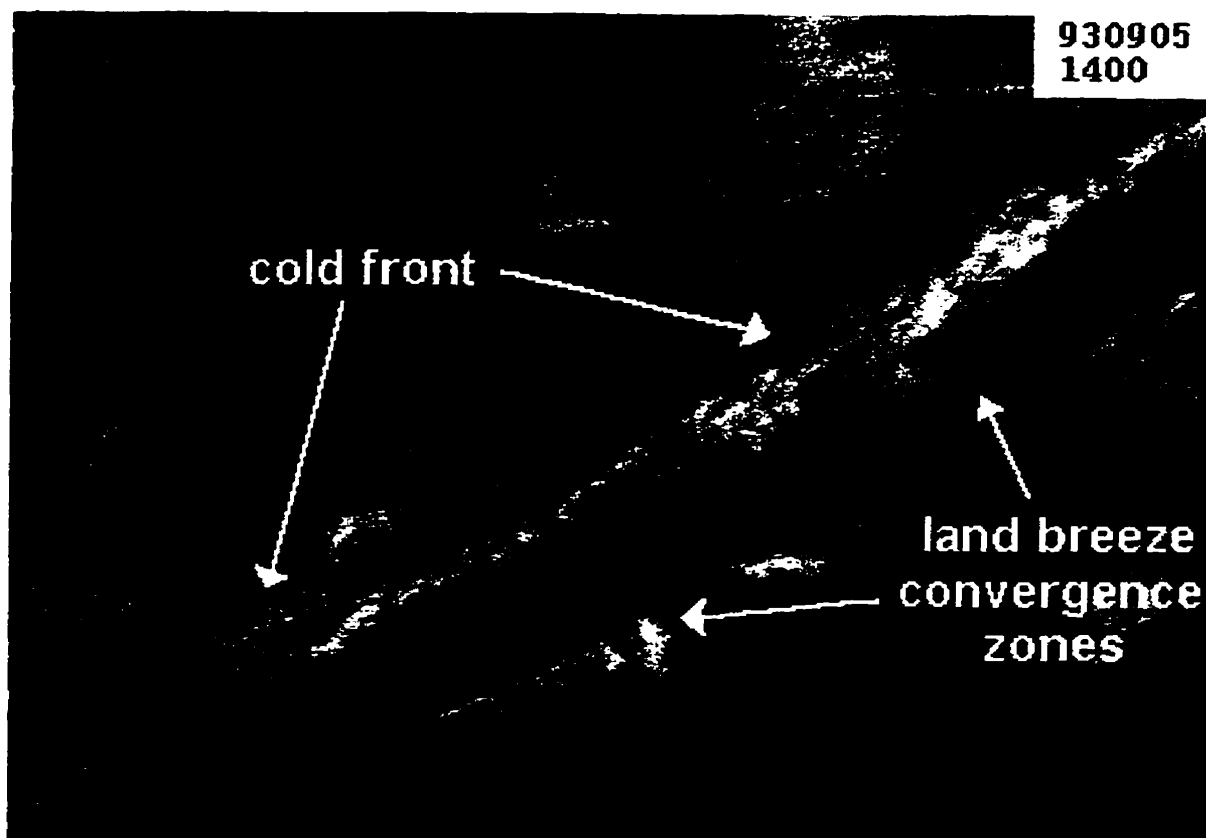


Figure 2.10. Remapped GOES-7 visible satellite image valid at 09 LST on September 5, 1993. A cold front extending across southern Ontario is labelled. Land breeze convergence lines are evident over Lake Erie and Lake Ontario and are also labelled. Deep, moist convection is forming along the eastern portion of the Lake Erie convergence line.

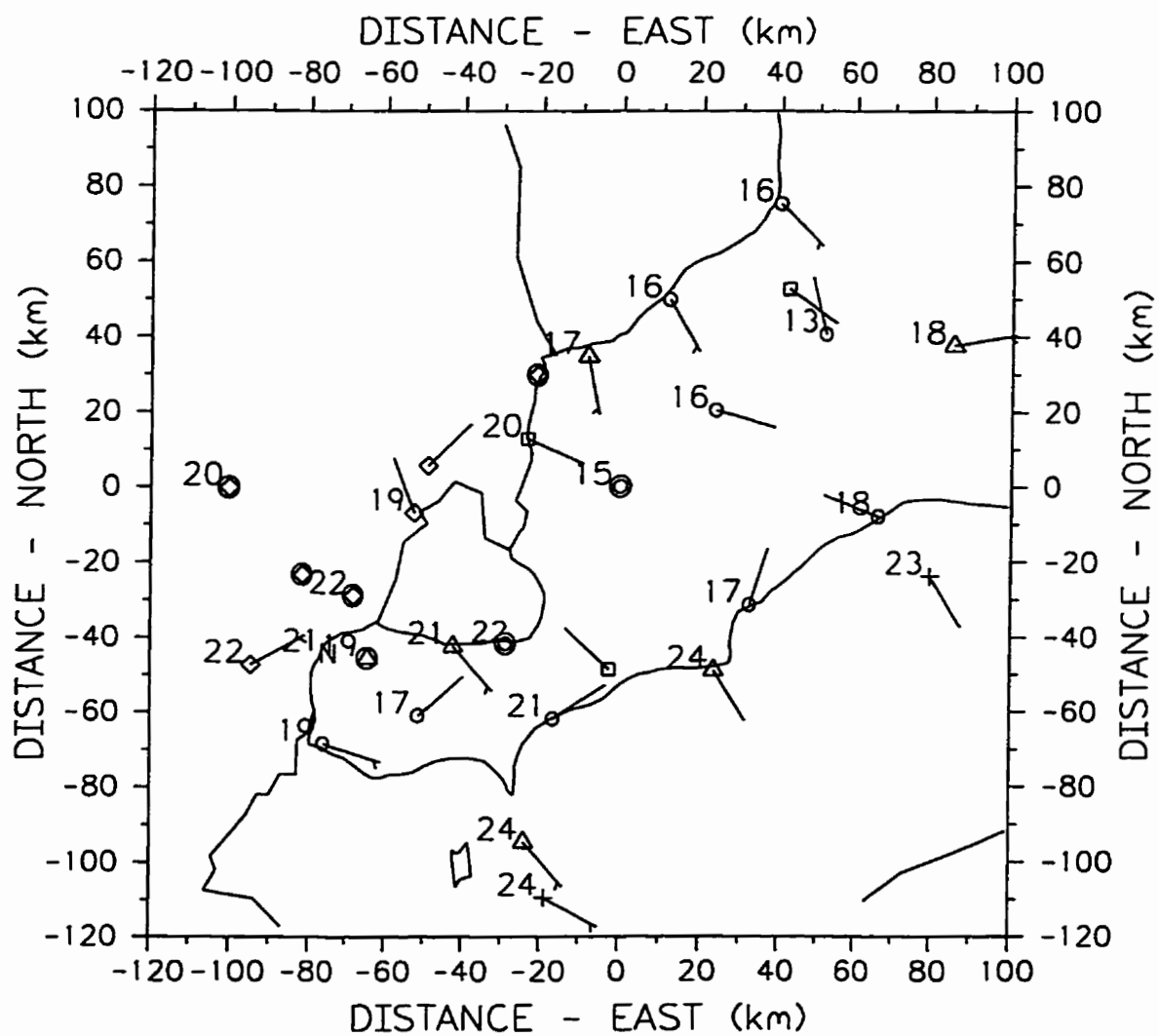


Figure 2.11. Plot of surface station data on August 26, 1993 at 05 LST showing offshore flow on the shores of each of the lakes. A land breeze convergence is implied along the north shore of Lake Erie.

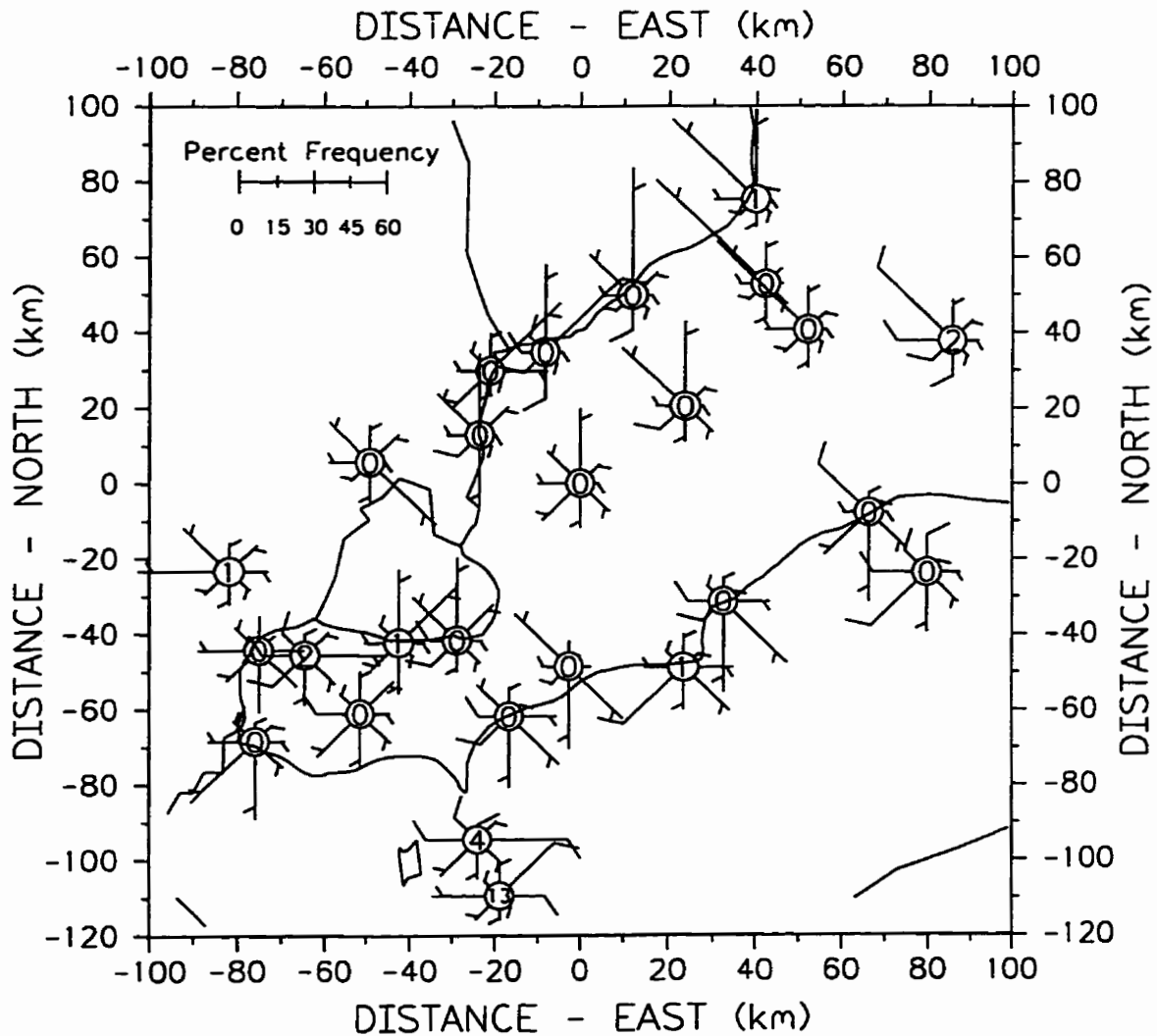


Figure 2.12a. Wind rose plot showing mean wind speed and direction frequencies between the hours of 12 LST and 18 LST for days with lake breezes on all lakeshores. The length of each 'petal' on a wind rose corresponds to the mean frequency of the wind from that octant. The frequency scale is shown in percent at the top left corner. The scale is the same for each plot for ease of comparison. Mean wind speeds are shown as barbs on the petals with short barbs representing 3-7 knots and long barbs representing 8-12 knots. The absence of a barb on a petal indicates a mean wind speed between calm and 3 knots. The frequency of calms is shown in percent inside the station marker.

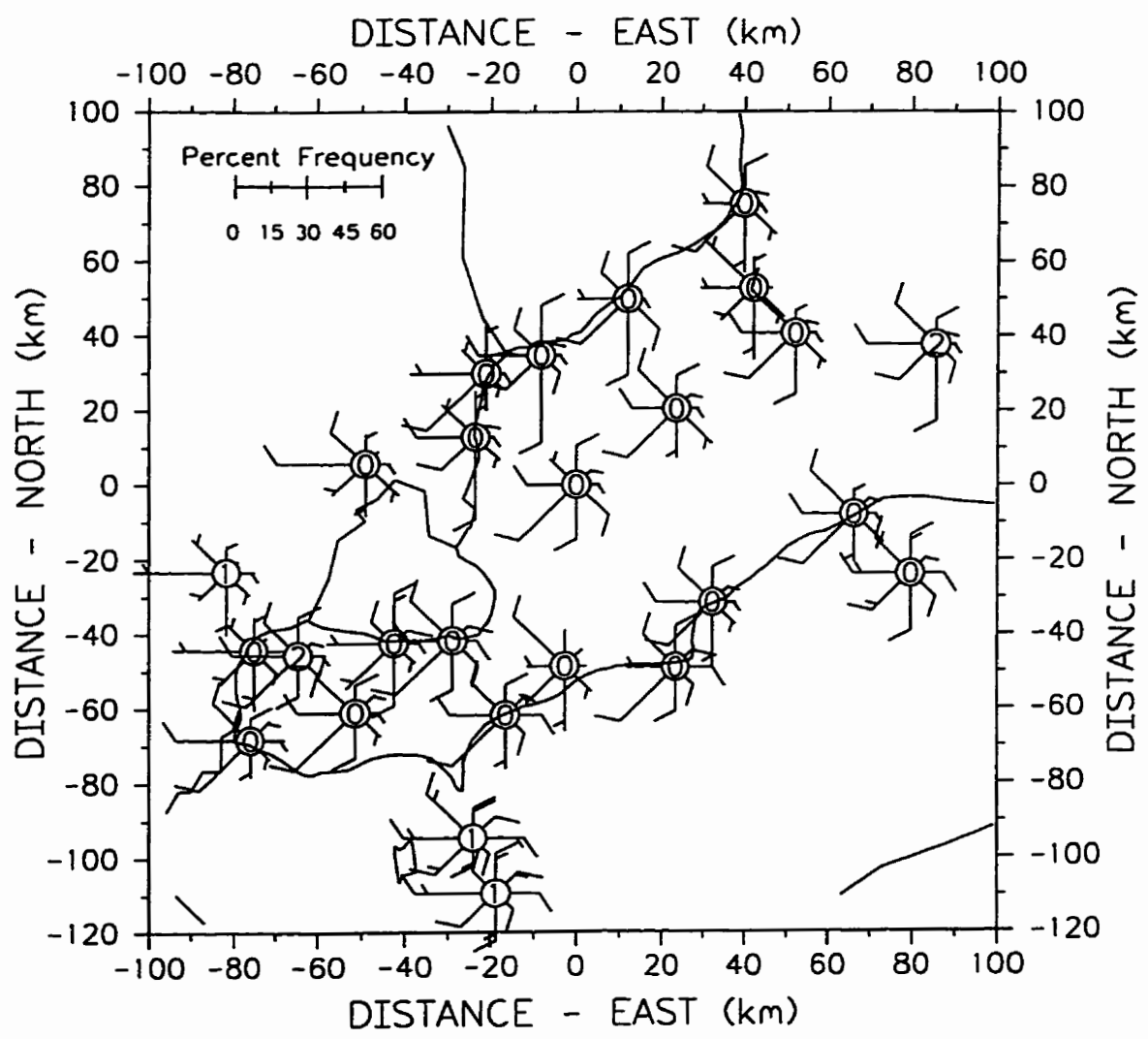


Figure 2.12b. As in Figure 2.12a, except for days with no lake breezes.

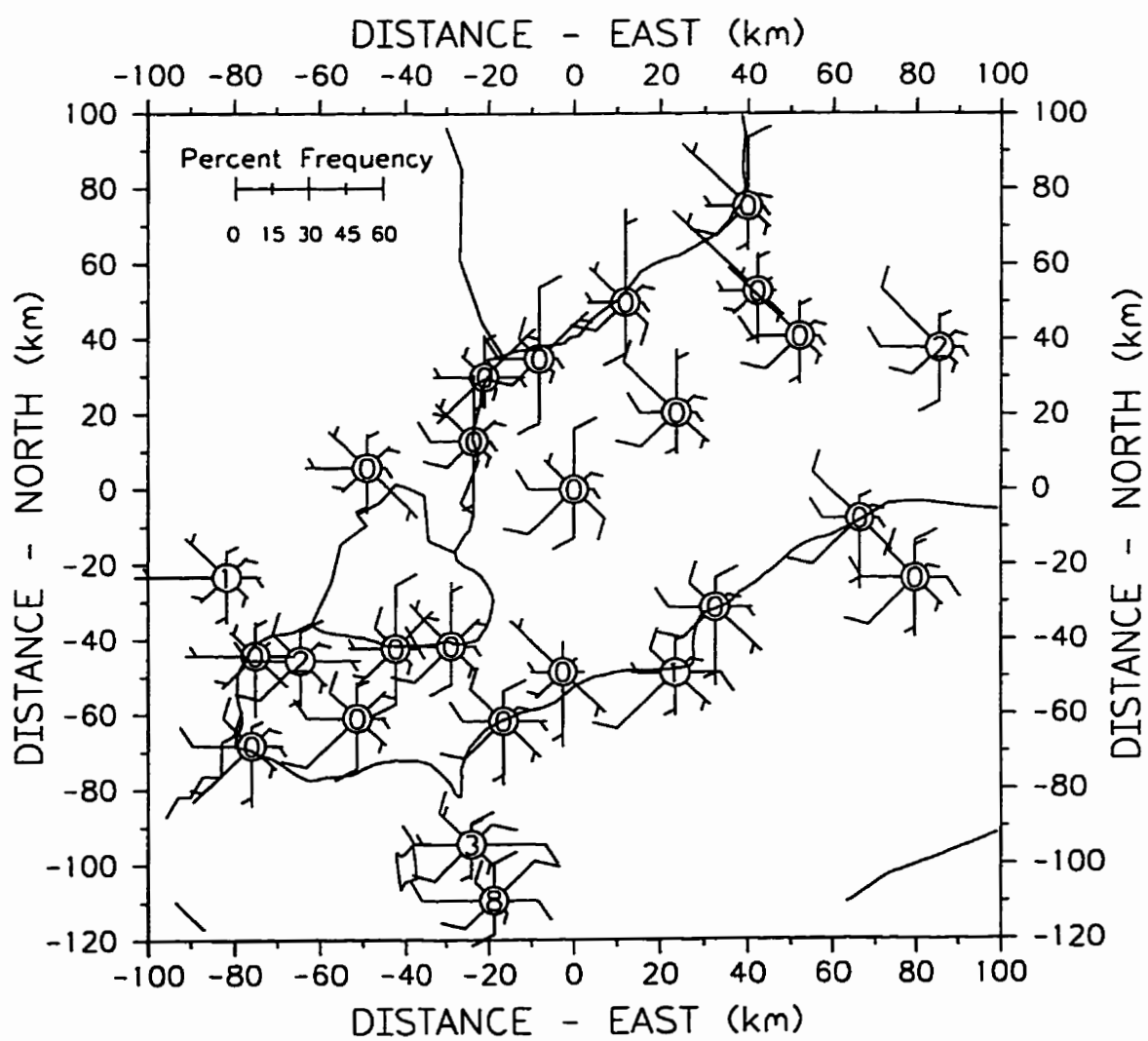


Figure 2.12c. As in Figure 2.12a, except for all study days.

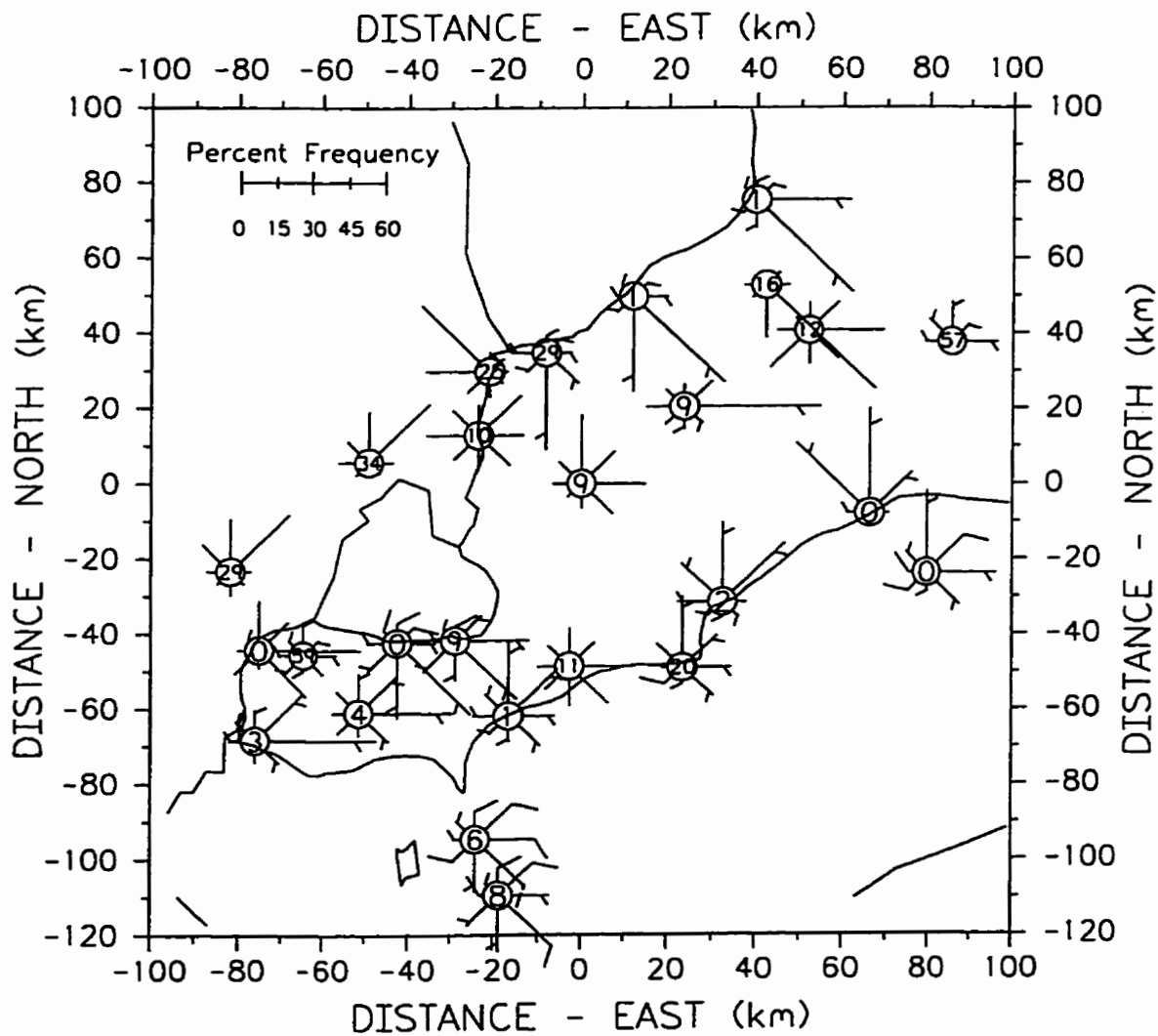


Figure 2.13a. Wind rose plot showing average wind speed (in knots) and direction frequencies between the hours of 00 LST and 06 LST for nights with land breezes on all lakeshores. The format is the same as that described for Figure 2.12.

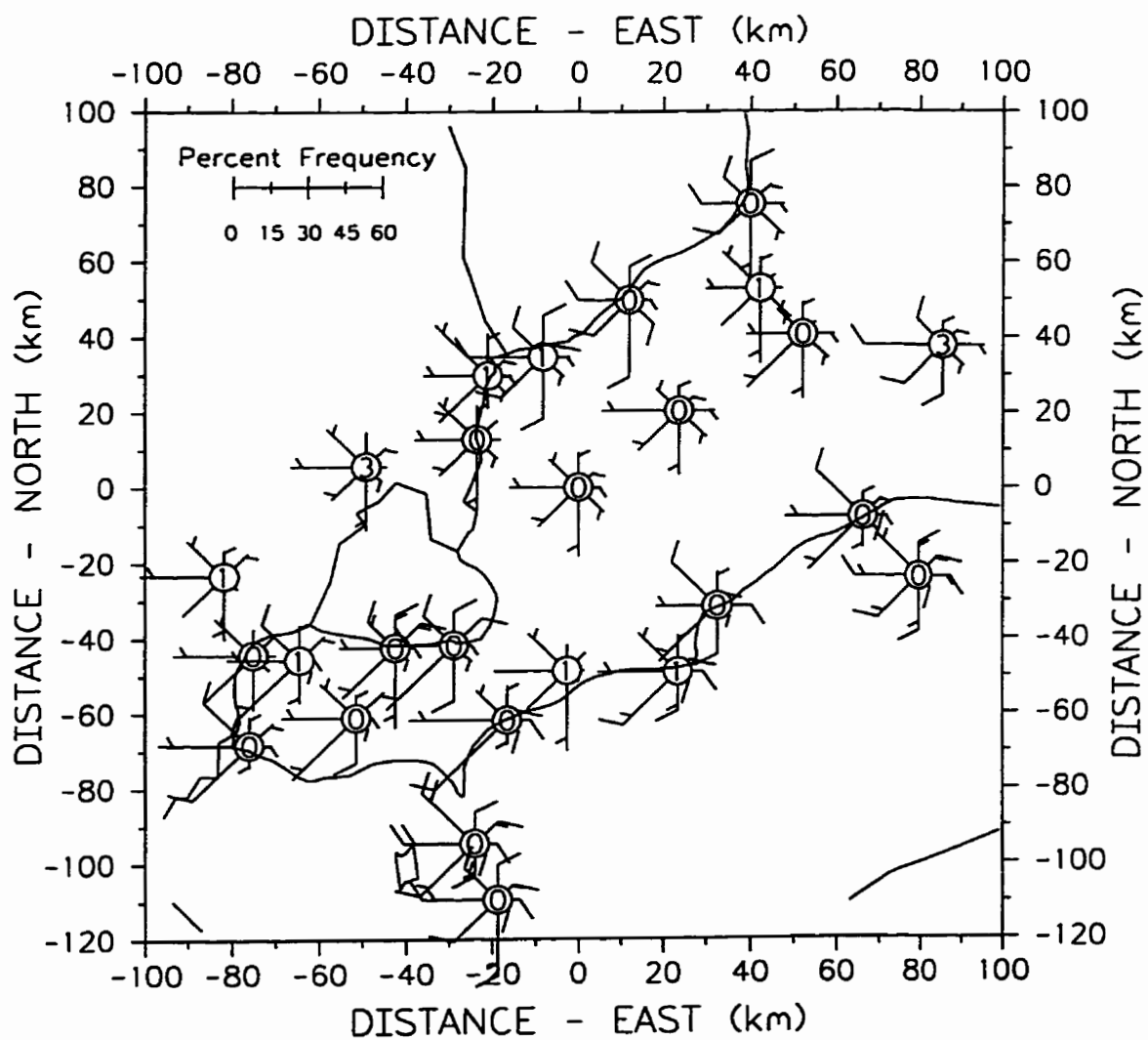


Figure 2.13b. As in Figure 2.13a, except for nights with no land breezes.

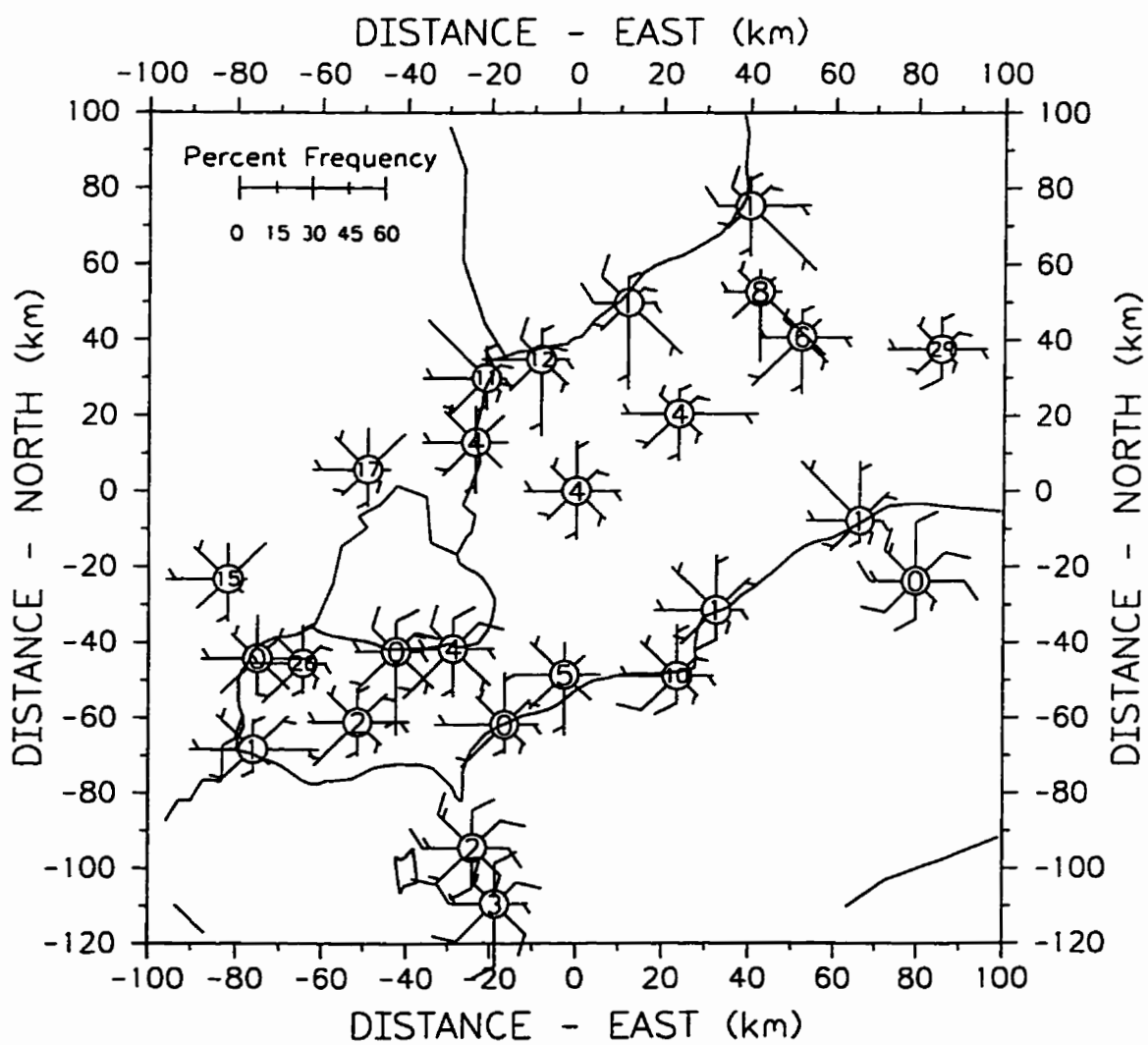


Figure 2.13c. As in Figure 2.13a, except for all study nights.

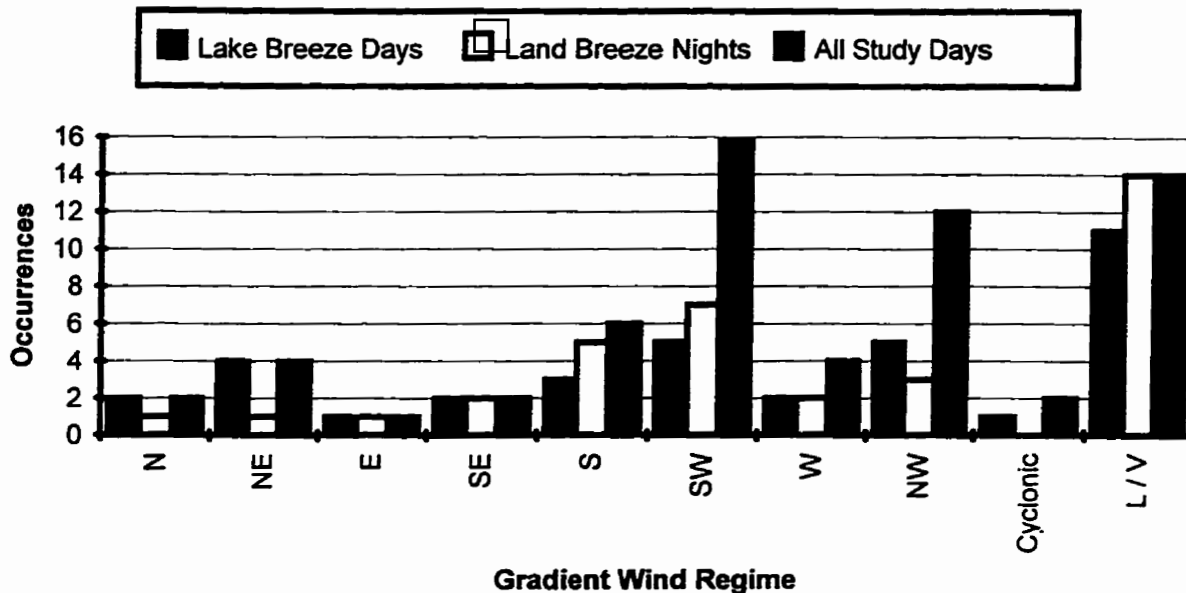


Figure 2.14. Bar graph showing the frequency of different gradient wind regimes and lake and land breeze occurrences (breeze on any shore) associated with each regime. Gradient winds were determined by analyzing 12 UTC mean sea level pressure patterns as depicted on NWS and AES surface analyses.

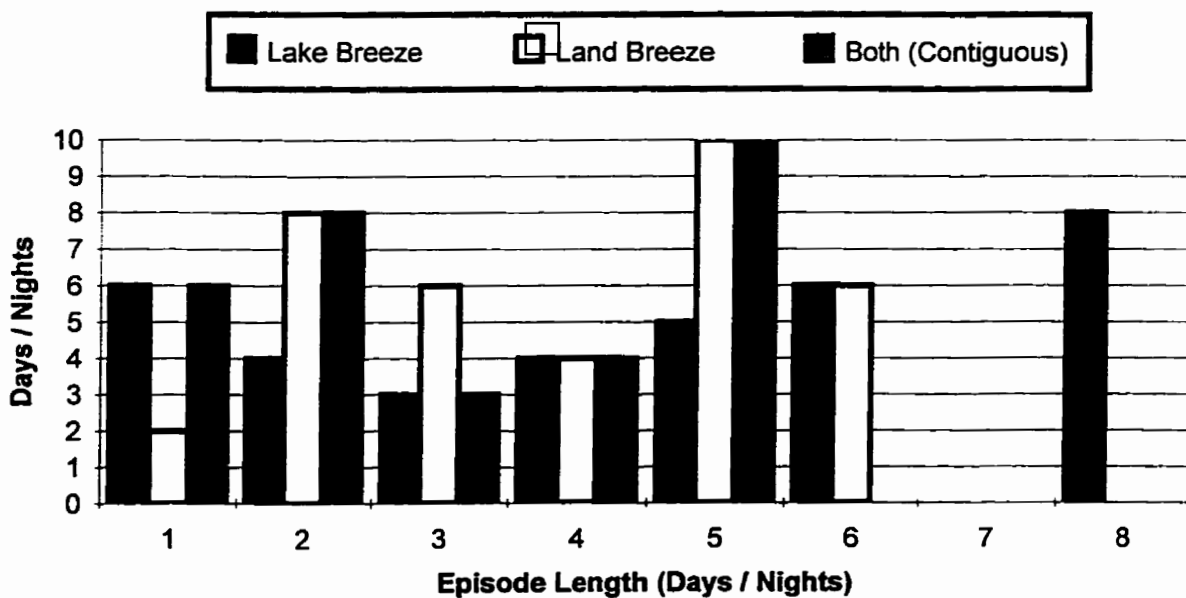


Figure 2.15. Bar graph showing lake and land breeze episode characteristics. Lake and land breeze occurrences include day / nights with breezes on any shore.

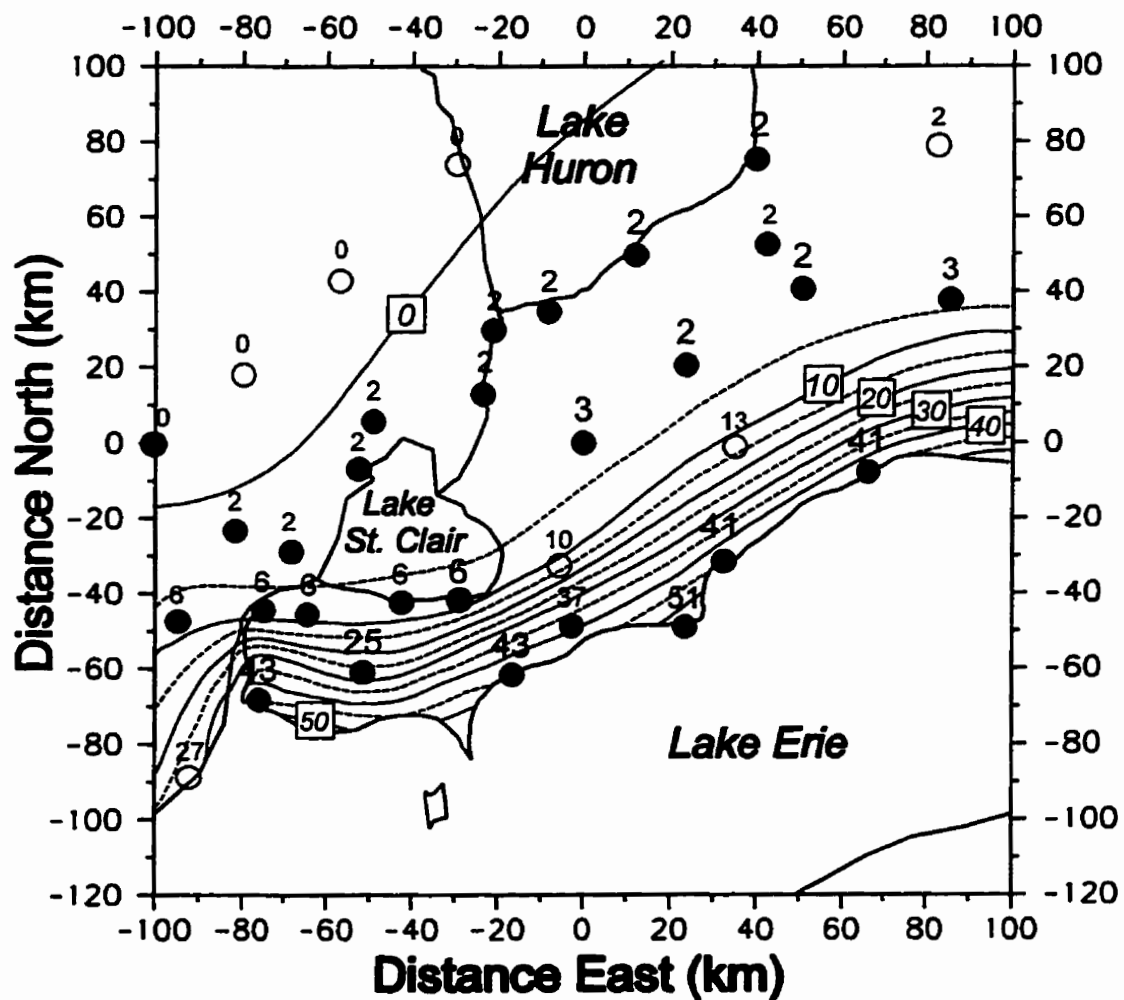


Figure 2.16a. Map showing the occurrence frequencies of the Lake Erie lake breeze. Station values are shown with the font size indicating the relative degree of confidence in the value. Stations with open circles are 'virtual stations' used as guide points for the contouring. The contour interval is 5% and solid contours are labelled.

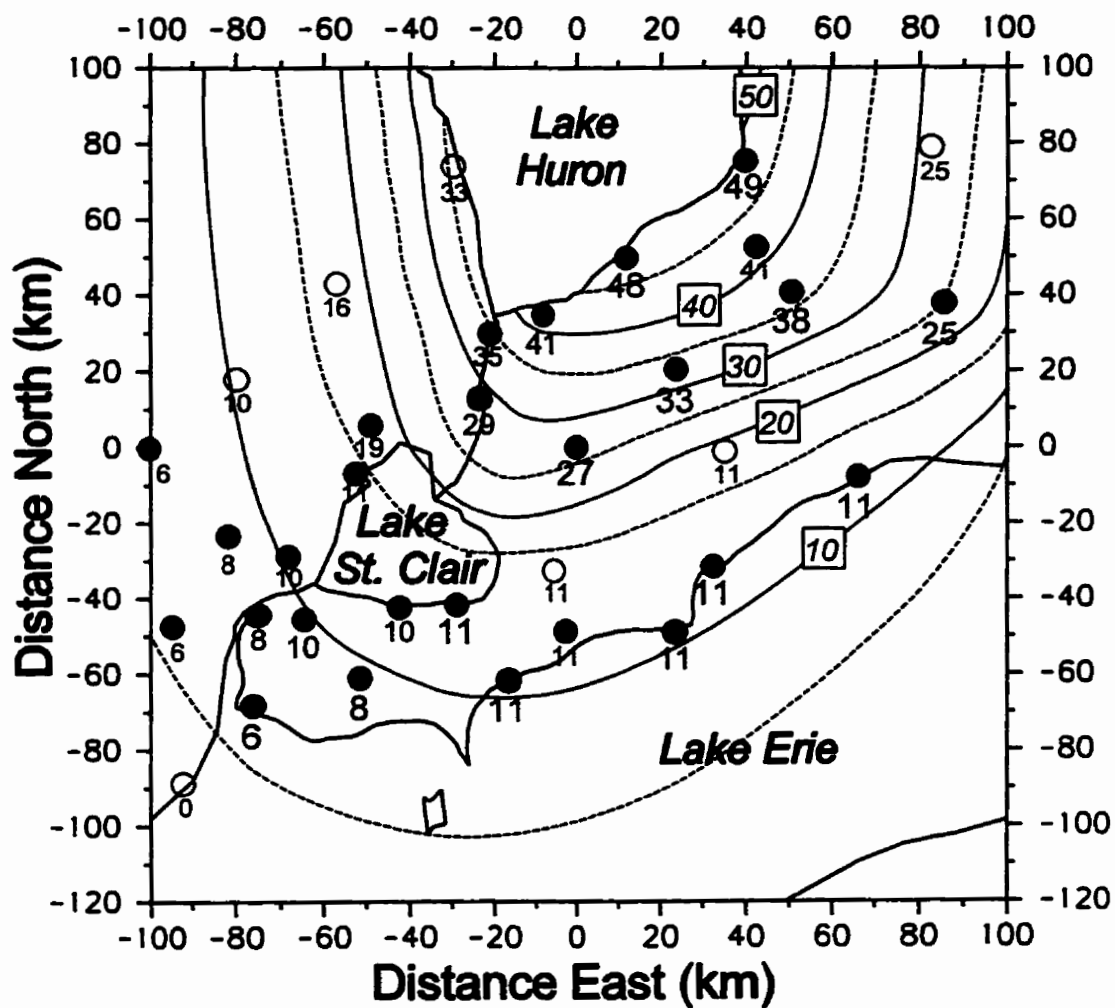


Figure 2.16b. As in Figure 2.16a, except for showing the occurrence frequencies of the Lake Huron lake breeze.

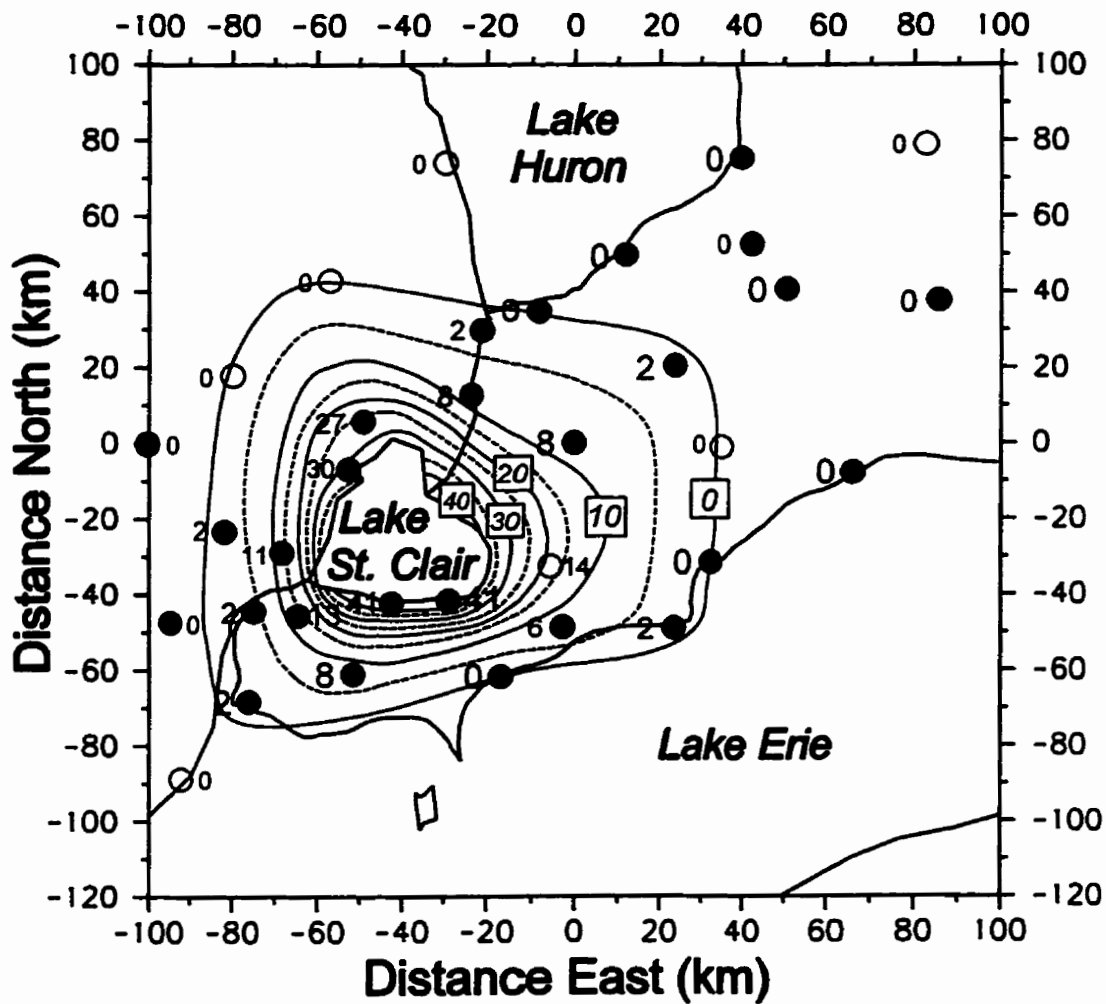


Figure 2.16c. As in Figure 2.16a, except for showing the occurrence frequencies of the Lake St. Clair lake breeze.

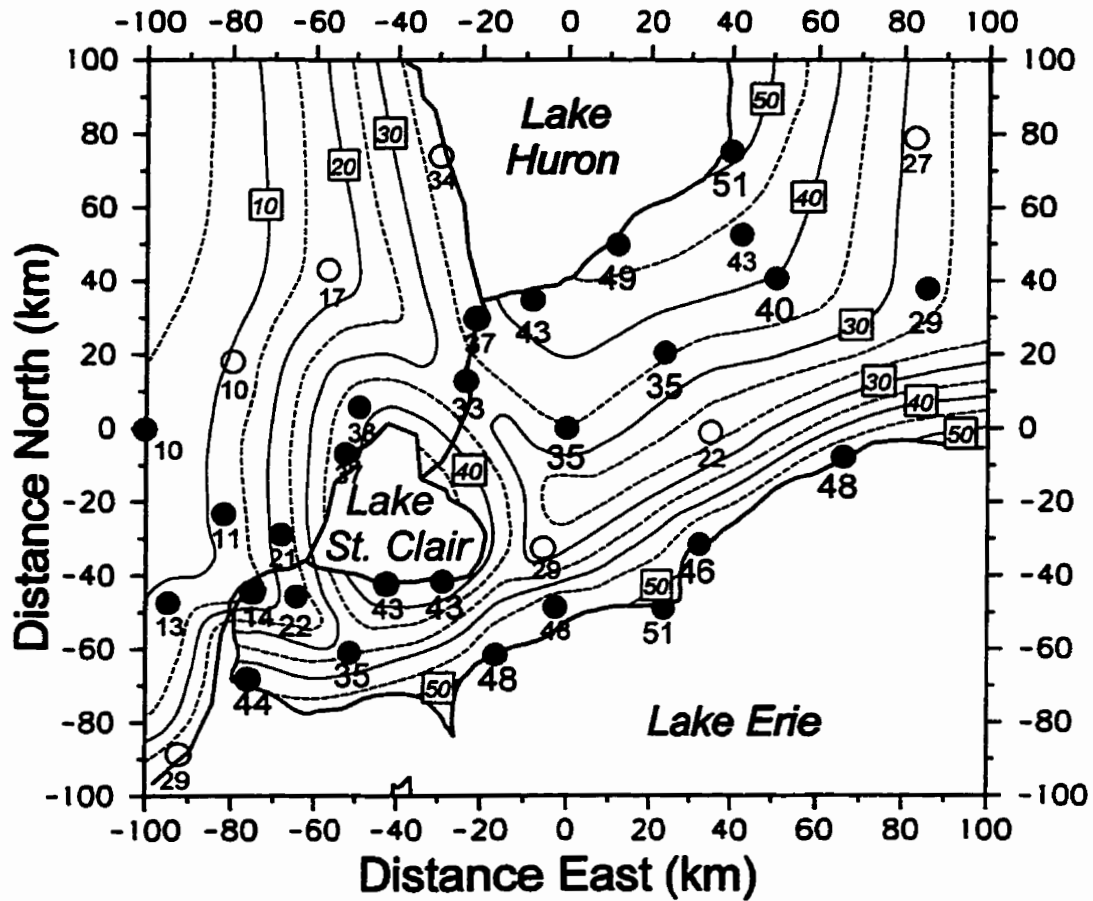


Figure 2.17. Map showing the occurrence frequency of lake breezes from any lake at stations in the study region. Labelling conventions are the same as those used in Figure 2.16. If a station experienced more than one lake breeze passage in a day, only one is counted.

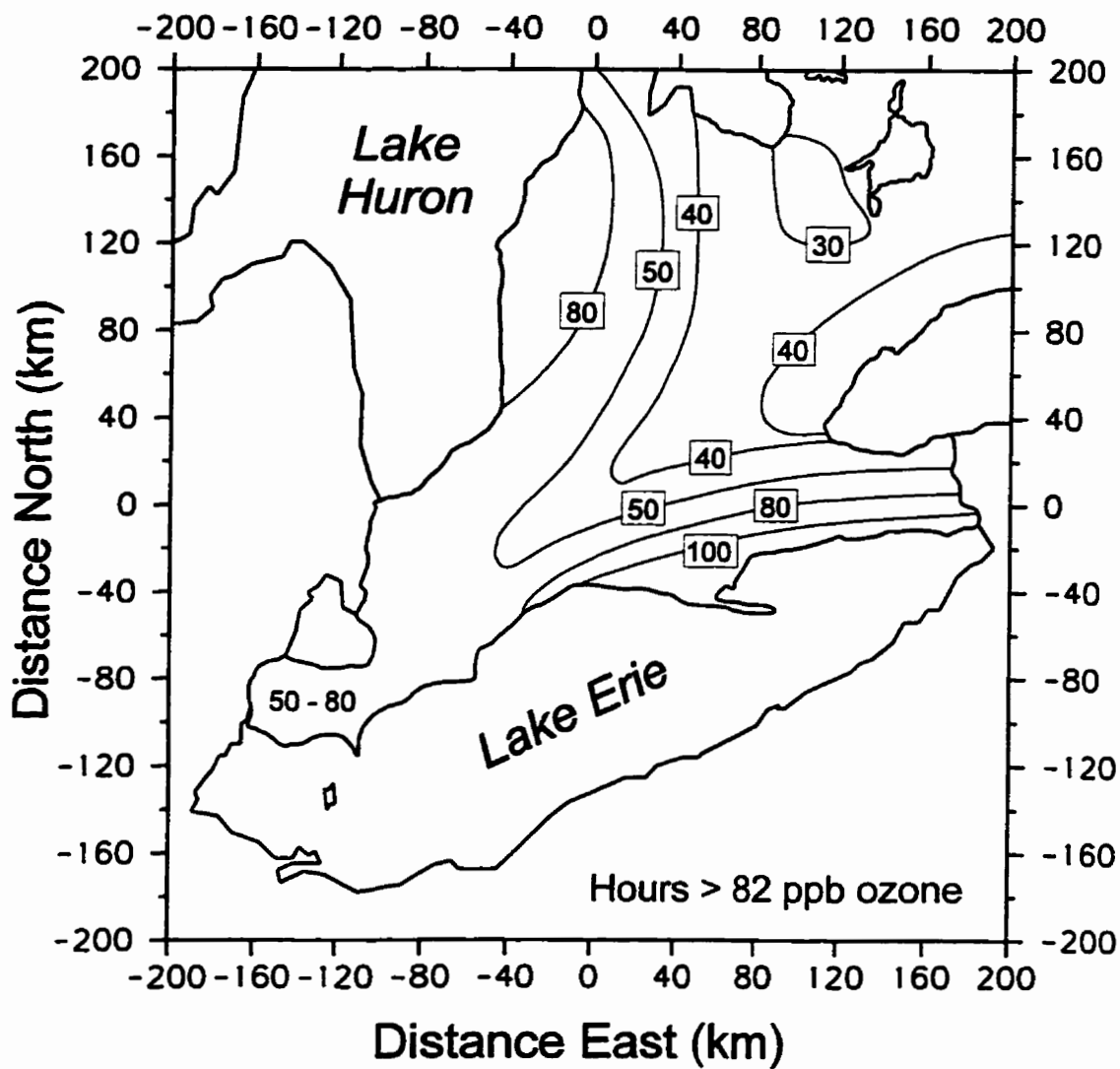


Figure 2.18. Map showing the number of hours of hourly-averaged ground-level ozone exceedances of the Canadian federal 82 ppb one-hour ozone criterion. (After Fuentes and Dann, 1994.)

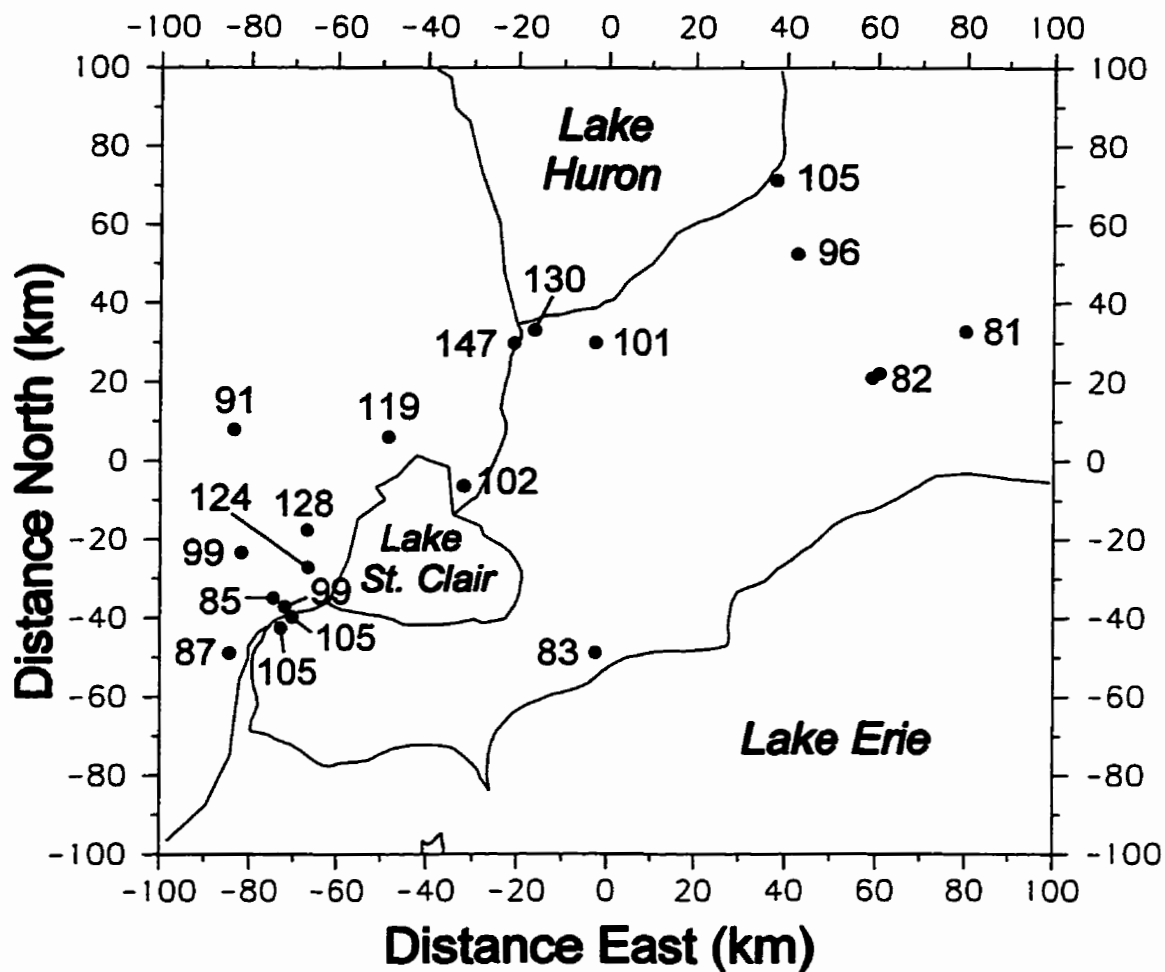


Figure 2.19. Map showing the maximum observed hourly-averaged ground-level ozone concentration during the study period at each station in the study region. The highest value was recorded at the Port Huron station while the lowest value was recorded at the London station.

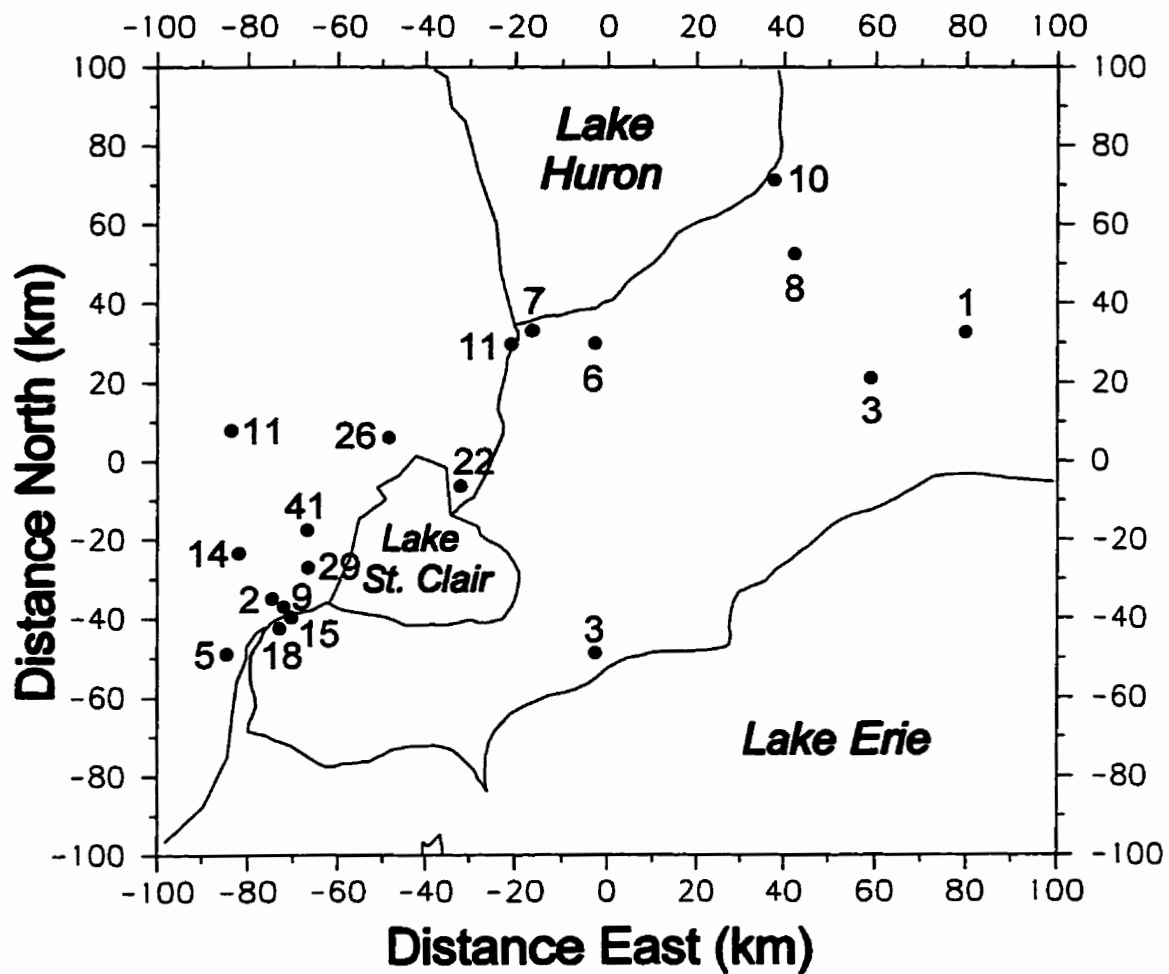


Figure 2.20. Map showing the number of hours of hourly-averaged ground-level ozone exceedances of the Ontario provincial 80 ppb one-hour ozone criterion during the SOMOS study period. The greatest number was reported at the Warren station while the lowest number was reported at the London station.

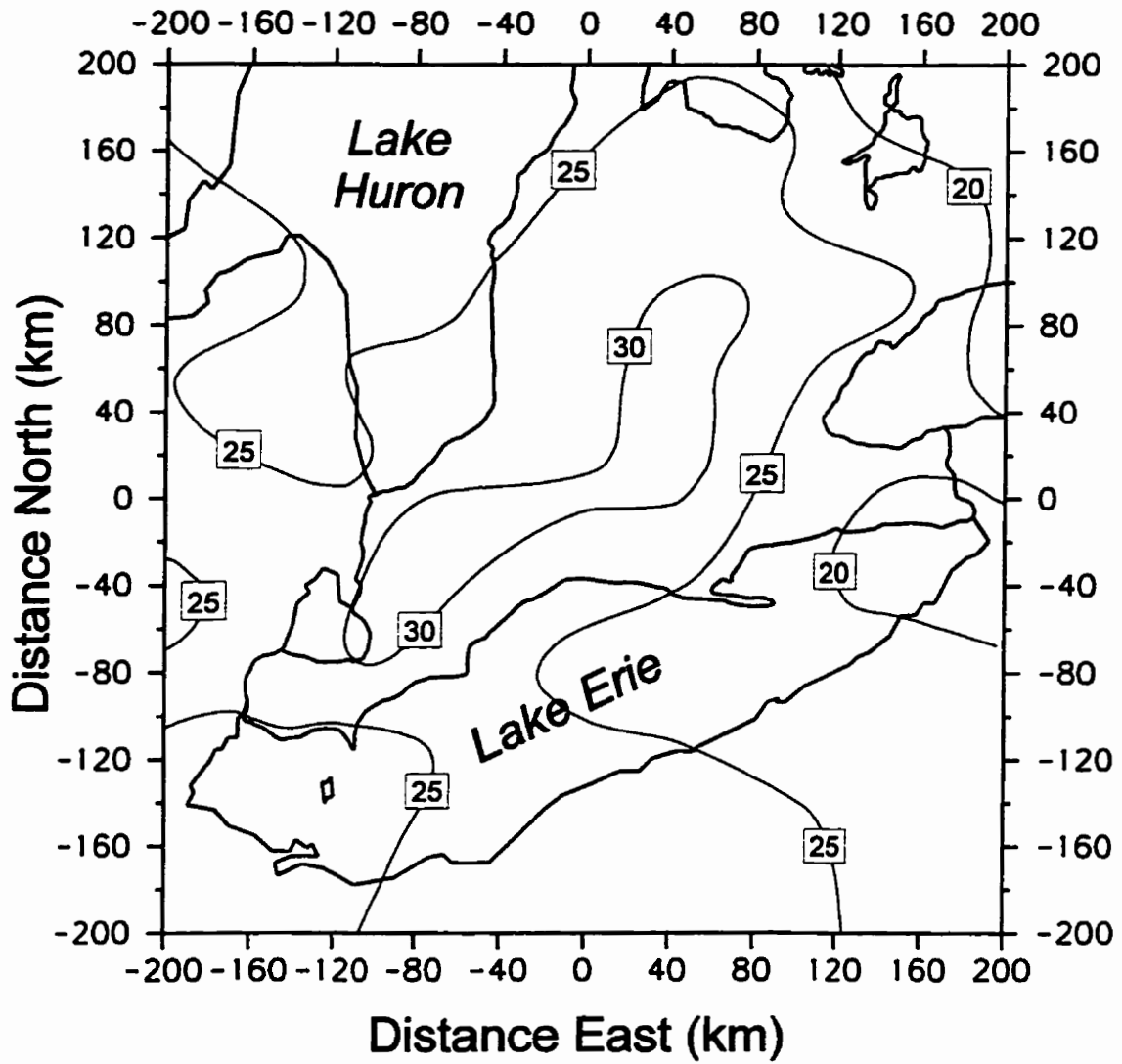


Figure 2.21. Map showing annually-averaged lightning day count for southern Ontario. A contour interval of 5 days is used. Data are from the warm seasons of 1989-1991. (After Clodman and Chisholm, 1996.)

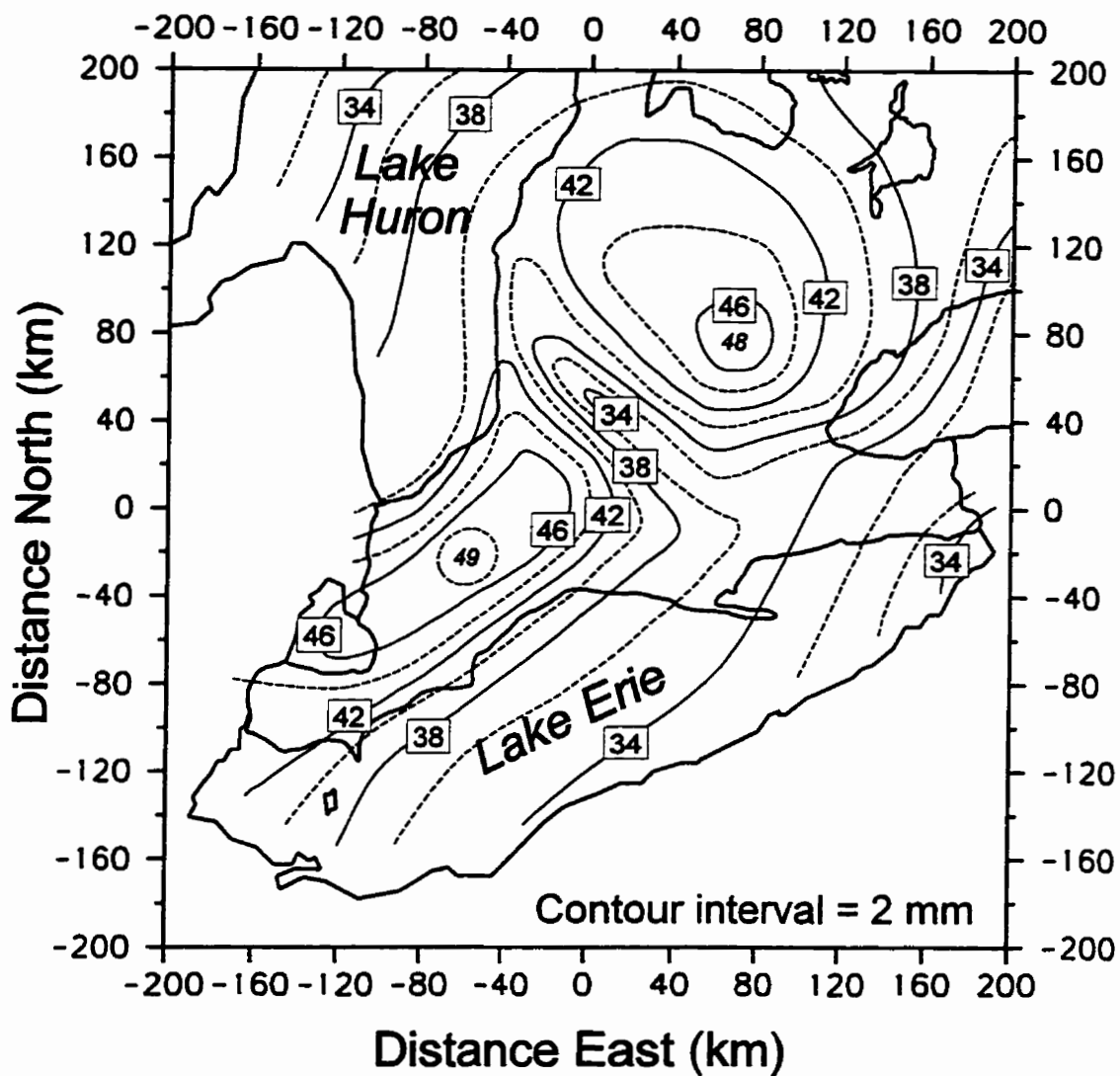


Figure 2.22. Map showing the annually-averaged ten year return period, one-hour rainfall over southern Ontario. A contour interval of 2 mm is used. (Data from Hogg and Carr, 1985.)

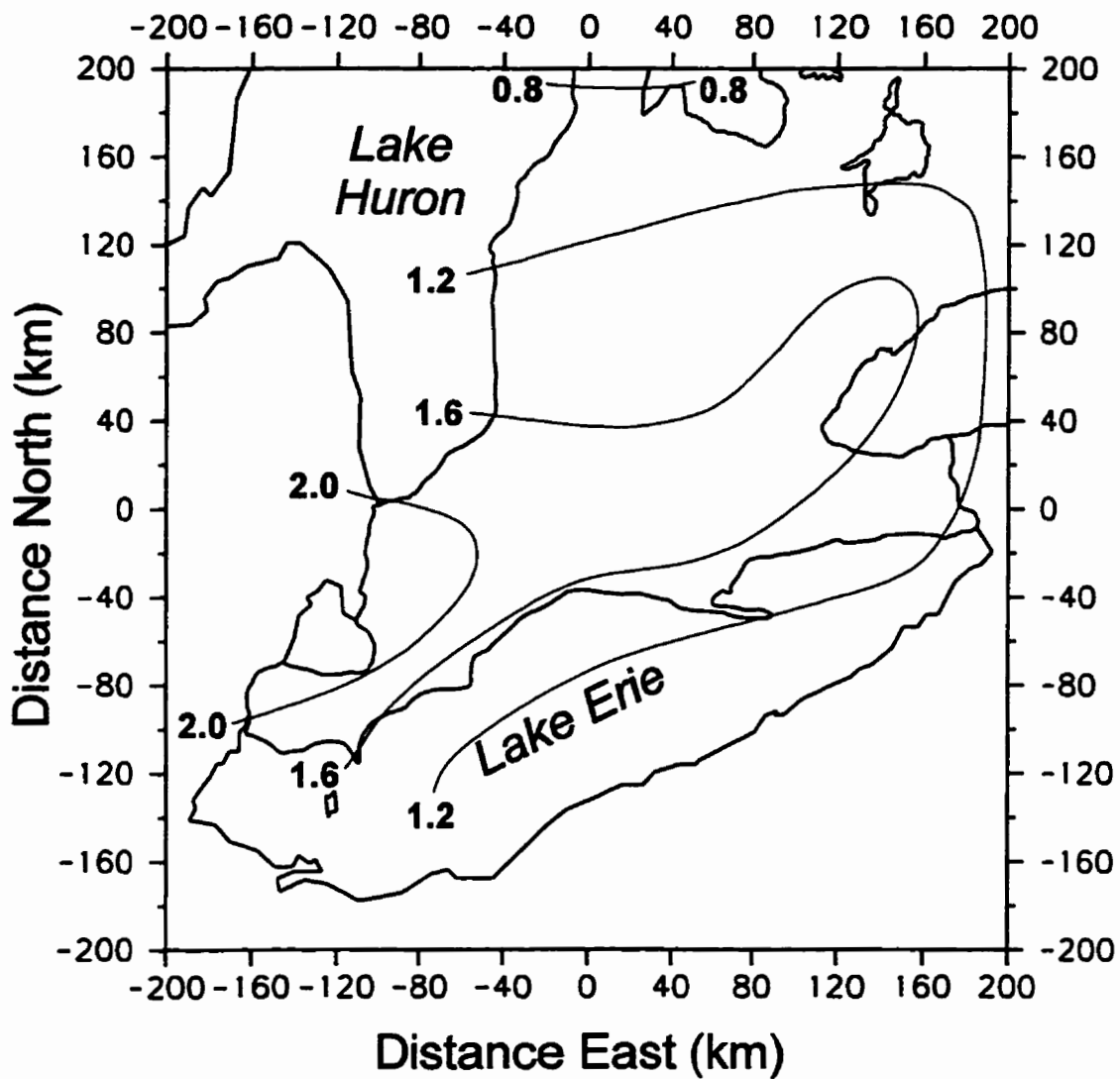


Figure 2.23. Map of average annual tornado incidence per 100² km². A contour interval of 0.4 tornadoes per 100² km² is used. (After Newark, 1984.)

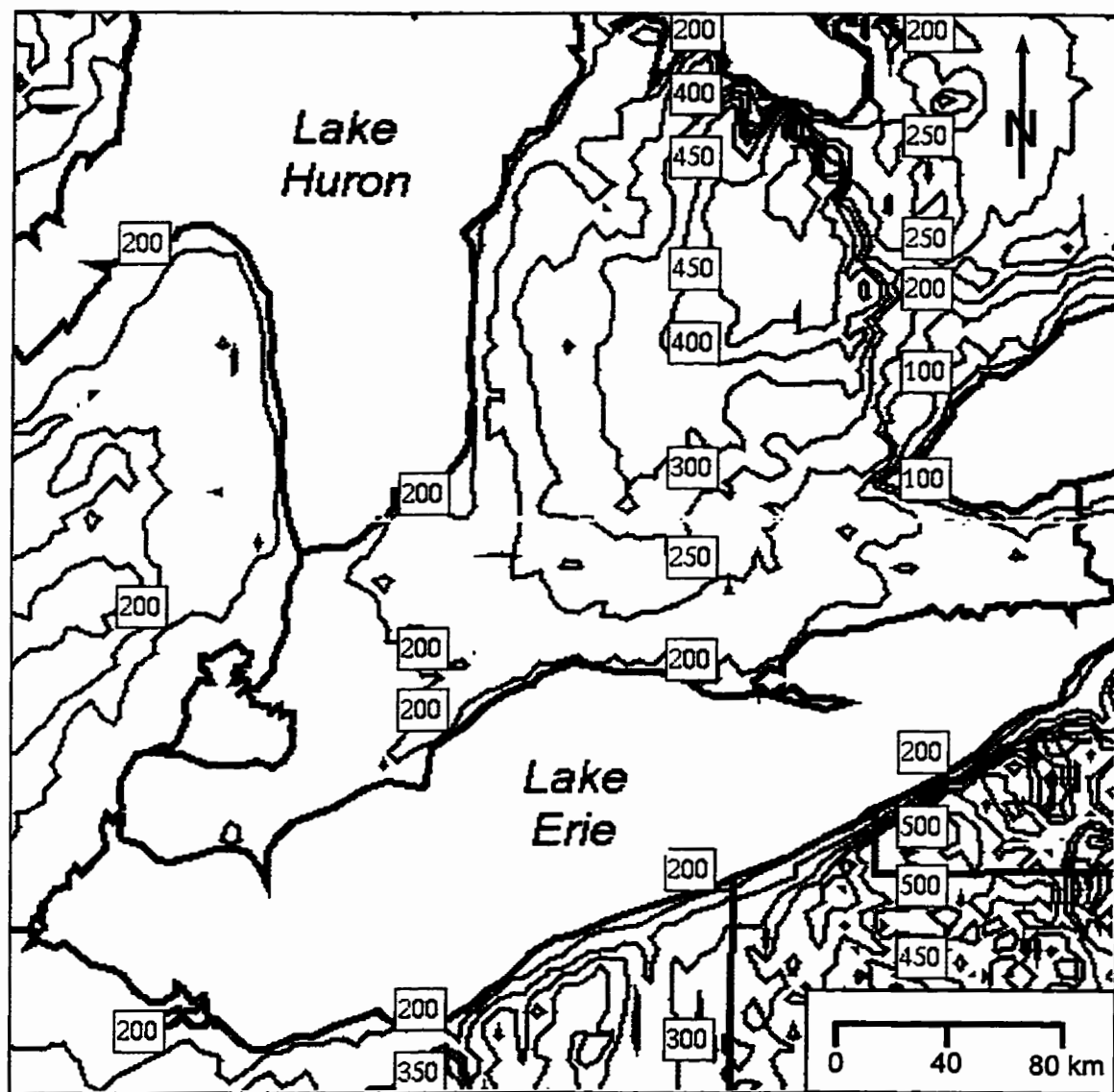


Figure 2.24. Map of the ELBOW study region and its topography. Elevations above mean sea level are in metres and the contour interval is 50 m.

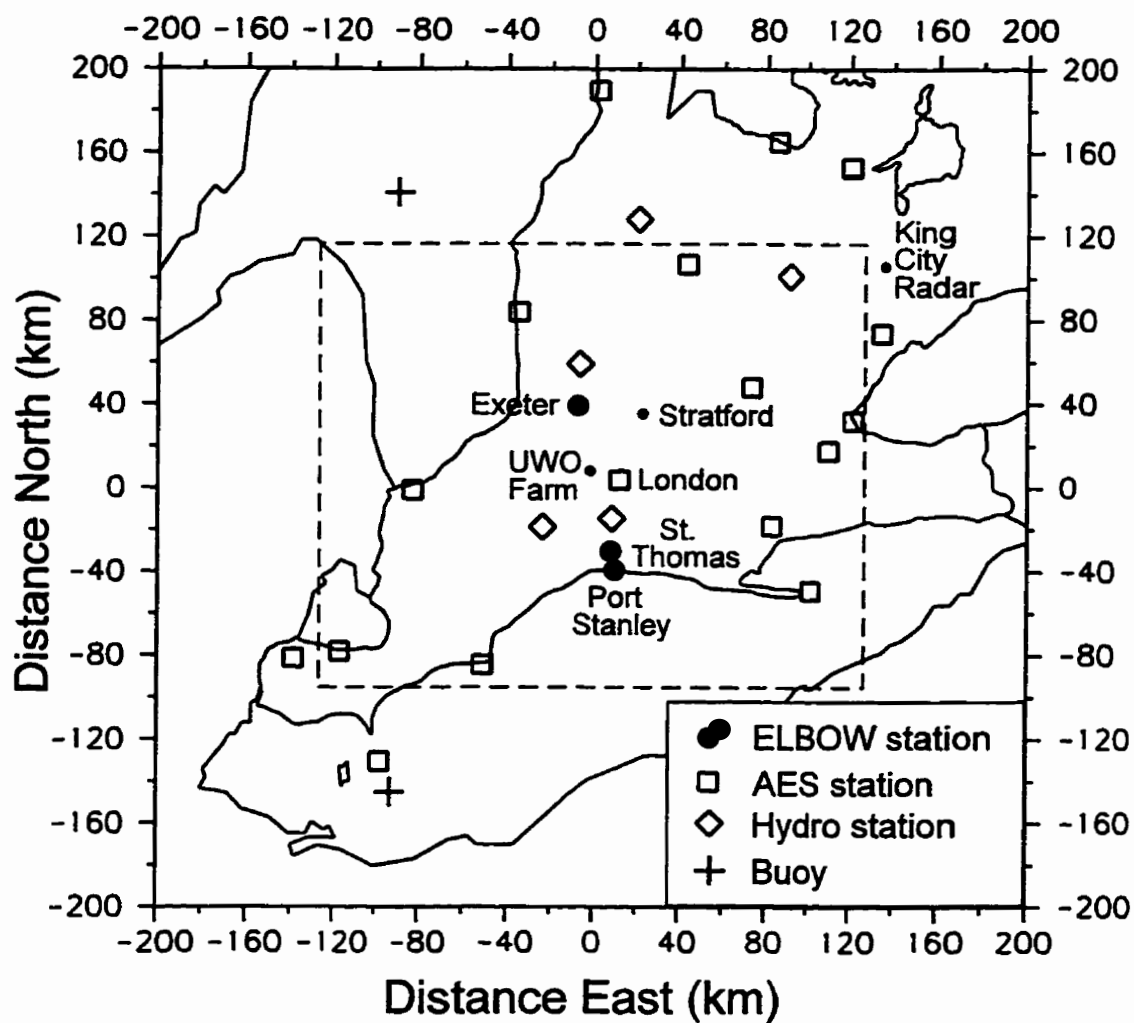


Figure 2.25. Map showing the locations of the ELBOW special surface stations and surface stations operated by AES and Ontario Hydro. Buoy locations are also shown. Stratford and the location of the UWO farm site are shown for reference. The main area of interest for the ELBOW project is enclosed by the dashed lines.

CHAPTER THREE - NUMERICAL MODELLING AND DISCUSSION

3.1 A Brief History of Lake and Land Breeze Modelling

The history of the numerical modelling of lake and land breezes begins with early theoretical studies of sea and land breezes. Much of the early work in this area has been summarized by Atkinson (1981) which provides the basis for this discussion up to the late 1970's. One of the first attempts at a quantitative theory of sea and land breezes was made by Jeffreys (1922). Using a simple dimensional analysis, Jeffreys found that sea and land breezes were examples of a type of wind that resulted from the balance between the pressure gradient force and viscous forces and gave reasonable first-order approximations of the magnitude of inflow and return flow winds. During the late 1940's and early 1950's, illuminating analytical investigations of sea and land breezes were carried out by Haurwitz (1947), Schmidt (1947) and Defant (1950) using linearized forms of the equations of motion. Though non-linear processes such as the development of the sea breeze front could not be resolved, these studies quantitatively elucidated relationships between sea and land breezes and external factors such as the land-sea temperature difference, the gradient flow, the Coriolis force, and friction. With the advent of computer technology in the 1950's, the non-linear equations of motion could be solved by numerical methods using equations written in discrete or finite-difference form. Pearce (1955) was one of the first researchers to use this new technology to predict a sea breeze circulation with two-dimensional, non-linear equations along a vertical cross-section

normal to the shore. Studies by Fisher (1961), Estoque (1961, 1962) and others proceeded in a similar vein while continuing to improve the accuracy with which the numerical models simulated the fundamental processes affecting sea and land breezes.

A study by Moroz (1967) investigating the lake breeze on the eastern shore of Lake Michigan was, to the author's knowledge, the first use of a model to simulate a lake breeze. Moroz used the model of Estoque (1961) modified to incorporate the effects of the bounded water surface. To simulate these effects, one side of a symmetric lake breeze was modelled. Recognizing that a symmetric lake breeze should only be observed if the effects of the large-scale wind were negligible, Moroz set the large-scale wind in the model to zero at all points. At the lake centreline, horizontal velocity perturbations and lateral derivatives of pressure and potential temperature perturbations were set to zero through the integration. Lateral derivatives of the horizontal velocity perturbations had identical values on either side of the lake centreline. The model results compared reasonably well with observations though numerical instabilities associated with the boundary conditions eventually dominated the solution. Both Physick (1976) and Estoque *et al.* (1976) continued this line of investigation using two-dimensional models with a vertical cross-section normal to the shore but spanning an entire lake. The main advantage of this approach was that the large-scale wind could be non-zero since symmetry was not required. Physick used this advantage to study the lake breeze as affected by gradient winds for several different directions and also found effects produced

by the interaction of circulations on the opposite shores that are not found when modelling along a single shoreline.

During the 1970's, three-dimensional numerical models began to be used in studies of the sea breeze problem. McPherson (1970) modified the two-dimensional model of Estoque (1961) to allow three-dimensional simulations of sea breezes along a square bay. He found that the variations along the coastline led to vertical velocities that were asymmetrical about the bay and attributed the differences to changes in the balance of forces due to the changing orientation of the coastline. Pielke (1974) investigated the characteristics of sea breezes over southern Florida using a three-dimensional numerical model. He found that predicted sea breeze convergence zones closely matched the locations of observed convective clouds and radar echoes and concluded that on days without significant synoptic-scale influence, sea breeze convergence patterns had a controlling influence on the spatial and temporal characteristics of deep moist convection.

The first study to use a three-dimensional, non-linear model to simulate lake breezes (again, to the author's knowledge) was that of Estoque and Gross (1981). Their domain included all of Lake Ontario and a small part of Lake Erie. They tested the sensitivity of the Lake Ontario lake breeze to changes in the direction of the gradient wind and to the inclusion of the local topography. When the large-scale flow was directed from the south across the long axis of the lake, it was found that a broad band of easterly winds was

produced at low levels apparently in response to the strong, lake-induced pressure gradients. Also, orographic effects associated with the local topography appeared to have a strong influence on the development of the lake breeze circulation. Arritt (1987) and Savijärvi and Alestalo (1988) used two-dimensional models at high resolution to further study the factors affecting lake breeze formation. Arritt investigated the effect of the water surface temperature on the lake breeze and concluded that the modelled development of the circulation was insensitive to the lake surface temperature if the temperature was cool enough to result in a stably-stratified surface layer over the lake. Savijärvi and Alestalo conducted a systematic investigation of the effect of the large-scale wind on the development and intensity of the lake breeze.

In the 1990's, non-linear, three-dimensional numerical models have become widely available for studies of mesoscale phenomena such as sea breezes, lake breezes and land breezes. Currently available mesoscale models include the Colorado State Regional Atmospheric Modeling System (RAMS), the Penn State / NCAR MM5 model and the Canadian Mesoscale Compressible Community (MC2) model. Comer and McKendry (1993) used the Colorado State University (CSU) mesoscale model (an early, hydrostatic version of the RAMS model) to simulate the Lake Ontario lake breeze in an extension of the study carried out by Estoque and Gross (1981). The results of this investigation are similar to those of Estoque and Gross in that gradient flow normal to the major axis of the lake induces low-level winds along this axis though Comer and McKendry disagree with

Estoque and Gross as to the cause. In any case, the results indicate the importance of including the entire lake in the modelling domain. Lyons *et al.* (1995) used the RAMS model coupled with a dispersion model to simulate the three-dimensional transport of pollutants on the western coast of Lake Michigan. They found that a portion of these pollutants were recirculated within the lake breeze circulation and that three-dimensional numerical modelling is essential for the accurate prediction of these complex motions. Segal *et al.* (1997) have recently published results of an experiment using a non-hydrostatic, quasi-compressible model in two dimensions to investigate cloud clearing over and downwind of lakes during lake breezes. They find that a combination of desiccation caused by dynamically-induced subsidence and suppression of the convective boundary layer behind the lake breeze front prevents clouds from developing.

It appears there will always be room for improvement of the representation of the governing equations and the numerical methods used to drive the new class of mesoscale models. However, much of the current research is focussed on improvements to the initial and boundary condition schemes and physical parameterizations that these models use and, concurrent with greatly increased processing power, very high resolution, non-hydrostatic simulations of mesoscale phenomena.

3.2 Mesoscale Numerical Modelling with MC2

The Mesoscale Compressible Community (MC2) Model (Benoit *et al.*, 1997) was chosen

for simulations of meteorological conditions in southwestern Ontario and nearby parts of southeastern Michigan on selected SOMOS and ELBOW days when lake or land breezes were occurring. These simulations were intended to:

- 1) permit an assessment of the performance of the MC2 model under these conditions by comparing model results with observations collected during SOMOS and ELBOW, and
- 2) provide four-dimensional insight to the mesoscale processes observed during SOMOS and ELBOW.

The following briefly describes the MC2 model and its use for this investigation.

3.2.1 MC2 Model Description

MC2 is a fully compressible, non-hydrostatic model based on the model of Tanguay *et al.* (1990) and developed in Canada by researchers at Recherche en Prévision Numérique (RPN) / AES and the University of Quebec at Montréal (UQAM). The model solves a complete set of Euler equations on a limited-area Cartesian domain of the polar projection in either two or three dimensions and uses a non-orthogonal terrain-following vertical coordinate with variable vertical resolution. It is likely the only three-dimensional, fully compressible model available that uses a semi-implicit semi-Lagrangian (SISL) time discretization scheme (Benoit *et al.*, 1997). Time-dependent nesting of lateral boundary conditions is provided by a larger-scale model or MC2 itself in self-nesting mode. The model dynamics are linked to a complete set of physical

parameterizations via the RPN Physics Library (see Mailhot *et al.* 1998). A detailed description of version 3.0 of the MC2 model is given in Benoit *et al.* (1997). Appendix B highlights changes to the numerical model and the physical parameterizations for the more recent version of MC2 (v3.4.3) used in this study.

The model can be implemented on several computer architectures including NEC supercomputers and various workstations such as the Hewlett-Packard (HP) workstation that was used for this study. Version 3.4.3 of the model was installed on the HP workstation at the AES King City Radar Research Facility where these simulations were conducted. The model code has been updated by RPN three times since the release of v3.4.3 (v4.0, v4.1, v4.2). Some of the more important changes include massively parallel computing capability (dynamics and physics) and access to a greater variety of physics parameterizations such as surface schemes and condensation and convection schemes. Since massively parallel computing was not an option at the King City facility and since model simulations with v3.4.3 were already well underway before v4.0 became available, a decision was made to continue using v3.4.3 for the present study.

3.2.2 Spatial and Temporal Modelling Considerations

To study lake and land breezes, careful consideration must be given to the choice of horizontal and vertical grid structures. Since lake and land breezes have been observed to typically occur within the first 2-3 km of the troposphere, a sufficient number of vertical

levels must be defined there to adequately resolve the circulations. Similarly, horizontal grid spacing must be small enough so that the entire meteorological phenomenon can be resolved. The choice of the horizontal grid domain should be large enough to ensure that boundary condition errors do not significantly affect the solution in the area of interest. Also, previous lake breeze simulations have shown that inclusion of only a portion of a lake may lead to inaccurate wind predictions (Estoque and Gross, 1981; Comer and McKendry, 1993). Lastly, the choice of vertical and horizontal grids has a direct impact on the time step that must be used for numerical integration.

3.2.3 Vertical Level Definition

Since the phenomena to be studied typically occur in the lowest few kilometres of the troposphere, variable resolution of vertical levels was used so that a greater number of levels could be specified there. Hence, 28 vertical thermodynamic levels were defined manually placing one half of the levels below 3000 m. Vertical levels in the model are staggered resulting in momentum levels centred between the thermodynamic levels. The first thermodynamic level was set to 20 m so that the lowest momentum level would be 10 m and thus match the standard anemometer height. For proper performance, MC2 requires that twice the difference between the ground and first thermodynamic level be used between the first and second thermodynamic levels (personal communication, M. Desgagné, 1995). Thus, the second thermodynamic level was set to 60 m. Values above 60 m up to 750 m were chosen arbitrarily keeping in mind that vertical level height

should increase smoothly and monotonically to minimize the generation of spurious waves. Above 750 m, a simple cubic relation, level height = (level number)³, was used to smoothly and monotonically define vertical thermodynamic levels to a height of 24389 m, the model lid. This vertical level definition, shown in Table 3.1, was used for all of the model runs. This helped to minimize errors due to interpolation onto new vertical levels between cascading runs.

The height of the model lid (> 24 km) may appear to be excessive considering the typical depth of the mesoscale circulation to be modelled (< 3 km). However, the model lid was placed in the lower stratosphere to ensure that gravity waves reflecting off this rigid lid would be far removed from the solution in the lower troposphere. To this end, the top nine levels were used as a vertical sponge layer to dampen vertically propagating gravity waves near the rigid model lid. This is accomplished by gradually increasing the horizontal diffusion coefficient at each of the nine levels so that the value of the coefficient beneath the model lid is ten times the value beneath the sponge layer.

3.2.4 Horizontal Dimensions and Nesting Strategy

Through preliminary model runs, it was found that lake breezes could be adequately resolved using 5 km horizontal grid spacing though much higher resolution was required to adequately resolve details of the lake breeze front, usually only 1-2 km wide. Due to computer hardware restrictions, the coarser 5 km grid spacing was used. To provide

initial and boundary conditions for the 5 km grid run, a series of cascading, self-nested runs were necessary. For each of the case study events, the model was used to cascade from 100 km to 25 km to 5 km grid meshes giving nested grid mesh ratios of 4 and 5, respectively. Thus, the maximum self-nesting horizontal grid size ratio of 5 recommended by RPN (Benoit *et al.*, 1997) was observed.

The nesting strategy is illustrated in Figure 3.1. First, regional and global analyses were required to provide nesting data for the 100 km model run. Regional 100 km analyses at 12 hour intervals from the Canadian Meteorological Centre (CMC) Regional Finite Element (RFE) model were used for the 1993 SOMOS simulations. Regional analyses were discontinued in 1997 and were not available for the ELBOW simulations. Instead, global 100 km analyses at 6 hour intervals from the CMC Spectral Finite Element (SEF) model were used. Thus, nesting data had 100 km grid spacing in the central domain (covering most of Canada and the United States). The 100 km MC2 model runs used 100 km horizontal grid spacing with the domain centred over the central domain of the RFE grid (the outer domain of the RFE uses a variable mesh grid) for the SOMOS cases and over the same area of the global domain for the ELBOW cases. This 87 x 59 node mesh, shown in Figure 3.2a, includes much of Canada and the United States. The 100 km run was integrated over a period of 24 hours from either the 1900 LST (0000 UTC) sounding time (lake breeze simulations) or the 0700 LST (1200 UTC) sounding time (land breeze simulation). The 100 km model run may appear unnecessary since 100 km

data are provided by the analyses. However, the 100 km run is able to provide boundary condition data to the 25 km model run at a much greater frequency and the vertical motion field is available for nesting. This strategy is also recommended by Benoit *et al.* (1997).

The 25 km run was initialized at the 10 hour mark so that it would be spun up sufficiently for a 5 km run initialized at the 12 hour mark. The 25 km run was carried out for 14 hours using nesting data every two hours from the 100 km run. The 25 km grid was centred over southwestern Ontario and included all of the Great Lakes area in an 80 x 64 node mesh as shown in Figure 3.2b. The 5 km run was carried out for 12 hours from the 12 hour mark to the 24 hour mark using nesting data every hour from the 25 km run.

The 5 km grid was centred over southwestern Ontario and was rotated to a configuration that maximized the area of the lakes included in the 100 x 100 node mesh (Figure 3.2c). All of Lakes Erie and St. Clair are contained within this domain. However, Lake Huron is a much larger lake that extends roughly 300 km north of the study region. Due to restrictions on computing power and data storage, less than half of the surface area of Lake Huron is included. A small portion of Lake Ontario is also present within this domain. The degree to which boundary condition errors entered the modelled domain will be discussed in a later section.

3.2.5 MC2 Settings

Selected MC2 settings for each of the model runs are shown in Table 3.2. Default values are used for most of the other settings that are not shown. Settings that are the same for each run and those that are grid-specific are discussed separately below.

Dynamic initialization is used to accelerate the spin-up process at the beginning of the integration. The model integrates forward a set number of time steps (10 for this study) at a reduced time step (1/3 of the actual time step for this study) without computing physics tendencies then integrates backward in a similar fashion before beginning the simulation. The acceleration factor is estimated by RPN to be about 2.5 times (personal communication, M. Desgagné, 1995). All runs use the latest version of the radiation package (NEWRAD), the turbulent vertical diffusion boundary-layer scheme with full free atmosphere vertical fluxes (CLEF), the force-restore surface scheme (FCREST), gravity wave drag parameterization and, as mentioned previously, a vertical sponge layer using the top nine levels.

The time step that was found to provide a satisfactory balance between efficiency and numerical stability for the 100 km grid model run was 20 minutes with 72 time steps required for the 24 hour integration. The NEWRAD radiation scheme was executed every 7 time steps or about every 2 hours. A simple condensation scheme (CONDS) and an older version of the Kuo convection scheme (OLDKUO) were used. The default

horizontal diffusion coefficient of $1.22 \times 10^5 \text{ m}^2 \text{ s}^{-1}$ provided adequate damping of numerical noise.

A 5 minute time step was found to be adequate for the 25 km run and 168 time steps were required for the 14 hour integration. The NEWRAD radiation scheme was executed every 13 time steps or about every hour. A new formulation of the Sundqvist condensation scheme (NEWSUND) and the Fritsch-Chappell convection scheme (FCP) were used. The default horizontal diffusion coefficient of $7.65 \times 10^3 \text{ m}^2 \text{ s}^{-1}$ provided sufficient damping to reduce numerical noise.

For the 5 km model run, a 60 second time step provided a satisfactory balance between efficiency and numerical stability and 720 time steps were required for the 12 hour integration. The NEWRAD radiation scheme was executed every 16 time steps or about every 15 minutes. The Tremblay single-equation condensation scheme (EXC1) was used but none of the convection schemes available were appropriate for use with a 5 km grid size. This is not indicative of any inadequacy on the part of MC2 but is a current problem throughout the mesoscale modelling community (see for example Molinari, 1993). Thus, no convection scheme (NIL) was used and only deep convection produced explicitly by the model (unlikely at 5 km grid spacing) was possible. Use of the default horizontal diffusion coefficient of $3.06 \times 10^2 \text{ m}^2 \text{ s}^{-1}$ resulted in a significant amount of numerical noise, especially near the surface. Several higher values were tested and it was felt that a

satisfactory compromise between damping of the numerical noise and damping of the useful solution was achieved with a value of $3.00 \times 10^3 \text{ m}^2 \text{ s}^{-1}$.

The execution interval for the radiation scheme was decreased with decreasing time step values since it was found that cloud cover generated diagnostically by the scheme had a tendency to induce mesoscale disturbances if an interval on the order of two hours was used at higher resolutions. These disturbances resulted from differential heating of land surfaces when thick, isolated clouds remained stationary over the two hour period.

3.2.6 Initialization and Boundary Condition Data

Dynamic variables used for initialization and boundary conditions, such as wind, temperature, moisture and pressure fields, are provided with CMC global and regional analyses and are generated by MC2 for self-nested runs. It can be much more difficult finding suitable geophysical data. For the 100 km model run, the CMC global or regional analysis provides surface, deep soil and sea / lake surface temperatures as well as surface albedo, ice and snow cover fields at the 100 km grid size. The topography, land-sea mask, surface roughness length and launching height (used with the gravity wave drag scheme) fields are also available at the 100 km grid size through CMC RFE archive file 'gftopoco'. The source for topography and land-sea mask grid point values in this file is a U.S. Navy $1/6^\circ \times 1/6^\circ$ data set. Roughness length and launching height grid point values are derived from these fields. For this study, soil moisture availability climate values for the

appropriate month were interpolated onto the 100 km grid from the CMC 25 km grid climate file 'regclim_25km'. The source of soil moisture values in this file is a 1.875° resolution dataset from the European Centre for Medium-Range Weather Forecasts (ECMWF).

Geophysical fields were replaced with fields at the 25 km grid size before beginning the 25 km grid model run. The topography, land-sea mask, surface roughness length, launching height, soil moisture availability, surface albedo and snow and ice cover were obtained via the CMC 25 km grid climate file 'regclim_25km'. The source for topography and land-sea mask grid point values in this file is a U.S. Navy 1/6° x 1/6° data set. Surface roughness and launching height grid point values are derived from these fields. Soil moisture values are from an ECMWF 1.875° resolution monthly climatology. Albedo values at 1° resolution are from a Canadian Climate Centre dataset. Surface, deep soil and lake surface temperatures were interpolated onto the 25 km grid from the 100 km grid analysis values.

For the 5 km grid model run, topography, land-sea mask and surface roughness length were obtained at the 5 km grid size via an RPN high resolution topography database. The Canadian data for this database has 900 m resolution and comes from the Canadian Communication Research Centre. The U.S. data is at 1 km resolution and comes from the Defense Mapping Agency. These fields were found to have several significant errors,

especially near the lake shorelines, and were manually corrected. The surface albedo, soil moisture availability, launching height and snow and ice cover were interpolated onto the 5 km grid from the CMC 25 km grid climate file 'regclim_25km'. Interpolation errors near the shorelines in the surface albedo and soil moisture availability fields were manually corrected using the corrected 5 km land-sea mask. The lake surface temperature field was manually entered at 5 km grid spacing using daily infrared temperature data from a NOAA satellite obtained via the CoastWatch program of the Great Lakes Environmental Research Laboratory (GLERL). These data compared well with morning lake surface temperatures measured by buoys on Lake Erie near the start of the lake breeze model runs at 0700 LST (1200 UTC) and were used unaltered. However, Lake Erie buoy temperatures near the start of the land breeze model run at 1900 LST (0000 UTC) were found to be about 2°C warmer than the infrared temperatures. Thus, a 2°C upward adjustment was applied to all points of the lake surface temperature field as entered using the infrared data. The surface and deep soil temperatures were interpolated onto the 5 km grid from the 100 km analysis.

3.2.7 Model Modifications

3.2.7.1 Implementing Passive Tracers

This version of the MC2 model (v3.4.3) was designed so that a user could add one or more three-dimensional variables for use as passive tracers through changes to the model source code. Tracer fields can take any three-dimensional form and must be constructed

manually before being input to the model as initial and boundary values. Passive tracers are implemented and used with MC2 in this study to simulate the movement of ozone, initially in pools near the surface (blobs) or in a layer aloft (sheet), in the vicinity of lake breeze circulations. Tracer variables are not passed to the physics module and therefore do not undergo turbulent vertical diffusion. Also, the amount of sub-grid scale horizontal diffusion applied to tracers was set to zero for this study. Thus, tracer motions represent pure semi-Lagrangian advection and any diffusion is numerical. This allows a greater focus on the way in which the lake breeze circulations affect the movement of the tracer.

Since ozone is a gas that can be generated and lost by chemical reactions, be removed by wet or dry deposition, or undergo substantial horizontal and vertical mixing in the planetary boundary layer, the use of an 'advective tracer', as described above, to simulate changes in concentration of ozone is crude at best. Indeed, a greater concern for the absolute concentrations of tracer would necessitate the inclusion of diffusive parameterizations. However, since ozone has a relatively long lifetime on the order of days, tracer motions should represent the local and regional transport of ozone with some skill and it is hoped that the model predictions will provide some valuable insights on the problem of ozone transport in the lower troposphere in the presence of lake breeze circulations.

3.2.7.2 Modification to Shallow Convection

The maximum cloud amount due to shallow convection is hard-coded in version 3.4.3 of the model source code at 5 tenths. In preliminary simulations conducted on several different days, this maximum cloud amount of five tenths was usually reached over land in the afternoon during maximum solar heating. However, in these regions with fair-weather cumulus over land, observed total cloud amounts usually ranged between 2 and 3 tenths. The significantly higher modelled cloud amounts resulted in decreased insolation at the surface and eventually affected the thermally-induced lake breeze circulations. This problem was also recognized by RPN as contributing to modelled temperatures that were slightly cooler than observations (personal communication, R. Benoit, 1996). Thus, based on the above comparisons with observations, the hard-coded limit in the model source code was changed for this study to give an upper limit of 2.5 tenths cloud cover.

Comparisons between simulations with the old and new upper limits at inland grid points near maximum daytime heating showed a nearly 40% increase in the incoming visible energy flux at the surface, an increase near 3 K for ground temperatures, and an increase near 1 °C for 1.5 m air temperatures. The increase in 1.5 m temperatures resulted in a closer match to observations at that level. This change in the model code was used for all subsequent model runs including those presented in this thesis.

3.2.8 Discussion of General Results

Model runs at all grid sizes maintained maximum three-dimensional Courant numbers

generally between 0.4 and 0.7. As expected, the 5 km grid size was too coarse to resolve most details of the lake breeze fronts as observed. However, the leading edges of the modelled circulations tended to exhibit lake breeze front characteristics, though with weaker gradients. An unexpected result was the degree to which lake breezes developed during the 25 km grid model runs.

The model failed to reproduce observed land breeze circulations over the period modelled. Reasons for this failure are discussed in Chapter Four (Case Studies). However, a simulation was attempted for only one period. Several more tests of the ability of the model to simulate land breeze circulations are required before the existence and nature of a systematic problem can be determined.

A tracer could be activated through the MC2 settings to show the extent to which boundary values were entering the solution. It was used to monitor contamination from the lateral boundary conditions. Contamination appeared not to be a problem in the SOMOS cases but the moderate southwesterly winds during the ELBOW case quickly brought boundary values well into the 5 km grid domain. By the end of the integration (12 hour mark), boundary values had permeated the entire domain. However, since the area of interest on that day was located in the northeast portion of the domain, contamination was generally restricted to points southwest of the area of interest during the time period of interest (all times before the 9th hour of the integration). Significant

differences between the lateral boundary values and the inner domain values frequently caused dynamical perturbations within the horizontal sponge zone, especially for the 5 km grid model runs. Model output from the 5 km model run that is presented in Chapter Four has had the sponge zone regions removed. In addition, the domain has been rotated back to an orientation in which north is towards the top of the domain near the centre of the image to facilitate comparisons with observations. Lastly, the RPN software tool used to display the MC2 results, XREC, uses the identifier 'Z' when displaying time values rather than 'UTC'. References to these diagrams in the text will assume the reader is aware that 'UTC' and 'Z' have the same meaning and will use the format 'LST (UTC)' used in the rest of the document.

3.3 Sensitivity Studies

An investigation of the sensitivity of the MC2 model to significant changes in fundamental geophysical fields on a day with well-developed lake breezes was conducted as part of a modelling extension to the SOMOS study called 'SOMOS II'. In particular, the effects of these changes to the character of the lake breeze circulation, mainly the speed of surface inflow, lake breeze front intensity and inland penetration distance, were assessed. The results, which will be only briefly summarized here, were published in a report to AES / OMEE (Sills *et al.*, 1997).

The geophysical fields tested were surface albedo, surface roughness length, soil moisture

availability, deep soil temperature and lake surface temperature. The study region included all of Lake Ontario and parts of Lake Erie, Georgian Bay and Lake Simcoe. MC2 Version 4.0 was used for these sensitivity tests. Only a few very minor changes were made to the parts of the model dynamics code and the physics parameterization code used for lake breeze simulations between the versions used in the present study and in the SOMOS II study. Thus, the results obtained in the SOMOS II study should apply equally well to Version 3.4.3 of the model used here. Values of the geophysical fields were changed only over land, with the exception of the lake surface temperature, since the values of these fields over water are relatively well-known while over land there is greater uncertainty. Thus, significant sensitivity to changes in a geophysical field over land may point to a need to examine the treatment of this field within the model. Perturbation values were initially chosen to reflect realistic potential changes to the physical system. However, for several of the parameters, these changes produced signals that were too weak to analyze and a greater perturbation value was chosen. Comparisons between model runs with increased, decreased and baseline geophysical field values were made at two times: 1500 LST (2000 UTC) corresponding with the approximate time of maximum daytime heating and 1700 LST (2200 UTC) corresponding approximately with the arrival time of the lake breeze at a meteorological research station roughly 40 km north of Lake Ontario. Changes to each of the geophysical parameters and the resulting sensitivity shown by the model will be discussed in the following sections.

3.3.1 Surface Albedo

Changes to land surface albedo affect the absorption of short wave (solar) radiation and thus the surface energy budget. Resulting changes in the air temperature over land can affect the land-lake temperature gradient and thus the strength of the lake breeze circulation. Albedo values over land were increased and decreased by 50% relative to baseline values (0.16 - 0.19). No significant change to the character of the lake breeze was identified in either case. The most significant change was to ground and 1.5 m air temperatures. Ground temperatures increased with decreasing albedo with a maximum change near 1 K relative to baseline values (294 K - 304 K). Air temperatures at 1.5 m also increased with decreasing albedo relative to baseline values (21 - 24°C) with a maximum difference near 1°C.

3.3.2 Surface Roughness Length

Changes to the surface roughness length over land affect the degree of vertical turbulent diffusion. Changes in the amount of diffusion alter the mixing of quantities such as heat in the planetary boundary layer and thus can have a significant influence on the strength of the lake breeze circulation. Values of surface roughness length (m) over land were increased and decreased by an order of magnitude relative to baseline values (0.2 - 1.8 m). Slight changes to the character of the lake breeze were identified with the most significant change being a 10 m wind speed increase of up to 3 knots in the lake breeze inflow over land with decreasing roughness length (baseline values 5 - 10 knots). This

was accompanied by significant decreases in surface momentum fluxes with decreasing roughness length. Though convergence at the lake breeze front was found to increase with decreasing roughness length, changes to inland penetration distance were negligible. Boundary-layer heights increased slightly with increasing roughness length due to enhanced boundary-layer turbulence.

3.3.3 Soil Moisture Availability

The soil moisture availability (kg kg^{-1}) plays a major role in land evaporation calculation in the model and changes can significantly affect the contribution of the latent heat flux in the surface energy budget. Changes in the latent heat flux affect the sensible heat available to drive the lake breeze circulation. Soil moisture availability values were increased and decreased by 50% relative to baseline values ($0.26 - 0.38 \text{ kg kg}^{-1}$). There was little change noted in the character of the lake breeze. Inland values of latent heat flux were found to increase by roughly 50 W m^{-2} with increasing soil moisture (baseline values $50 - 200 \text{ W m}^{-2}$). This significantly altered the surface energy budget and resulted in significant changes to the ground and 1.5 m air temperatures. Both ground temperatures and 1.5 m air temperatures (baseline values given previously) increased with decreasing soil moisture availability with maximum changes near $1^\circ\text{C} / 1 \text{ K}$, respectively. Boundary-layer heights also increased significantly with decreasing soil moisture availability.

3.3.4 Deep Soil Temperature

Changes to deep soil temperature affect the land surface energy balance and thus have an impact on lake breeze circulation strength through subsequent changes to air temperature. Deep soil temperatures (K) were increased and decreased by 10 K relative to baseline values (290 K - 292 K). No significant changes in the character of the lake breeze were observed though there was a slight increase in 10 m wind speed in the lake breeze inflow and an associated slight increase in convergence at the lake breeze front with increasing deep soil temperature. The most significant changes were observed for ground and 1.5 m air temperatures. Ground temperatures increased with increasing deep soil temperature with a maximum difference of approximately 5°C from baseline values (given previously). Air temperatures at 1.5 m also increased with increasing deep soil temperature and reached a maximum difference of about 1.5°C from baseline values (given previously). In the decreased deep soil temperature case, ground temperatures and 1.5 m air temperatures over land were still slightly warmer than those over water at 1500 LST. The difference between ground and 1.5 m temperatures reached up to 12°C for the increased deep soil temperature case (baseline maximum near 9°C), mainly at grid points with low surface roughness values and thus reduced turbulent fluxes. Sensible heat flux values over land increased by 20 - 40 W m⁻² (baseline values 40 - 155 W m⁻²) while boundary-layer heights increased significantly with increasing deep soil temperature.

3.3.5 Lake Surface Temperatures

Lake surface water temperatures (K) were increased and decreased by 10 K relative to baseline values (near 294 K). In the former case, the increase resulted in the lake surface temperatures being higher than inland ground temperatures. These changes significantly altered the character of the lake breeze. The intensity of the lake breeze circulation, as gauged by the speed of surface inflow and the strength of the front, increased significantly with decreasing lake surface temperature. The inland penetration distance also increased with decreasing lake surface temperature but with a maximum difference of only a few kilometres relative to the baseline case (near 20 km). The 10 m wind fields for the increased, decreased and baseline lake surface temperature cases are shown in Figures 3.3a, b, and c. Changes in lake surface temperature also greatly affected the boundary-layer height over the lake. In the baseline case, boundary-layer heights over the lake were generally near 400 m except in the vicinity of the mesohigh in the southwest corner of the lake where the boundary-layer heights fell to below 200 m. When the lake surface temperature was increased, boundary-layer heights increased to heights over 1000 m over a large part of the lake mainly on its southeastern side. When lake surface temperatures were decreased, the boundary-layer height over the entire lake fell below 200 m.

An interesting aspect of this sensitivity test was that, when lake surface temperatures were increased, a weak lake breeze still formed on Lake Ontario even though lake surface temperatures were warmer than ground temperatures over land. Air temperatures at 1.5 m

responded slowly to the warm, underlying, water surface temperatures resulting in differences in these values exceeding 10°C early in the integration. The slow adjustment rate was apparently the result of greatly reduced turbulent fluxes associated with very low surface roughness values over the lake. Since heat could not be quickly distributed to the layers of air above the lake, air temperatures over land were greater than those over water and a weak lake breeze resulted. This problem might have been avoided if the air overlying the lake had been given sufficient time to adjust to the lake surface temperature before the onset of the lake breeze circulation.

3.3.6 Sensitivity Test Conclusions

Overall, the MC2 model showed surprisingly weak sensitivity to significant changes to the fundamental geophysical parameters. Changing the surface albedo had the greatest effect on ground and 1.5 m air temperatures while varying the surface roughness length had significant impacts on 10 m wind speeds in the lake breeze inflow and the intensity of the front. Changes to the soil moisture availability had a significant effect on latent heat flux and thus the surface energy balance but changed the character of the lake breeze circulation very little. The same was true when values of deep soil moisture were changed though the greatest change was in the sensible heat flux and its effect on the surface energy balance.

Lake breezes simulated by the MC2 model showed the greatest sensitivity to changes in

lake surface temperature. When the lake surface temperature was increased by 10°C, a weak lake breeze developed even though lake surface temperatures were greater than ground temperatures over land. This was attributed to the slow rate at which heat was transferred to the layers of air over the lake in the absence of significant turbulence.

When the lake surface temperature was decreased by 10°C, a significantly stronger lake breeze circulation developed relative to the baseline case and a small increase in penetration distance was observed. However, even this stronger lake breeze failed to reach inland to the meteorological research site roughly 40 km north of the lake as the observed lake breeze had done. This suggests that the primary factor controlling inland penetration of the lake breeze on this day, for at least the north shore of Lake Ontario, was the strength and direction of the gradient wind. The observed gradient wind for August 8 was light (~ 5 knots) and backed from northwest at 0700 LST (1200 UTC) to west-southwest at 1900 LST (0000 UTC). However, the modelled gradient wind in this case was roughly 1 - 2 knots stronger and veered in the afternoon to northwest before backing to west by 1900 LST (0000 UTC). The enhanced offshore component of the modelled gradient wind likely retarded the inland penetration of the lake breeze along the north shore.

CHAPTER THREE TABLES

Table 3.1. Vertical thermodynamic and momentum level heights (m) used for all MC2 runs. Levels 1 through 9 were manually defined while levels 10 through 28 were defined using the function Level Height = (Level Number)³. The height of the model lid (m) is also given.

Level	Thermodynamic	Function	Momentum
	Levels (m)		Levels (m)
1	0	manual	10
2	20		40
3	60		80
4	100		125
5	150		175
6	200		250
7	300		400
8	500		625
9	750		875
10	1000	LH=LN ³	1165
11	1331		1530
12	1728		1963
13	2197		2471
14	2744		3060
15	3375		3736
16	4096		4505
17	4913		5373
18	5832		6346
19	6859		7430
20	8000		8631
21	9261		9955
22	10648		11408
23	12167		12996
24	13824		14725
25	15625		16601
26	17576		18630
27	19683		20818
28	21952		23171
Model lid	24389		

Table 3.2. Settings selected for 100 km, 25 km, and 5 km grid MC2 model runs.

Model Run	100 km	25 km	5 km
Initialization method	dynamic	dynamic	dynamic
Time step	20 minutes	5 minutes	60 seconds
Number of time steps	72	168	720
Radiation scheme, interval	NEWRAD, every 7 time steps	NEWRAD, every 13 time steps	NEWRAD, every 16 time steps
Boundary-layer parameterization	CLEF	CLEF	CLEF
Surface scheme	FCREST	FCREST	FCREST
Condensation scheme	CONDS	NEWSUND	EXC1
Convection scheme	OLDKUO	FCP	NIL
Nested quantities?	none	vertical motion, liquid water content, TKE	vertical motion, liquid water content, TKE
Horizontal diffusion coefficient ($\text{m}^2 \text{s}^{-1}$)	1.22×10^5 (default)	7.65×10^3 (default)	3.00×10^3
Gravity wave drag parameterization	turned on	turned on	turned on
Levels in vertical sponge layer	9	9	9

CHAPTER THREE FIGURES

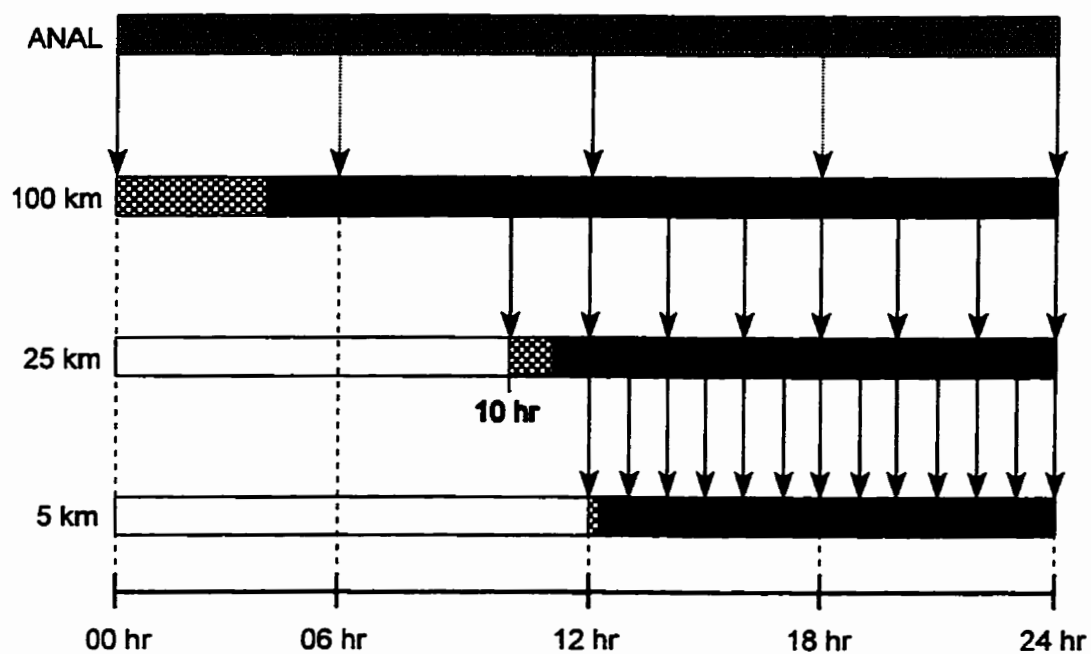


Figure 3.1. Diagram illustrating the nesting strategy used for MC2 runs. The grey bar indicates the analysis data. Model run intervals are shown by black bars with checkered regions indicating the length of the spin-up period. Arrows indicate the times at which nesting data were made available to the higher resolution model run.

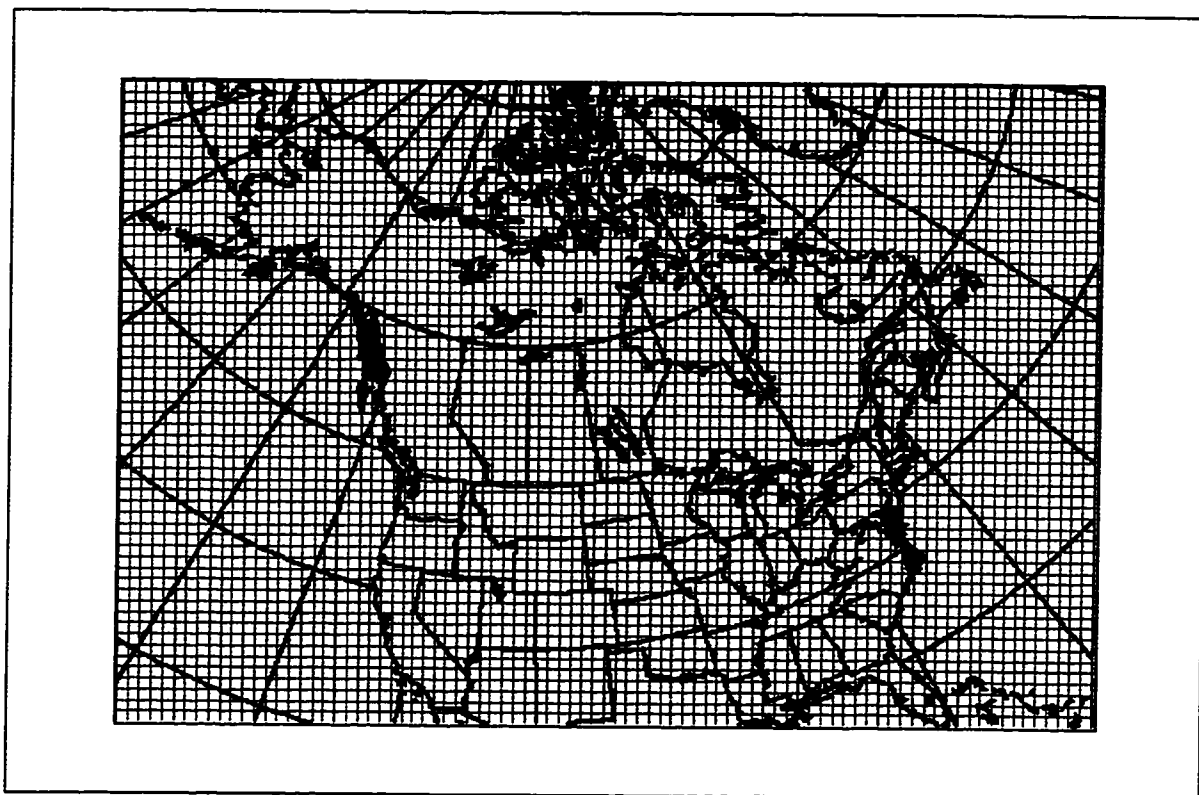


Figure 3.2a. MC2 domain for the 100 km grid model runs showing the geographical area of the domain and the grid mesh.

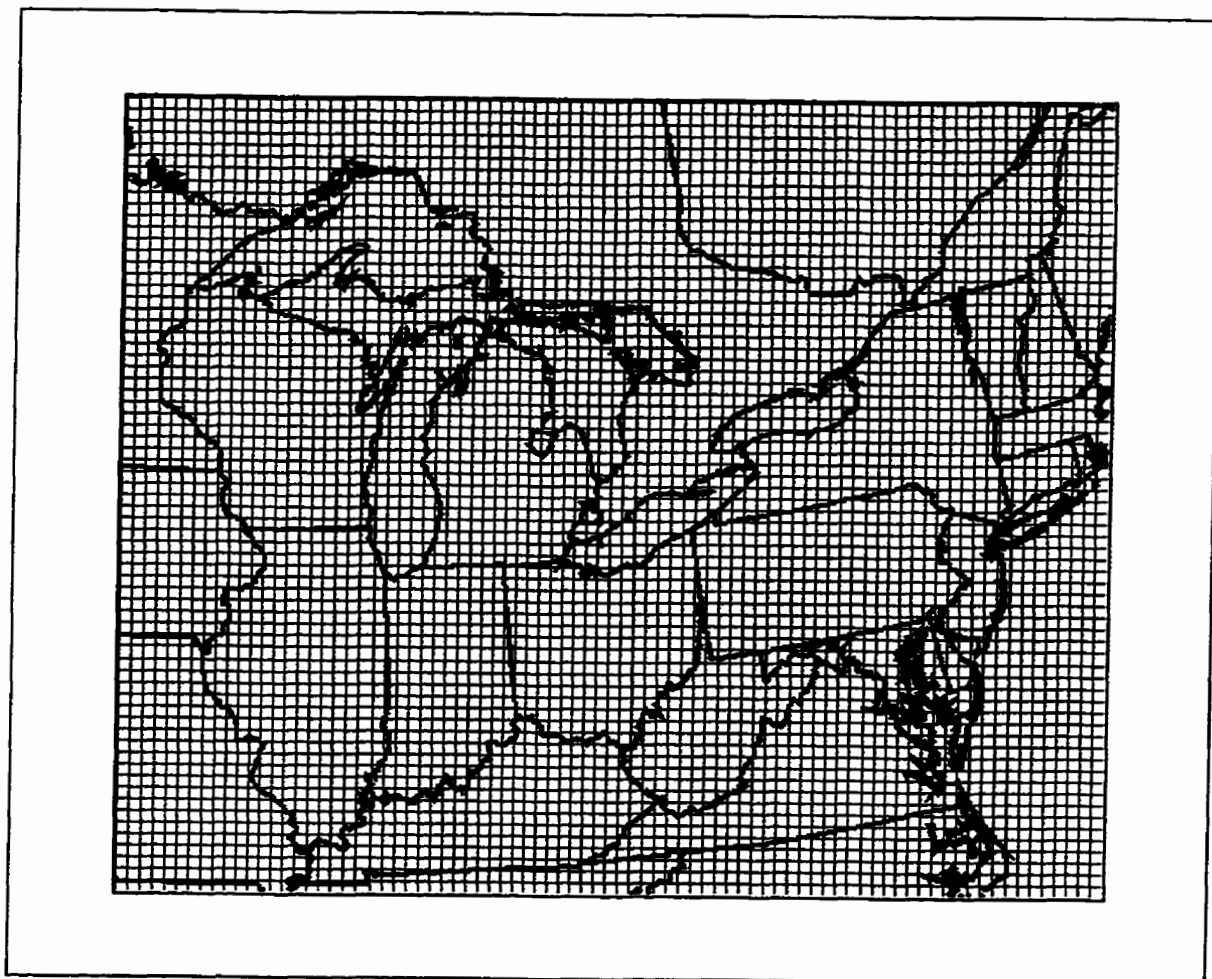


Figure 3.2b. As in Figure 3.2a, except for the 25 km grid mesh.

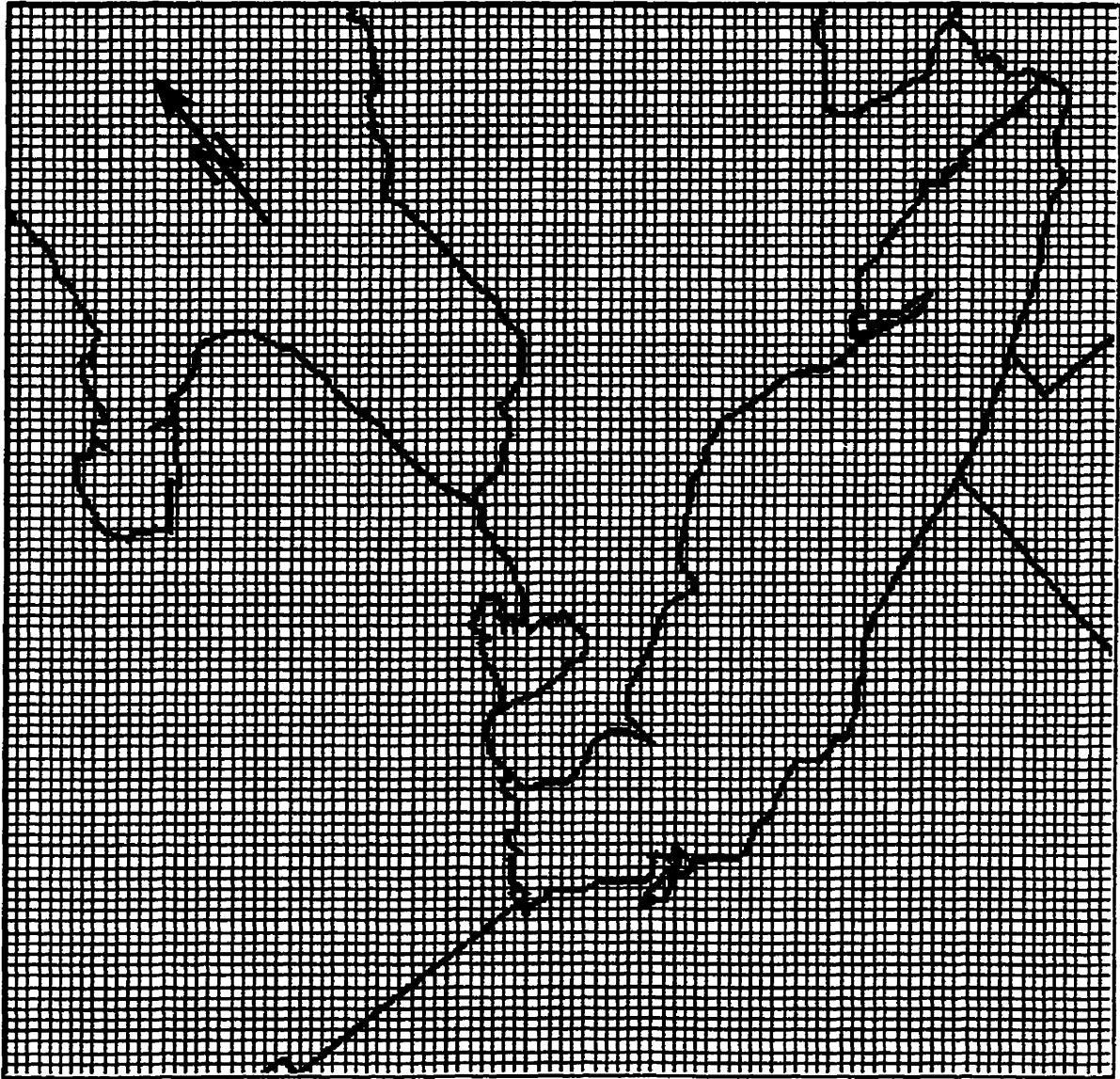


Figure 3.2c. As in Figure 3.2a, except for the 5 km grid mesh. The 5 km grid mesh is rotated roughly 40° to maximize the area of the lakes included in the domain.

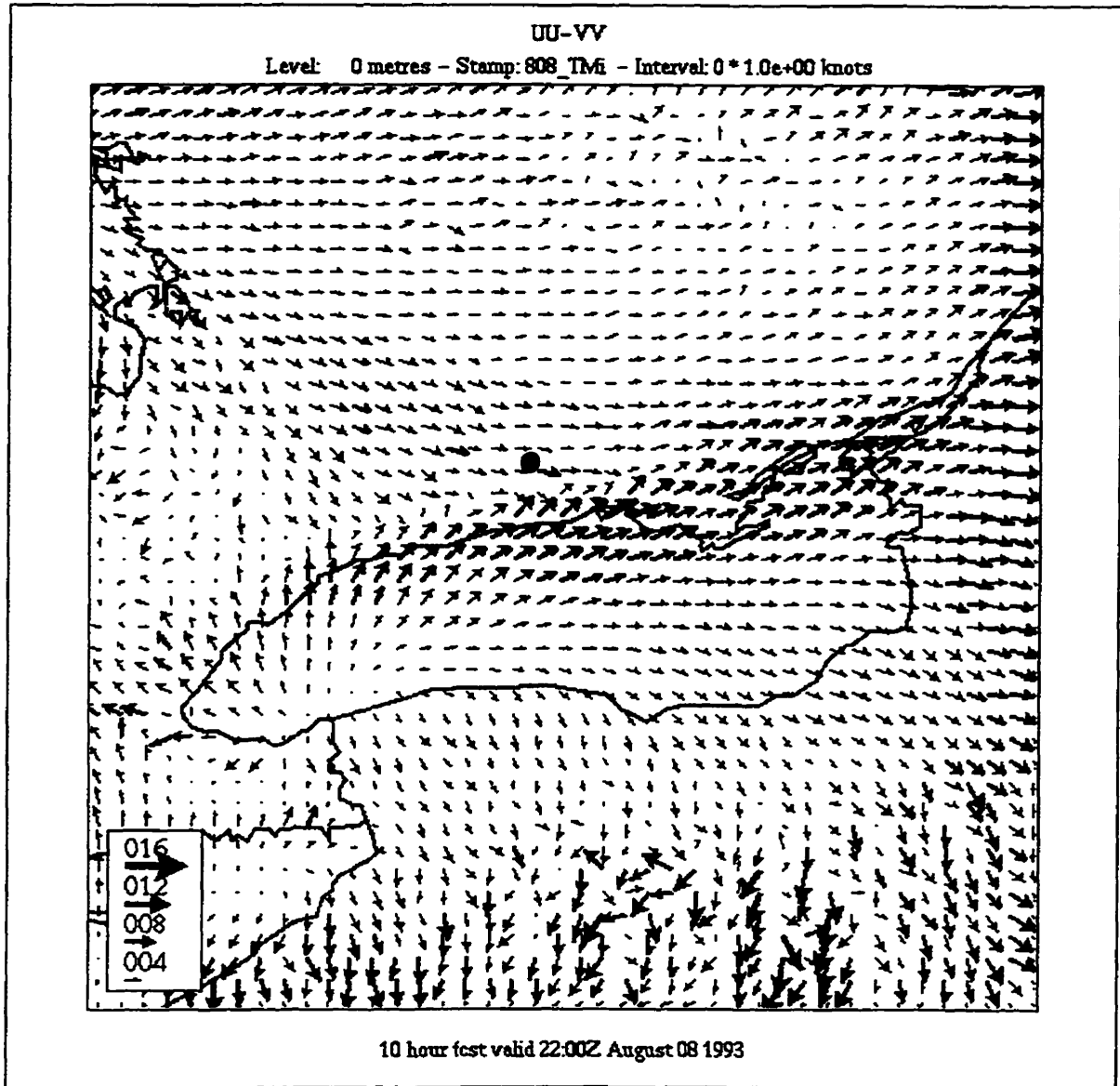


Figure 3.3a. 10 m winds (knots) from the 5 km grid model run valid at 2200 UTC on August 8, 1993 for increased lake surface temperatures. The Lake Ontario lake breeze front passed the meteorological research site shown by the darkened circle at this time.

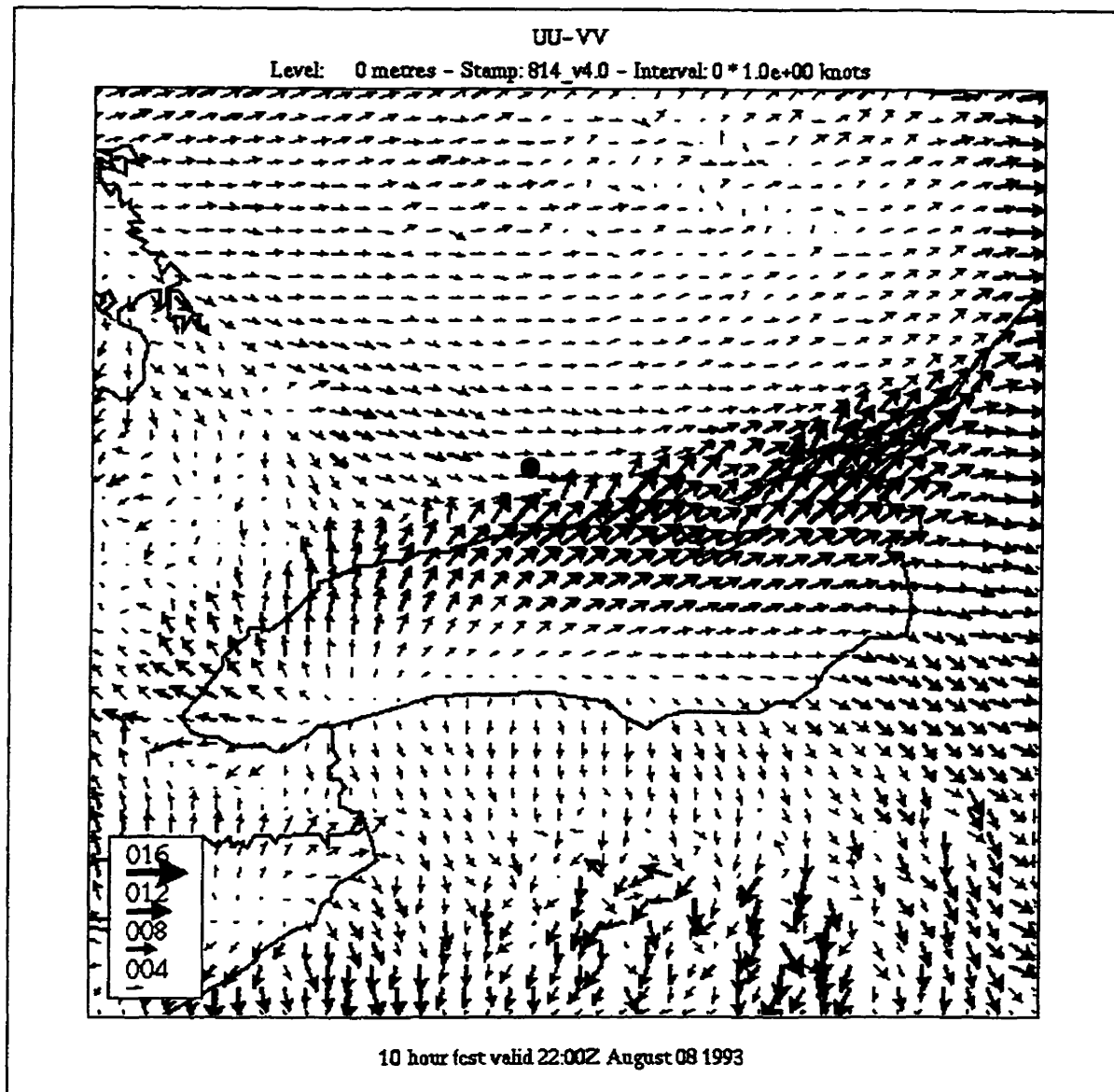


Figure 3.3b. As in Figure 3.3a, except for baseline lake surface temperatures.

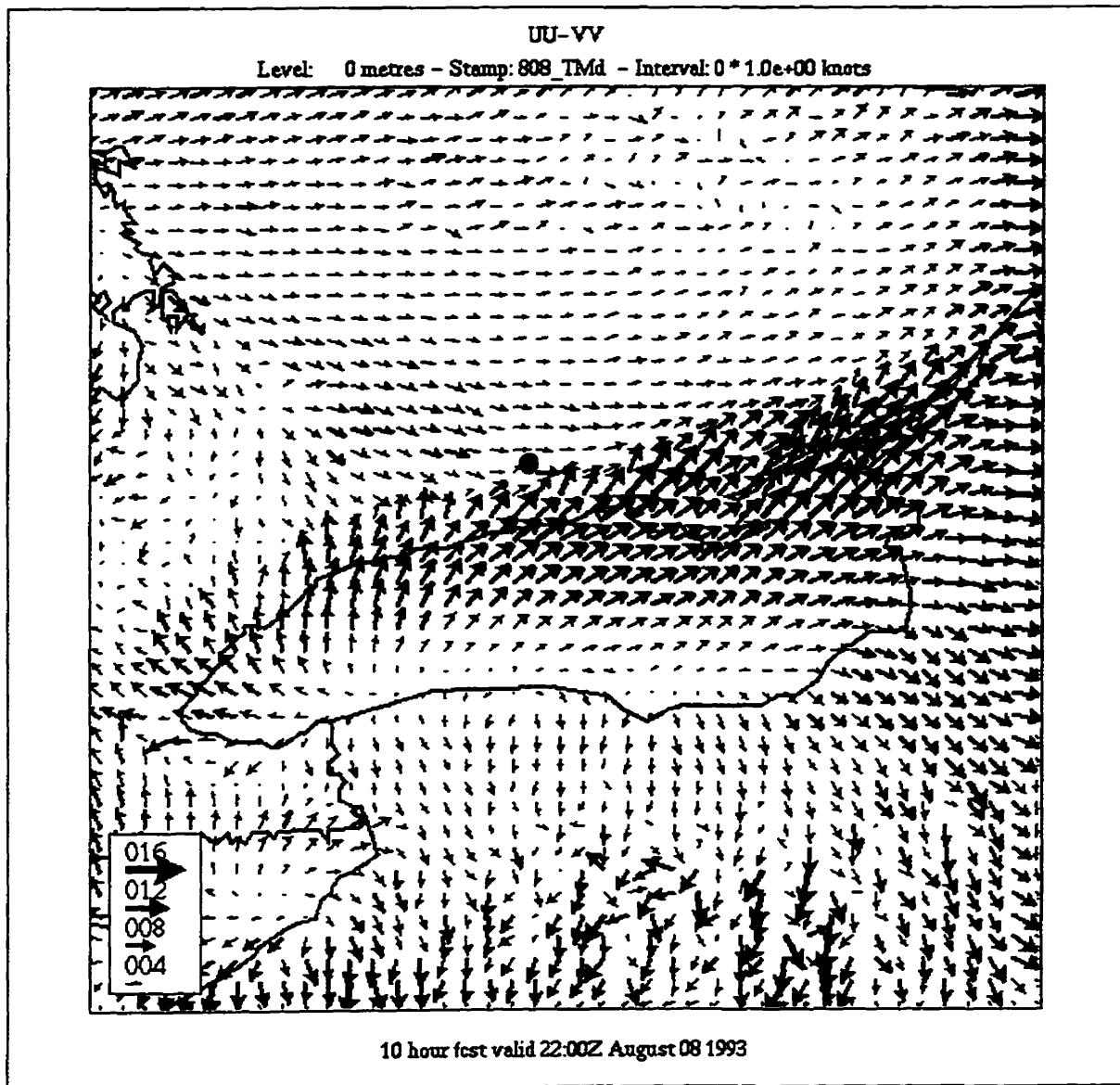


Figure 3.3c. As in Figure 3.3a, except for decreased lake surface temperatures.

CHAPTER FOUR - CASE STUDIES

4.1 Introduction

Two periods were chosen for detailed observational analysis and simulation with the MC2 mesoscale model: August 14 - 15, 1993 and July 14, 1997. Well-developed lake and land breezes occurred in the period from the morning of August 14 to the evening of August 15. Under light and variable gradient winds, these circulations had characteristics common to most lake and land breezes described in the literature and are thus referred to as 'classic' lake and land breezes. This period was also chosen because at least four severe weather events and several of the highest one-hour ozone concentrations recorded in Ontario and Michigan during 1993 occurred in association with lake breezes in the SOMOS study region during the period. Separate MC2 simulations were conducted for the lake breezes of August 14, the land breezes of August 14 - 15, and the lake breezes of August 15. The spatial and temporal characteristics of these lake and land breezes will be examined using a combination of observational and model data. For this period, the relationships between lake breezes and thunderstorms and lake breezes and high ozone concentrations will also be investigated.

Conditions observed on July 14, 1997 differed significantly from those of the August 14 - 15, 1993 period. A moderate westerly gradient wind was present and resulted in the development of highly-perturbed lake breezes in the ELBOW study region. In fact,

observing conditions in this type of situation was one of the main goals of the ELBOW project. Several thunderstorms, including a severe thunderstorm, appeared to be initiated at lake breeze fronts. The spatial and temporal characteristics of these highly-perturbed lake breezes are investigated and the role of these circulations in initiating and maintaining thunderstorms is discussed.

The lake breezes on August 14, 1993 exhibited the most 'classic' traits and much of the discussion on the spatial and temporal characteristics of the lake breeze in southern Ontario will be focussed there. Lake breeze signatures in ground-level ozone data were also most apparent on this day and discussion of mesoscale ozone transport will be centred on August 14. The main focus of discussion for August 15, 1993 will be on lake breezes and their relationship to severe weather events that occurred on that day. For the July 14, 1997 case, the discussion will concentrate on highly-perturbed lake breezes and their links to severe weather in the region.

The performance of the MC2 model will also be evaluated for each case using the method of Pielke (1984). Pielke states that a model may be validated with observations using either 'subjective evaluation' or 'point and pattern quantitative validation'. Using subjective evaluation, the spatial and temporal characteristics of a predicted field are qualitatively compared to observations of that parameter or a justifiably-related field. For example, modelled vertical velocity values near the top of the boundary layer might be

compared to observed locations of convective cloud or precipitation. Pielke's second method, point and pattern validation, involves quantitative point-to-point comparisons between predicted and observed parameters and the use of set theory to describe the correlation between observed and predicted patterns. For this study, a combination of subjective evaluation and point-to-point quantitative validation will be used to assess the utility and skill of the MC2 model under lake and land breeze conditions.

4.2 'Classic' Lake and Land Breezes during SOMOS: August 14 - 15, 1993

4.2.1 Overview

This case study period occurred within the longest period of stagnant synoptic conditions in the SOMOS study. From August 11 to August 18, a 500 hPa ridge was maintained over central North America and the sea level pressure gradient in the Great Lakes region remained weak. On each of these days, well-developed lake breezes occurred on all shores in the study region. In addition, contiguous lake and land breezes occurred from August 11 to August 15. Figure 4.1 shows divergence values through this period for the areas between Lakes Erie and St. Clair (Triangle A) and Lakes Erie and Huron (Triangle B) depicted in Figure 4.2. The method of calculation is discussed in Appendix C. The oscillation between convergence during the day and divergence during the night between the lakes is clearly evident with relatively high convergence and divergence values calculated for August 14 and 15. Hourly-averaged ozone concentrations exceeding 80 ppb were also recorded in the study region from August 11 to August 16 with the highest

concentrations observed on August 14. Severe weather, including weak tornadoes and heavy rain, occurred during the afternoon hours on both August 14 and August 15.

4.2.2 Synoptic Conditions

As discussed in Chapter One, the gradient wind is one of the most important factors affecting the development of lake and land breezes. Objectively analyzed synoptic data and surface analyses will be discussed briefly to assess the gradient wind and other synoptic-scale parameters through the period. These data are also compared to similar fields predicted by the MC2 model.

Figure 4.3 shows Canadian Meteorological Centre (CMC) objectively analyzed sea level pressure at twelve hours intervals beginning on August 14 at 0700 LST (1200 UTC). The main feature affecting the Great Lakes region is the broad ridge of high pressure extending from Hudson Bay south into the Mississippi Valley. The pressure gradient is clearly weak throughout the period. A weak low pressure disturbance is apparent over the southeastern U.S. in the first image but is shown to quickly dissipate. A light gradient wind with a dominant northerly component is suggested over the study region. Sea level pressures as predicted by the 100 km MC2 model run are shown for the same times in Figure 4.4 for comparison with the objectively analyzed fields. MC2 successfully generates the ridge of high pressure that was observed from Hudson Bay toward the southern U.S. However, the model brings the 1016 hPa contour farther north than

observed by 1900 LST (0000 UTC) resulting in a greater pressure gradient. Twelve hours later, the 1016 hPa contour is close to the observed location, but the pressure gradient over the western Great Lakes is greater than observed with the 1012 hPa contour located farther east than observed. The enhancement of the pressure gradient over the western Great Lakes region by the model will result in a gradient wind there that is slightly stronger than observed. However, the coarse grid simulation was considered to be sufficiently accurate for use as nesting data for the 25 km grid run.

Regional surface analyses courtesy of AES at 12 hour intervals beginning at 1300 LST (1800 UTC) on August 14 are shown in Figures 4.5, 4.6 and 4.7. At 1300 LST (1800 UTC) on August 14, a broad ridge was present over the Great Lakes region with a northeasterly gradient wind over the study region suggested by the orientation of the isobars. Inland temperatures up to around 29°C were reported in the Great Lakes region accompanied by haze. A weakening cold front was cutting across the northern Great Lakes. By 0100 LST (0600 UTC) on August 15, the pressure pattern was largely unchanged and fog had developed over a large area. Inland temperatures in the Great Lakes region down to around 15°C were reported. Two quasi-stationary fronts were analyzed associated with a developing low pressure system centred over extreme western Ontario. Finally, by 1300 LST (1800 UTC) on August 15, two baroclinic waves were beginning to enter the western Great Lakes region accompanied by an extensive cloud shield and showers and thunderstorms. The pressure gradient over the Great Lakes

remained relatively weak but the orientation of the isobars suggests that the gradient wind had acquired a dominant southerly component. Inland temperatures reaching up to 28°C were reported. Figure 4.8 shows the sea level pressure patterns for the same time periods as computed by the MC2 model on the 25 km grid. Modelled sea level pressure values are nearly 3 hPa lower than observed suggesting a possible loss of mass in the model volume between the 100 km run and the 25 km run. The model appears to have been overly aggressive in deepening the low pressure system centred over Wisconsin by 1300 LST (1800 UTC) on August 15. This resulted in a modelled surface pressure gradient greater than observed over the western Great Lakes. However, the modelled surface pressure gradient remained relatively weak over the study region resulting in light modelled gradient winds. This is supported by modelled 850 hPa winds for the afternoon hours of August 14 and August 15 from the 25 km grid model runs (Figure 4.9). For August 14, winds over the study region were generally light from the north with anticyclonic flow centred just to the west. For August 15, the anticyclonic flow centre had drifted to the southeast and winds over the study region were light from southwest to west. Much stronger winds were predicted over the western Great Lakes region associated with the tighter pressure gradient there. Overall, the 25 km prediction was found suitable for use as nesting data for the 5 km grid model run.

4.2.3 Mesoscale Observations, Model Results and Comparisons

Another important factor affecting the development of lake and land breezes is the

difference in temperature between air over land and air over the lakes. The temperature of the air over water is strongly correlated with the lake surface temperature. Figure 4.10 shows Great Lakes water surface temperatures as measured by satellite-borne infrared sensors. Lake surface temperatures valid for the afternoon of August 14 ranged spatially between 19°C and 25°C over Lakes Huron and Erie and between 20°C and 23°C over Lake St. Clair. Satellite-derived lake surface temperatures valid for August 15 (not shown) were slightly warmer (< 1°C difference) than those of August 14. The air temperatures over land and over the lakes as well as various other mesoscale parameters are discussed for each time period in the following sections.

4.2.3.1 August 14 Lake Breezes

Figure 4.11 is a sequence of mesonet station plots for August 14 at 0900 LST, 1200 LST, 1500 LST and 1900 LST. At 0900 LST, light land breeze winds were present south of Lake Huron and the Lake Erie lake breeze was detected at a few stations along the north shore of Lake Erie. In other areas, winds were either light or calm. Air temperatures ranged from 23°C to 27°C and dew points were reported between 18°C and 22°C. Temperatures over land were 1-2°C greater than over Lake Erie. By 1200 LST, lake breezes were occurring on each of the lakes. Inland temperatures had reached up to 32°C and dew points had changed very little since 0900 LST. At 1500 LST, onshore winds associated with lake breezes dominated surface flow over southwestern Ontario. Stations over inland parts of Michigan that were unaffected by lake breezes had northwest winds.

Temperatures at most stations reached their maximum value near this time. Dew point values at some shoreline stations were 1-2°C greater than at 1200 LST. Inland temperatures were up to 7°C greater than air temperatures over Lake Erie and roughly 9°C and 10°C warmer than lake surface temperatures for Lakes Huron and St. Clair, respectively. Finally, at 1900 LST, diffluent lake breeze flow off of Lake Huron was continuing to penetrate inland to the southwest and had already begun to displace the Lake St. Clair lake breeze. The Lake Erie lake breeze was beginning to dissipate with air temperatures over water greater than or equal to that over land. Some stations had their highest dew point values near this time.

Modelled surface winds, temperatures and dew points for the same times as above are shown in Figures 4.12, 4.13 and 4.14 respectively. At 0900 LST (1400 UTC), modelled surface winds were light to calm over land and up to 6 knots over the lakes. Winds across the study region had a northerly component though onshore flow was just beginning to occur along the north shore of central Lake Erie. Though land breeze winds were observed at this time south of Lake Huron, modelled winds show onshore flow. By 1200 LST, onshore winds were predicted by the model on all of the lakeshores. In areas not yet affected by lake breezes, winds generally had a northern component. Each of the lake breezes had penetrated inland by 1500 LST with Lake Huron having the greatest penetration distance. By 1900 LST, the Lake Huron lake breeze was meeting both the Lake Erie and Lake St. Clair breezes. Modelled temperatures increased gradually over

land reaching values up to 30°C by 1500 LST. Air temperatures over water continued to increase until the end of the integration at 1900 LST, reaching near 25°C over western Lake Erie. Large temperature gradients are evident inland from each of the lakes. At 1500 LST, the land-lake temperature difference was roughly 7°C for each of the lakes. Modelled dew points were closely related to topography at 0900 LST with the lowest values over the highest terrain. However, by 1500 LST, lake breeze effects on dew point values became dominant with tight gradients inland of each of the lakes. At 1900 LST, areas not affected by the modelled lake breezes had dew points down to near 14°C while dew points remained between 19°C and 22°C over the lakes and near-shore areas.

Comparing the observed and modelled values described above reveals several important differences. Observed winds over inland parts of southeastern Michigan were northwesterly for much of the period and observed winds over western Lake Erie remained out of the southwest. In contrast, modelled winds in these areas were approximately reversed. Modelled temperatures at times up to 1500 LST were generally 1-2°C cooler than observations. Modelled land-lake temperature differences for Lakes Huron and St. Clair were generally 2-3°C lower than observed likely resulting in weaker lake breeze circulations. Lastly, modelled dew points became several degrees Celsius too low over land by 1900 LST.

A diagram showing observed lake breeze penetration distances over time is shown in

Figure 4.15 The positions of lake breeze fronts were inferred using a combination of mesonet station data and visible satellite images in the same manner as described in Chapter Two. Due to surface station spacing (~ 25 km), the time between surface observations (up to one hour), and possible errors in the correlation between cloud lines on visible satellite imagery and the actual positions of lake breeze fronts near the surface, errors of approximately ± 5 km are likely with the frontal positions given. Frontal positions in the diagram are estimates and assume a continuous inland progression of the front over time to interpolate between stations and observations in locations such as the north shore of Lake Erie.

Aided by a light northwesterly gradient wind, the Lake Huron lake breeze rapidly penetrated inland and appeared to reach distances up to 120 km from its shores by 0100 LST on August 15 before dissipating. This extraordinary penetration distance is certainly not one of the 'classic' lake breeze features observed on this day. Its most rapid rates of penetration occurred between 1300 LST and 1500 LST, and between 2300 LST and 0100 LST. In the evening hours, the lake breeze probably penetrated inland in the form of a detached lake breeze vortex, as has been discussed in Chapter Two.

In contrast, the opposing gradient wind held the Lake Erie lake breeze close to its shoreline. The Lake Erie breeze penetrated only 10-25 km inland in the study region before being forced to retreat by the approaching Lake Huron lake breeze after 1700 LST.

Similarly, the Lake St. Clair lake breeze reached a maximum penetration distance of about 25 km before being displaced by the Lake Huron lake breeze after 1600 LST.

A similarly formatted diagram of modelled lake breeze penetration distances is shown in Figure 4.16. The inland extent of a lake breeze in this case was inferred using the modelled surface wind field and divergence field at various heights up to 625 m. In particular, the surface winds were used to locate wind shift lines and divergent patterns emanating from a lake while the surface divergence field was analyzed for elongated lines of convergence indicating a lake breeze front. At some times, the surface divergence showed only a weak frontal signature but a stronger frontal signature was present at levels above the surface up to 625 m. Since the horizontal grid spacing is 5 km, the error in the lake breeze frontal positions shown is estimated at ± 5 km. As with the observed frontal positions, a continuous inland progression of the front over time is assumed to interpolate between grid points in locations such as the north shore of Lake Erie.

Lake breezes are not detectable until 1000 LST. The leading edge of the lake breeze in areas of onshore gradient flow such as the southern shore of Lake Huron does not become discernable until 1600 LST. The modelled penetration pattern is similar to the observed pattern with a few important differences. First, the observed Lake St. Clair lake breeze penetrated nearly 30 km to the east before being displaced by the Lake Huron circulation while the modelled Lake St. Clair lake breeze remained nearly stationary less than 10 km

east of the shore through most of the period. Second, the observed Lake Huron lake breeze penetrated well to the east of the lake while the modelled circulation remained relatively close to the shore. The observed circulation also extends farther to the south meeting the Lake Erie lake breeze by 1900 LST. Inland penetration distances inferred using the 10 m wind field from the 25 km grid model run (not shown) are very similar to those predicted by the 5 km grid model run. This suggests that differences between the observed penetration distances and those predicted by the 5 km grid model run are attributable mainly to inaccuracies in the nesting data.

Figure 4.17 compares time series data from the Cedar Point station located about 750 m from the Lake Huron shoreline with those of the Walnut station located about 32 km farther inland. The arrival of the Lake Huron lake breeze front at Cedar Point is clearly shown at 0950 LST. As the front passed, the temperature fell from 26.9°C to 24.3°C and the dew point temperature reached a maximum value of 22.1°C. The wind speed increased from 0.5 m s⁻¹ to 2.1 m s⁻¹ and the wind direction shifted from offshore to onshore. Through the rest of the day, the temperature increased at a reduced rate to a maximum of 26.9°C at 1510 LST and the dew point temperature remained elevated. The wind reached speeds of 4.7 m s⁻¹ by 1530 LST and slowly veered toward the northeast through the day, perhaps due in part to the Coriolis force. The dissipation of the circulation at Cedar Point is evident after 1945 LST. Wind speed and direction time series for the inland station Walnut are similar to those of Cedar Point. However, the Lake

Huron lake breeze at Walnut appears to have arrived in a series of pulses before a steady onshore flow was established at 1340 LST. This 'pulsing' or 'surging' effect at inland stations was also reported by Moroz (1967) and Munn and Richards (1964). Both of these papers also showed that temperature and moisture parameters at inland stations may show little or no lake breeze front characteristics when the lake breeze arrives since the air associated with the lake breeze is modified as it moves inland over the warm surface. This modification is evident in the temperature and dew point time series data from Walnut with only very weak frontal characteristics detectable.

Modelled time series for the grid points at these station locations are also shown in Figure 4.17. Instantaneous model values are shown at one-hour intervals. Comparing the modelled time series, the inland temperature is the same as that at the shore at the start of the integration but becomes about 5°C warmer by mid-afternoon. The difference in dew point temperature also increases gradually through the day to a maximum of about 3°C. Modelled inland wind speeds are generally about 1.5 m s⁻¹ greater than those at the shore. This difference is not as evident in the observed time series. Wind directions are nearly the same through the period.

Comparing observed and modelled time series, there are clearly some significant differences. Modelled temperature values at both locations are generally 1-2°C lower than observed through the morning and early afternoon but become warmer than observed

by late afternoon. At the inland location, the modelled maximum temperature occurs two hours later than observed. Modelled dew point temperatures at both locations are higher than observed by more than 1°C at the start of the integration at 0700 LST. The dew point at the shore location remains generally within 1°C of observed dew points. However, the dew point at the inland station decreases gradually through the day and is about 3°C less than the observed value at the end of the integration at 19 LST. Modelled wind speeds at both locations are slightly greater than observed at the start of the integration at 0700 LST and the shoreline location continues this trend with wind speeds about 1 m s^{-1} greater than observed through the period. The inland wind speed remains within 1 m s^{-1} of observed values through the afternoon. Finally, modelled wind direction at both stations poorly matches observations in the morning hours but begin to closely match observed wind directions after noon.

Observed time series data for the Morpeth station on the shore of Lake Erie are shown in Figure 4.18. The observations suggest the arrival of the Lake Erie lake breeze front at 0925 LST. The temperature decreased from 26.1°C to 24.6°C , the dew point increased nearly 2°C and the wind direction became onshore. Several hours after the passage of the lake breeze front at 1315 LST, the temperature reached a maximum of 27.9°C . Dew points varied by as much as 3°C through the afternoon but appeared to generally increase until the lake breeze dissipated after 1900 LST. The wind speed reached a maximum value of 5.1 m s^{-1} at 1435 LST then began to decrease. After the passage of the front, the

wind direction remained steady out of the south until the circulation dissipated after 1900 LST. A thunderstorm that appeared to be initiated on the Lake Erie lake breeze front just north of Morpeth drifted south over the station near 1515 LST. Its effects can be evident in the time series. The temperature fell about 3°C, the dew point increased about 1°C and winds increased in speed and backed slightly. However, it appears that the thunderstorm did not disrupt the lake breeze circulation which continued for several more hours.

Modelled time series for the grid point at the Morpeth station location are also shown in Figure 4.18. Modelled temperatures and dew points at the start of the integration are 1-2°C greater than observed but were close to observations by late morning. Though modelled surface wind speeds increase at a slower rate than those observed, the maximum wind speed reached matches very closely. Lastly, the modelled surface wind direction poorly matches the observations near the beginning of the integration.

Observations show that the wind backs with time while between land and lake breeze regimes. However, the modelled surface wind gradually veers with time. After the observed lake breeze has become established, modelled wind direction is within about 45° or less of observed values.

One significant difference between the observed and modelled time series discussed above is the lack of any sharp changes in the modelled data associated with the arrival of the lake breeze. This absence is apparent even with modelled data at half hour intervals

(not shown). The observed lake breeze front is generally thought to be between 1-2 km across (see Chapter One) so its passage brings very rapid changes to meteorological parameters. In contrast, the model uses a grid size of 5 km and changes associated with the arrival of the lake breeze are significantly muted.

Returning to the observed 10 m divergence values of Figure 4.1, the divergence time series indicates that values in Triangle A (between Lakes Erie and St. Clair) on August 14 (Julian Day 226) reached a minimum of about $-35 \times 10^{-5} \text{ s}^{-1}$ near 1300 LST while values in Triangle B (between Lakes Erie and Huron) reached a minimum near $-10 \times 10^{-5} \text{ s}^{-1}$ at about the same time. Modelled 10 m divergence at 1300 LST (1800 UTC) is shown in Figure 4.19. The grid point value at the centre of Triangle A is about $-8 \times 10^{-5} \text{ s}^{-1}$ while the grid point value at the centre of Triangle B is about $-4 \times 10^{-5} \text{ s}^{-1}$. These values are somewhat lower than those observed. However, minimum divergence values in areas to the north of Lake Erie are concentrated along the lake breeze front. While this effect should be represented in the observed divergence values that include lakeshore measurements, the modelled divergence values at inland grid points away from the frontal zone can be expected to be correspondingly lower. Also, the very coarse resolution of the observational values of divergence could contribute to these differences.

4.2.3.2 August 14 - 15 Land Breezes

Land breezes in the study region were later than usual getting started due to the very robust Lake Huron lake breeze. A land breeze was first detected in the mesonet on the Lake Huron shore near 2200 LST. It is unclear when land breezes began on the north shore of Lake Erie since the passage of the Lake Huron lake breeze front there had already resulted in offshore winds. Land breezes were detected on the Lake St. Clair shore near 0100 LST. Figure 4.20 shows time series data from the Stoney Point mesonet station on the south shore of Lake St. Clair. The arrival of the Lake Huron lake breeze front is signalled between 2100 and 2200 LST, most prominently for wind speed. Near 0200 LST, the lake breeze circulation gives way to a land breeze circulation. The wind speed time series shows that the land breeze occurred in a series of pulses with an average period of roughly 45 minutes. The land breeze circulation appears to dissipate near 0500 LST after which calm conditions prevail. Similar land breeze behaviour is described by Wexler (1946). He found the land breeze to be "hardly discernible" and "characterized by a few long thrusts interrupting at intervals the nightly calm".

A time series plot for the same period at the Cedar Point station on the shore of Lake Huron is shown in Figure 4.21. The land breeze at this station appears to commence between 0100 and 0200 LST on August 15. Its arrival is indicated by a sharp shift to offshore winds and an increase in wind speed. Again, there appears to be a pulsatory nature to the flow shown by the wind speed. Both temperature and dew point begin to

increase after 0600 LST. The increase in dew point is likely due to condensed water at the surface evaporating into the air as insolation increases. The land breeze circulation at Cedar Point is abruptly replaced by a lake breeze circulation near 0900 LST.

The evolution of the land breeze is shown by a sequence of station plots in Figure 4.22. Plots are shown for 2100 LST on August 14 and 0400 LST and 0700 LST on August 15. In the first image at 2100 LST, the Lake Huron lake breeze is continuing its southward progression having reached as far southwest as Willow Beach station. However, the Dashwood station on the Lake Huron shore is beginning to exhibit offshore flow. By 0400 LST, the land breeze appears to have become well established on eastern portions of the Lake Huron and Lake Erie shores. Stations along the Lake St. Clair shoreline also have an offshore component. There appears to be a diffluent character to the flow over the eastern portion of the study region but a mesohigh is not clearly indicated by the sea level pressure reports at this time. By 0700 LST, the land breeze on the north shore of western Lake Erie has intensified but the land breeze on Lake St. Clair appears to have dissipated. The diffluent flow over the eastern portion of the study region is still apparent and the sea level pressure at the London station indicates the possibility that a mesohigh is now in place. Calculated divergence values at 10 m for both the areas between Lakes Erie and St. Clair (Triangle A) and Lakes Huron and Erie (Triangle B) are positive for much of the overnight period (Figure 4.1). Surface convergence is implied between the stations along the north shores of Lake Erie and the buoys over the Lake at 0700 LST. In fact, a

persistent, thin line of clouds appears to exist along the major axis of Lake Erie in satellite animations for the morning of August 15 (not shown). Thickening cirrus clouds prevent the line from being traced to the western basin of Lake Erie. However, the station data appear to support its existence there. At 0400 LST, the difference between the air temperature over land and the air temperature over water near the Lake Erie shore was generally near 4°C. No observations are available over water for Lake Huron and Lake St. Clair though lake surface temperature data shown in Figure 4.10 suggest that differences would be smaller than that found at the Lake Erie shore.

Plots of modelled wind, temperature and dew point fields for the periods specified above are given in Figures 4.23, 4.24, and 4.25. At 2100 LST on August 14 (0200 UTC on August 15), modelled 10 m winds are generally out of the northeast with an average speed of 6-9 knots over land. By 0400 LST (0900 UTC) on August 15, winds over the entire study region have veered to become southeasterly with speeds remaining generally in the range from 6-9 knots. Modelled winds over the study region at 0700 LST (1200 UTC) retain a southerly component but the range of speeds becomes 3-12 knots. No land breezes are apparent in the wind pattern at any time though offshore winds are present along some shoreline segments. In fact, a detailed examination of the model output through the period revealed no clear land breeze signatures. Modelled lake-land air temperature differences for Lakes Huron and St. Clair appear to be small at 1-2°C. The modelled temperature difference near the Lake Erie shore exceeds 3°C in places. Plots of

modelled dew point values show that marine air over the lakes was gradually advected northwest over inland areas.

Apart from the absence of clearly detectable land breezes, the modelled fields differed from observations in several respects. Modelled winds were generally about 5 knots higher than observed winds. Though air temperatures over Lake Erie were generally well handled by the model, modelled inland air temperatures were consistently 4-5°C higher than observed (excessive cloud cover does not appear to be the cause). This was likely an important factor in the absence of model land breezes. Lastly, modelled dew points were 1-2°C higher than observed values at many inland locations.

4.2.3.3 August 15 Lake Breezes

Lake breezes developed during the morning of August 15 replacing the land breezes of the preceding period. Time series of station data at Stoney Point on the shore of Lake St. Clair are shown in Figure 4.20. As discussed earlier, the land breeze at this location subsided shortly after 0500 LST. The lake breeze is shown to arrive shortly after 0900 LST accompanied by a decrease in temperature, sharp increases in dew point temperature and wind speed and the onset of onshore flow. The lake breeze continued until outflow from a nearby thunderstorm disrupted the circulation shortly after 1300 LST. Figure 4.21 shows time series of station data at Cedar Point on the shore of Lake Huron. Offshore flow associated with a land breeze is evident until the onset of a lake breeze after

0900 LST. The passage of the lake breeze front is marked by a decrease in temperature and sharp changes in dew point and wind direction. The lake breeze at this station ends abruptly near 1400 LST with a short period of calm then a return to offshore flow. The effect of thunderstorm outflow on the given fields is evident shortly after 1630 LST.

A sequence of mesonet station plots for 0900 LST, 1200 LST and 1500 LST on August 15 is shown in Figure 4.26. At 0900 LST, a land breeze was still active on the Lake Huron shore but a lake breeze had already developed along the north shore of Lake Erie. Temperatures at this time ranged from 23°C over Lake Erie to 27°C at the Stoney Point station while dew points ranged from 17°C to 24°C. By 1200 LST, lake breezes had developed on each of the lakes with the greatest penetration occurring on the northwestern sides. Temperatures at this time ranged from 24°C over Lake Erie to 30°C in Windsor while dew points ranged from 24°C on Lake Erie to 14°C inland at London. By 1500 LST, the Lakes Huron and St. Clair lake breeze circulations had shifted northwestward bringing an end to onshore flow at stations along the southern shores of these lakes. The Lake Erie breeze remained fully developed. Most temperatures and dew points at this time are similar to those at 1200 LST. From mesonet data and visible satellite pictures (not shown), the maximum inland penetration distance of the Lake Erie lake breeze front appeared to be about 25-30 km.

Plots of modelled wind, temperature and dew point fields for the periods specified above

are given in Figures 4.27, 4.28, and 4.29. At 0900 LST (1400 UTC), the modelled winds are out of the south over land and out of the east to southeast over water. There are suggestions of diffluent flow from the southeast sides of each of the lakes. By 1200 LST, lake breezes have developed on each of the lakes but divergent wind patterns suggest that mesohighs are located to the southeast rather than over the centre of the lake in response to the increasing southwesterly gradient wind. At 1500 LST, lake breezes are well-developed but moderately perturbed by the gradient wind. Divergence centres implying mesohighs have reached the southeastern shores of Lakes Huron and St. Clair and have weakened the branch of the lake breeze inflow there. The gradual shifting of the mesohigh in the direction of the gradient wind is also apparent in results over Lake Okeechobee from Pielke (1974), though Pielke fails to comment on this feature. The model predicts an end to onshore flow along the south shore of Lake St. Clair at this time. Easterlies and southeasterlies have become prevalent over the western shores of the lakes with wind speeds near 12 knots.

Modelled temperatures over land gradually increase through the day to 28-29°C at 1500 LST while temperatures over the lakes increase slightly to generally lie between 22°C and 24°C. Tight temperature gradients are evident along the shores of each of the lakes though the gradient along the north shore of Lake Erie extends farther inland behind the lake breeze front. Dew point temperatures at 0900 LST appear to be related to the topography of the region with the lowest values occurring over the highest terrain. By

1500 LST, the influence of the lakes can be clearly seen with tongues of moist air with dew points greater than 21 °C being advected inland to the northwest of the lakes.

When the modelled winds are compared to observed winds, several important similarities and differences are revealed. The MC2 model predicted lake breeze circulations with enhanced penetration on the northwest sides and limited penetration on the southeast sides of the lakes. This closely matches the observed lake breeze evolution and is believed to be due to the influence of the prevailing synoptic wind on this day. However, the model seems to have shifted the circulations slightly too far to the northwest so that locations on the southeast sides of Lakes Huron and St. Clair were not affected by the modelled lake breezes. Rather, the modelled lake breezes stayed just offshore in these areas. The development of moderate southeasterly winds on the western sides of the lakes appear not to be supported by the observations. The New Haven station to the northwest of Lake St. Clair did report a southeasterly wind but its speed was roughly 5 knots lower than the model predicted. In the western Lake Erie basin, shore and buoy winds gave a light south to southwesterly wind rather than the predicted moderate southeasterlies.

Modelled temperatures are generally 1-2°C cooler than observed temperatures at 0900 LST, but closely match observed values by 1500 LST. Lastly, both modelled and observed dew points at 0900 LST show an inverse relationship with terrain elevation though modelled dew points were 1-2°C higher than observed over the northeastern part

of the study region. Both the modelled and observed dew points had the highest values above 20° occurring along the lakeshores.

4.2.4 Evaluation of Model Performance

For both the August 14 and 15 lake breeze simulations, the model demonstrated considerable skill in predicting the general characteristics of the lake breeze circulations with the 5 km grid, based on the above comparisons between the predicted and observed conditions. In both cases, the horizontal extents of the modelled circulations and the predicted surface wind fields were similar to those observed. However, the model was unable to fully recreate the complex wind field on these days, particularly over the western basin of Lake Erie, parts of southeastern Michigan, and in the area near London. Modelled surface temperatures were generally 1 - 2°C below observed values over land which resulted in lower land-lake air temperature differences. In addition, inland dew point temperatures on August 14 generally fell several degrees below observed values by the end of the integration. It is felt that many of the above differences between observed and predicted values may be due to insufficient resolution of the geophysical fields and/or inaccuracies in the nesting data available for the high resolution simulations. Increased resolution of the final model simulation might also help to improve accuracy.

For the August 14-15 land breeze simulation, the model skill was poor. No land breeze circulations could be identified in the model output. Modelled surface winds were

roughly 5 knots higher than observed and modelled inland surface temperatures were generally 4 - 5°C higher than observed. The main problem appears to be that modelled radiational cooling of land surfaces failed to provide low enough air temperatures to decouple near-surface winds from the gradient flow aloft. Lower land temperatures would also have resulted in a greater lake-land air temperature difference and would possibly have led to the development of land breeze circulations. It is possible that this problem is addressed in later versions of MC2. In particular, recent versions that allow the use of the more sophisticated Canadian Land Surface Scheme (CLASS) (Verseghy, 1991;1993) instead of the force-restore surface scheme over land may show improved results in land breeze situations.

Overall, the model appears to be quite useful for 'classic' lake breeze simulations but its utility for 'classic' land breeze simulations appears to be considerably less. This assessment, however, is based on application of the model to only one land breeze case. Application of the model (perhaps a more up-to-date version) to a greater number of 'classic' land breeze problems would help to elucidate this issue.

4.2.5 Severe Weather

As mentioned previously, four reported severe weather events occurred during the case study period. On August 14, a thunderstorm initiated in a lake breeze frontal zone produced a reported funnel cloud that was likely a weak tornado. On August 15,

thunderstorms that formed in the vicinity of the Lake Erie lake breeze front produced a weak tornado and localized heavy rainfall events. A detailed discussion of these events and the synoptic and mesoscale conditions that preceded them follows beginning with a brief discussion of the synoptic-scale dynamics during the case study period.

4.2.5.1 Synoptic-Scale Dynamics

The synoptic-scale features important to severe convective potential throughout the period are briefly discussed using a combination of objectively analyzed upper-air data and morning soundings. The 250 hPa charts with geopotential heights and wind vectors for 0700 LST (1200 UTC) on August 14 and 15 are shown in Figure 4.30. Jet stream winds to 90 knots were occurring over the central United States at 0700 LST (1200 UTC) on August 14. A weaker branch of this jet stream can be seen over southern Ontario with northwesterly winds near 60 knots. By 0700 LST (1200 UTC) on August 15, the height contour pattern had moved north over the eastern part of the continent but was otherwise mostly unchanged. However, the magnitude of jet stream winds over southern Ontario had slightly decreased. Charts showing geopotential heights on the 500 hPa surface are shown in Figure 4.31 with the 500-1000 hPa thickness pattern superimposed. A ridge migrated toward the study region from the west from 0700 LST (1200 UTC) on August 14 to 0700 LST (1200 UTC) on August 15. The thickness pattern remained mostly unchanged over the period with very weak positive thickness advection occurring to the northwest of the Great Lakes. Charts of 850 hPa geopotential heights and temperatures

are shown in Figure 4.32 for August 14 at 0700 LST (1200 UTC) and August 15 at 1900 LST (0000 UTC) and 0700 LST (1200 UTC). The height contours remain relatively unchanged over the period in the Great Lakes region. However, some warming at this level is apparent with the 16°C isotherm reaching the region by 1900 LST (0000 UTC) on August 15. Winds at 850 hPa are shown in Figure 4.33 and are a good representation of the gradient wind throughout the period. The gradient wind over the SOMOS study region was light out of the north-northwest at 0700 LST (1200 UTC) on August 14 then backed slightly to northwest and increased slightly in speed by 1900 LST (0000 UTC) on August 15. By 0700 LST (1200 UTC) on August 15, the gradient wind had decreased in strength and had backed to west. Throughout the period, a broad band of strong southwesterly winds shifted slowly from the central U.S. to the western Great Lakes region. Overall, the above charts suggest little in the way of synoptic-scale enhancement of upward vertical motion in the study region until the late afternoon and evening hours of August 15 when the southwesterly low-level jet occurring ahead of a cold front began to affect the area.

Rawinsonde data from Flint, Michigan (see Figure 2.1 for location) at 0700 LST (1200 UTC) on August 14 and 15 show many similarities, as shown in Figure 4.34. Both soundings had deep conditional instability, weak capping inversions, convective available potential energy (CAPE) values of 1500-2500 J kg⁻¹, and low storm-relative helicity values. The CAPE value for August 14 increases only marginally when the sounding is

modified at the surface with the inland surface temperature and dew point from later in the afternoon. In contrast, the CAPE value for August 15 more than doubles when this modification is applied. Both wind profiles had westerly to northwesterly winds above 800 hPa. On August 14, the west-northwest winds were apparent down to just above the surface level while on August 15, gradual veering of the wind from southerly at the surface to westerly at 800 hPa is evident. In both cases, large amounts of buoyant energy and low storm-relative helicity / wind shear values at low levels point to the likelihood of brief, single-cycle, isolated thunderstorms known as 'pulse' storms (Ford, 1995). A computed storm motion (75% of and 30° to the right of the 0-6 km mean wind) from the northwest near 10 knots in both cases indicates that thunderstorms will be slow-moving.

4.2.5.2 Mesoscale Analysis

August 14

In the presence of warm, moist air and invading lake breezes, deep moist convection commenced in the study region shortly after 1300 LST. The shower and thundershower activity was confined to inland areas where lake breeze fronts had not yet passed.

Showers and thunderstorms that developed in the area between the Lake Huron and Lake St. Clair lake breezes appeared to be forming when outflow boundaries collided with the fronts. Thunderstorms that formed quickly dissipated while drifting to the southeast. A funnel cloud with light damage at the ground, likely a very weak tornado, was reported to have occurred during the afternoon hours on this day though no exact time was given

(Appendix D). The location was near the hamlet of Tupperville about 20 km to the northeast of Lake St. Clair. From animations of radar and satellite images, it appears that a thunderstorm occurred close to this location at about 1500 LST. Figure 4.35 shows the visible satellite image at this time while Figure 4.36 shows mesonet station data and composite maximum radar reflectivity data from 1515 LST (weak echoes over and south of Lake Huron appear to be anomalous). The thunderstorm near Tupperville developed in the vicinity of the Lake St. Clair lake breeze front. Tupperville is located near the northwest edge of the radar echo produced by this storm. The intensity of rainfall was moderate to heavy at this time with reflectivity cores between 46 dbZ and 49 dbZ. Other thunderstorms occurring near the Essex and Morpeth stations appear to have been initiated along lake breeze fronts as well. All of these storms existed for less than an hour. Since the tornado that occurred was apparently associated with a brief thunderstorm, it is likely that it was a 'landspout' type of tornado as described in Chapter 1. Even then, the initial storm development appears not to have been strong enough to generate more than a very weak tornado.

A vertical cross-section through the combined horizontal and vertical wind fields from the model in this region at 1500 LST is shown in Figure 4.37a. The cross-section arrow from west of Lake St. Clair to over Lake Erie is shown with the modelled 10 m wind field at 1500 LST in Figure 4.37b. The cross-section shows well-developed lake breeze circulations over the western shore of Lake St. Clair and the northern shore of Lake Erie.

A shallower circulation cell is evident over the eastern shore of Lake St. Clair. However, vertical velocities reaching over 8 cm s^{-1} are present in the updraft of the eastern Lake St. Clair front and vertical velocities reach over 12 cm s^{-1} along the Lake Erie front. These values are much lower than the 100 cm s^{-1} lake breeze front updraft speed estimated by Lyons (1972) but this is likely attributable to the coarse 5 km grid resolution relative to the 1 - 2 km scale of the observed front. A cross-section along the same arrow through the potential temperature field at 1500 LST is shown in Figure 4.38. Intensely stable air is evident over Lakes Erie and St. Clair but the boundary-layer quickly increases with increasing distance from the lakes. The boundary-layer height between the lakes is about 1000 m. The boundary layer over Michigan west of Lake St. Clair is significantly higher at around 1300 m. Another interesting feature is the region of higher potential temperature than has been lifted from the surface within the Lake Erie lake breeze front.

A modelled profile of wind and thermodynamics variables is plotted for 1500 LST on a skew-T log-P or 'skew-T' diagram in Figure 4.39. The profile location is at a grid point near the Tupperville site. Winds near the surface are out of the northeast and back to northwest above 1.5 km. The wind speed increases with height reaching 65 knots near 12 km. The calculated storm motion is from 355° at 10 knots and the calculated storm-relative helicity values for 0-2 km and 0-3 km are 5 and $6 \text{ m}^2 \text{ s}^{-2}$, respectively. The temperature near the surface increases dry adiabatically to about 1 km then begins to generally follow a moist adiabatic lapse rate to the tropopause. No cap is present in the

sounding. The dew point temperature closely follows a line of constant mixing ratio up to nearly 1 km indicating well-mixed air. Dry layers are present near 2 km and between 4 km and 7 km. The CAPE value is near 920 J kg^{-1} . Modelled wind and temperature profiles are similar to those from the 0700 LST (1200 UTC) Flint rawinsonde data, shown in Figure 4.34a. However, modelled dew point temperature values are significantly lower than those from the rawinsonde data between 4 km and 7 km. The CAPE calculated using the modelled data is also significantly lower than that from the rawinsonde data, mainly due to lower dew point temperatures near the surface.

Clearly, during the afternoon of August 14, the ingredients necessary for the development of thunderstorms were present: a large amount of instability, moist lower layers, and a lifting mechanism - the lake breeze front. However, these ingredients in the modelled atmosphere existed only in diminished quantities. The modelled CAPE was significantly lower, the lower layers were somewhat drier, and the lift generated at the lake breeze fronts was only on the order of 10 cm s^{-1} . Thus, if the conditions predicted by the model had actually occurred on this day, the observed thunderstorms would likely not have developed.

August 15, 1993

The thunderstorms that occurred on this day shall be described with the aid of maximum reflectivity radar images (Figure 4.40) that show each of the August 15 storms at its

maximum intensity. The first deep, moist convection in the study region on August 15 began near 1230 LST near the Town of Tilbury, located on the narrow strip of land between Lakes St. Clair and Erie. Lake breezes from these lakes generated strong convergence there for several hours previous to the convective development. A thunderstorm quickly developed to the east of the town and remained nearly stationary for about one hour. Maximum radar reflectivities in the storm core at 1245 LST (1745 UTC) ranged from 50 dbZ to 57 dbZ. Several funnel clouds and at least one weak tornado occurred in Tilbury near this time (see Appendix D). The vortices were reported to have occurred under cloudy but precipitation-free skies suggesting that the thunderstorm flanking line may have been aligned along the lake breeze convergence zone. In addition, witness reports suggest that the tornado began moving east toward the storm core then moved back along nearly the same path to the west before dissipating. This appears to indicate tornado motion parallel to the lake shore and suggests a link to the lake breeze convergence zone in the vicinity. This tornado, like the one that occurred on August 14, was likely a 'landspout' type of tornado described in Chapter 1 since storm-relative helicity values were very low and since the storm was brief in nature. Also, at the time that the tornado was reported to have occurred, the thunderstorm was undergoing explosive growth - a condition required for the necessary spin-up of a pre-existing vertical vortex.

A stationary thunderstorm developed to the northeast of the first storm near Glencoe by

1430 LST (1930 UTC) and remained stationary for around two hours. Maximum radar reflectivities again reached 50-57 dbZ. The location of this storm was near the estimated location of the Lake Erie lake breeze front at that time. Another thunderstorm formed farther to the east near Dorchester by 1515 LST (2015 UTC). This storm behaved much like the Glencoe storm remaining stationary for nearly two hours and having maximum radar reflectivities of 50-57 dbZ. Again, the location of this storm, roughly 40 km inland from the Lake Erie shore, was very close to the estimated position of the Lake Erie lake breeze front at that time. At a meteorological station near Dorchester, 42 mm of rain was recorded in one hour near 1500 LST (Chadwick, 1994). Rainfall accumulation estimated from the radar data (not shown) suggests that the accumulation rate may have been even greater for the Glencoe storm. It appears that some of the weakest echoes and echoes on the eastern shore of Lake Huron at 1245 LST (1745 UTC) are anomalous. However, strong thunderstorms did also occur on the western shore of Lake Huron and appear to have continually redeveloped on their southwest flanks along a lake breeze front there. Precipitation associated with a low pressure system moving into the area from the west can be seen in the last image at 1515 LST (2015 UTC).

A vertical cross-section through the combined horizontal and vertical wind fields from the model in the vicinity of Tilbury at 1330 LST (1830 UTC) is shown in Figure 4.41. The cross-section arrow from northwest of Lake St. Clair to over Lake Erie is shown in Figure 4.40b. The cross-section shows well-developed lake breeze circulations over the

northwestern shore of Lake St. Clair and the northern shore of Lake Erie. A weaker circulation cell is evident over the southeastern shore of Lake St. Clair. Vertical velocities reaching over 8 cm s^{-1} are present in the updraft of the northwestern Lake St. Clair front and in the region where the Lake St. Clair and Lake Erie fronts meet. A second vertical cross-section through the combined model winds in the vicinity of Dorchester valid at 1500 LST (2000 UTC) is shown in Figure 4.42. The cross-section arrow runs from southeast of Lake Huron to well over Lake Erie as shown in Figure 4.40b. Maximum modelled vertical velocities in the updraft region of the Lake Erie lake breeze front are lower than that near Tilbury at around 4 cm s^{-1} . As with the modelled lake breeze front near Tilbury, upward vertical velocities are significant only up to about the 1000 m level.

Profiles of modelled wind, temperature and dew point fields at 1300 LST (1800 UTC) on August 15 are plotted on a skew-T diagram in Figure 4.43. Winds near the surface are light and southerly but veer gradually with height to northwesterly at 60 knots at about 13 km. The computed storm motion is from 304° at 8 knots and the calculated storm-relative helicity values for 0-2 km and 0-3 km are both $12 \text{ m}^2 \text{ s}^{-2}$. The temperature increases from the surface to greater than 1 km nearly dry adiabatically at which height there is a very weak capping inversion. The sounding has a significant region of conditional instability between 3 km and 9 km. The dew point value is greater than 20°C at the surface and remained within a few degrees of the temperature through most of the sounding. A CAPE value of nearly 2000 J kg^{-1} is computed indicating a significant degree

of instability. The modelled wind profile is very similar to that obtained via the 0700 LST (1200 UTC) Flint rawinsonde shown in Figure 4.34b. Values for storm motion and storm-relative helicity are also very similar. The modelled temperature profile also shows many similarities to the rawinsonde data above the surface. In contrast with the August 14 model data, the modelled dew point temperatures on August 15 appear to be warmer than observed through most of the troposphere. The most significant differences occur between roughly 6 km and 10 km. The CAPE value derived from the model data is roughly 300 J kg^{-1} higher than that derived from the rawinsonde data, though observed CAPE values at Flint likely would have been higher in the afternoon. As with the August 14 case, the modelled storm environment on August 15 appears to be lacking in the ingredients required for the development of thunderstorms, with the possible exception of instability which the model was able to generate in moderate quantities.

An interesting aspect of the storms on August 15 was their quasi-stationary nature. For the Glencoe and Dorchester storms, it was clearly this characteristic that led to heavy rainfall over small areas. For the Tilbury storm, it may have been the quasi-stationary storm motion that resulted in the unusual tornado movement reported there. Similar types of storms over southwestern Ontario have been investigated by Clodman and Chisholm (1994), as mentioned in Chapter One. These storms were quasi-circular having a diameter near 15 km, usually lasted about two hours, were quasi-stationary producing heavy rainfall over small areas, occurred in groups of two or more separated by clear areas, and

developed in environments of relatively low wind speeds and wind shears in the low to middle troposphere and moderate instability and moisture. They suspect that lake breezes were occurring when these storms developed. This storm type certainly appears to apply to the storms of August 15 and the observations and modelling on this day seem to confirm their suspicion that lake breezes, in particular the lake breeze fronts, contribute greatly to the development and maintenance of these storms.

4.2.6 Ozone Transport

4.2.6.1 August 14 Lake Breezes

Forty-eight hour 900 hPa back trajectories obtained from OMEE for Windsor and Sarnia at 1300 LST (not shown) suggest that the air mass on August 14 was effectively stagnant. Air originating near western Lake Erie at $t - 48$ hours had travelled north to near Flint, Michigan before arriving at Windsor during the afternoon. Air arriving at Sarnia originated near London at $t - 48$ hours and had travelled north over southern Lake Huron before arriving at the site. Summer high ground-level ozone events in southern Ontario are most frequently associated with southerly or southwesterly air flow on the back side of an anti-cyclone (Heidorn and Yap, 1986). In that situation, a large fraction of the ozone in southern Ontario is likely to have originated in heavily industrialized areas of the United States to the south and southwest of Ontario (Yap *et al.*, 1988). However, in a flow situation that has been stagnant for 48 hours, most of the ozone precursors (NO_x and RHC) and residual ozone would likely have originated within or near the SOMOS

study region. The most likely area and point sources of ozone precursors in the study region are located in the urban and industrialized areas of Windsor-Detroit and Sarnia-Port Huron. Significant local impacts on ozone levels have been observed downwind of these areas (Yap *et al.*, 1988; Kelly *et al.*, 1986). It will be shown later that maximum ozone concentrations on August 14 were highest near these locations.

Early morning ground-level ozone concentrations in the study region on August 14 ranged from near 0 ppb to 20 ppb. Light winds with land breezes overnight resulted in most ozone within the nocturnal boundary layer over land being scavenged either by dry deposition or by titration with NO emitted into the layer. However, ozone concentrations at all stations increased rapidly as the nocturnal inversion began to break down around 0800 LST and ozone-rich air that resided above the nocturnal boundary layer was mixed down to the surface. Most stations reported a 15-35 ppb increase in ozone concentration between 0800 LST and 1000 LST. Morning ozone increases of this magnitude are only slightly greater than that typically due to photochemical production, so down-mixing of ozone appears to be of secondary importance at these stations. However, the Warren and East 7 Mile stations north of Detroit had ozone increases in this time period greater than 50 ppb and the Sarnia and Port Huron stations showed increases greater than 80 ppb. These rapid and substantial increases are attributable mainly to down-mixing. The Port Huron station also reported a large but relatively brief increase in the primary pollutant SO₂ as the nocturnal inversion broke down. A similar large increase in SO₂ was not

reported at other stations in the study region that measured this pollutant including Sarnia and those in the vicinity of Windsor-Detroit.

Maximum ozone concentrations at sites in the study region on August 14 are shown in Figure 4.44. Hourly-averaged ozone maxima were greater than 80 ppb (the Ontario one-hour ozone criterion) at many of the stations between Windsor-Detroit and southern Lake Huron. The region that experienced the highest ozone concentrations was Sarnia-Port Huron with stations reporting one-hour average values up to 147 ppb. The region to the southwest of Lake St. Clair including Windsor and Detroit also experienced high ozone concentrations with the Warren station reporting a one-hour average concentration of 128 ppb.

It is quite difficult to detect changes due to the arrival of the lake breeze circulation with hourly-averaged ozone data. Large changes at the lake breeze front can occur over a period of few minutes so any signature in hourly-averaged data is often smoothed to varying degrees. Hourly averaging also causes a lag in response from five minutes to over one hour depending on the point within the hour that the front passed the station. Thus, in cases with changes in ozone concentration occurring at the time of the lake breeze frontal passage, it is occasionally impossible to tell whether an increase or a decrease in ozone has occurred. A data set with a minimum of 5 minute, perhaps 10 minute, time resolution would be required to accurately analyze ozone response to lake breeze frontal

passages. Ozone is also a dynamic variable in that temporal changes are caused by chemistry as well as meteorology. Nevertheless, an attempt is made here to investigate the impact of lake breeze frontal passages on surface ozone concentrations.

Times series of wind direction and ozone concentration at Sarnia (Figure 4.45a) and Port Huron (Figure 4.45b) suggest that increases in ozone occurred with the passage of the Lake Huron lake breeze front. At Sarnia, the wind direction shifted to onshore by 1100 LST and the one-hour average ozone concentration rapidly increased by 20 ppb from 1100 LST to 1200 LST. Ozone reached a maximum concentration of 130 ppb at 1300 LST before beginning a rapid decline. The lake breeze front passed Port Huron by 1400 LST, as indicated by the shift to onshore winds, and was likely better developed than when it had passed Sarnia. This may explain the ozone 'spike' to 147 ppb at 1400 LST observed at Port Huron compared to the slightly more gradual rise and fall in ozone concentrations after the front passed through Sarnia. SO₂ concentrations at both of these stations (not shown) increased rapidly with the arrival of the lake breeze front then decreased at a somewhat slower rate behind it.

Figure 4.46 shows the observed surface wind field, estimated lake breeze front positions and one-hour average ozone values valid at 1300 LST in the SOMOS study region. Ozone concentrations varied greatly across the region at this time. The highest (130 ppb at Sarnia) and lowest (59 ppb at Grand Bend) values were both reported at stations along

the Lake Huron shore. Other than for Sarnia and Port Huron, ozone concentrations differences across the lake breeze fronts appear to be insignificant. Concentrations at stations southeast of Lake Huron and north of Lake Erie were well below the one-hour criterion of 80 ppb and ozone time series at these stations (not shown) failed to indicate any significant changes with the passage of a lake breeze front. Ozone time series at stations along the western shore of Lake St. Clair (not shown) indicate that an initial peak in concentrations occurred at 1300 LST with one-hour average concentrations of 102 ppb at the East 7 Mile station and 94 ppb at the Warren station. However, ozone increased by 30-40 ppb as the Lake St. Clair lake breeze front passed near 1600 LST reaching secondary peak values of 124 ppb and 128 ppb, respectively (there is also a suggestion of a tertiary peak in the ozone time series at these stations as the Lake Huron lake breeze passed between 1900 LST and 2100 LST). The above observations suggest that lake breezes delivered high concentrations of ozone mainly to locations in the vicinity of Sarnia-Port Huron and north of Detroit. Little or no change in ozone concentration with the passage of a lake breeze front was observed at stations in other locations.

There are several possible reasons why some areas experienced a large increase in ozone with a lake breeze frontal passage while others did not. One hypothesis, illustrated in Figure 4.47a, is that localized pools of ozone precursors over Lakes Huron and St. Clair, originating from sources in the Windsor-Detroit and Sarnia-Port Huron areas, underwent photochemical processing after sunrise to produce high ozone concentrations offshore. A

temperature inversion may also have helped to confine the high ozone concentrations to a near-surface layer over the lake but this process is not considered in this simplified model. As lake breezes advected marine air inland, concentrations of ozone rose sharply at observation stations in the path of these ozone pools while little change was observed elsewhere. A similar mechanism has been invoked for such locations as the western shore of Lake Michigan (Lyons and Cole, 1976) and the north shore of Lake Ontario (Hastie *et al.*, 1998).

However, the confirmed presence of an ozone-rich layer aloft, greatly enhanced near urban / industrial areas (Windsor-Detroit, Sarnia-Port Huron), leads to another hypothesis as illustrated in Figure 4.47b. Suppose that relatively high concentrations of ozone remained in a layer above the deepening daytime boundary layer over land near Windsor-Detroit and Sarnia-Port Huron. This ozone-rich air would likely have been entrained by lake breeze circulations as they moved inland and downward motion in the wake of lake breeze fronts accompanied by mixing in the thermal internal boundary layer may have delivered ozone to the surface in these areas. In locations where air above the boundary layer had roughly the same ozone burden as air near the surface, downward motion and mixing behind the lake breeze fronts would have delivered air that had little effect on ozone concentrations at the surface. The fact that ozone and SO₂ increases were observed at Port Huron both when the nocturnal inversion broke down and when the lake breeze front passed also lends support to this hypothesis since this suggests that a similar supply

of polluted air was being tapped in both instances. If air from aloft was delivered to the surface, one would expect that air to be drier than the marine air it replaced. Indeed, the dew point temperature time series for Cedar Point, Walnut and Morpeth stations, shown previously in Figures 4.20 and 4.21, show a period of decreasing values following the initial surge in dew point associated with the passage of the lake breeze front.

Both of these hypotheses were investigated using passive tracers with 5 km grid MC2 model runs. Recall that tracer variables are not passed through vertical or horizontal boundary-layer diffusion parameterizations so that tracer motions represent pure semi-Lagrangian advection. Also, only initial values at 0700 LST (1200 UTC) are provided. Boundary values are set to zero through the integration. To test the first hypothesis, the model tracer was initialized to 120 units from the surface up to 200 m over extreme southern Lake Huron, Lake St. Clair, and western and eastern Lake Erie. Tracer values in other locations were set to zero through the vertical column. These tracer pools or 'blobs' were intended to represent ozone that had formed after sunrise in a shallow layer over the lakes. The movement of tracer within the modelled wind field is illustrated in Figure 4.48. Figure 4.48a shows the initial state of the tracer field at 0700 LST (1200 UTC). By 1100 LST (1600 UTC), the tracer blobs have moved to the southwest with tracer spreading out along the lake breeze front south of Lake Huron (Figure 4.48b). The amount of tracer remaining at the surface had decreased substantially by 1500 LST (2000 UTC), shown in Figure 4.48c. Tracer has continued to spread out along and ahead of the

Lake Huron and Lake St. Clair lake breeze fronts and tracer from Lake Erie has moved well inland over the southern shore. By 1900 LST (not shown), almost none of the tracer can be found at the surface level. A vertical cross-section through the tracer field along the lake breeze fronts, shown in Figure 4.48d, reveals that tracer was lofted to heights above 1000 m at the fronts. By 1900 LST, all of the tracer that had initially been at the surface over Lakes Huron and St. Clair had been transported aloft by lake breeze circulations. Similar behaviour was reported by Lyons *et al.* (1995). Using a three-dimensional mesoscale meteorological model coupled with a Lagrangian particle dispersion model over Lake Michigan, they showed that an ozone plume at the surface can be entirely translocated aloft in the updrafts of a lake breeze front. The present tracer simulation shows some similarities with the observed ozone data. In particular, large amounts of tracer moved inland over Sarnia and Port Huron and the amount of tracer left at the surface later in the day was substantially less. However, large amounts of tracer moved southwest of Lake St. Clair over Windsor and did not affect the areas to the west of the lake that showed large ozone increases associated with the passage of the lake breeze front.

The second hypothesis was tested using a sheet of tracer initialized at 120 units between 500 m and 1000 m and at 0 units at all other levels. A layer at this height would reside above the top of a typical nocturnal boundary layer over land as well as a boundary layer developing after sunrise. In this case, the tracer was intended to represent a layer of

residual, elevated ozone aloft. The tracer was initialized in this layer over the entire study region rather than over just the urban / industrialized areas so that the tracer behaviour could be gauged over a wider region. To examine the movement of tracer within the modelled wind field, a sequence of cross-sections were made through the tracer field. The cross-section location used here, shown in Figure 4.49f, is the same that was used in the previous section for the severe weather discussion on August 14 (see Figure 4.37b). The cross-section runs from west of Lake St. Clair to over Lake Erie. Since the modelled lake breeze front south of Lake Huron was weaker than observed, it was felt that cross-sections through the more intense Lake St. Clair and Lake Erie lake breeze fronts provide a better illustration of this mechanism. Winds at 1500 LST (2000 UTC) in the vicinity of the lake breeze circulations are shown along this cross-section in Figure 4.37a. Figures 4.49a through 4.49e show that the tracer aloft was transported downwards behind the lake breeze fronts and, to a lesser extent, upwards just ahead of the lake breeze fronts. By 1500 LST (2000 UTC), significant amounts of tracer began to reach the surface over Lake St. Clair and tracer had been transported downward over Lake Erie and was beginning to move inland with the lake breeze inflow above 60 m. At 1900 LST (0000 UTC), tracer had reached the surface over Lake Erie and had also started to recirculate in the frontal vortex. Significant amounts of tracer had also been lofted by the lake breeze front updrafts to heights greater than 1700 m. Tracer amounts at the 200 m level at 1500 LST (2000 UTC) are shown in Figure 4.49f. Large amounts of tracer are evident at this level on the lakeward side of the lake breeze fronts, including Sarnia-Port Huron and areas

west of Lake St. Clair. Clearly, tracer takes several hours to reach the surface but testing of the model at 2 km grid spacing has shown that vertical velocities at the lake breeze front increase with increasing model resolution, presumably up to the resolution of the actual front (roughly 1 km across). Thus, downward movement of tracer is too slow at 5 km resolution to explain the rapid increases in observed ozone concentration at some stations but would be much faster (possibly several times faster) if the model grid spacing was on the order of the width of the lake breeze front. Also, tracer may have reached the surface at a somewhat faster rate if the tracer variable were diffused vertically and horizontally.

The results of the tracer experiments suggest that motions within the lake breeze circulation can dominate the local transport of ozone and that the initial level at which the ozone resides is important. In addition, the two transport mechanisms discussed above would have been further complicated by motion parallel to the shore, a factor not considered for these simplified models. In the case of August 14, either scenario (or possibly some combination thereof) may have occurred. Since ozone data exist neither in the vertical nor over the lakes for August 14, it is difficult to speculate further on the scenario responsible.

4.2.6.2 August 14 - 15 Land Breezes

Ozone concentrations between August 14 at 1800 LST and August 15 at 1200 LST at the

19 observation stations (not shown) fell gradually overnight reaching minimum values near 0700 LST with no concentration greater than 22 ppb and several stations near 0 ppb at that time. Concentrations increased rapidly as the nocturnal inversion began to break up at 0900 LST on August 15, again revealing an ozone-rich layer aloft. Since ozone concentrations remained relatively low overnight, this pool of ozone-rich air aloft must not have been tapped. This suggests that weak subsidence over land associated with the land breezes must not have brought air down from this level, possibly due to the shallow nature of this circulation. Since no chemistry observations were made over the lakes, the behaviour of ozone concentrations in the vicinity of a land breeze front could not be examined.

4.2.6.3 August 15 Lake Breezes

Ozone concentrations in the study region on this day did not reach levels as high as those reported on August 14. The maximum one-hour ozone concentration recorded in the Ontario portion of the study region was 81 ppb at the Windsor Main station at 1500 LST and 1600 LST while all other stations had maximum one-hour concentrations below the 80 ppb criterion. In the Michigan portion of the study region, ozone concentrations climbed above the 80 ppb criterion north of Detroit and near the northern portion of Lake St. Clair. The Warren station west of Lake St. Clair and north of Detroit had the highest maximum ozone concentration in the study region on August 15 with a value of 101 ppb at 1600 LST. The location of high ozone concentrations near and north of Windsor-

Detroit and Lake St. Clair is mainly attributable to the south-southwesterly general flow on this day. Lake breezes that occurred on all of the lakes likely had some degree of influence on the locations of high concentrations and possibly low concentrations as well but signatures due to lake breezes were too weak to arrive at any conclusions.

4.3 'Highly-Perturbed' Lake Breezes during ELBOW: July 14, 1997

4.3.1 Overview

One goal of the ELBOW field project was to collect meteorological observations in the vicinity of lake-induced cloud lines that tend to occur in association with moderate surface winds, especially those from the southwest that blow along parallel Lake Huron and Lake Erie shoreline segments. It is suspected that these cloud lines, which have been implicated in the initiation of severe weather (King, 1996), are fronts associated with highly-perturbed lake breeze circulations. However, their true nature has been difficult to characterize due to sparsity of observational data, ambiguous signatures in satellite and surface data, and suspected frictional and topographical effects in the region. ELBOW field observations, GOES-8 visible imagery, weather radar data and MC2 modelling results are used here to elucidate the origins and evolutions of lake-induced cloud lines observed during an ELBOW IOP on July 14, 1997. The importance of these lines to the development of thunderstorms, including a severe storm, on this day will also be discussed.

4.3.2 Synoptic Conditions

To determine the effect of synoptic-scale weather patterns on the lake breezes of July 14, 0700 LST (1200 UTC) analyses from the Canadian SEF (spectral finite element) global numerical model are examined. The gradient wind strength and direction are of particular importance. For brevity, the discussion will be focussed on features that directly affected the conditions in and near the study region on July 14. Additionally, upper-air dynamics will be discussed in the severe weather section.

The mean sea level pressure analysis is shown in Figure 4.50a. A weak area of low pressure was centred over northern Ontario with a central pressure of about 1003 hPa (1003 mb). A broad area of high pressure was located over the southeastern U.S. A cold front was situated along the pressure trough from northern Ontario southwest into Texas while a warm front extended east from the low centre along a secondary pressure trough. The study region was located in the warm sector of this large, open, baroclinic wave. Isobars in the warm sector had a WSW-ENE orientation suggesting a nearly westerly gradient wind. Winds at the 850 hPa level over the study region, just above the friction layer, were also westerly at about 20 knots (Figure 4.51b).

The sea-level pressure pattern from the coarse resolution MC2 run with 100 km grid spacing is shown in Figure 4.50b. A 999 hPa low pressure centre was located at the Ontario / Minnesota border. Although suggested by the 850 hPa wind analysis

(Figure 4.51b), this low was not found on the sea-level pressure analysis. Examination of the model data indicates that both low pressure areas were present in weaker forms in the early morning hours of July 14. The model weakened the more northerly low and deepened the more southerly low. The opposite appears to have occurred in the analyses (an experimental 100 km grid run with a later version of the MC2 model produced a solution much closer to the analyses in this case). Though shifted slightly to the south, the model isobars have nearly the same orientation and spacing as those in the analysis. Also, the modelled pressure pattern is somewhat different over the southeastern U.S.. The high pressure region produced by the model is weaker and not as well defined as in the analysis. Even with the above differences, the pressure patterns near the study region were considered sufficiently similar to provide adequate nesting data for the intermediate run.

The pressure pattern from the intermediate run with 25 km grid spacing valid at 1600 LST (2100 UTC) is shown in Figure 4.52. The modelled low centre had deepened to 996 hPa over northwestern Ontario and pressure values over the study region varied from 1004 hPa to 1008 hPa. These values are significantly less than observed values at mesonet stations (not shown) which ranged from 1008 hPa to 1011 hPa. The model pressure gradient is also significantly greater than that in the station data. This suggests that the modelled gradient wind was somewhat greater than observed though this comparison may be complicated by the lake-breeze-induced pressure perturbations in this region.

The 0700 LST (1200 UTC) sounding from the DTX station northwest of Detroit, Michigan showed considerable instability even with the nocturnal inversion present near the surface. As shown in Figure 4.53, the temperature at 850 hPa was near 20°C with dew point temperatures near the surface also around 20°C. Winds near the surface were light though the maximum wind speed of the sounding occurred near the 800 hPa level indicating the presence of a low-level jet. Winds above 400 hPa were relatively light and were generally from the southeast.

In the study region, a moderate southwesterly surface wind was accompanied by inland temperatures up to 34°C and unusually high dew point temperatures up to 27°C. Lake surface temperatures, shown in Figure 4.54, varied significantly across the Great Lakes and also on each Lake. Values in the study region ranged from a minimum of 16°C on Lake Huron to a maximum of 24°C on western Lake Erie. Typical land-lake air temperature difference values at 1500 LST were around 12°C across the Lake Huron shore, 7°C across the Lake Erie shore and 9°C across the Lake St. Clair shore.

4.3.3 Mesoscale Observations, Model Results and Comparisons

The mesoscale conditions prior to the development of intense afternoon convection over southwestern Ontario will be described with the assistance of four visible satellite images, shown in Figure 4.55. Near 0500 LST, several hours before the time of the first satellite image shown, a band of scattered showers and thunderstorms began to move into western

parts of southern Ontario. Initially, the band stretched from Lake St. Clair to eastern Lake Huron. By 0615 LST, only the portion of the band east of Lake Huron remained and continued to move slowly to the east. By 0745 LST, the band of showers and thunderstorms east of Lake Huron began to weaken and a new line of thunderstorms developed to the southeast of Lake Huron. This line took on squall-line characteristics and moved inland as far as eastern Lake Erie as shown in Figure 4.55a valid at 1032 LST (1532 UTC). These showers and thunderstorms dissipated shortly after 1100 LST. ELBOW mobile observers reported light tree damage and a few flooded fields with these storms. Convective debris from these storms moved slowly off to the north with the weak upper-level winds and thunderstorm outflow boundaries appeared to rapidly dissipate. Except when affected by showers and thunderstorms, observed early morning surface winds across the study region were out of the south or southwest while inland surface temperatures remained between 19°C and 24°C and dew points generally remained above 15°C.

Figure 4.55b shows the clouds observed at 1232 LST (1732 UTC). Convective debris (mainly cirroform) from the earlier showers and thunderstorms was present east of Lake Huron. A small area of convective debris was also located southwest of Lake Huron over Michigan. Fair weather cumulus had begun to develop south and west of Lake Erie as well as east of Lake Huron. A line of these cumuli is evident to the southeast of Lake Erie. Skies over the lakes were relatively free of cumulus clouds.

By 1402 LST (1902 UTC), the amount of cumulus cloud had increased except in areas over and downwind of the lakes (Figure 4.55c). Over southwestern Ontario, two cloud lines had developed aligned with the southwesterly wind. Animation of these satellite images suggests that these lines originated from headlands along the north shore of Lake Erie. These cloud lines remained nearly stationary with respect to the Lake Erie shore while gradually extending farther inland to the northeast into the region of convective debris. Thunderstorms had also developed near the south shore of Lake Erie with cirrus anvils blown off to the northwest. The skies over the lakes remained relatively free of convective cloud.

In the last image in this sequence, shown in Figure 4.55d, an area of enhanced cumulus convection is apparent east of the Exeter base site near the centre of the image. The area is bounded by clear regions to the northwest and to the southeast that extend inland from Lakes Huron and Erie. Other clouds lines and cloud 'edges' are evident from west of Lake St. Clair to over western Lake Huron, to the southeast of Lake Erie, and to the north of Lake Ontario. Thunderstorms that formed near the south shore of Lake Erie were continuing to eject cirrus anvil clouds to the northwest. Again, the skies over the lakes remained relatively free of convective clouds.

Figure 4.56 shows a visible satellite image valid at 1545 LST and centred over the study region. The positions of cloud lines, estimated from animations of satellite imagery, are

indicated using dashed lines on the lakeward edges of the cloud lines. Rapidly developing convection can be seen where the Lake Huron and Lake Erie lines appear to meet. Showers and thunderstorms were also forming along the lakeshores of eastern Michigan. Convective debris from thunderstorms initiated at a cloud line along Lake Erie's south shore are evident over Lake Erie. Convective debris from morning showers and thunderstorms is also visible east of Lake Huron. Figure 4.57 is a close-up satellite view of the study region at 1545 LST with surface observations superimposed. The ELBOW base station at Exeter (solid station marker) had a temperature of 33°C and a dew point of 25°C at 1545 LST. The temperature and dew point at the Lake Huron shore were 31°C and 25°C. At the Lake Erie shore, the temperature and dew point were 26°C and 23°C. Thus, temperatures increased and relative humidity decreased with increasing inland distance. Differences between inland temperatures and air temperatures at buoys (not shown) were about 7°C for Lake Erie and 13°C for Lake Huron. Surface parameters on either side of the cloud lines present at this time showed small or negligible differences. Any lake breeze signals were very weak. However, winds at stations between Lakes Huron and Erie suggest larger-scale surface convergence.

A rawinsonde was launched from the Exeter base station at 1511 LST (2011 UTC) as part of the ELBOW IOP measurements that day. It gathered atmospheric profile data just as intense convection commenced in the area. A skew-T diagram with data from this sounding is shown in Figure 4.58a. Unusually high dew points were clearly limited to the

near-surface layer supporting the notion that they were likely the result of enhanced evapotranspiration due to heavy morning showers and thunderstorms and high temperatures on that day.

After 1545 LST, convection intensified at the apparent point of merger of the Lake Huron and Lake Erie cloud lines and at cloud lines along the lakeshores of eastern Michigan. A more detailed discussion of the subsequent storms and the 1511 LST rawinsonde data is given in a later section.

The 5 km model run was initialized at 0700 LST and was carried out to 1900 LST. The development of convergence lines was studied using cross-sections and animations of various fields such as the horizontal and vertical wind fields. Weak lake breezes began to form by 0800 LST but were limited to about 300 m in depth (inflow depth plus return flow depth). As the circulations increased in strength and depth, they were shifted downwind by the southwesterly flow causing lake breeze fronts approximately aligned with the wind to stretch toward the northeast. By 1130 LST, lake breeze circulations had grown to about 900 m in depth and lake breeze fronts along the lakeshores of eastern Michigan (from western Lake Erie to western Lake St. Clair to western Lake Huron) began to link together. Lake breeze circulations were near their maximum depth at 1600 LST with updraft regions reaching up to 2000 m in height. Figure 4.59 shows positive vertical motion at 500 m valid at 1600 LST with the modelled surface wind field

superimposed. Several convergence lines are apparent. The strongest is the line associated with the linked lake breeze fronts along the lakeshores of eastern Michigan from western Lake Erie to western Lake Huron. Other strong convergence lines are associated with lake breeze fronts along the north and south shores of Lake Erie with the convergence line north of Lake Erie extending inland to the northeast. A much weaker convergence line associated with a lake breeze front south of Lake Huron also extends inland to the northeast. Another weak line is located over inland southeastern Michigan northwest of Lake St. Clair and is likely caused by a topographic feature there (see the topographic map in Figure 2.24). The general pattern of lines is similar to that indicated in Figure 4.56 though the lines observed by satellite north of Lake Erie appear to be located farther inland. A cross-section through both the Lake Huron and Lake Erie convergence lines is shown in Figure 4.60 valid at 1600 LST. The entire Lake Huron lake breeze circulation has been shifted to the northeast. Thus, its western front is located over water on the western side of the lake and its descending branch is located nearly over the southern shore. As a result, its southern front, located near the southern shore, is much weaker with a severely restricted inflow depth. The Lake Erie front is located well inland with a narrow but intense region of upward vertical motion exceeding 10 cm s^{-1} . Air temperatures over land exceed 32°C while much cooler temperatures between 22°C and 24°C are evident over the Lakes Huron and Erie, respectively. A nearly dry adiabatic lapse rate near 9°C km^{-1} exists in the lowest kilometre over land while strong temperature inversions are evident over the lakes. Based on these and other cross-sections, and

animations of the development of these lines, it is believed that most of the cloud lines indicated in Figure 4.56 are indeed lake breeze fronts though the front south of Lake Erie is likely enhanced by the steep topography there. Clearly, lake breeze circulations and their associated fronts are highly perturbed by the large-scale wind field on this day.

Weak, modelled convergence lines also appear along the eastern shore of Lake Huron and the northern shore of central Lake Erie (Figure 4.59). Animations show that these lines are nearly stationary over the shorelines. They appear to be caused by frictional drag as fast-moving air over water encounters the rough and quickly rising terrain. Potential temperature profiles over these areas (not shown) give boundary layer heights of less than 100 m. Thus, clouds would not be expected to form with these convergence lines and are not apparent at those locations in the satellite imagery (Figure 4.56).

Figure 4.61 summarizes the suggested causes of convergence and cloud lines at 1545 LST based on satellite and surface observations and the MC2 model output. The Lake Erie lake breeze front along the north shore begins at the extreme western edge of Lake Erie and continues northeast as a series of frontal segments originating from segments of coastline aligned with the southwesterly wind. The model output suggests that these frontal segments begin as convergence lines in the lowest few vertical levels and grow in depth north of the shore. The weak lake breeze front southeast of Lake Huron is shown extending inland to the northeast and merging with the Lake Erie front. The western-most

segment of the Lake Erie front also joins the lake breeze front along the western shore of Lake St. Clair. At 1545 LST, the front along western Lake St. Clair is also linked to the front over western Lake Huron. Cross-sections of a combination of horizontal and vertical wind fields (not shown) show a continuous horizontal vortex along the length of these fronts from western Lake Erie to western Lake Huron. A lake breeze front on the southeast shore of Saginaw Bay in Michigan intersects the western Lake Huron front over the lake. The modelled vertical velocity field (not shown) indicates enhanced vertical motion at the point of intersection of these fronts. As stated previously, it is believed that the cloud line along the southeastern shore of Lake Erie is a lake breeze front enhanced by upslope flow along steep terrain near the shore. Also, the topography of inland southeastern Michigan appears to cause a weak convergence zone there. Lastly, weak convergence zones are thought to be caused by frictional effects as fast-moving air over water encounters relatively rough and steeply rising terrain along the eastern shore of Lake Huron and the northern shore of central Lake Erie. For each of the lakes, the southwesternmost and northeasternmost parts of the lake breeze circulation appears not to support a front.

As with the August 14 case, estimates of frontal positions are expected to have an associated error of about ± 5 km due to surface station spacing, the time between surface observations, and possible errors in the correlation between cloud lines on visible satellite imagery and the actual positions of lake breeze fronts near the surface.

An estimate of the skill and utility of the model predictions on the 5 km grid can be made by comparing model parameters to observed parameters at selected times. Three times were selected for comparison: 1000 LST (lake breezes just beginning), 1300 LST (lake breezes underway on all lakes) and 1600 LST (lake breezes fully developed before severe storm begins). Comparisons beyond this time are inappropriate since deep convective processes not fully represented by the model physics begin to dominate. The discussion will consider modelled surface winds (Figure 4.62), temperatures (Figure 4.63), dew points (Figure 4.64) and observed values of these fields (Figure 4.65). A modelled temperature, dew point and wind profile at 1500 LST will also be compared to the 1511 LST rawinsonde profile.

At 1000 LST (1500 UTC), modelled winds are mainly out of the southwest except over much of Lake Huron where southerly flow is predicted (Figure 4.62a). The strong deviation in winds over Lake Huron appears to be the combination of lake breeze effects and stability effects. The modelled Lake Huron lake breeze circulation extends from the surface to about 250 m at this time. The lake breeze inflow has a component from the southeast that appears to cause part of the deviation of the wind over the lake. In addition, an intense temperature inversion is present over the first several levels of the model over Lake Huron. Changes in vertical gradients of the horizontal Reynolds stress that occur in a stably-stratified layer can alter the balance of forces in this layer and can cause a deviation of up to 20° in the surface wind toward lower pressure (Sorbján, 1989). Thus,

in the stably-stratified layer near the surface over Lake Huron, this effect could also contribute to the deviation in the surface wind. In fact, wind profiles over the lake (not shown) indicate that the deviation is strongest at the lowest levels where the inversion is most intense. On Lake Erie and Lake St. Clair, lake breezes are just beginning to develop. Modelled wind directions closely match observations but modelled wind speeds are, on average, about 5 knots higher than observed. Modelled temperatures are slightly warmer over land on average but temperatures over the lakes appear to closely match. Modelled dew points temperatures are slightly greater than observations across the study region.

At 1300 LST (1800 UTC), modelled winds over Lake Huron continue to be from the south though the lake breeze circulation at this time has grown to about 1200 m in depth. Deviations in the wind field due to a lake breeze component from the southeast are apparent in the northwest corners of Lakes Erie and St. Clair. Modelled wind speeds again appear to be roughly 5 knots higher than observations on average. Modelled temperatures across the study region at this time appear to closely match the observations. However, modelled dew point temperatures have begun to fall several degrees Celsius below observed values on average.

Finally, at 1600 LST (2100 UTC), the modelled wind field is showing widespread deviations in direction from southwest. These deviations are also evident in the observed wind field. Important similarities exist between modelled and observed wind directions

over western Lake Erie and near Lake Huron. Modelled wind speeds remain roughly 5 knots greater than observed in general. Modelled temperatures are generally within 1°C of observed values. However, the differences between the modelled and observed dew points have increased since 1300 LST. Whereas the model appears to bring drier air to the surface east of Lake Huron with dew point temperatures falling below 19°C, observations show dew point values near 25°C in the same region. Dew point values are generally less than observed across the study area at this time.

A modelled vertical profile of wind and thermodynamic variables, shown in Figure 4.58b, was produced for 1500 LST at the grid point corresponding to Exeter for comparison with the rawinsonde data measured there beginning at 1511 LST. Near the surface, the modelled and observed soundings are similar with nearly dry adiabatic lapse rates, surface temperatures near 33°C and a nearly constant mixing ratio. However, a very moist observed surface dew point of 25.9° was not predicted by the model. This causes a large difference in the modelled surface-based CAPE value calculation. For the observed sounding, a CAPE near 6200 J kg⁻¹ was calculated while a CAPE of less than 1700 J kg⁻¹ was calculated from the modelled profile values. However, if the modelled surface dew point is modified to match the observed surface dew point, a CAPE near 5200 J kg⁻¹ is obtained. The modelled profile above the near-surface layer is different from the observed profile in several respects. First, the modelled profile has a relatively warm, moist layer at 700 hPa (700 mb) that acts as a capping inversion. This feature is not present in the

observed profile data. Second, the observed sounding has a prominent dry layer between 300 hPa and 400 hPa. This dry layer is missing from the modelled profile with modelled dew point depressions at 300 hPa about 23°C less than that observed. The modelled wind profile closely matches the observed wind profile below 11 km with the exception of modelled wind speeds near the layer between 700 hPa and 800 hPa that are roughly 10 knots weaker than those observed. Due partly to this difference, storm-relative helicity values calculated from the modelled wind profile data are much less than those calculated from the observed profile data. Above 11 km, modelled winds back from southwest to southeast with height while the opposite occurs in the observed profile data.

4.3.4 Evaluation of Model Performance

Based on the above comparisons, the model appears to predict wind direction and temperature at the surface with considerable skill but produces winds that are consistently higher than observations by roughly 5 knots and dew point temperatures significantly lower than observed. The unusually high observed surface dew points on this day were likely the result of enhanced evapotranspiration following localized heavy rain from morning showers and thunderstorms. Thus, the dew point difference may be attributable to the lack of representation of this process in the model. Consistently high wind speeds may be due to inaccurate nesting data and/or inaccuracies in geophysical fields such as the surface roughness. There appears to be a good match between observed indicators of lake breeze penetration, such as convective cloud lines and precipitation, and indicators

predicted by the model such as vertical motion and divergence. Overall, the results suggest that the model is useful for simulations of 'highly-perturbed' lake breeze circulations.

4.3.5 Thunderstorms and Severe Weather

The development of thunderstorms, including at least one severe storm now referred to as "the Punkeydoodle's Corners storm" (King *et al.*, 1998), appeared to be closely related to lake breeze circulations on this day. In this section, this relationship will be examined beginning with a discussion of the synoptic-scale conditions on this day to determine if synoptic-scale dynamics were a contributing factor to the development of these storms. A discussion of the mesoscale convective conditions follows, including descriptions of the development of the storms. Lastly, the modelled storm environment will be compared to that observed.

4.3.5.1 Synoptic Conditions

The synoptic scale-features important to severe convective potential on July 14 are briefly described in this section using a combination of 0700 LST (1200 UTC) objectively analyzed upper-air data and rawinsonde data. The goal is to determine if synoptic-scale dynamics were a contributing factor to storm development.

The 250 hPa chart shown in Figure 4.66 shows a strong jet stream with winds up to about

120 knots over eastern Canada. A weaker jet stream associated with an upper-level trough existed over the extreme western Great Lakes region with winds to roughly 90 knots. Over the study region in southern Ontario, an anticyclonic vortex was present at 250 hPa. Winds within this vortex were light to near zero over southern Ontario. Figure 4.67 shows the 500 hPa heights with 500-1000 hPa thicknesses superimposed. A weak trough was present to the west of the Great Lakes region while a stronger ridge stretched from the upper Mississippi Valley, through the study region and into Hudson Bay. A thickness ridge stretched from the southwestern U.S. states into the study region. Some weak negative thickness advection was present to the west of the Great Lakes region. At the 850 hPa level, a weak trough existed to the west of the Great Lakes and the height gradient was relatively tight from the U.S. Midwest into southern Ontario, as shown in Figure 4.51a. An 850 hPa temperature ridge ran from the Great Plains states to the area around southern Lake Michigan. Temperatures in the ridge were greater than 20°C. A temperature minimum was present south of Manitoba. A baroclinic zone was apparent to the west of the Great Lakes region between the temperature ridge and minimum. Winds at the 850 hPa level, shown in Figure 4.51b, indicate cyclonic flow over northern Ontario and to a lesser extent over northern Minnesota. A low-level jet extended from North Dakota through to Indiana though the jet weakened somewhat as it entered the Great Lakes region. 850 hPa winds over the study region were westerly at about 20 knots. Considering the above synoptic-scale dynamics, areas to the southwest and northeast of the Great Lakes region had environments favourable for the development of severe

storms. However, synoptic-scale dynamics could be expected to contribute very little to the development of thunderstorms over the study region.

The 0700 LST (1200 UTC) sounding data from the DTX station near Detroit, Michigan (not shown) giving a CAPE near 2500 J kg^{-1} and a Lifted Index near -7°C showed considerable instability even with the nocturnal inversion present near the surface.

However, the weak wind profile suggested that any thunderstorms would likely be of the 'pulse' (brief, single-cell) variety. The temperature at 850 hPa was near 20°C . Dew point temperatures near the surface were also near 20°C . Winds near the surface were light though the maximum wind speed of the sounding occurred near the 800 hPa level indicating the presence of a low-level jet. Winds above 400 hPa were relatively light and were generally from the southeast.

The rawinsonde launched at 1511 LST (2011 UTC) (Figure 4.58a) showed that mesoscale thermodynamic effects were likely more important than synoptic-scale dynamics for severe storm development in the study region. The sounding gave a surface-based CAPE near 6200 J kg^{-1} , storm motion from 304° at 13 knots, and a storm-relative helicity value near $160 \text{ m}^2 \text{ s}^{-2}$ below 3 km. No capping inversion is indicated. The high CAPE value suggested the possibility of intense updrafts with the potential for hail. However, the freezing level was quite high on this day indicating that most of the precipitation would likely fall as rain. The storm-relative helicity value indicated the possibility of weak

mesocyclones. Temperature and dew point data profiles from the sounding are very similar to the those described by Caracena *et al.* (1983) as typical of a wet microburst environment (not shown). Thus, wet microbursts were a possibility with any storm that developed. The wind profile veered from west-southwest to northwest in the lowest 4 km then backed to the south up to 14 km. Winds above 14 km were out of the southwest. The highest wind speeds in the profile occurred at 2700 m (from 305° at 29 knots) and 9400 m (from 200° at 29 knots) indicating the absence of both upper- and low-level jets. This profile was not significantly different from that measured earlier in the morning at the DTX station in Michigan. The most significant differences were the eradication of the nocturnal boundary layer with surface heating, a drier layer between 300 hPa and 400 hPa, and stronger, more-southerly winds above 9 km.

4.3.5.2 Mesoscale Conditions and Analysis

A sequence of four GOES-8 visible satellite images illustrating the development of thunderstorms in the study region and over eastern Michigan is shown in Figure 4.68. The accompanying sequence of King City radar images is shown in Figure 4.69. Radar from the King City radar facility north of Toronto is used for the discussion here since after the heavy rainfall on this day it was found that the Exeter radar was severely underestimating rainfall rates. At 1545 LST (2045 UTC), deep moist convection was developing near the Exeter base station at the apparent merger point of the Lake Huron and Lake Erie lake breeze fronts and over the shores of eastern Michigan along a series of linked lake breeze

fronts. The King radar recorded a single cell with a maximum reflectivity value of 49 dbZ (rain rate of 32-64 mm h⁻¹) near this time. Explosive convective development continued to occur east of Exeter with the King City radar measuring echo top heights up to 19 km at 1610 LST (not shown). A well-formed, quasi-circular anvil had formed by 1632 LST (2132 UTC) (Figure 4.68b). Lake breeze fronts inferred from lines of cloud to the west and southwest of the storm appear to be feeding the storm. Radar at this time (Figure 4.69b) shows a grouping of thunderstorm cells. However, the main cell has moved very little from the previous image. The maximum reflectivity value had increased to 54 dbZ (rain rate above 64 mm h⁻¹). By 1700 LST (2200 UTC), the anvil area had approximately doubled in size and a line of clouds is apparent to the southwest along the Lake Erie lake breeze front (Figure 4.68c). Radar at this time (Figure 4.69c) shows three main cells with a new cell developing to the west. The easternmost cell was moving away from the main cell along an outflow boundary. Two planes were flipped over at the Waterloo-Wellington Regional Airport and winds were measured to have gusts to 115 km h⁻¹ as this cell passed. This could possibly have been due to a microburst. Close inspection of Doppler radar images of the storm at this time (not shown) have indicated several brief mesocyclones in the lower levels of the storm. However, no reports of funnel clouds or tornadoes were received. Again, the main cell had moved very little from its original position. The satellite image at 1815 LST (2315 UTC) (Figure 4.68d) shows that the anvil had again nearly doubled in size and moved to the north-northeast with the upper-level winds. An overshooting cloud-top, indicative of a very intense updraft, is made visible by

the shadow near the southwest edge of the storm. In addition, the extent of the outflow boundary can be seen to the southeast of the storm made visible by an arced cloud line. On radar (Figure 4.69d), it is evident that storms had formed along the outflow boundary and were propagating toward the southwest as the gust front continued to rotate about the anchored main cell. A plot of station wind and pressure data in the study region at 1900 LST is shown in Figure 4.70 accompanied by a subjective isobaric analysis. A large area of divergent surface flow and increased sea level pressure is evident west of Lake Ontario associated with outflow from the Punkeydoodle's Corners storm (the estimated leading edge of the outflow is indicated by the cold-front type symbol).

The sequence of satellite images shown in Figure 4.68 also shows the development of thunderstorms along the linked lake breeze fronts on the shores of eastern Michigan. By 1815 LST (2315 UTC), these storms had begun to move across the lake. Storms that developed along an approaching cold front are also apparent in the most western part of the 1815 LST satellite image (Figure 4.68d). Thunderstorms continued as these three areas of convection converged over the study region. Intense convection was re-activated in the study region as the cold front passed through resulting in more heavy rain. Some of this re-activation appeared to occur along old thunderstorm and lake breeze frontal boundaries. Heavy precipitation ended in the study region near 0000 LST on July 15. Figure 4.71 is a map showing precipitation accumulation in the Great Lakes region between 0700 LST (1200 UTC) on July 14 and 0700 LST (1200 UTC) on July 15 as

estimated by NEXRAD Doppler radars in the United States. The image was downloaded from the internet on July 15 courtesy of WSI Corporation. In the study region, these precipitation accumulations include amounts from localized heavy rain from morning showers and thunderstorms though most of the high accumulation amounts are associated with storms that occurred after that time. The area of precipitation stretching from Lake Huron southwestward to Illinois is associated with the passage of the cold front. However, high precipitation amounts are evident along the lakeshores of eastern Michigan where showers and thunderstorms formed on the linked lake breeze fronts. The greatest accumulations occurred over southwestern Ontario. A small region of 8-10 inch (about 200-250 mm) accumulation is located where the severe thunderstorm occurred on July 14 at the merger point of the Lake Huron and Lake Erie lake breeze fronts. Most of this appears to have fallen in a five-hour period after the initiation of the storm according to a report from operators of the NEXRAD radar in Buffalo. Another large area of high accumulation is located to the northwest of this point. The rains here fell from storms that intensified with the passage of the cold front overnight. Many of the storms that occurred in the Great Lakes region on July 14 produced very heavy rain. Clearly, it was the quasi-stationary nature of the Punkeydoodle's Corners storm on July 14 that resulted in such remarkably high rainfall accumulations.

Divergence at the 10 m level was measured in several areas of the study region in the manner described in Appendix C. Figure 4.72 shows the stations selected to be vertices of

triangles for the divergence calculations. AES stations provided the best triangles and were used exclusively. Triangle A was chosen to represent the region between Lakes Erie and Huron, Triangle B was selected to represent the Punkeydoodle's Corners storm region and Triangle C was chosen to represent the region affected by the thunderstorm outflow. Time series of divergence from these triangles are shown in Figure 4.73. Oscillation between weak divergence and weak convergence is evident for Triangle A until 1900 LST after which there was a significant increase in convergence. This was mainly due to the Punkeydoodle's Corners storm outflow reaching the London station. For Triangle B, weak divergence is present until 1400 LST after which oscillation between weak divergence and weak convergence begins. Divergence increases significantly after 1900 LST associated with the thunderstorm outflow at London and Waterloo. Finally, for Triangle C, weak to moderate divergence is apparent most times with the greatest divergence value occurring at 1900 LST again in association with the thunderstorm outflow, this time affecting stations at each vertex. Part of the difference in absolute values of divergence at this triangle compared to the other two triangles is attributable to its reduced area. Overall, the divergence values for Triangles A and B are surprising since lake breezes on the shores of Lakes Erie and Huron and their merger failed to generate significant convergence values. This may indicate that the convergence associated with the initiation of the Punkeydoodle's Corners storm was highly localized.

4.3.5.3 Mechanism for Storm Initiation and Maintenance

The Punkeydoodle's Corners severe storm exhibited the traits of a 'multicell cluster' storm. Essentially, this means that thunderstorms were maintained by new cells replacing older ones at a flanking line and that several of these 'multicell' thunderstorms occurred in close proximity, interacting and behaving as a system. In contrast, a 'supercell' type storm has one intense, persistent cell and tends to occur in isolation. In terms of severe winds and hail, this storm was not extraordinary. No tornadoes or funnel clouds were sighted. A report of two planes being flipped by winds up to 115 km h^{-1} was received and observations were made of several felled trees. These very localized incidents suggest that wind damage was caused by microbursts. This storm produced some hail but no large hailstones were reported. However, when heavy rainfall is considered, this storm was remarkable. Approximately 200 mm of rain fell in the vicinity of Punkeydoodle's Corners in five hours. Observations were made of badly flooded roads, fields and yards. Severe damage due to erosion was also recorded. This aspect of the storm is arguably the most interesting and is directly related to its quasi-stationary nature. No other storms that occurred in and near the study region on this day exhibited this type of behaviour. Was it the merger of lake breeze fronts that led to the initiation and evolution of such a unique storm?

Unfortunately, the data collected during the ELBOW IOP are insufficient to answer this question unequivocally. However, the data that were collected, supported by three-

dimensional results from the MC2 model, are sufficient to propose a conceptual model of the storm's formation and maintenance. As the Lake Huron and Lake Erie lake breeze fronts merged east of Exeter, southwesterly winds delivering very warm and moist air were forced to converge and rise up over the more dense wedges of air on either side, as shown in Figure 4.74. In addition, upward vertical motion was present along the lake breeze fronts. Thus, the sum of vertical motion due to converging southwesterly winds, lake breeze fronts and, to a lesser extent, upslope flow resulted in a region of enhanced vertical velocities in the vicinity of the merger point of the lake breeze fronts. This enhanced lift was sufficient for air parcels to reach their level of free convection allowing large amounts of CAPE to be tapped. Warm, moist air was continually fed into the region of active deep moist convection by southwest winds funnelled along the lake breeze fronts. Once the main thunderstorm was initiated, outflow began to affect the near-storm environment. Two separate cells, one to the northeast and one to the east of the main cell, appeared to form in association with this outflow. However, the outflow along the rear of the storm may have been balanced by the southwest flow. This would have created a quasi-steady-state inflow from which the main storm region could feed resulting in nearly continuous redevelopment at the rear of the storm, as illustrated in Figure 4.74. This is supported by animations of radar data (not shown) that show a quasi-stationary southwest edge to the main storm region with several smaller cells that develop, move toward and eventually merge with the main cell from the southwest. In addition, intense convection appears to be repeatedly re-invigorated in this area. The result of the last of these re-

invigorations is presented in Figure 4.75a which shows King radar at 2210 LST (0310 UTC). Widespread showers and heavy thunderstorms migrated across Lake Huron from Michigan and were present east of the Lake. However, a line of very intense thunderstorms developed at this time along a line from northern Lake Erie to east of Stratford (roughly azimuth 250° , range 90 km). This line appears to be in a location just downstream from the location of the Lake Erie lake breeze front that had initiated the original thunderstorm. Figure 4.75b shows that winds north of the Lake Erie shoreline had changed very little from earlier in the afternoon (see Figure 4.65). Also, temperatures and dew points were still relatively high inland and temperatures inland remain several degrees higher than those over the Lake. This suggests that the Lake Erie lake breeze front was probably still active and that deep convection along the front was still possible. Further, it suggests that the Lake Erie lake breeze front had remained nearly stationary since at least 1600 LST. Looking again at the precipitation accumulation map in Figure 4.71, the effects of the intense precipitation along this line are evident.

4.3.5.4 Frequency of Occurrence of the July 14 Lake Breeze Pattern

The highly-perturbed lake breeze pattern suggested above deviates significantly from that observed on days with more 'typical' lake breeze circulations. This may lead one to think that the occurrence of this particular lake breeze pattern is uncommon. However, similar lake breeze patterns produced by the MC2 model on two other days indicate the possibility that this pattern may occur in the study region on a regular basis. Figure 4.76

shows 500 m positive vertical motion at 1500 LST (2000 UTC) on three days: July 14 1997, July 2 1997 and August 15 1993. The July 14 and August 15 simulations have already been described in detail. The July 2 simulation was conducted separately but used the same MC2 settings and nesting strategy as the July 14 case. In all three cases, strong lake breeze fronts are indicated by enhanced vertical motion over parts of the north and south shores of Lake Erie and along the lakeshores of eastern Michigan. A weaker lake breeze front is also present in each case south of Lake Huron. On each of these days, surface winds were from between the southwest and the south. The modelled gradient wind is the lightest on August 15 and modelled lake breeze fronts are more well-defined around the perimeters of the lakes. The frequency at which this pattern occurs could have important implications for severe weather forecasting in the region since the air mass in this type of synoptic regime is frequently conducive to severe thunderstorms. In fact, severe thunderstorms occurred in the study region on each of these days.

4.4 Summary

In this chapter, observations and results from MC2 model simulations were discussed in detail for two periods. For the first period, 14-15 August 1993, lake and land breezes that exhibited typical or 'classic' characteristics were examined. The effects of these circulations on the development of severe weather and the transport of ozone near the surface were also discussed. Lake breezes that occurred during the second period, 14 July 1997, were highly perturbed by the gradient wind and were shown to have characteristics

quite different from those of lake breezes during the first period. The association between these 'highly-perturbed' lake breezes and the development of thunderstorms, including a severe storm, on this day were also discussed. For both periods, observations were used to subjectively evaluate the MC2 model. In Chapter Five - Discussions and Conclusions, results from this chapter and Chapter Two will be discussed in order to synthesize the data and arrive at some final conclusions for this study.

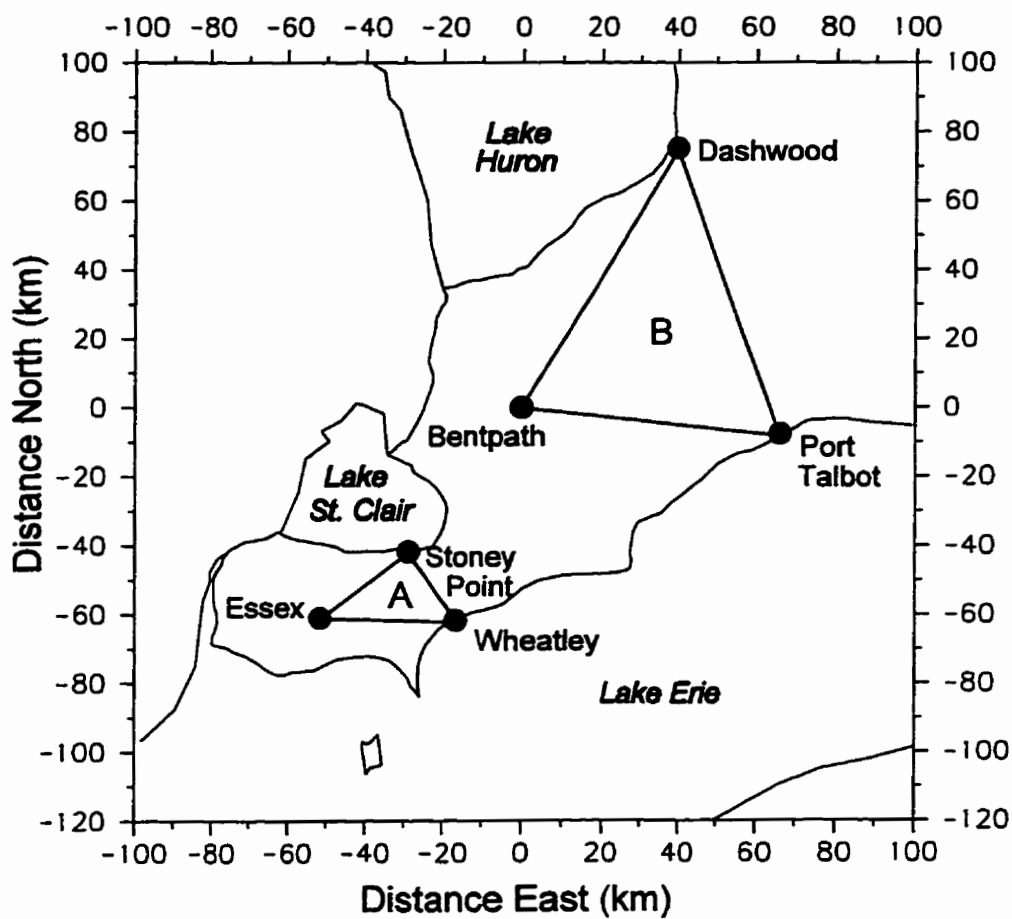


Figure 4.2. Map showing the locations of triangles A and B and their vertices used for the divergence calculations. Divergence values from these triangle are shown in Figure 4.1

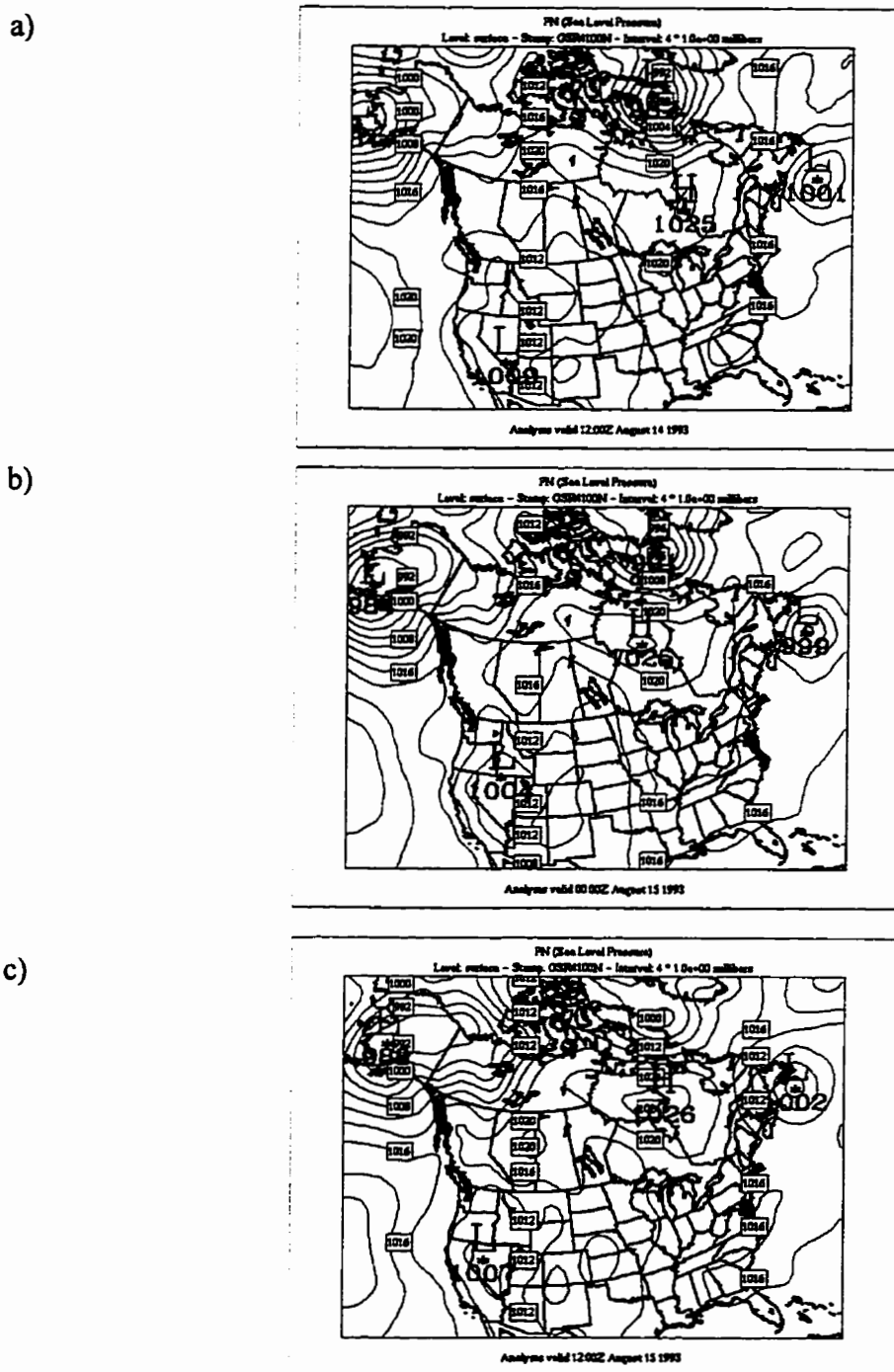


Figure 4.3. CMC objectively analyzed sea level pressure for 1200 UTC on August 14 (a) and 0000 UTC (b) and 1200 UTC (c) on August 15. The pressure contour interval is 4 hPa. Contour labels are attached to contours at their right, lower corner.

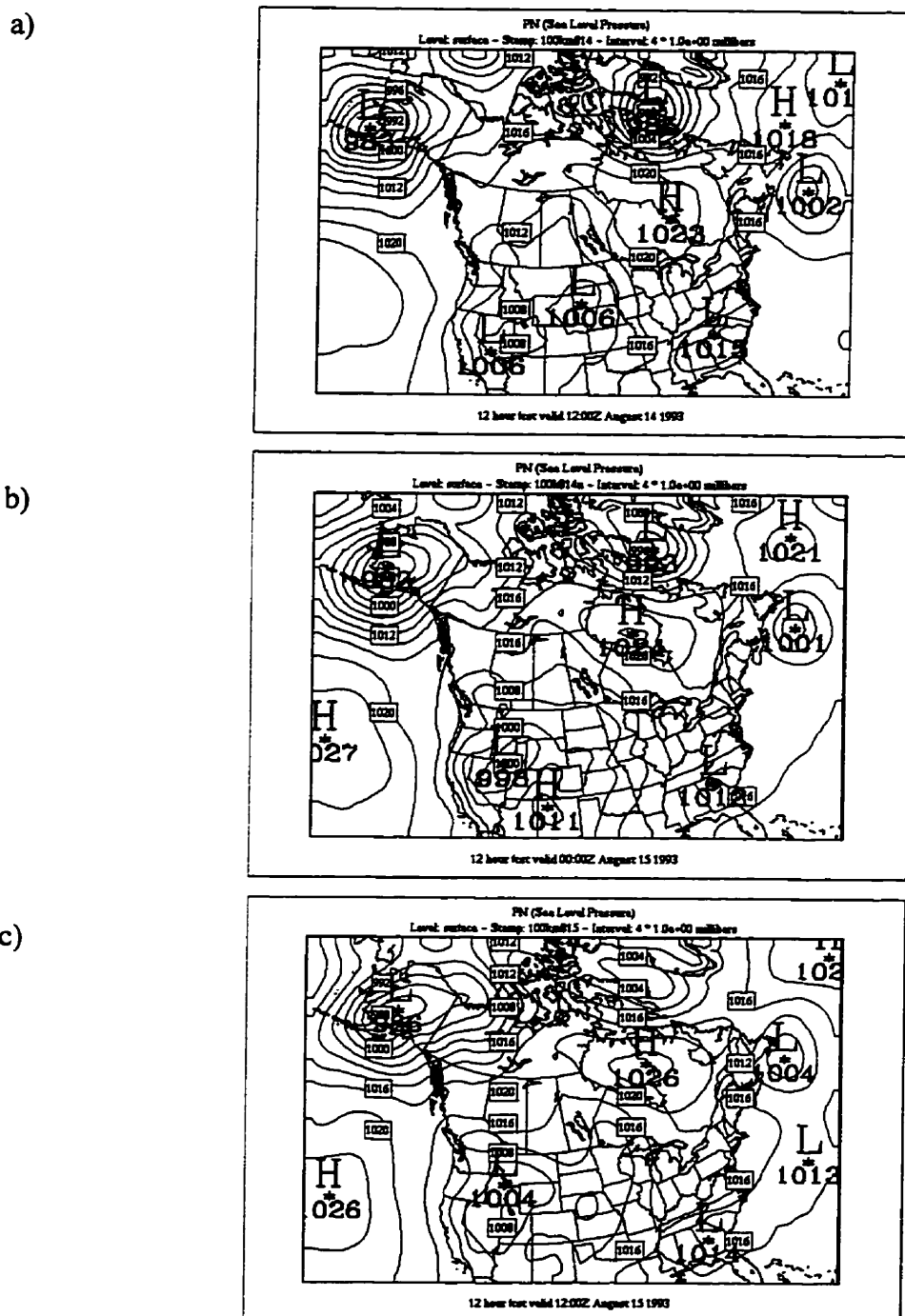


Figure 4.4. As in Figure 4.3, except that sea level pressure values are those predicted by the 100 km MC2 model run.

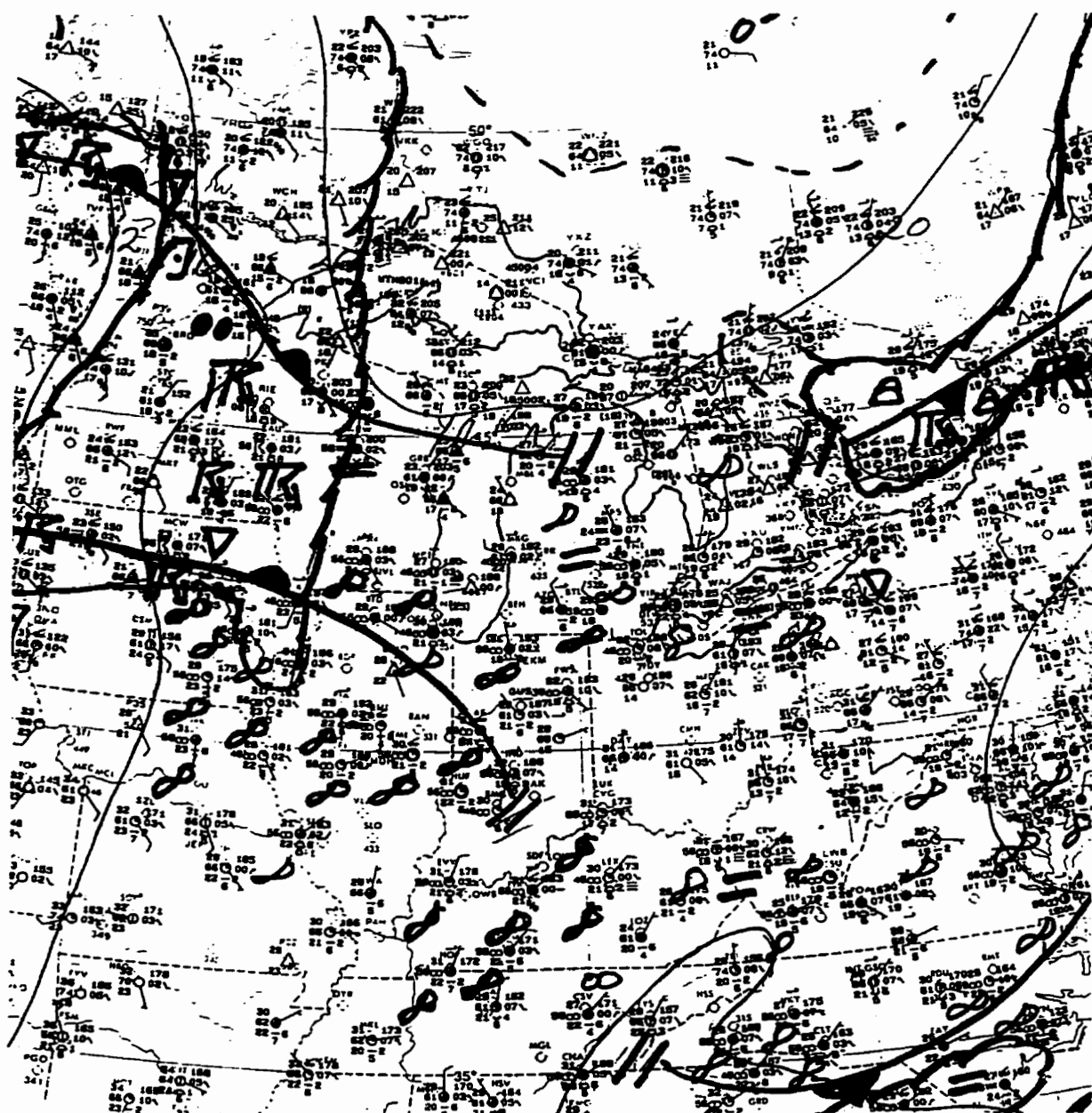


Figure 4.5. Regional operational surface analysis valid at 1800 UTC on August 14. The isobars have 4 hPa spacing. Coastlines in the study region have been outlined. Courtesy of AES.

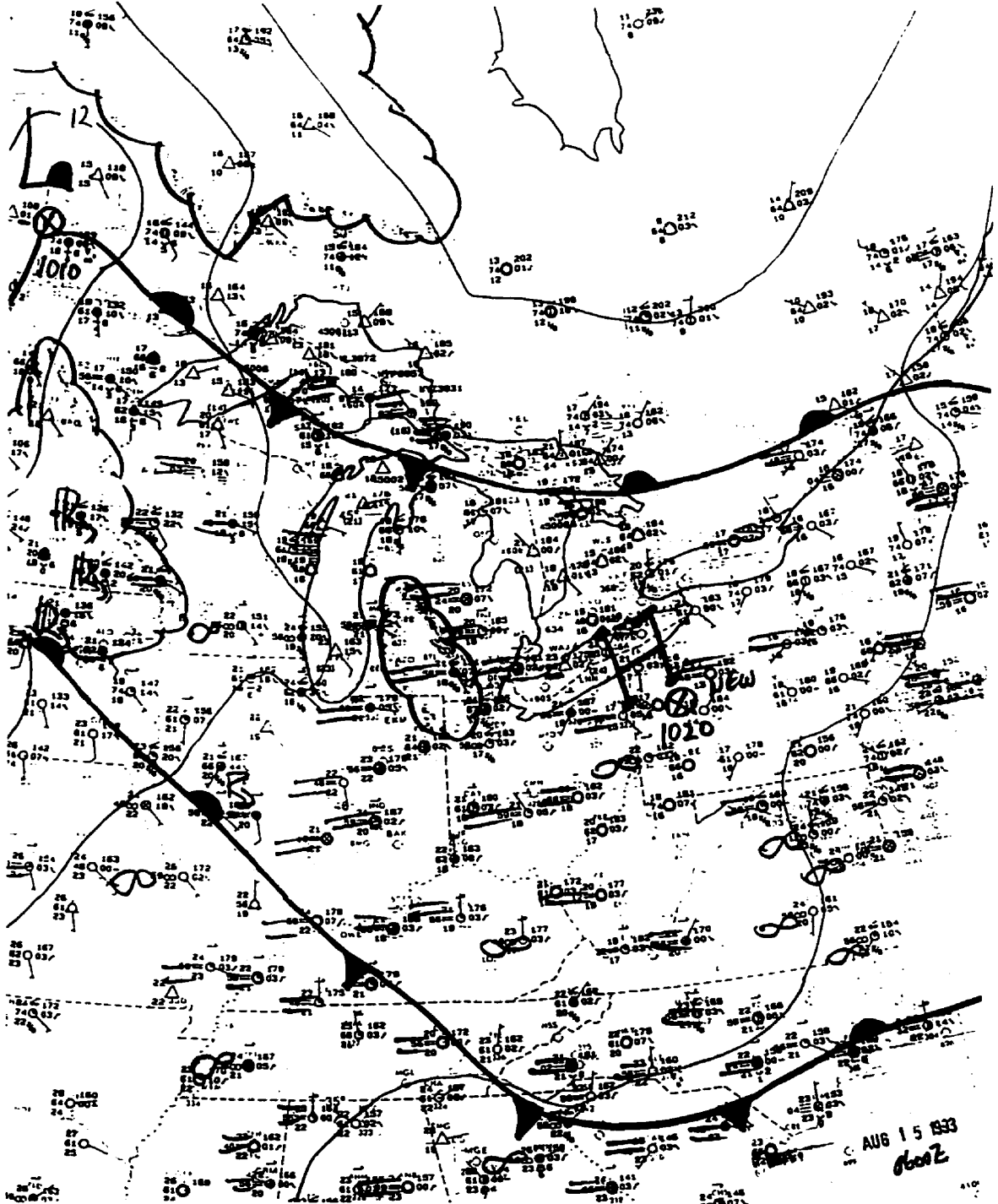


Figure 4.6. As in Figure 4.5, except valid for 0600 UTC on August 15.

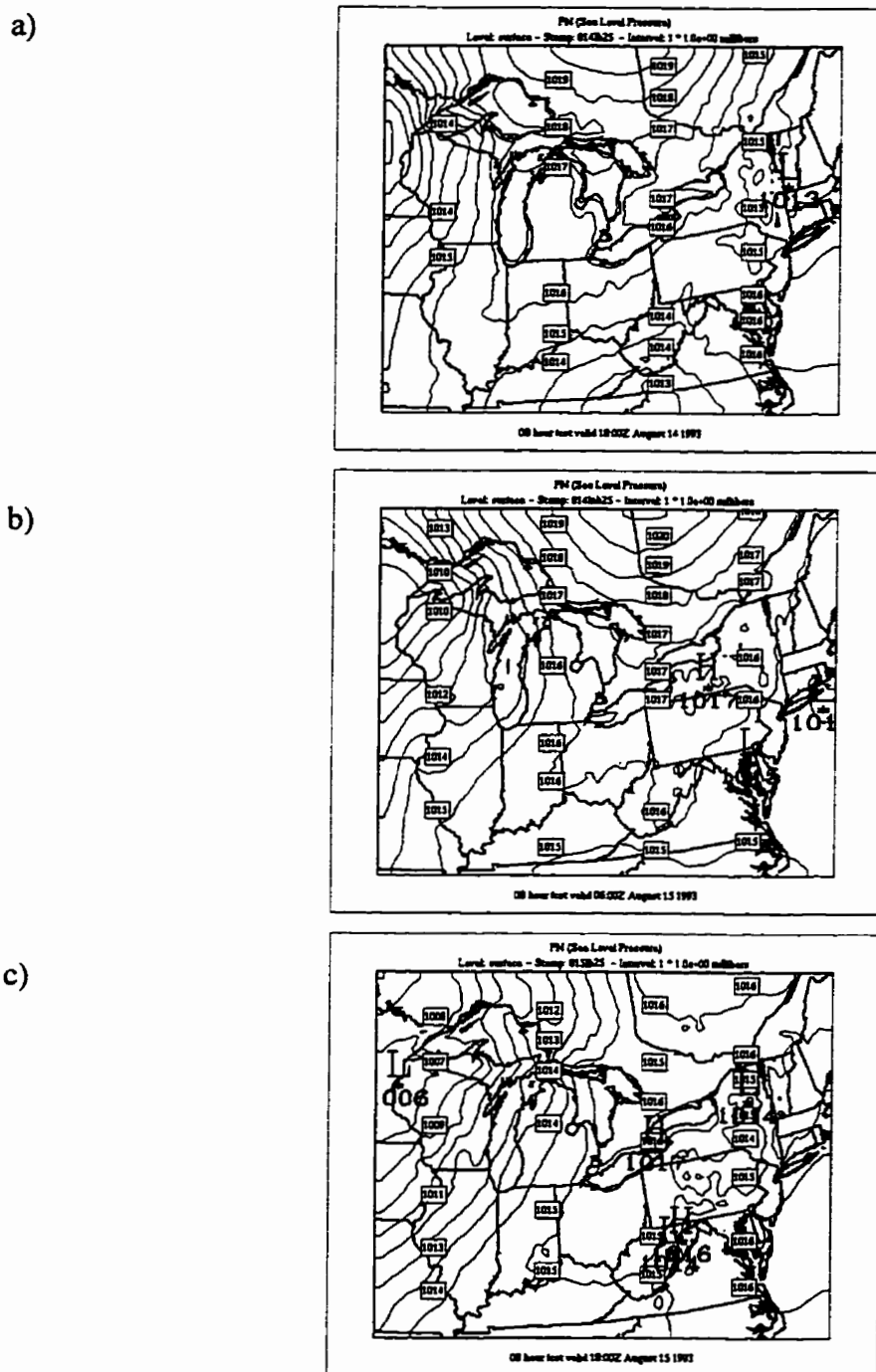
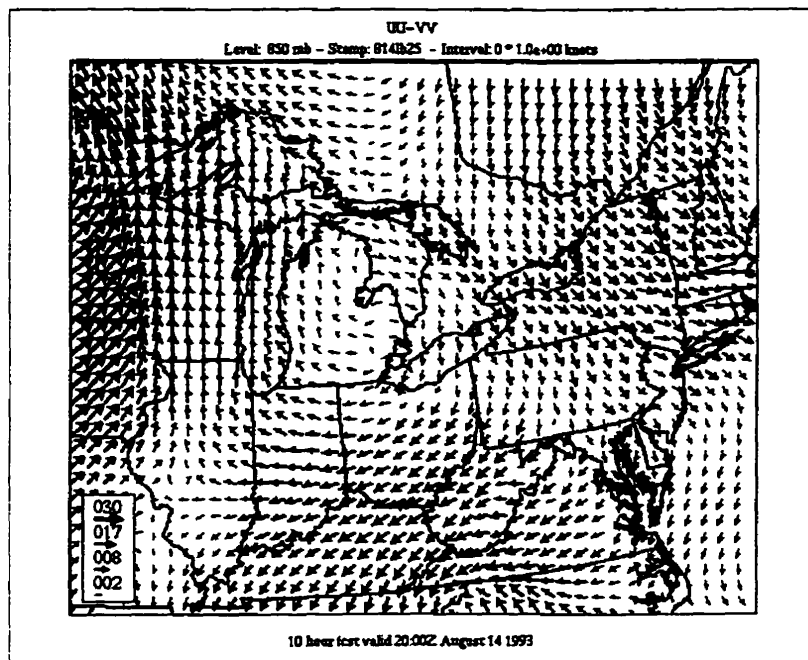


Figure 4.8. Sea level pressure patterns as computed by the MC2 model on the 25 km grid valid for 1800 UTC on August 14 (a) and 0600 UTC (b) and 1800 UTC (c) on August 15. The contour interval is 1 hPa.

a)



b)

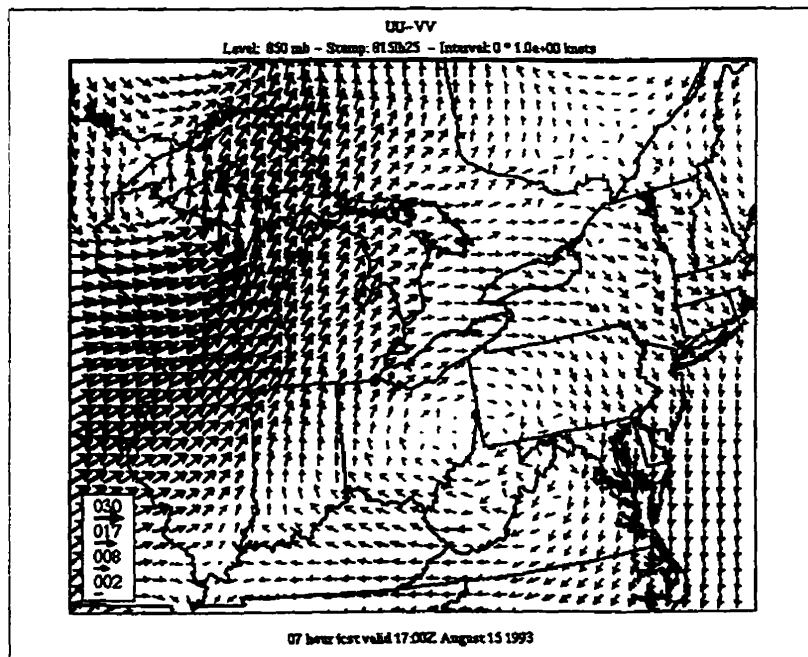


Figure 4.9. Winds at the 850 hPa level as predicted by the MC2 model on the 25 km grid for 2000 UTC on August 14 (a) and 1700 UTC on August 15 (b). Wind speeds are in knots.

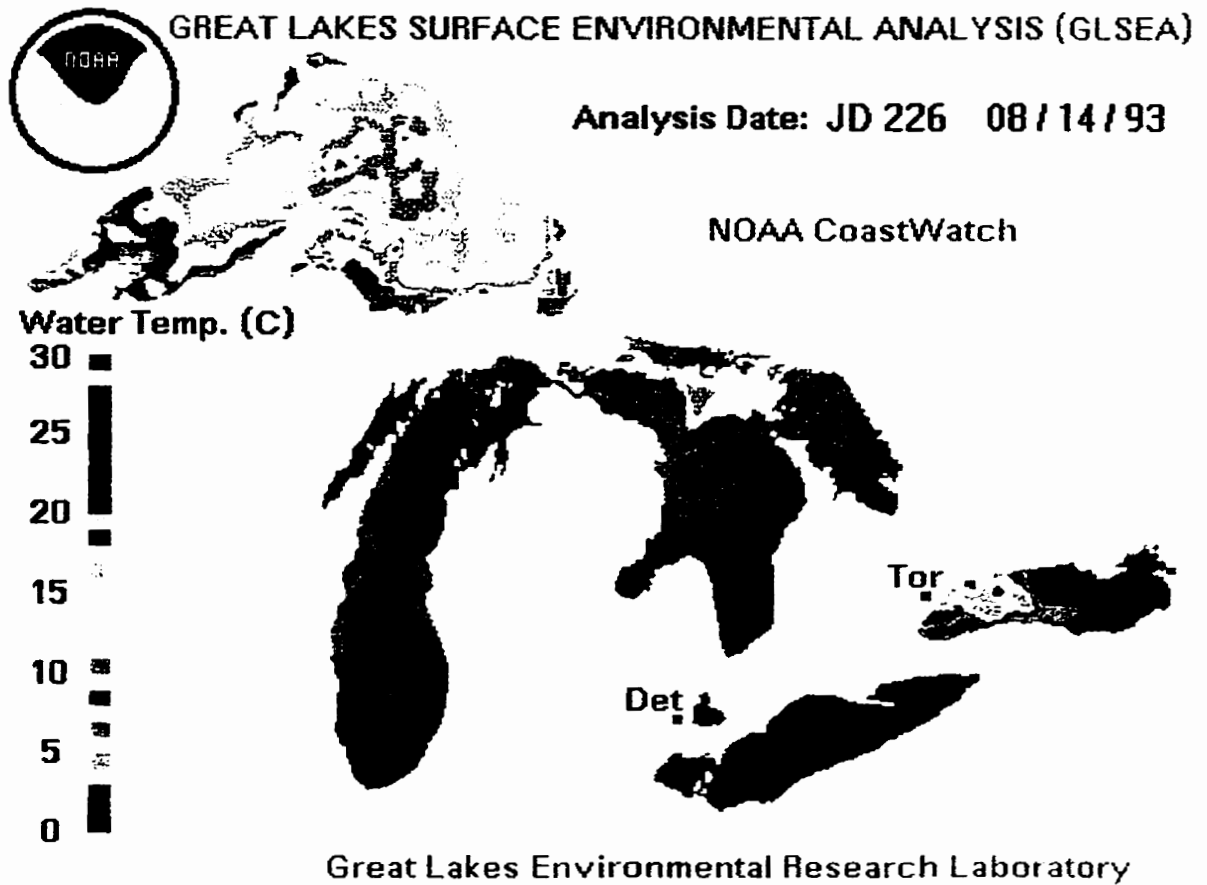


Figure 4.10. Lake surface temperatures as measured by a satellite-borne infrared sensor. Water temperatures are given in °C. Temperatures are valid for mid-afternoon on August 14. Courtesy of NOAA CoastWatch.

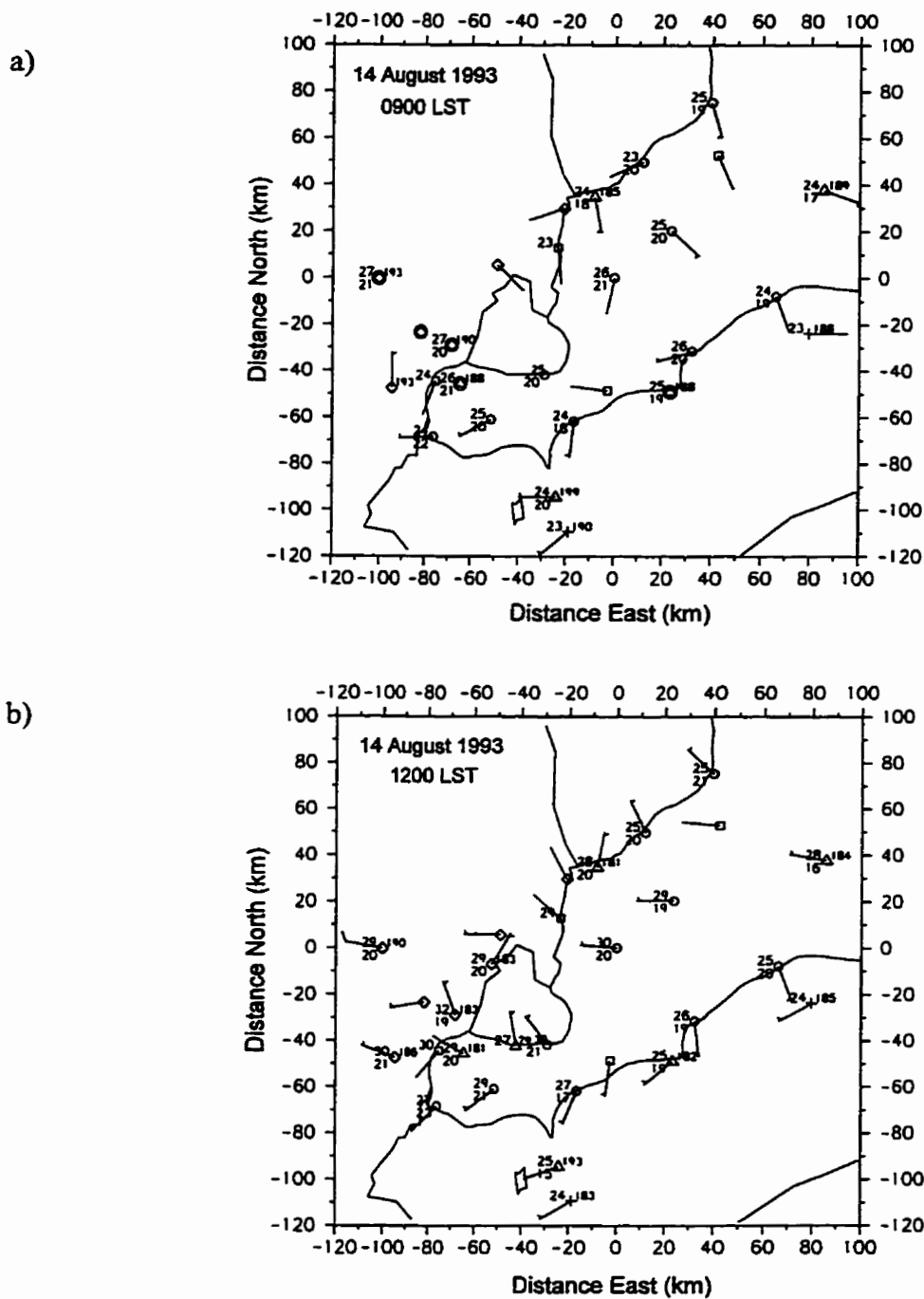
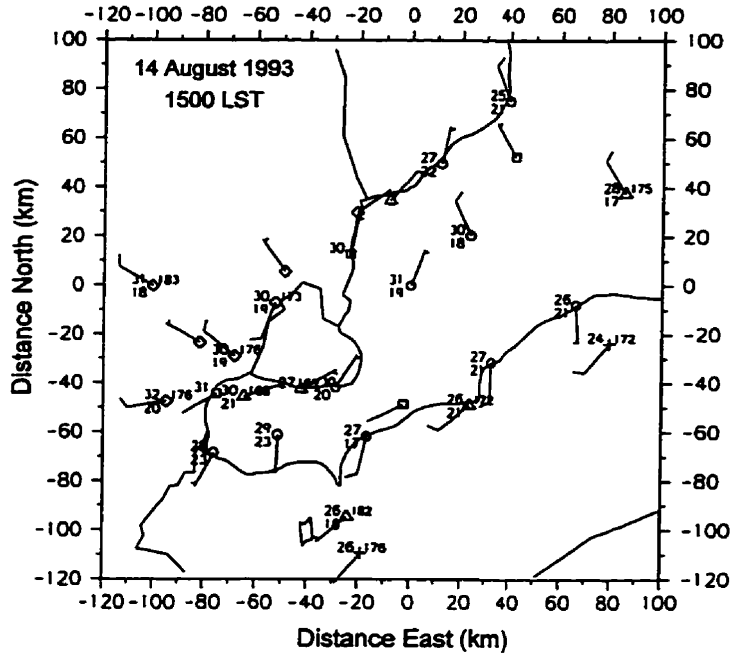


Figure 4.11. A sequence of mesonet station plots for August 14 at 0900 LST (a), 1200 LST (b), 1500 LST (c) and 1900 LST (d). The standard synoptic plotting format is used (small wind barb = 5 knots, temperatures in $^{\circ}\text{C}$, pressure in tenths of a hPa). *continued*

c)



d)

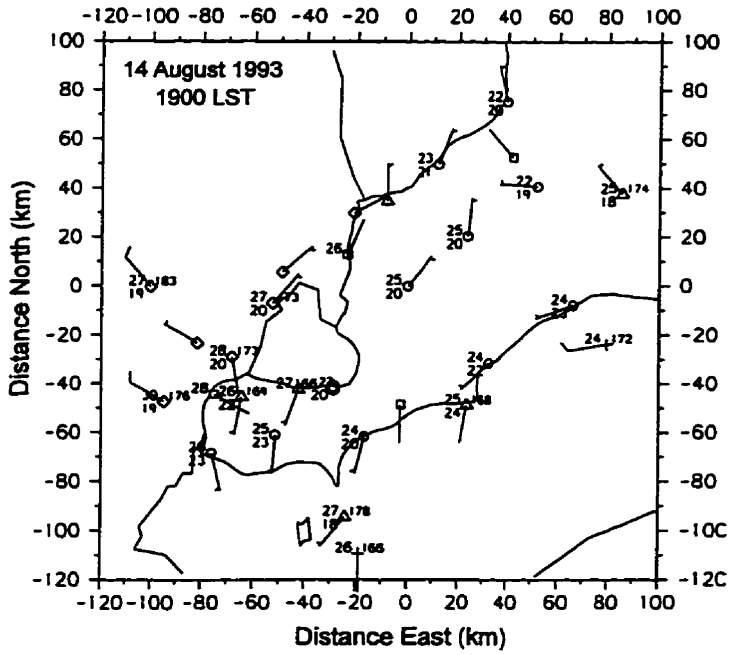


Figure 4.11., continued.

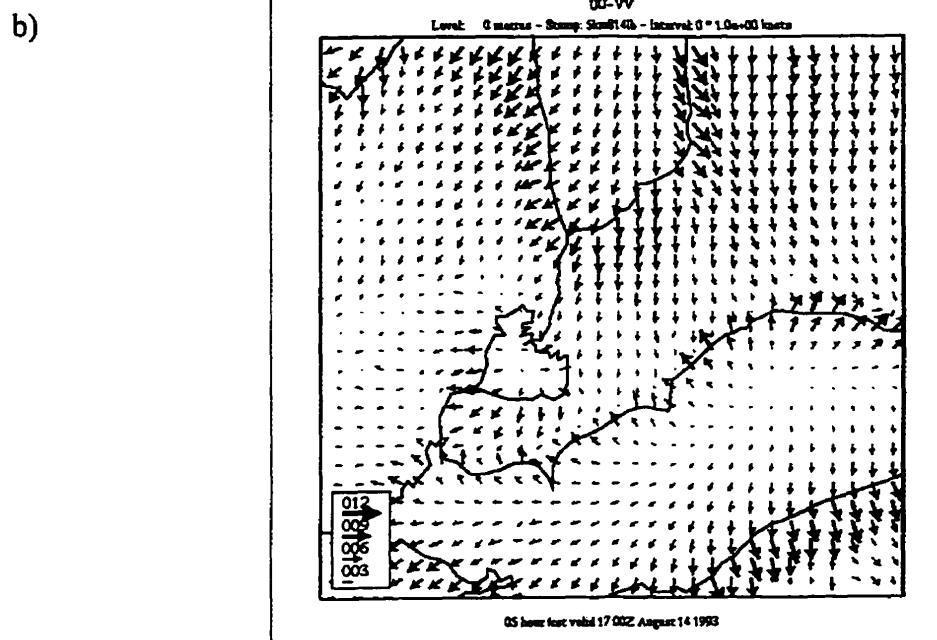
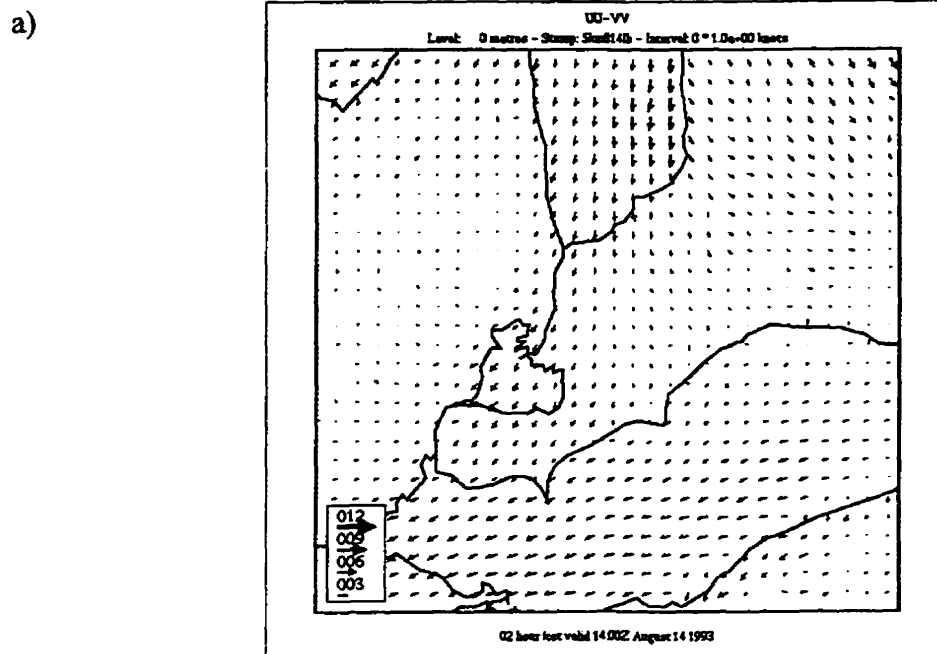
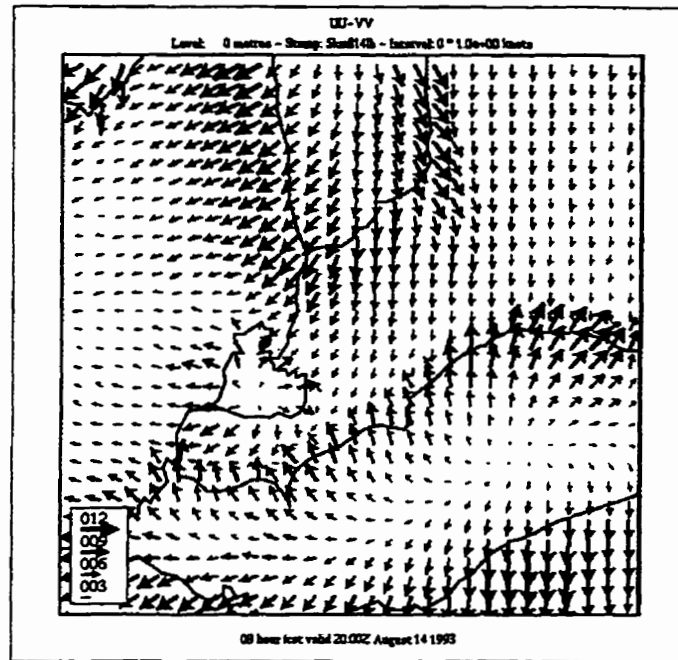


Figure 4.12. Modelled 10 m winds for August 14 at 1400 UTC (a), 1700 UTC (b) and 2000 UTC (c) on August 14 and 0000 UTC (d) on August 15. Winds are in knots and north is toward the top of the image. *continued*

c)



d)

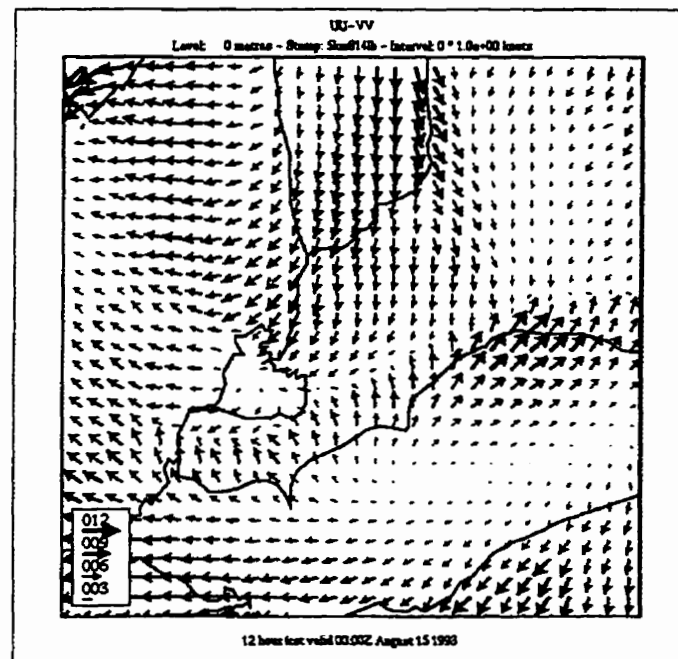
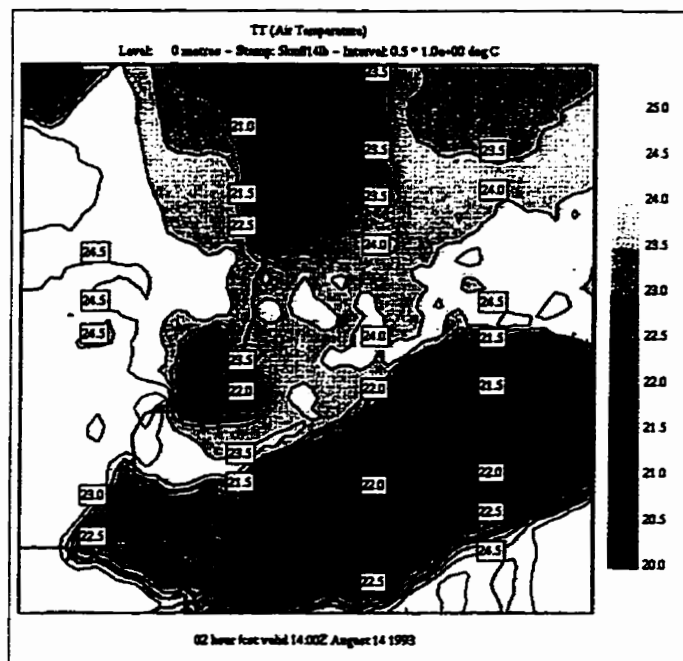


Figure 4.12., continued.

a)



b)

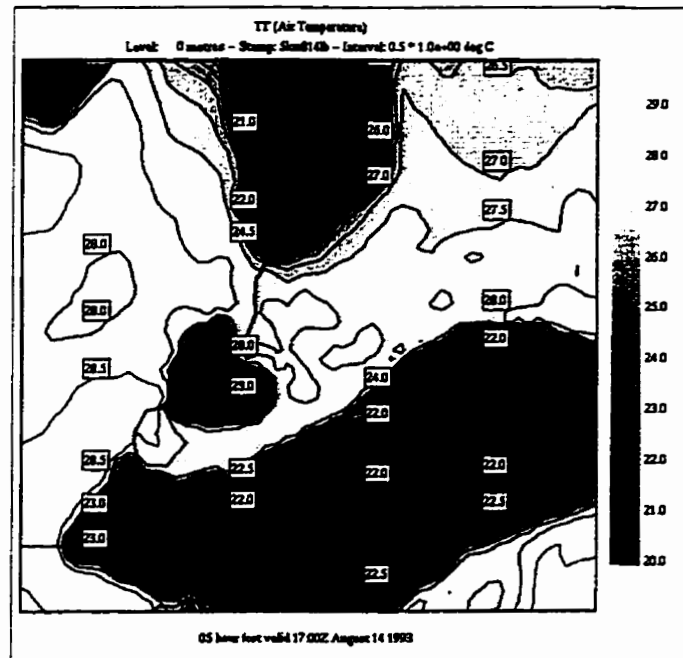
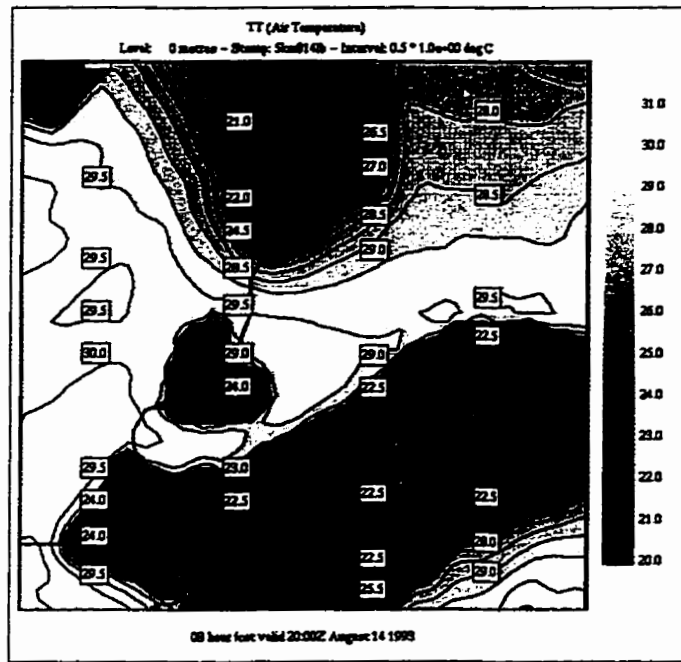


Figure 4.13. Modelled 1.5 m temperatures for August 14 at 1400 UTC (a), 1700 UTC (b) and 2000 UTC (c) on August 14 and 0000 UTC (d) on August 15. A 0.5°C temperature contour interval is used. *continued*

c)



d)

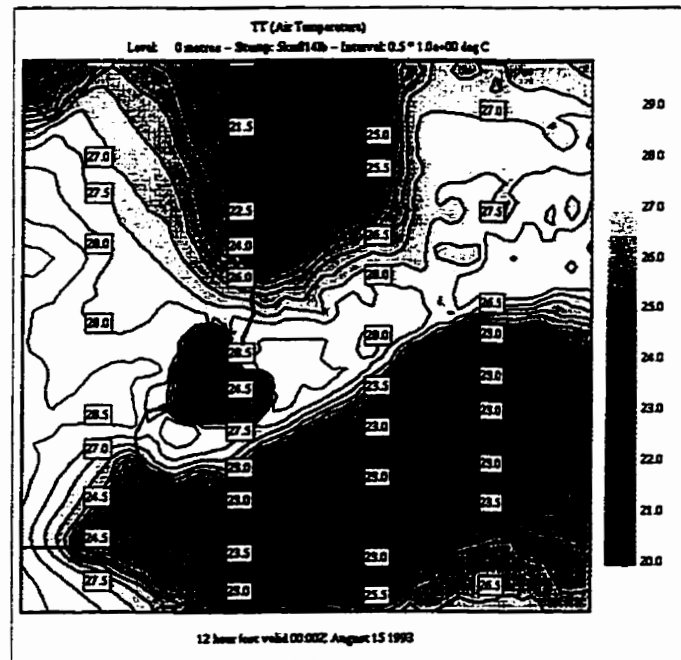
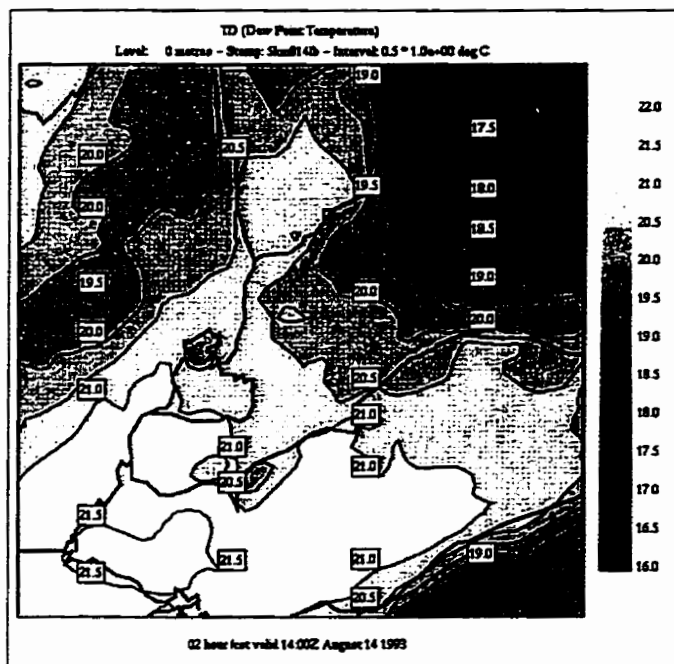


Figure 4.13., continued.

a)



b)

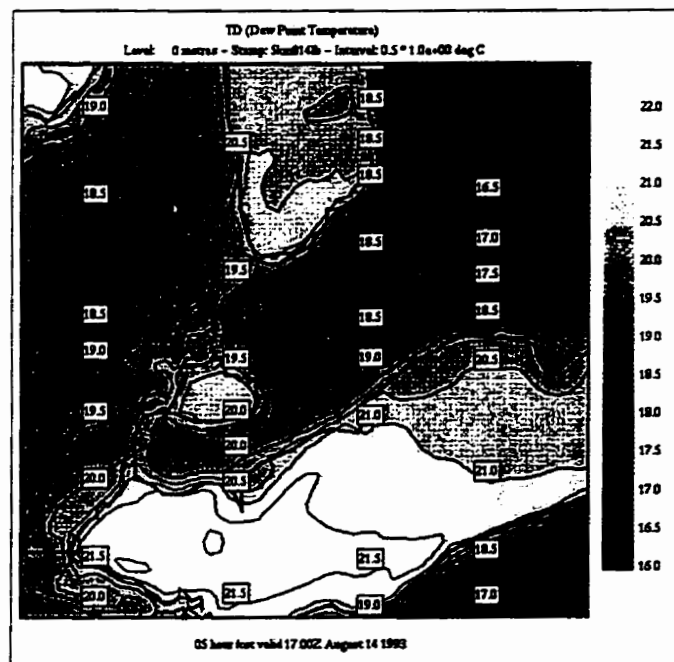
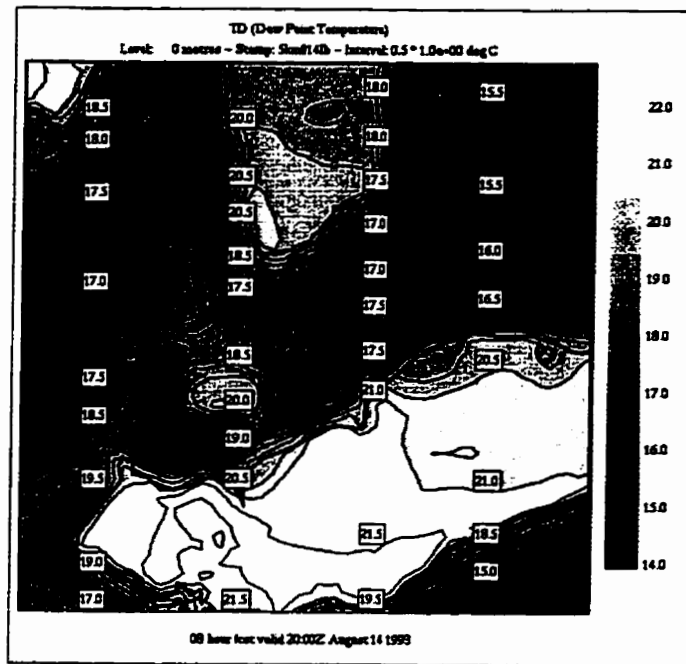


Figure 4.14. As in Figure 4.13, except values are 1.5 m dew point temperatures.
continued

c)



d)

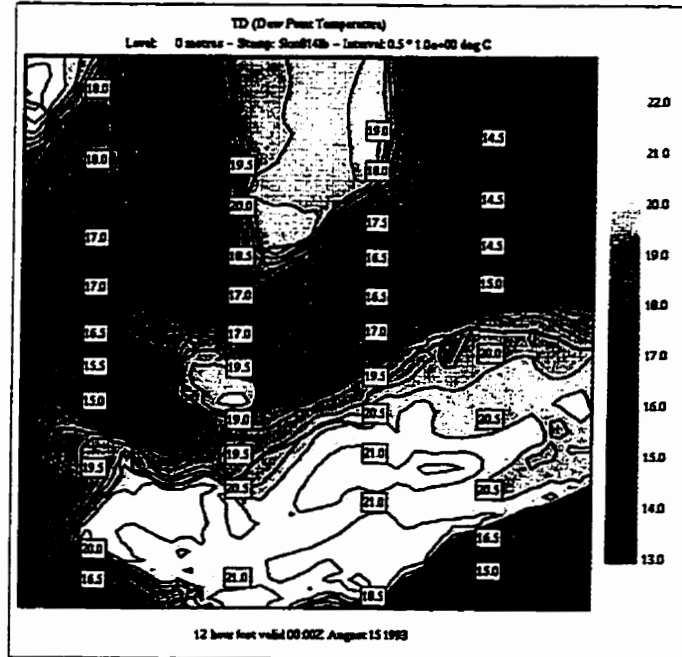


Figure 4.14., continued.

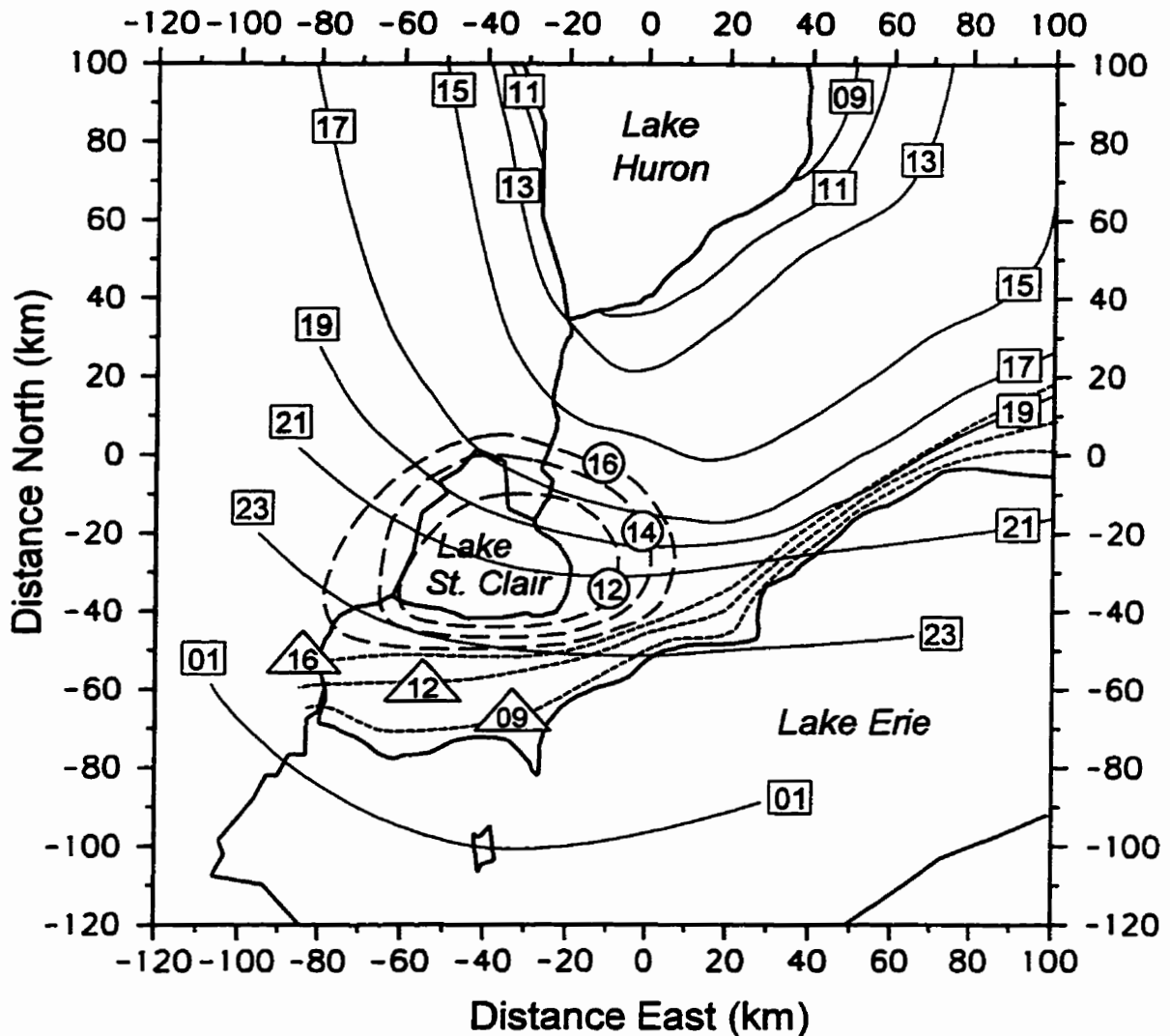


Figure 4.15. Map showing the inland penetration distance of the Lake Huron (solid line, square labels), Lake Erie (long dashed line, circle labels) and Lake St. Clair (short dashed line, triangle labels) lake breezes over time as estimated using visible satellite imagery and mesonet station data. Only the penetration contours up to the time of maximum penetration distance are shown for Lakes Erie and St. Clair. All times are in LST.

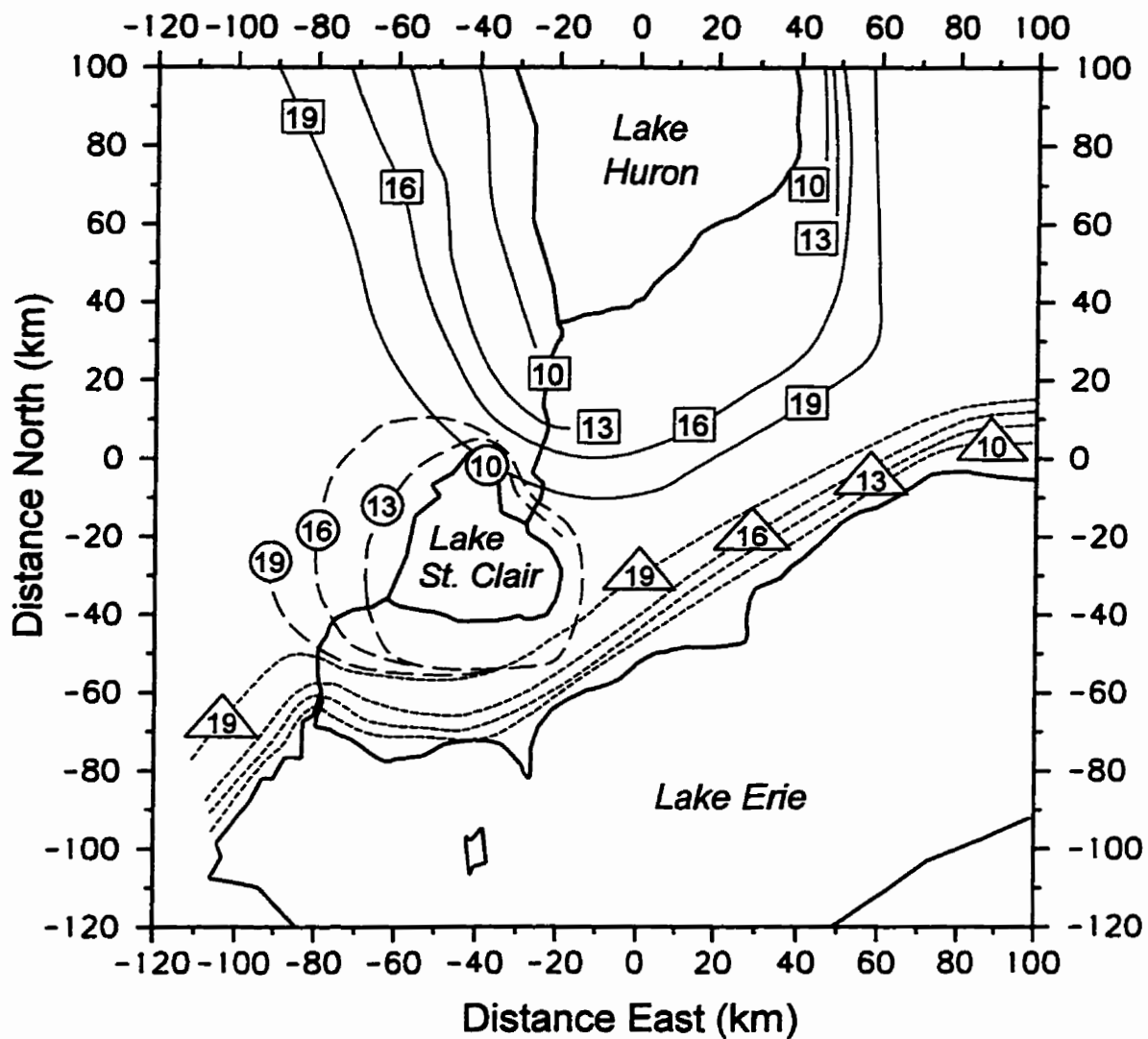


Figure 4.16. As in Figure 4.15, except that inland penetration distances are inferred from MC2 modelled winds and divergence values. Contours are shown at three hour intervals. Contours are plotted for times up until the end of the model run (1900 LST) for each lake.

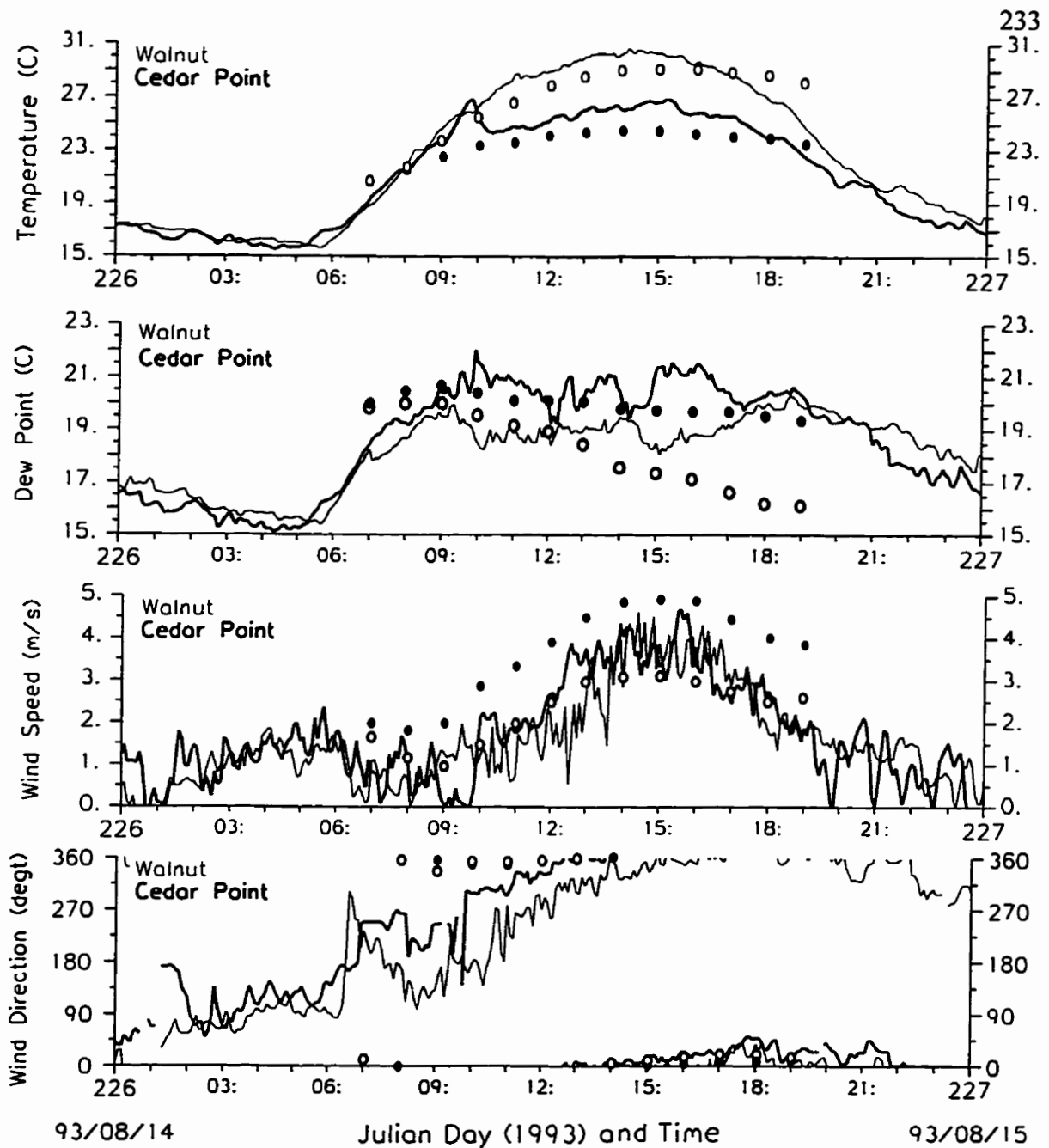


Figure 4.17. Time series plots of temperature, dew point and wind and wind direction for the Cedar Point station on the shore of Lake Huron and the inland Walnut station. Observed values are shown by light and dark lines while modelled values are shown by light and dark circles. Plots show values from 0000 LST August 14 to 0000 LST August 15. Observed data are at 5 minute intervals while modelled data are at 1 hour intervals.

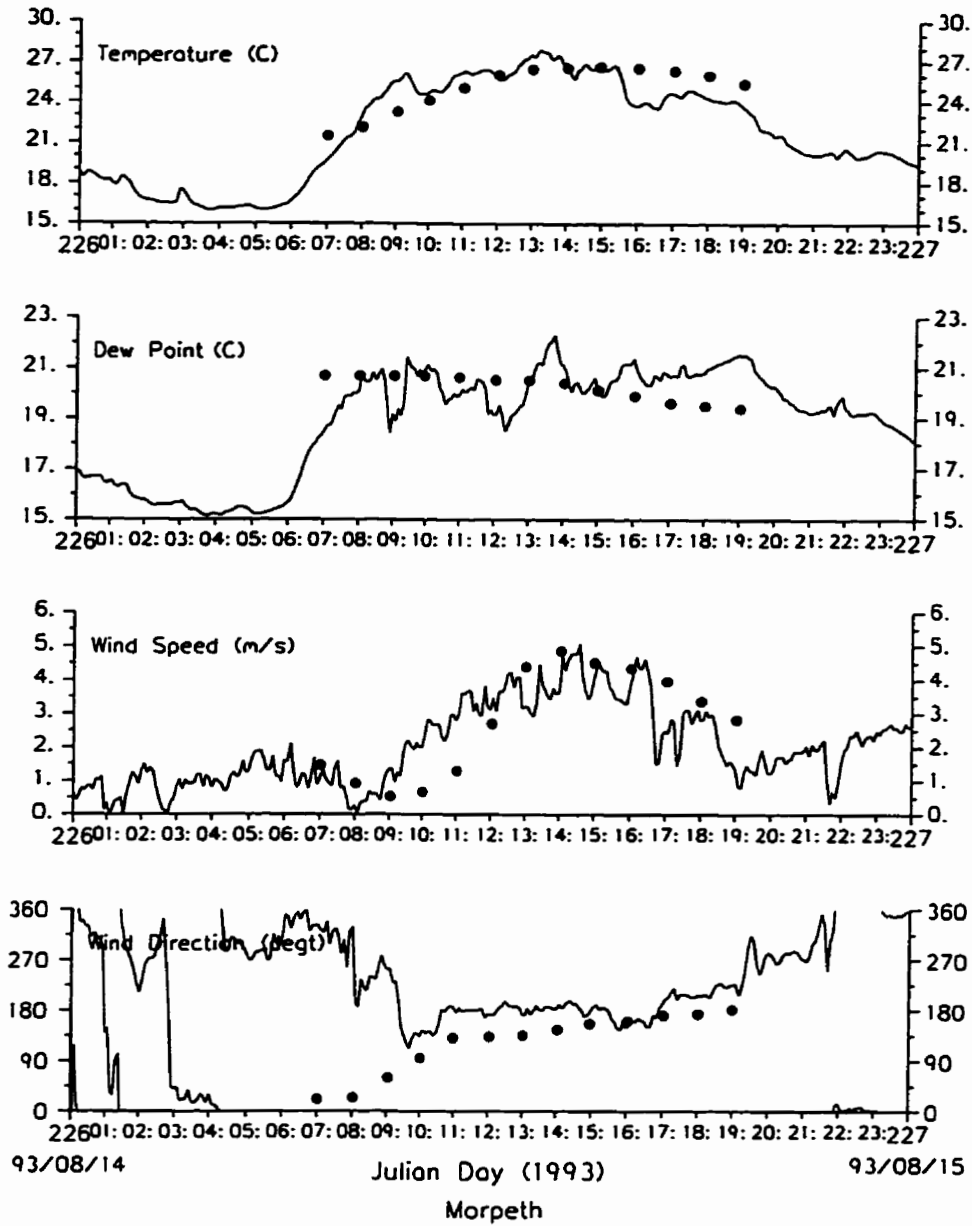


Figure 4.18. As in 4.17, except that observed and modelled time series values are for the Morpeth station location on the shore of Lake Erie.

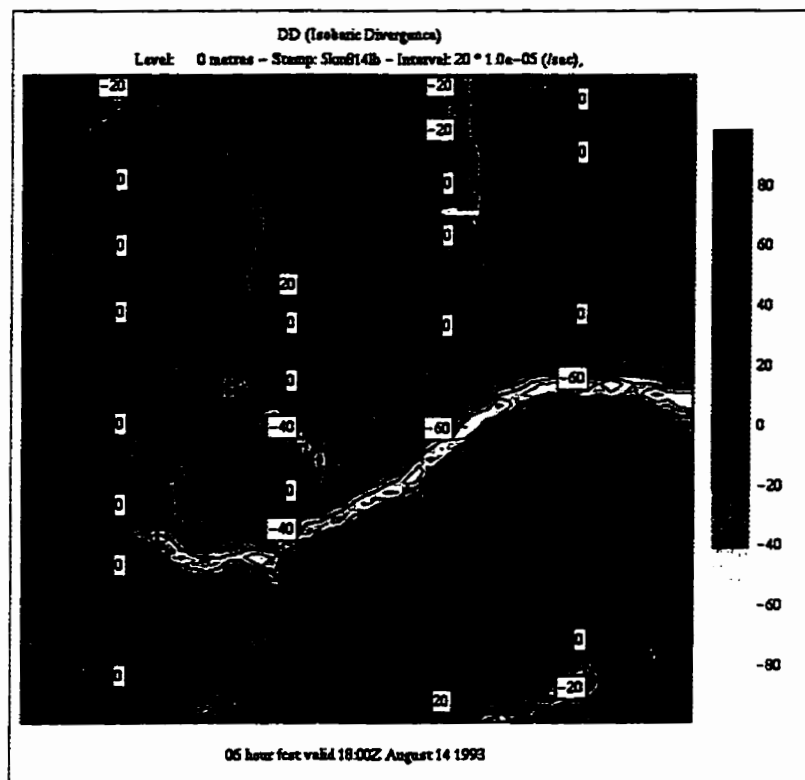


Figure 4.19. Divergence at the 10 m level at 1800 UTC on August 14 as predicted by the MC2 5 km grid model run. The divergence contour interval is $20 \times 10^{-5} \text{ s}^{-1}$.

STATION DATA

1993 SOMOS 10m Mesonet

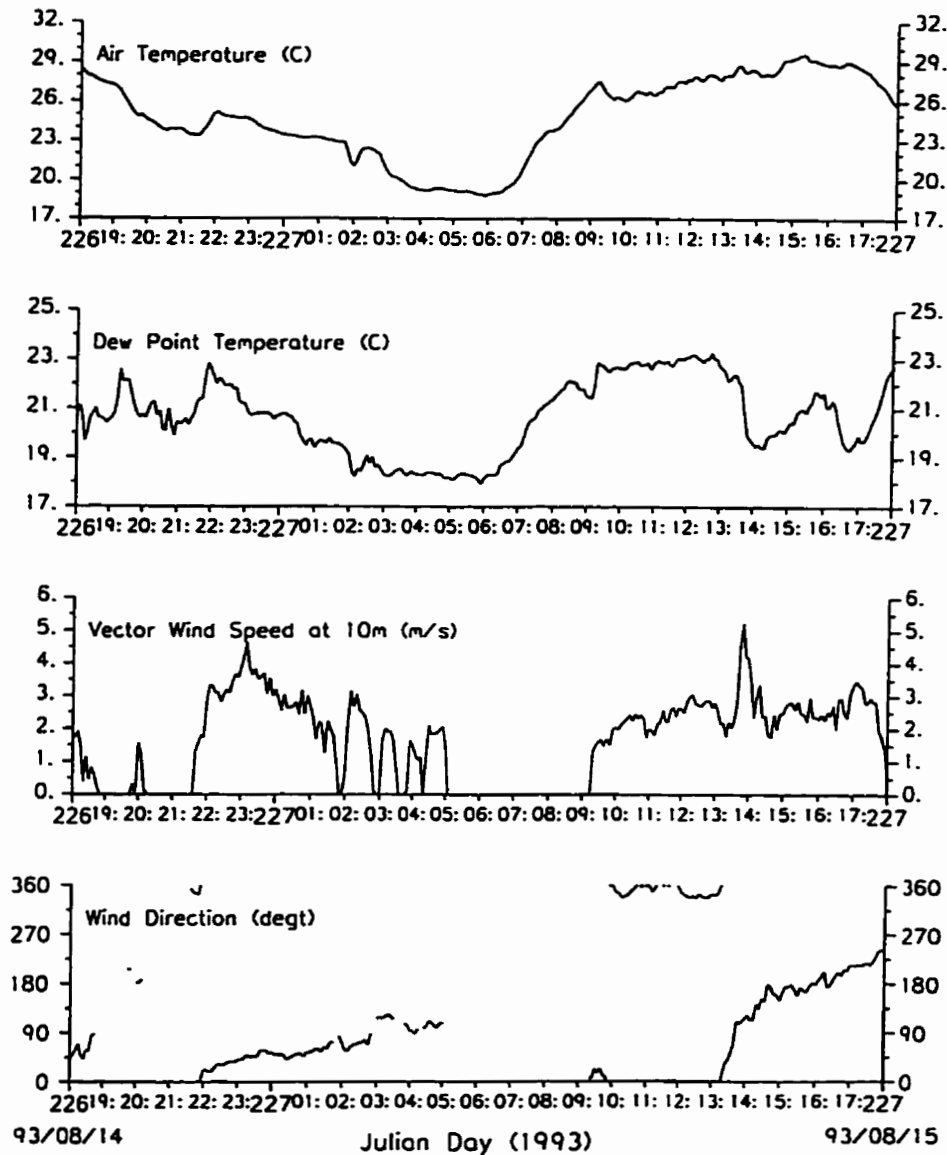
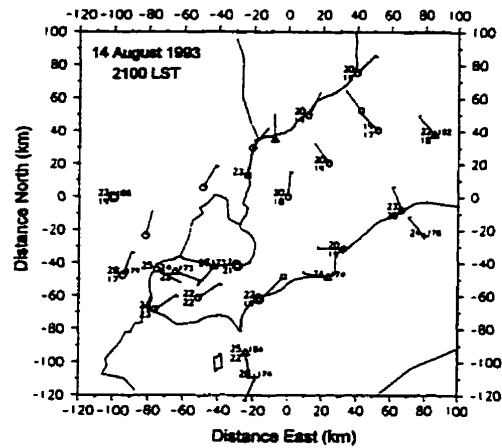
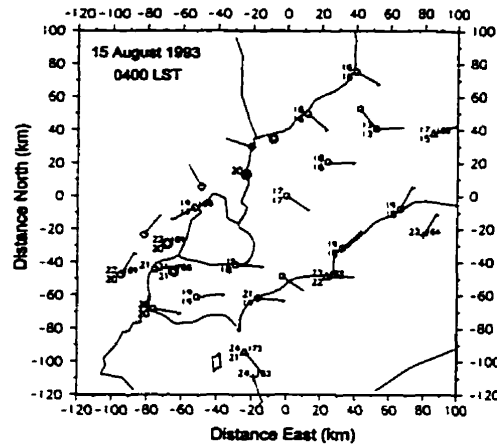


Figure 4.20. A plot of 1.5 m temperature, 1.5 m dew point, and 10 m wind speed and wind direction time series data from the Stoney Point mesonet station on the south shore of Lake St. Clair. Values are shown from 1800 LST on August 14 to 1800 LST on August 15. Data are shown at a five-minute time interval.

a)



b)



c)

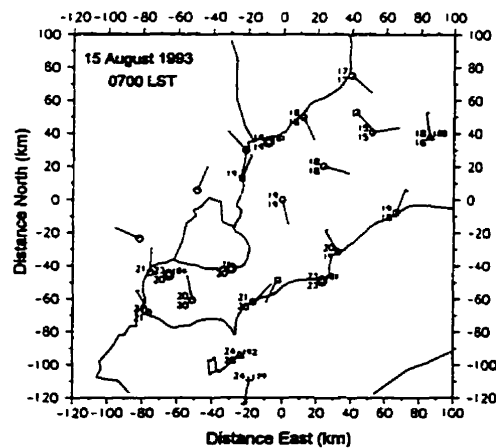


Figure 4.22. A sequence of mesonet station plots for 2100 LST (a) on August 14, and 0400 LST (b) and 0700 LST (c) on August 15. The standard synoptic plotting format is used (small wind barb = 5 knots, temperatures in $^{\circ}\text{C}$, pressure in tenths of a hPa).

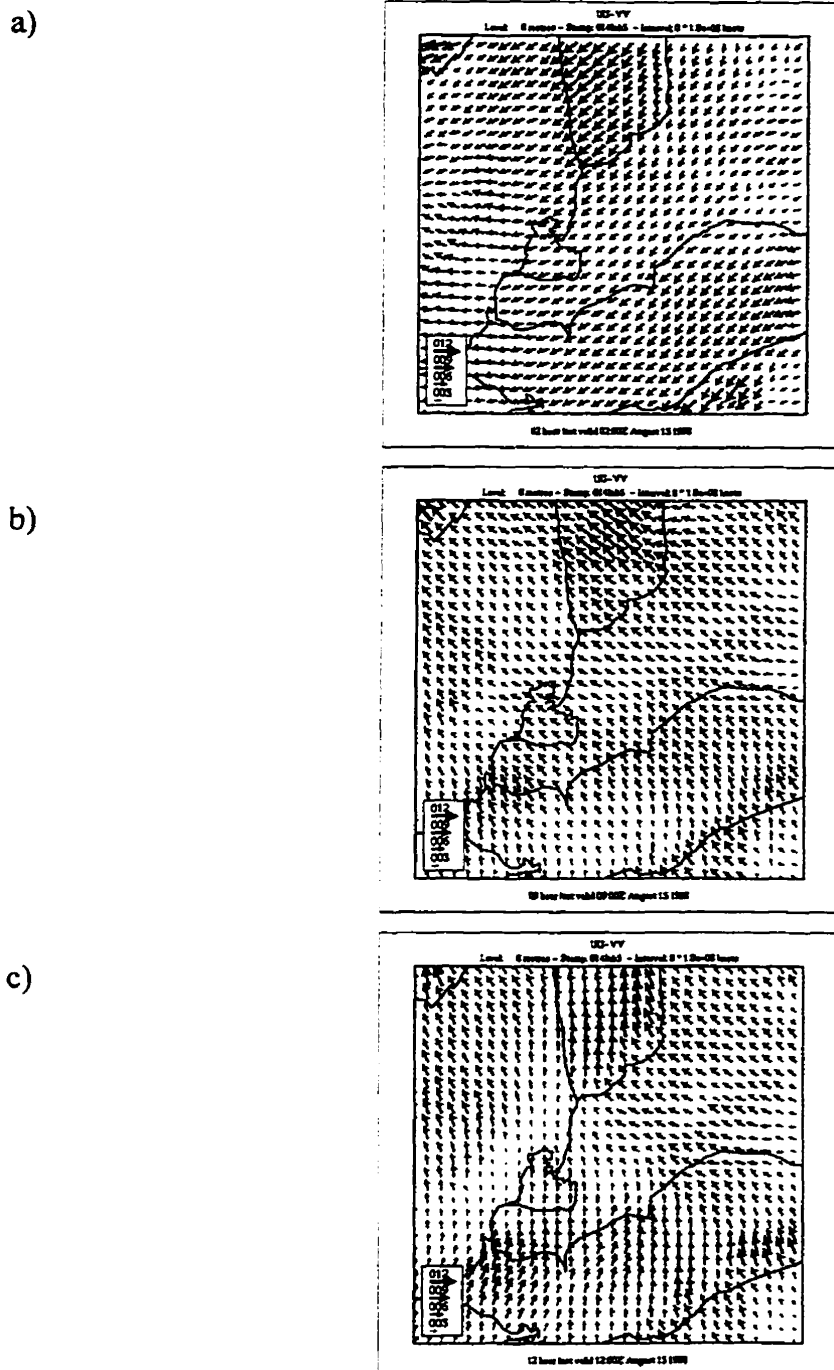


Figure 4.23. Modelled 10 m winds for 0200 UTC (a), 0900 UTC (b) and 1200 UTC (c) on August 15. Winds are in knots and north is toward the top of the image.

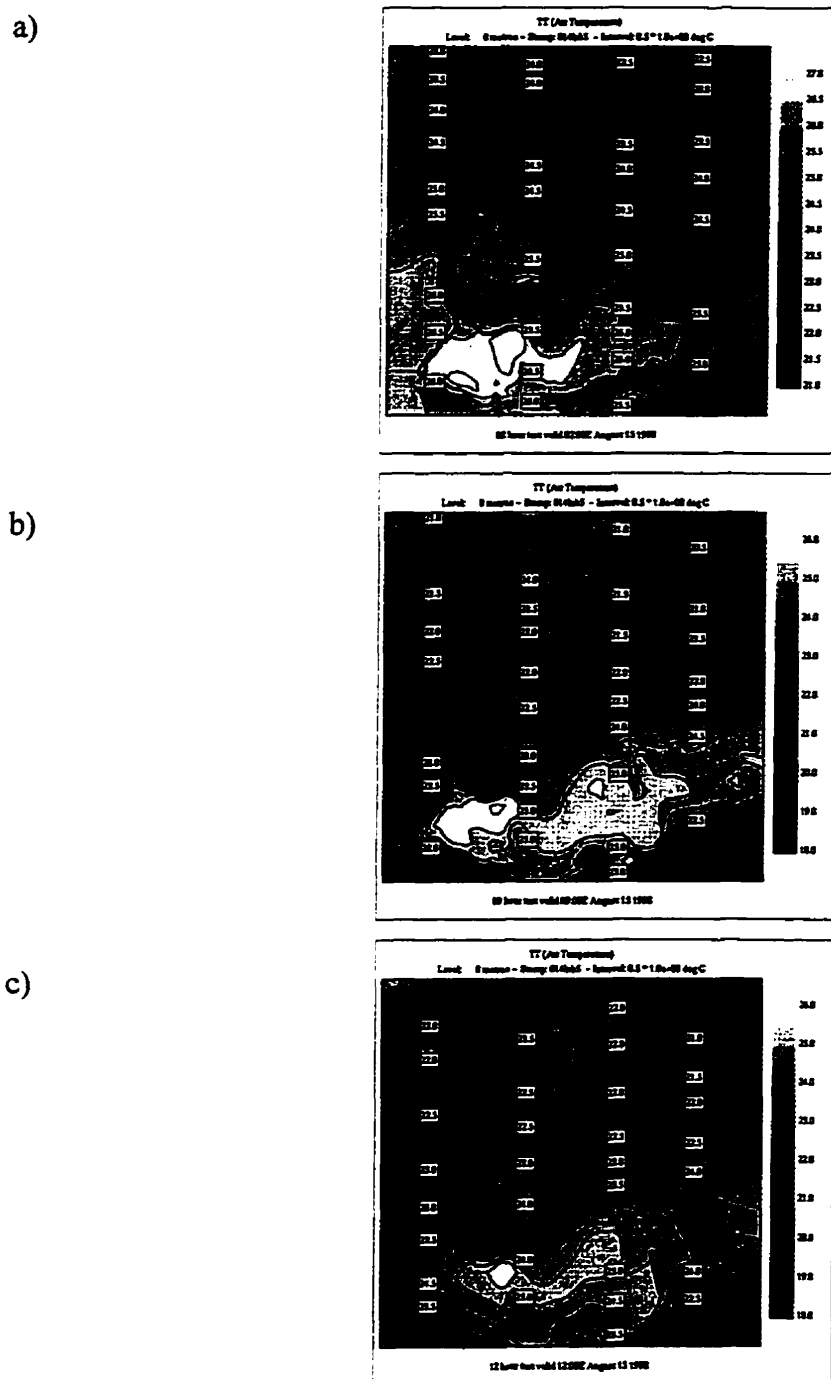


Figure 4.24. Modelled 1.5 m temperatures for 0200 UTC (a), 0900 UTC (b) and 1200 UTC (c) on August 15. A 0.5°C temperature contour interval is used.

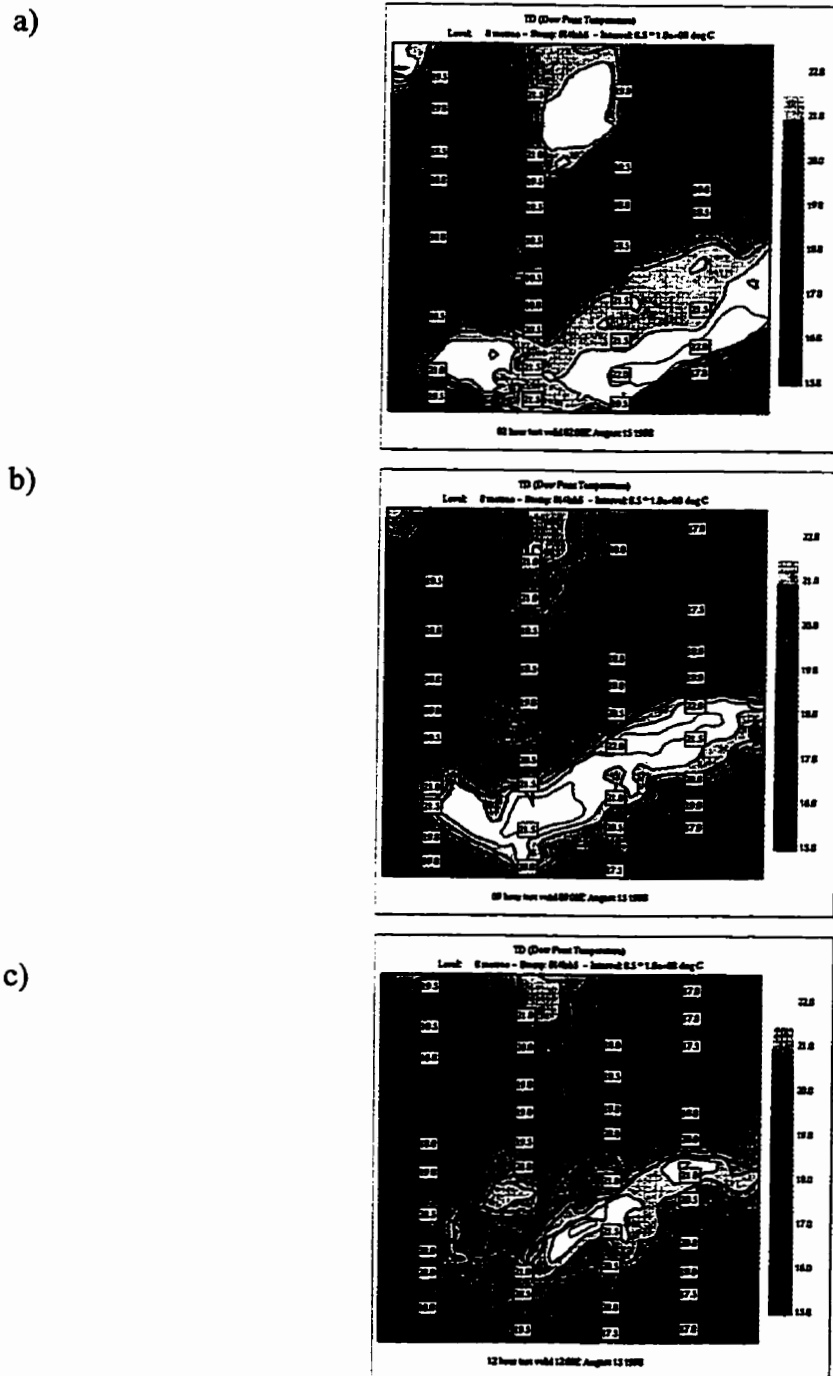
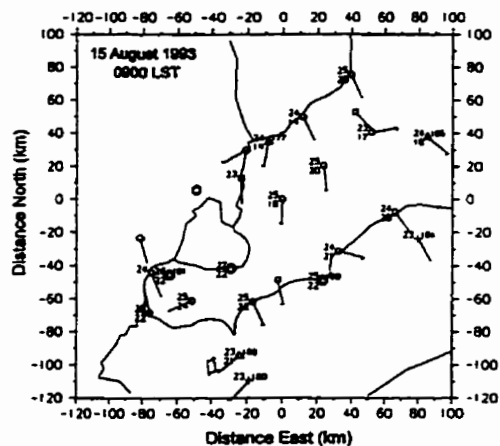
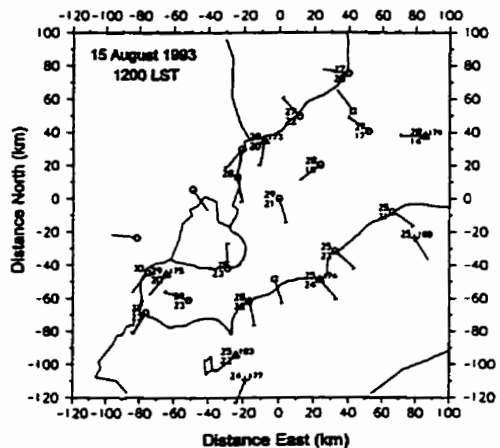


Figure 4.25. As in Figure 4.24, except values are 1.5 m dew point temperatures.

a)



b)



c)

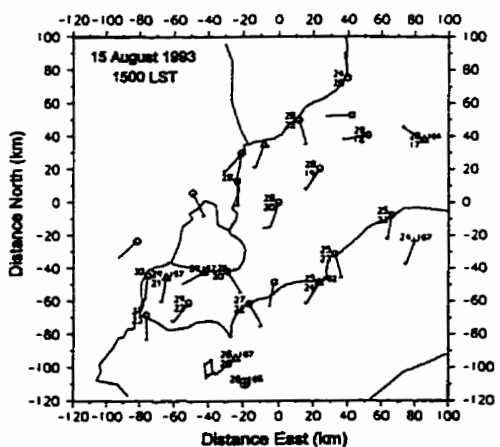


Figure 4.26. A sequence of mesonet station plots for 0900 LST (a), 1200 LST (b) and 1500 LST (c) on August 15. The standard synoptic plotting format is used (small wind barb = 5 knots, temperatures in $^{\circ}\text{C}$, pressure in tenths of a hPa).

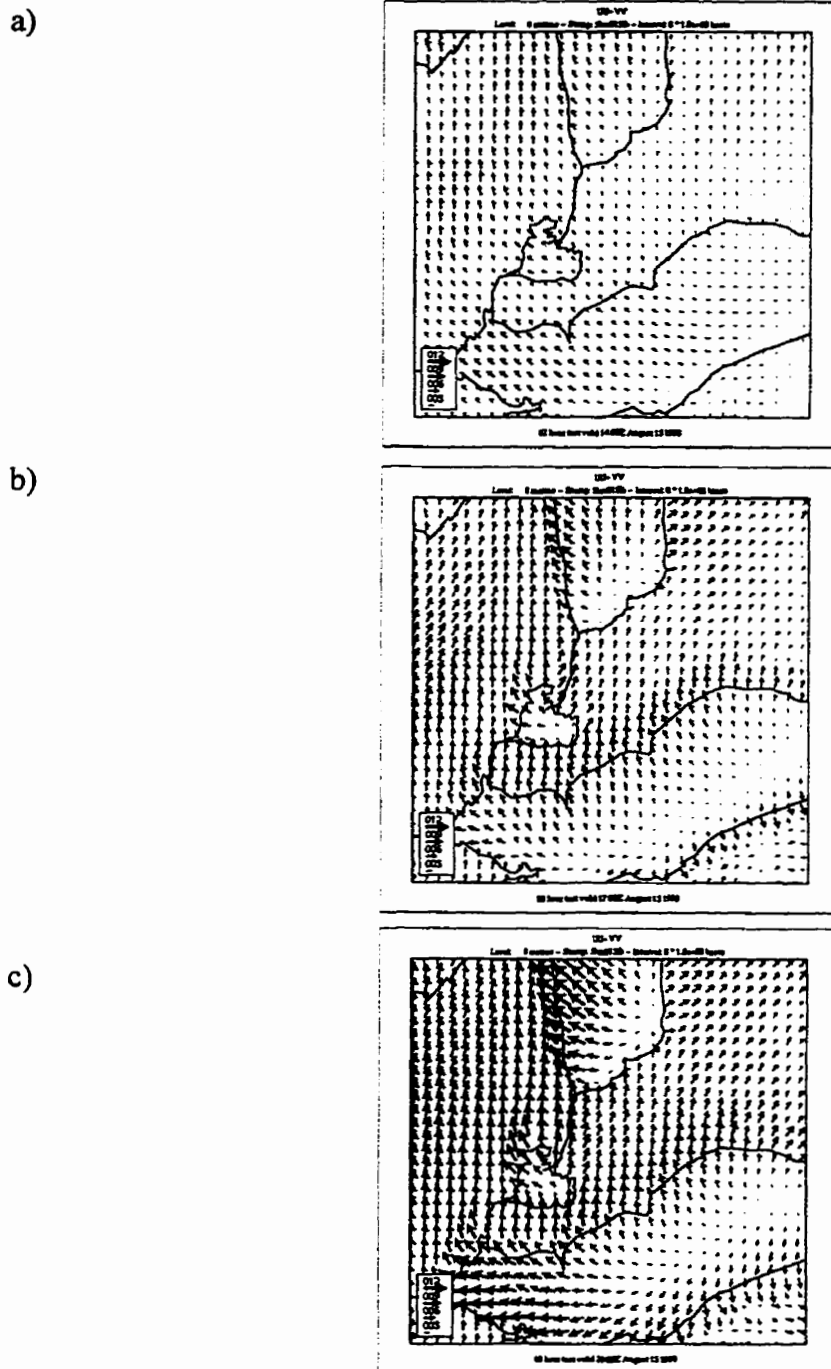


Figure 4.27. Modelled 10 m winds for 1400 UTC (a), 1700 UTC (b) and 2000 UTC (c) on August 15. Winds are in knots and north is toward the top of the image.

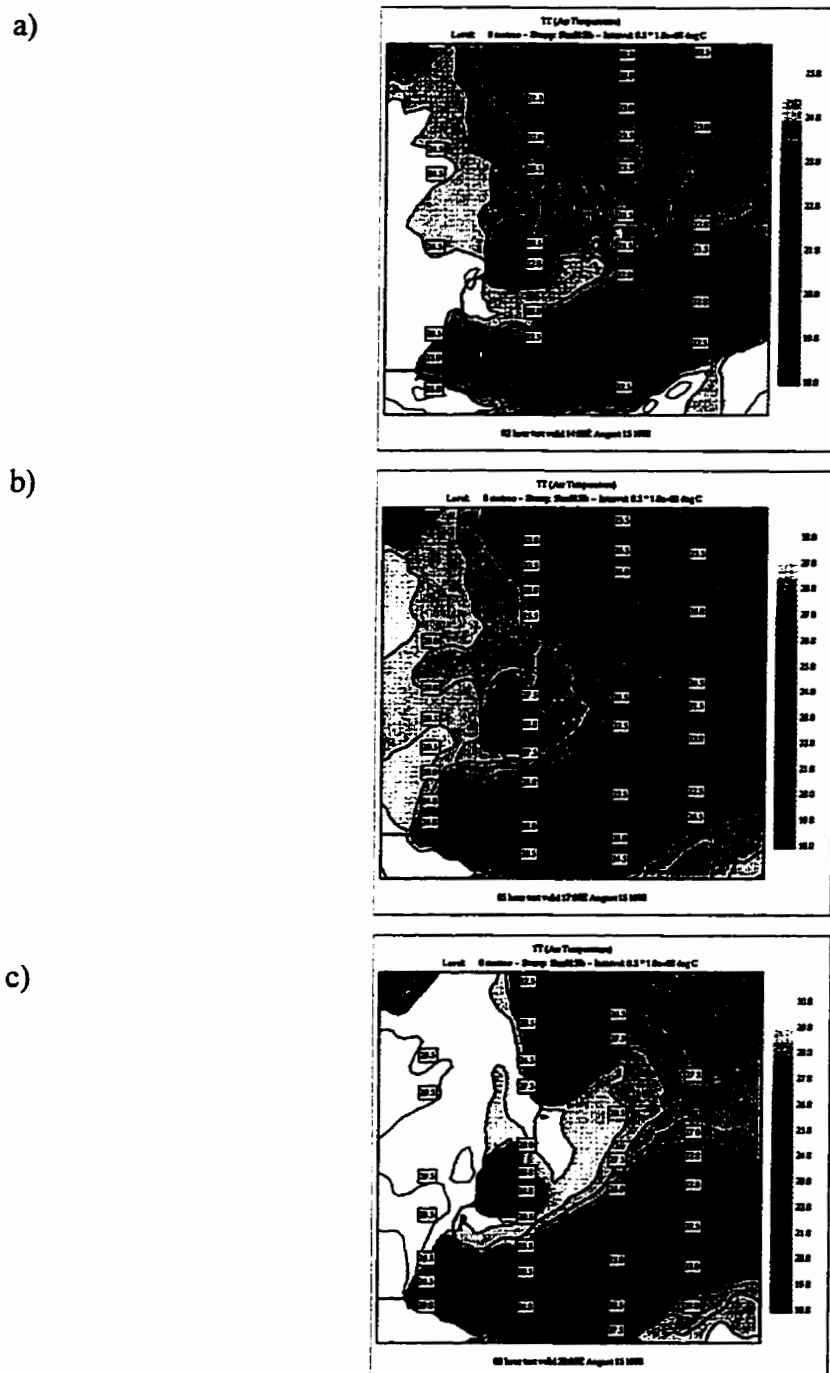
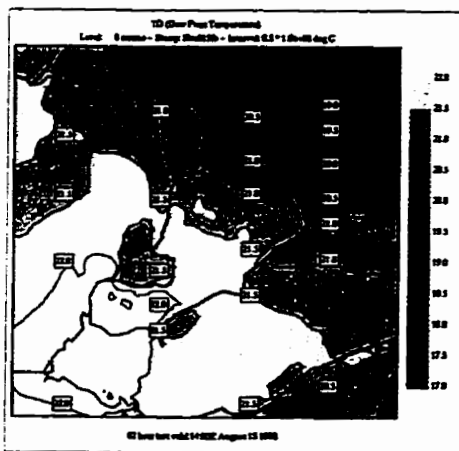
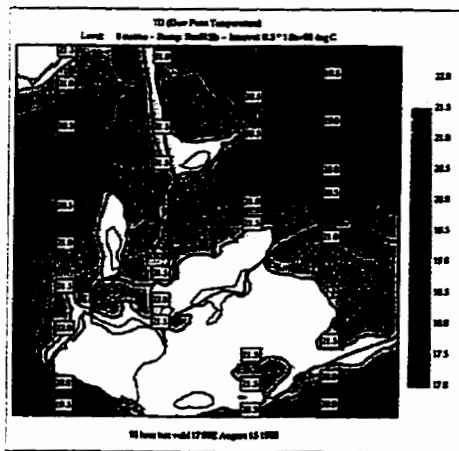


Figure 4.28. Modelled 1.5 m temperatures for 1400 UTC (a), 1700 UTC (b) and 2000 UTC (c) on August 15. A 0.5°C temperature contour interval is used.

a)



b)



c)

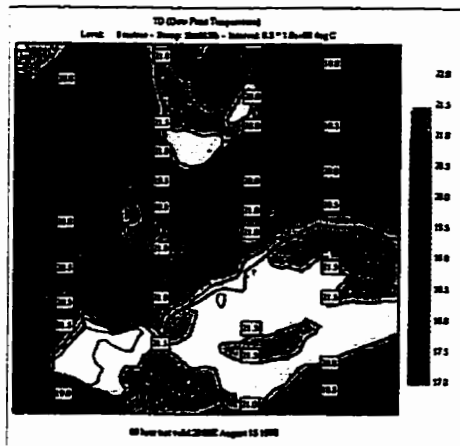


Figure 4.29. As in Figure 4.28, except values are 1.5 m dew point temperatures.

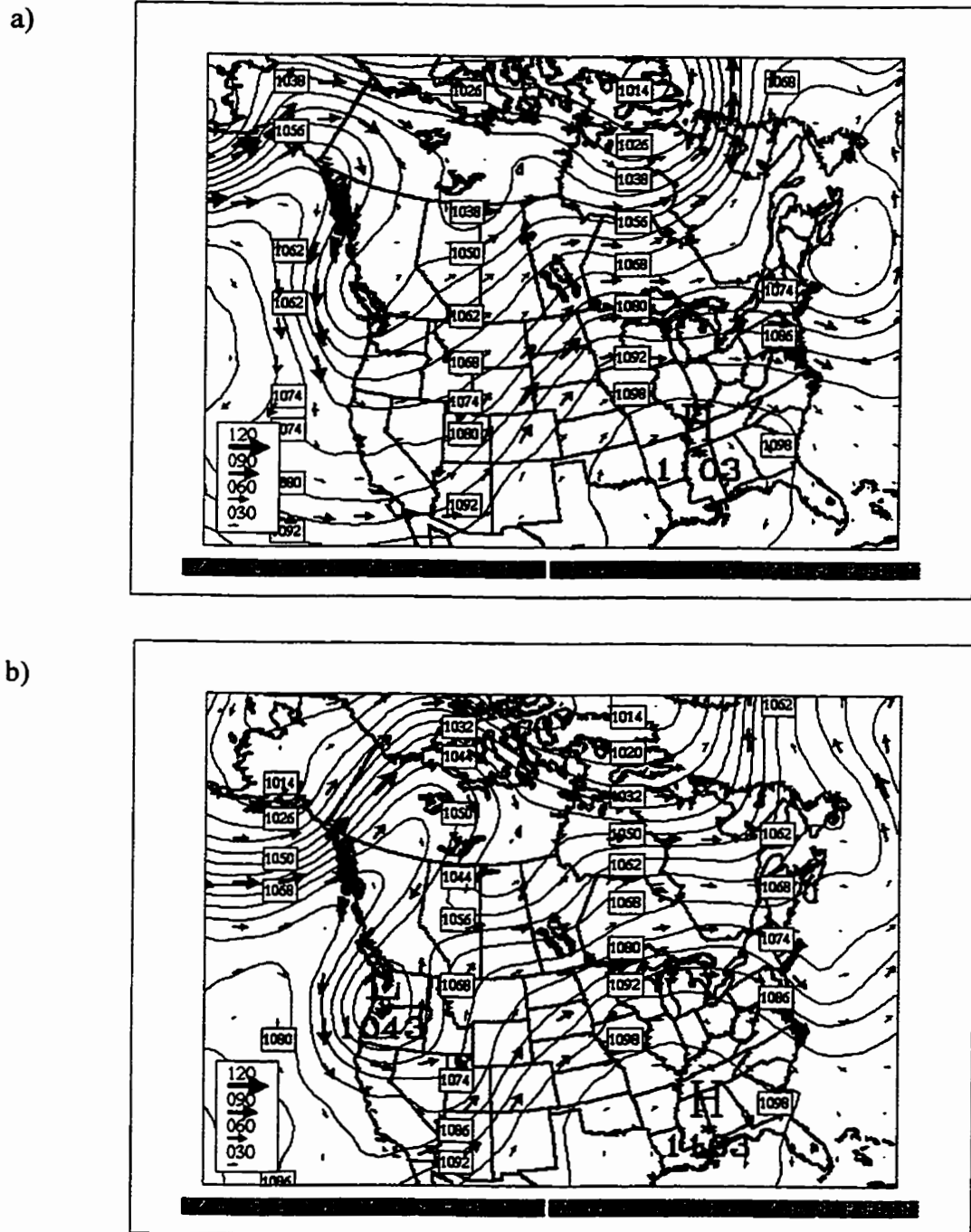


Figure 4.30. Analyzed 250 hPa charts valid for 1200 UTC on August 14 (a) and August 15 (b). The geopotential height contour is 6 dam. Winds are given in knots.

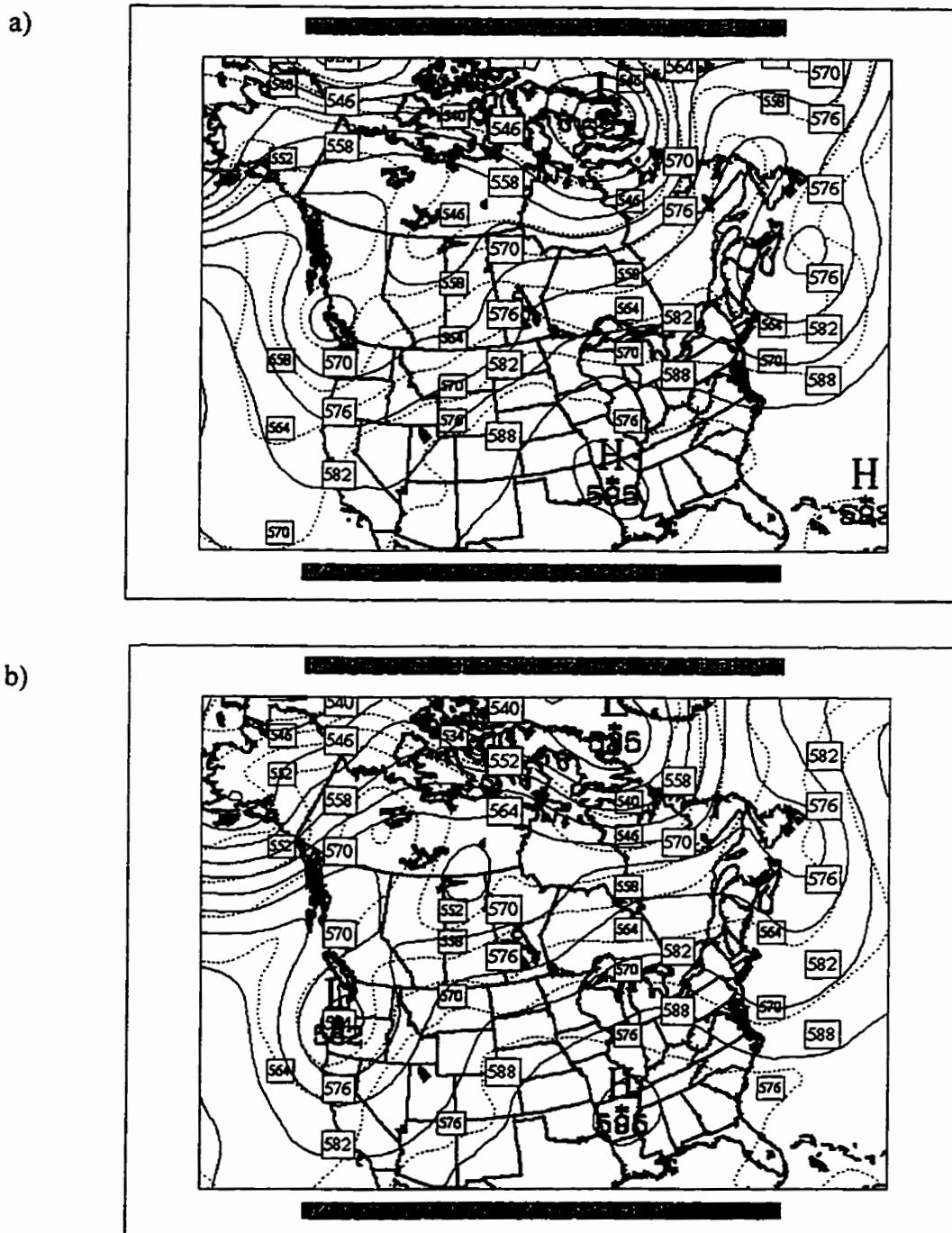
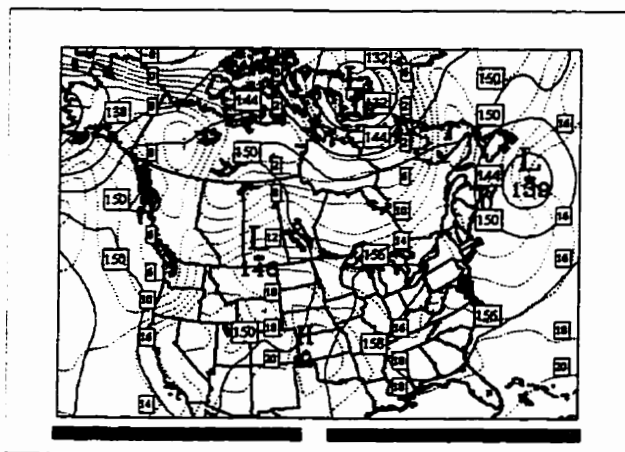
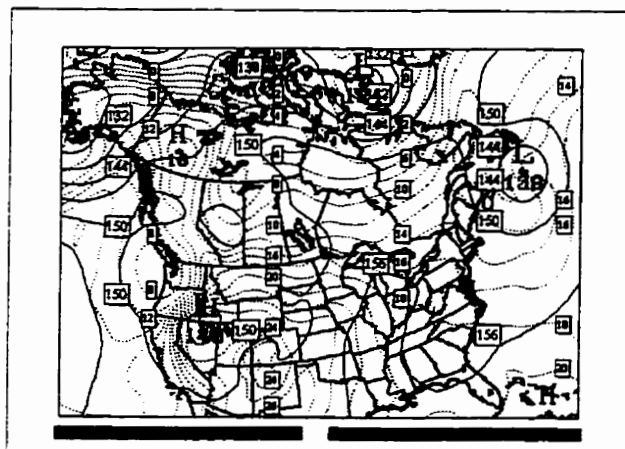


Figure 4.31. Analyzed 500 hPa charts for 1200 UTC on August 14 (a) and August 15 (b) showing geopotential heights on the 500 hPa surface (solid line) with the 500-1000 hPa thickness pattern superimposed (broken line). Contour intervals are 6 dam.

a)



b)



c)

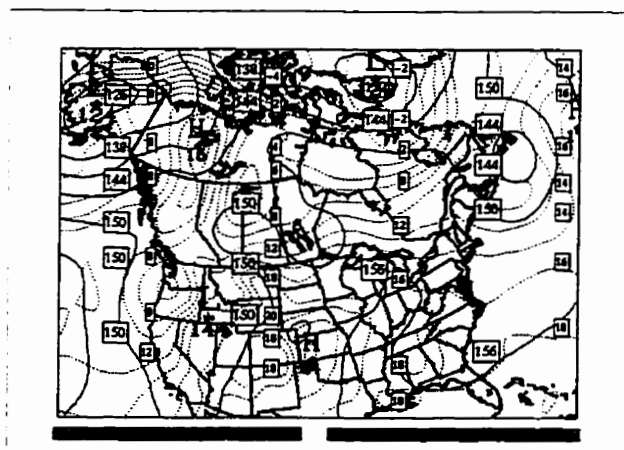


Figure 4.32. Analyzed 850 hPa charts for August 14 at 1200 UTC (a) and August 15 at 0000 UTC (b) and 1200 UTC (c). Geopotential heights are shown (solid line) using a 6 dam interval and temperatures are shown (broken line) using a 2°C interval.

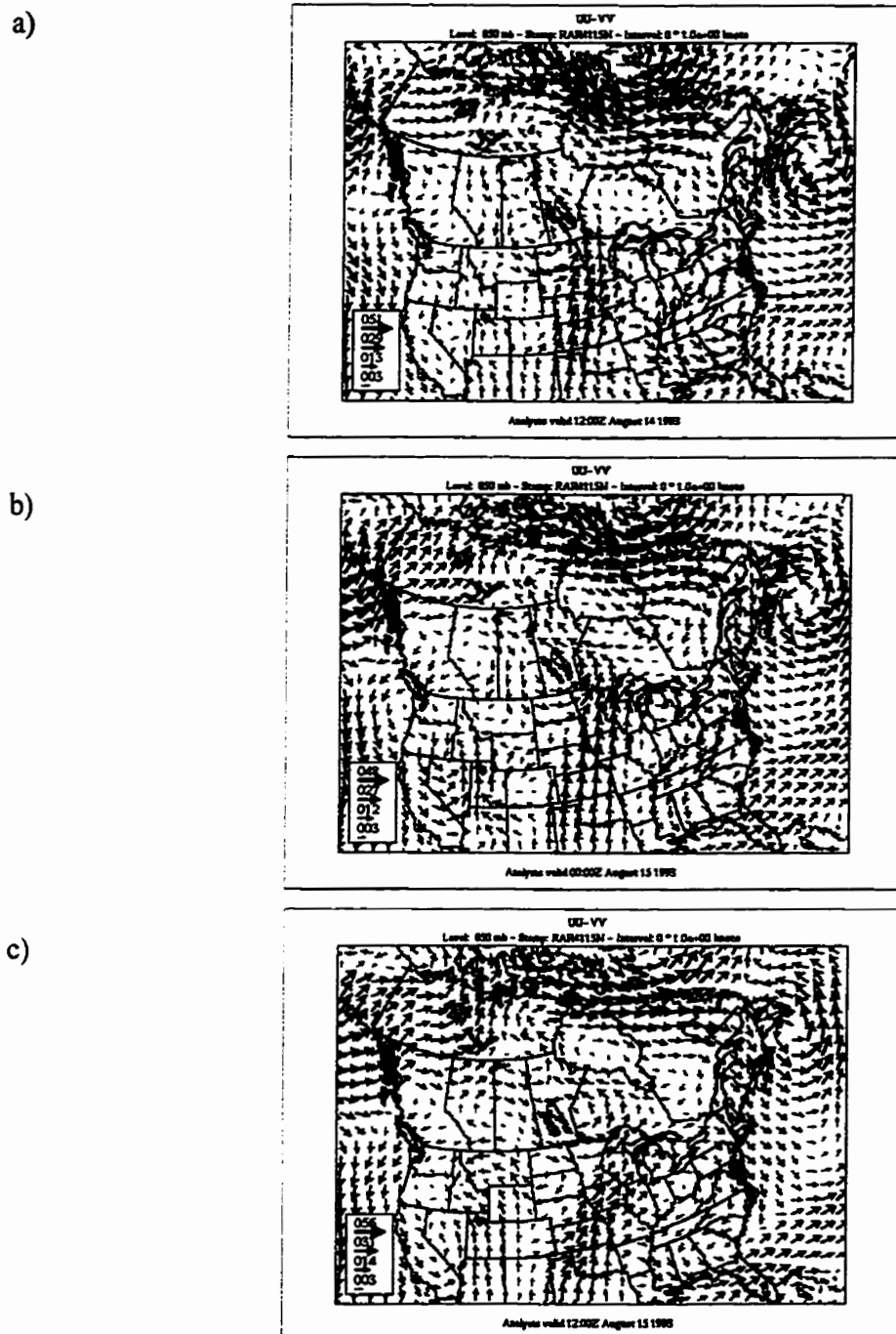


Figure 4.33. Analyzed 850 hPa winds for August 14 at 1200 UTC (a) and August 15 at 0000 UTC (b) and 1200 UTC (c). Winds are in knots.



Figure 4.35. Visible GOES-7 satellite image valid at 2000 UTC on August 14 over an area including the study region. North is toward the top of the image.

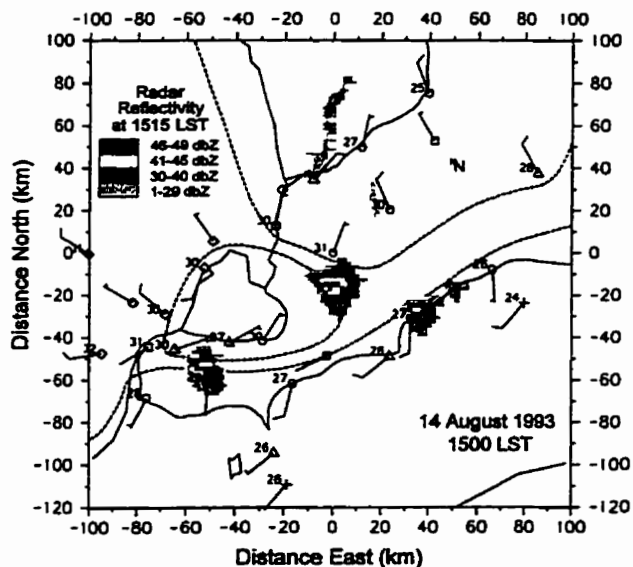


Figure 4.36. Plot of mesonet station winds and temperatures at 1500 LST (2000 UTC) on August 14 using the standard synoptic plotting format. The estimated extent of the inland penetration a lake breeze is indicated by a broken line. Composite maximum reflectivity radar data from 1515 LST are superimposed.

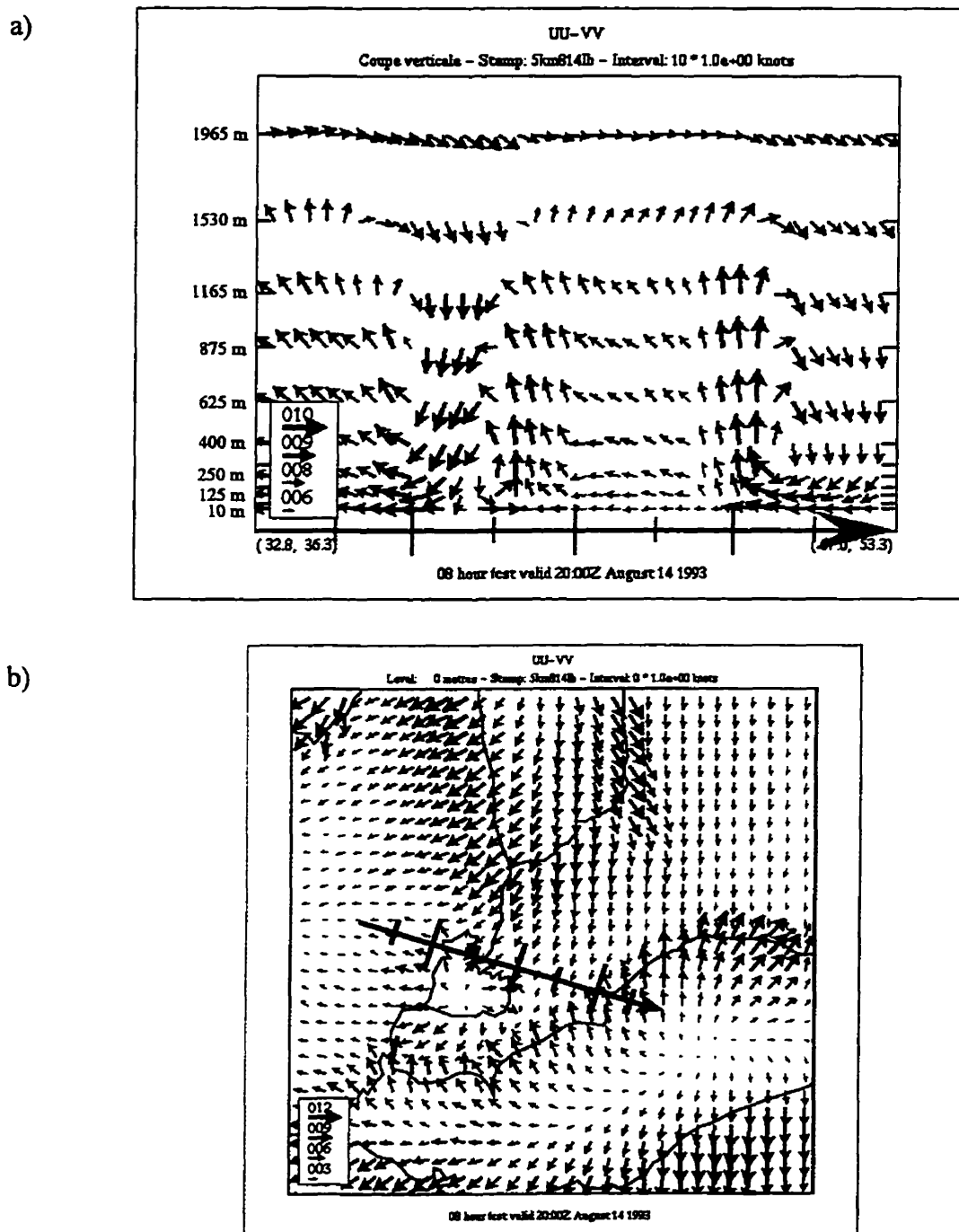


Figure 4.37. A vertical cross-section (a) through the combined horizontal and vertical modelled wind fields at 2000 UTC on August 14 following the arrow shown in (b). Cross-section winds are in knots and vertical winds are multiplied by 50. Winds at 10 m (b) at 2000 UTC on August 14 are also in knots.

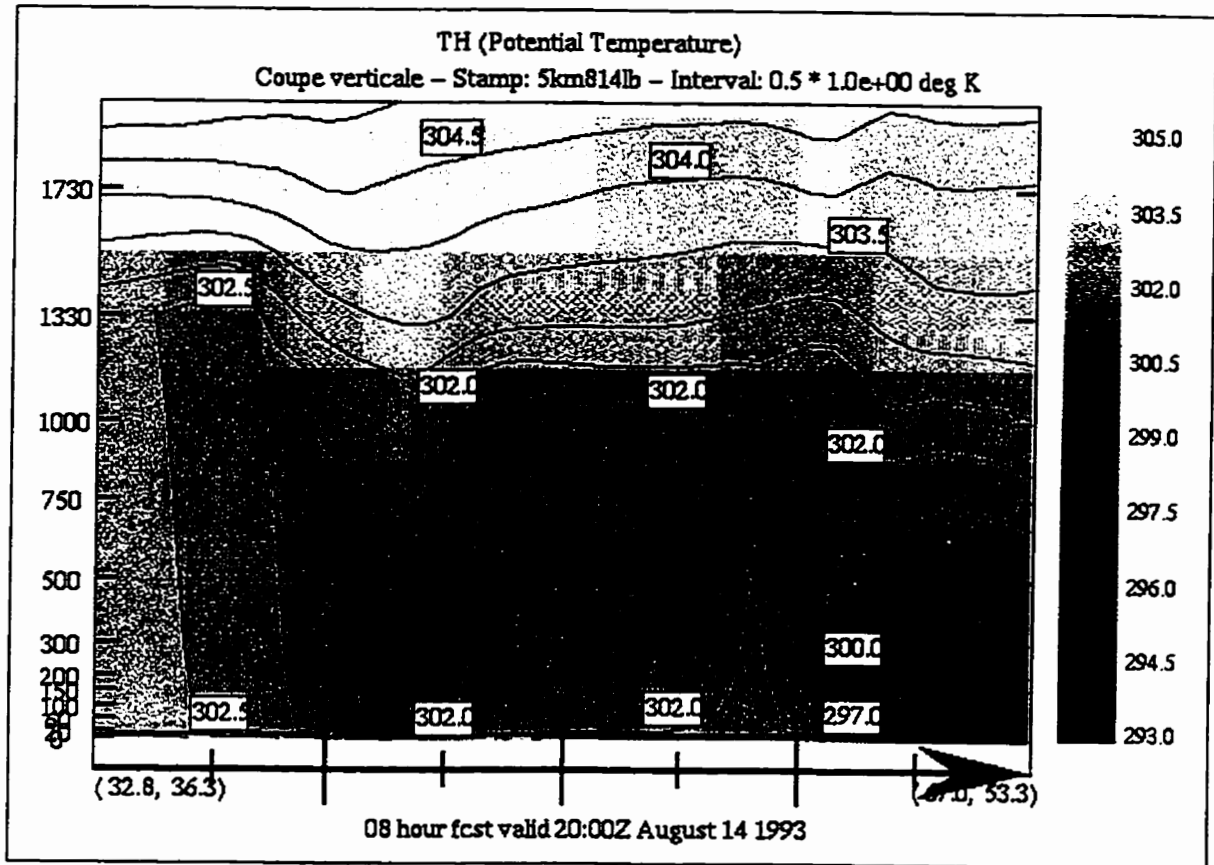


Figure 4.38. A vertical cross-section through the potential temperature field at 2000 UTC along the arrow shown in Figure 4.37b. A contour interval of 0.5 K is used.

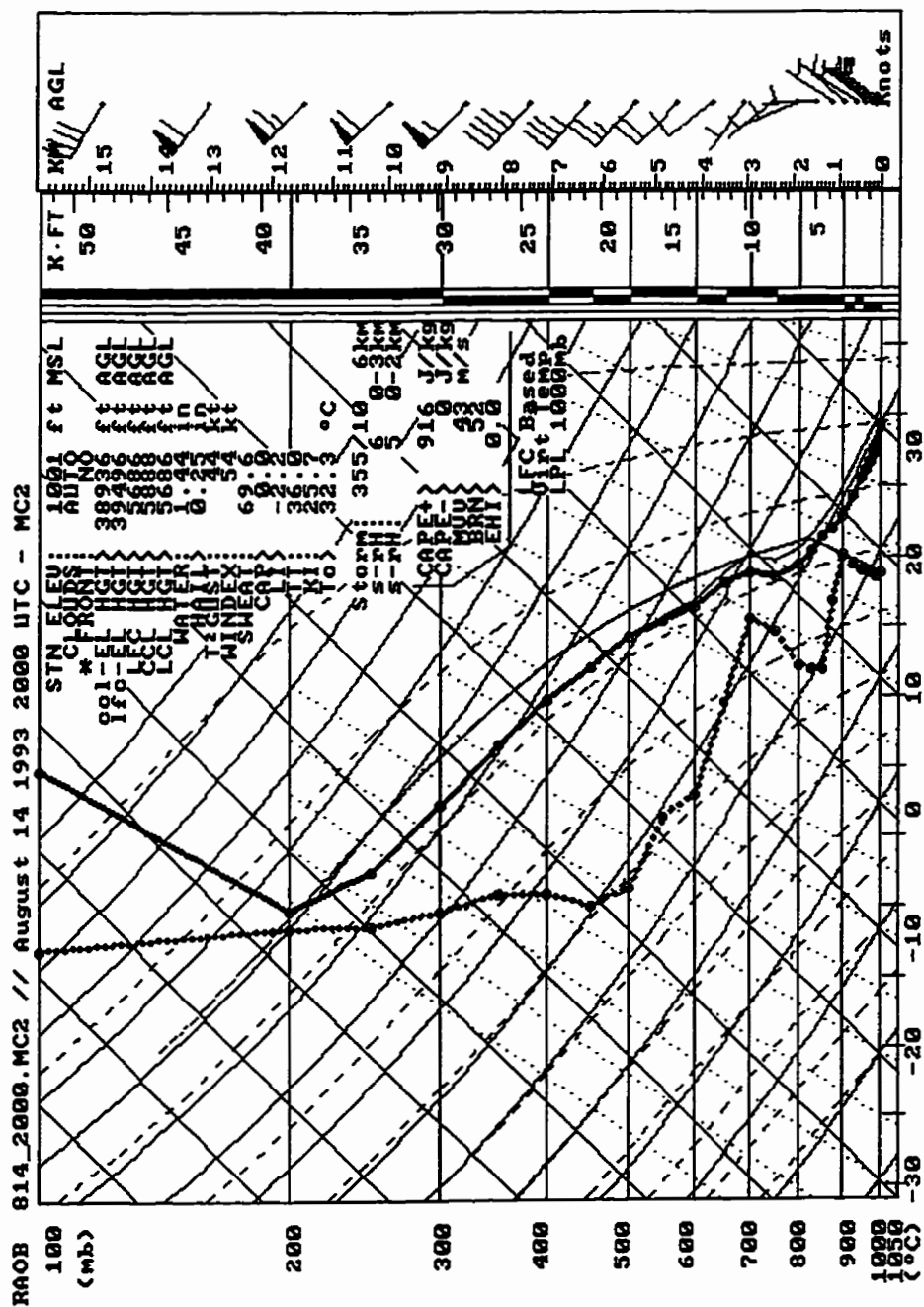


Figure 4.39. Modelled wind, temperature and dew point profiles at 2000 UTC on August 14 plotted on a skew-T diagram using RAOB software. Winds along the right side are in knots. The temperature curve is a solid line while the dew point curve is a broken line.

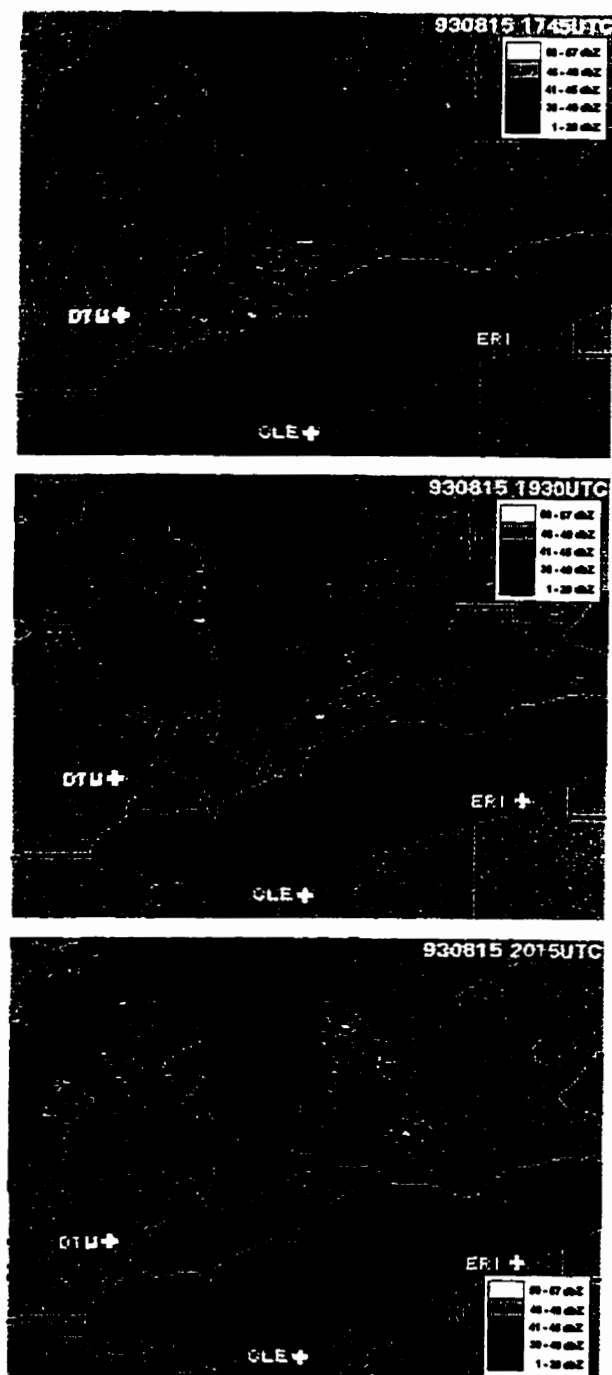


Figure 4.40. Composite maximum reflectivity radar data in the study region for 1745 UTC (a), 1930 UTC (b) and 2015 UTC (c) on August 15. The Tilbury, Glencoe and Dorchester storms are shown at their maximum intensities. The arrows in (b) mark the locations for cross-sections in Figures 4.41 and 4.42.

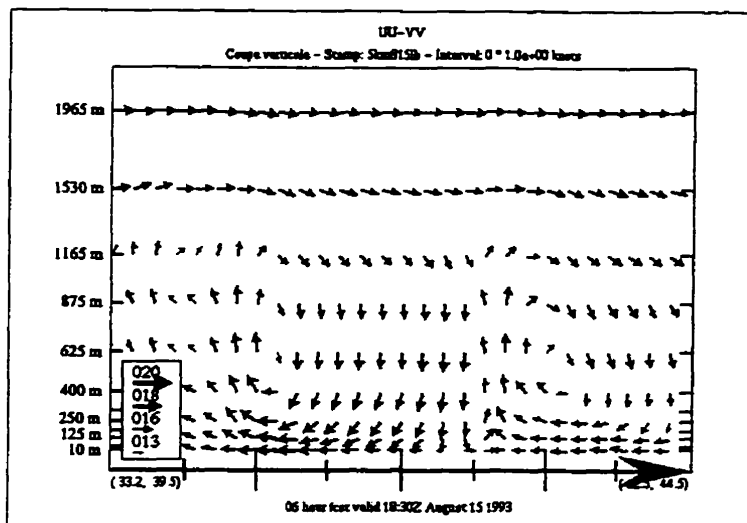


Figure 4.41. Vertical cross-section through the combined horizontal and vertical modelled wind fields at 1830 UTC on August 15 following the arrow shown in Figure 4.40b through Lake St. Clair (left arrow). Winds are in knots and the vertical wind is multiplied by 100.

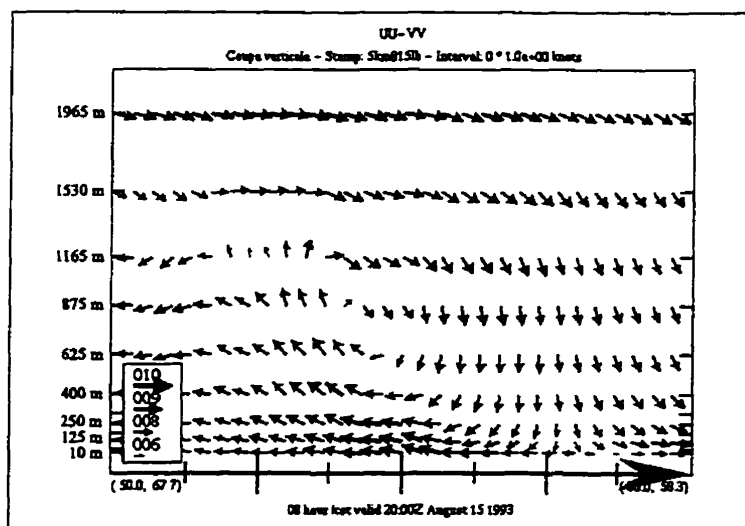


Figure 4.42. Vertical cross-section through the combined horizontal and vertical modelled wind fields at 2000 UTC on August 15 following the arrow shown in Figure 4.40b across the Lake Erie shore (right arrow). Winds are in knots and the vertical wind is multiplied by 100.

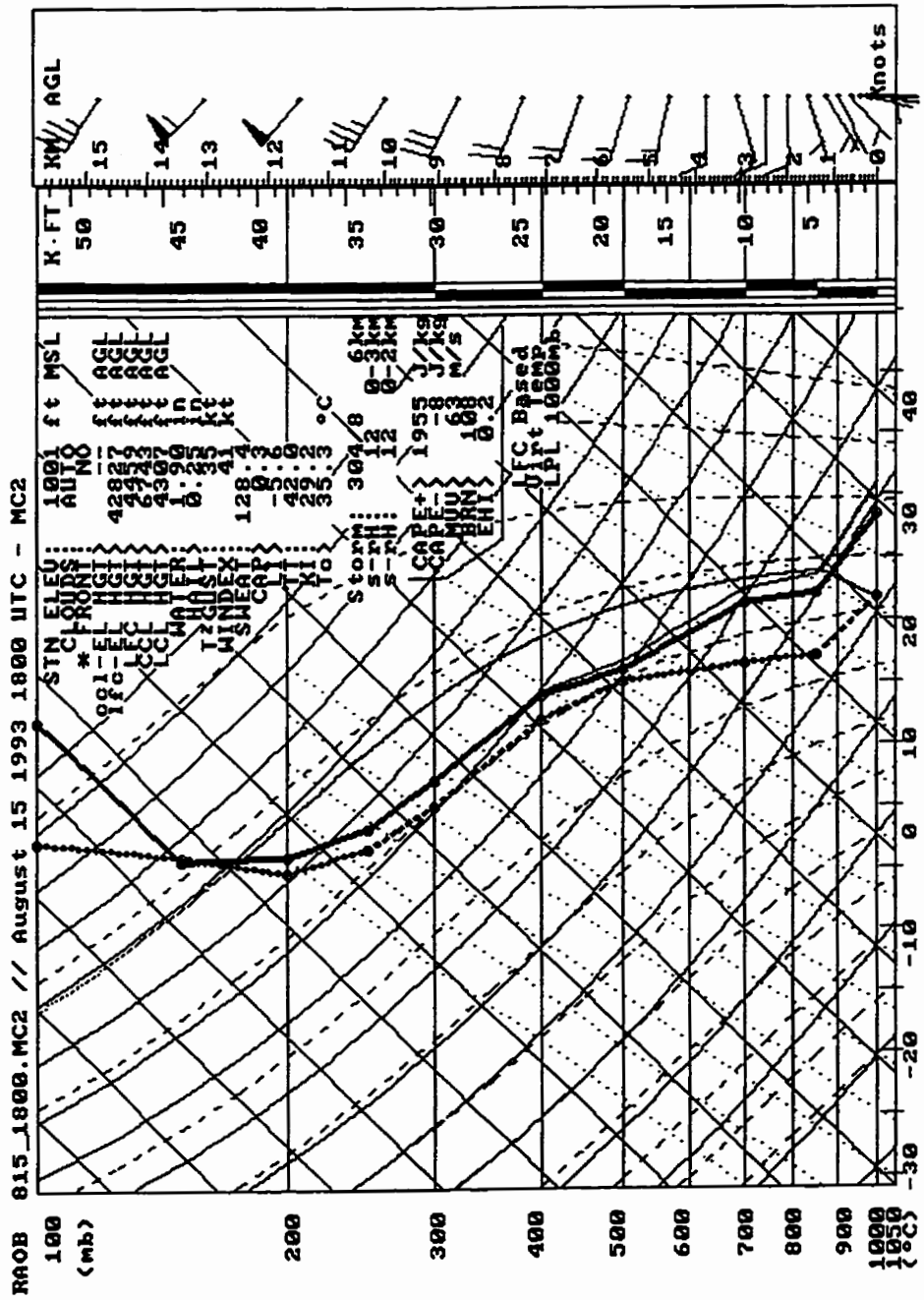


Figure 4.43. Modelled wind, temperature and dew point profiles at 1800 UTC on August 15 plotted on a skew-T diagram using RAOB software. Winds along the right side are in knots. The temperature curve is a solid line while the dew point curve is a broken line.

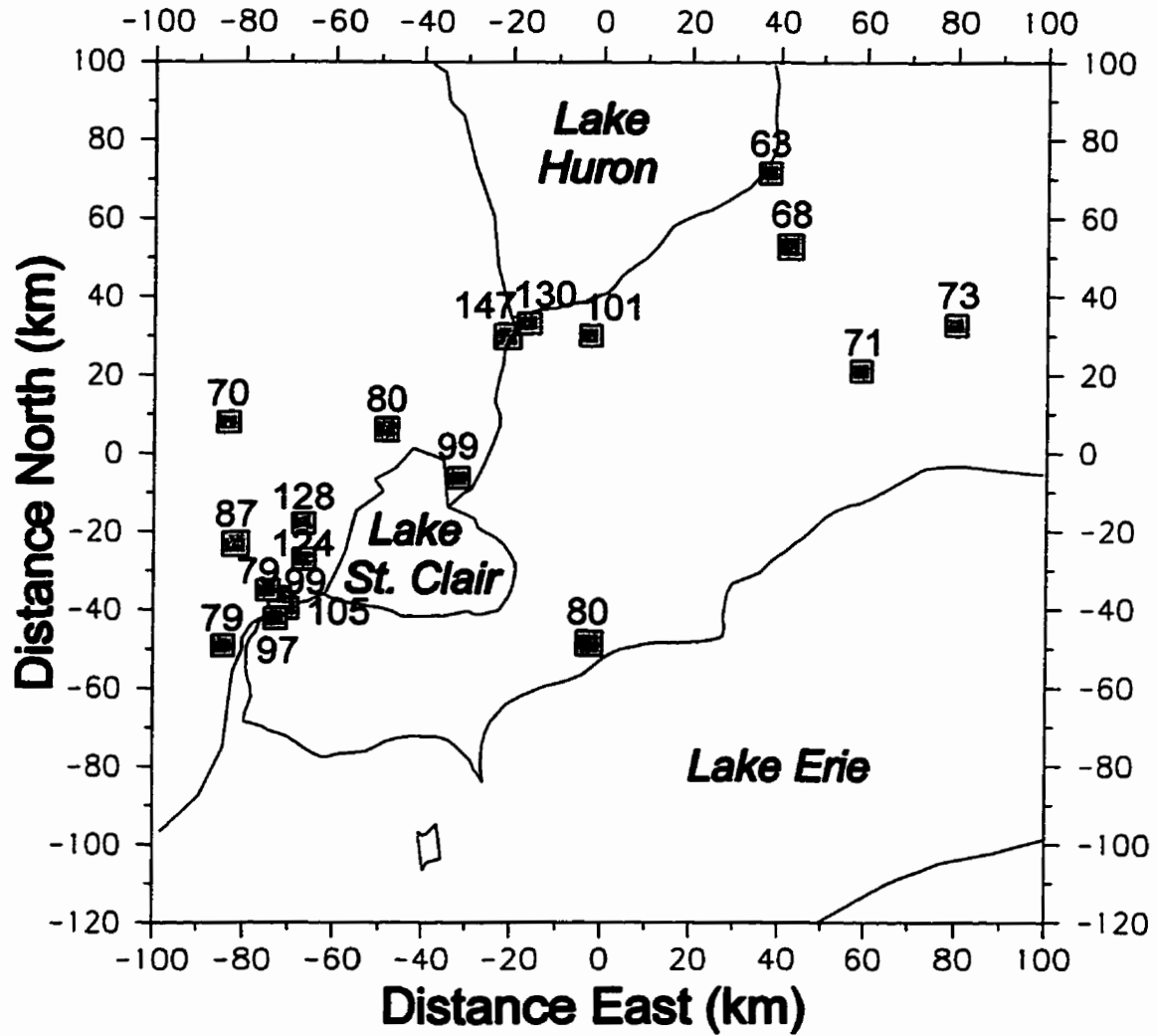


Figure 4.44. Map showing maximum one-hour average ozone concentrations on August 14 recorded at sites in the study region.

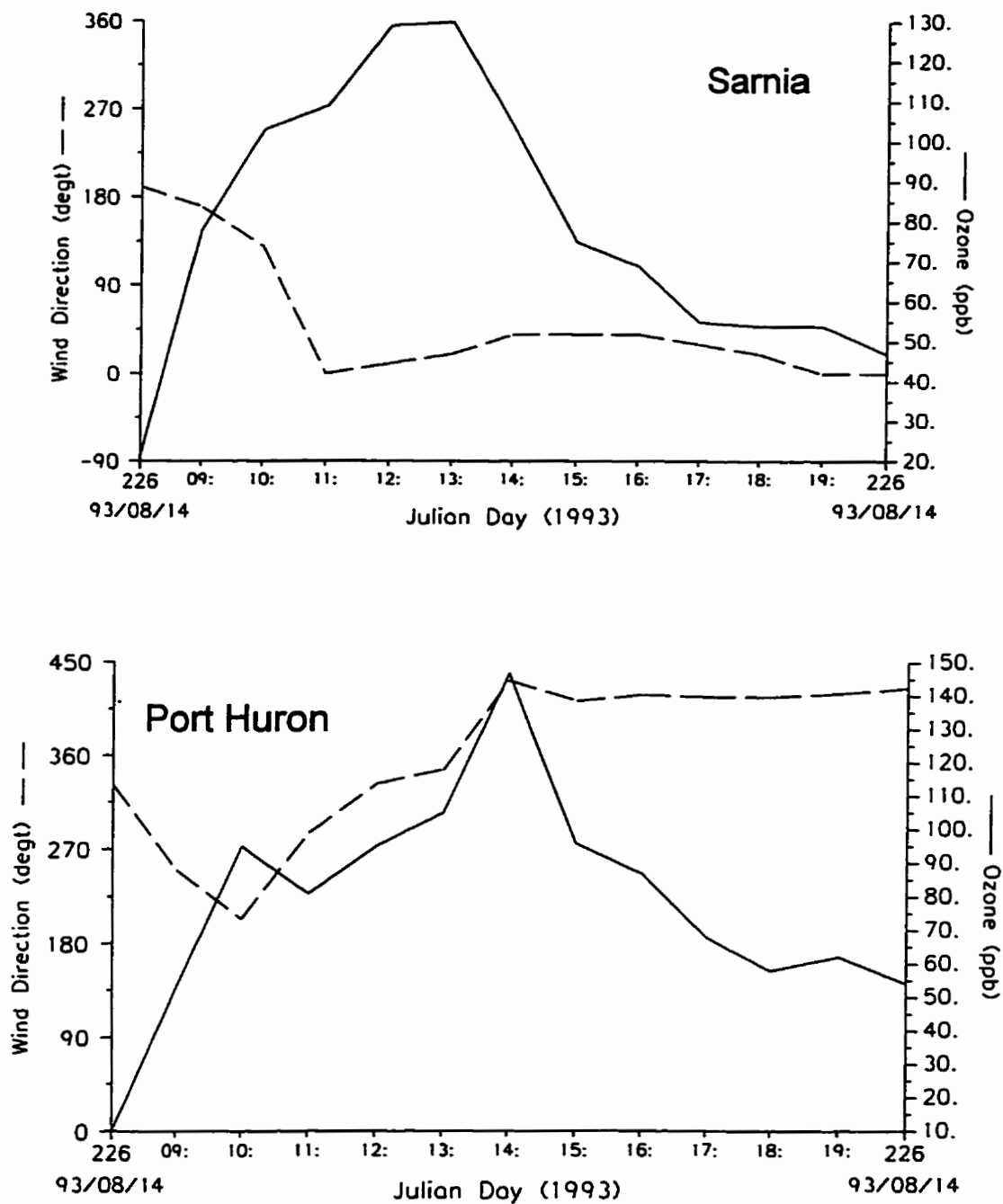


Figure 4.45. Times series of wind direction and ozone concentration data at Sarnia (a) and Port Huron (b). Data are shown from 0800 LST to 2000 LST on August 14. The Lake Huron lake breeze arrived at Sarnia by 1100 LST and at Port Huron by 1400 LST.

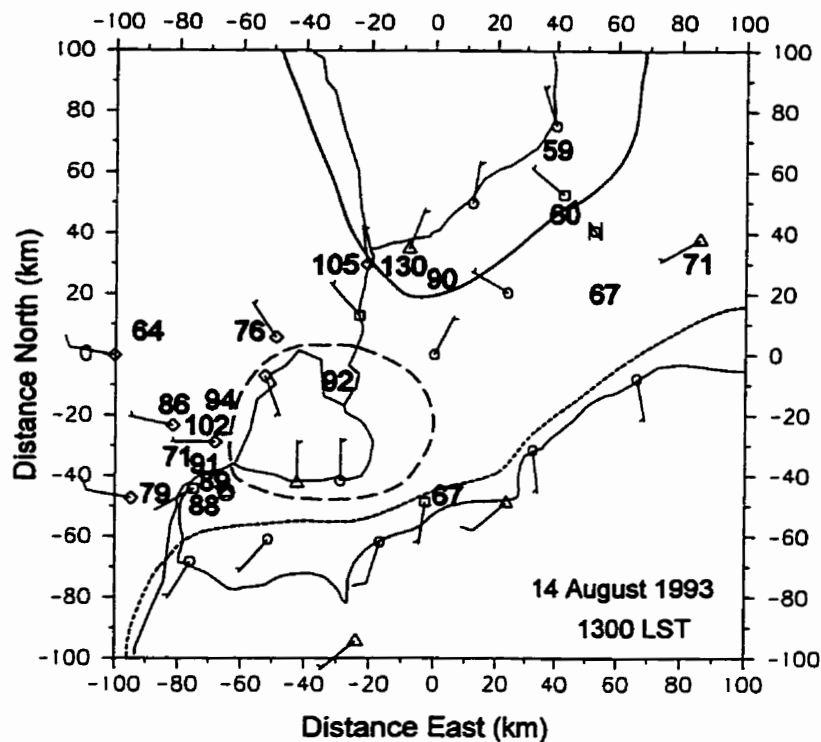


Figure 4.46. Map showing station winds (short barb = 5 knots), the estimated lake breeze penetration distances and observed surface ozone concentrations (ppb) at 1300 LST on August 14.

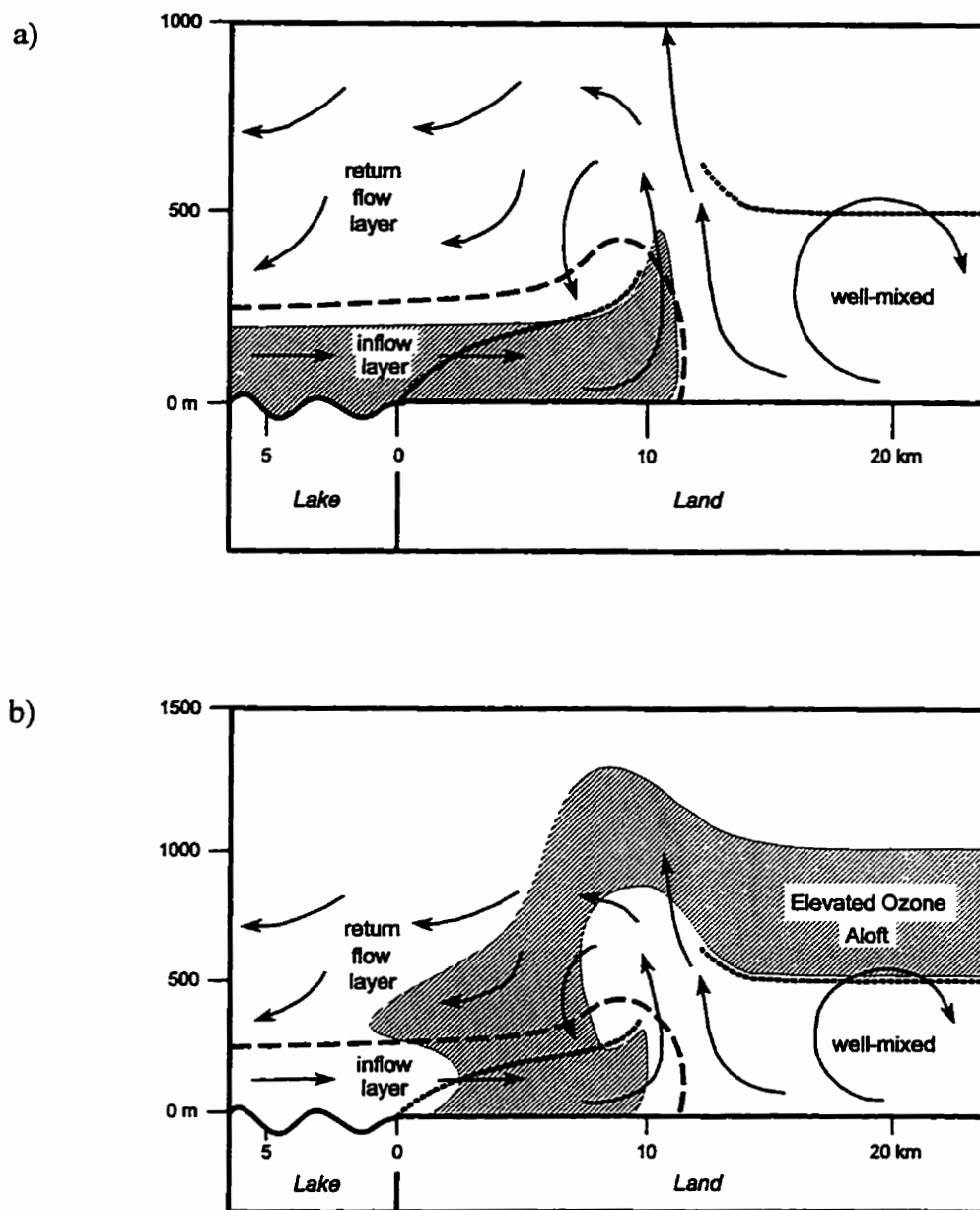
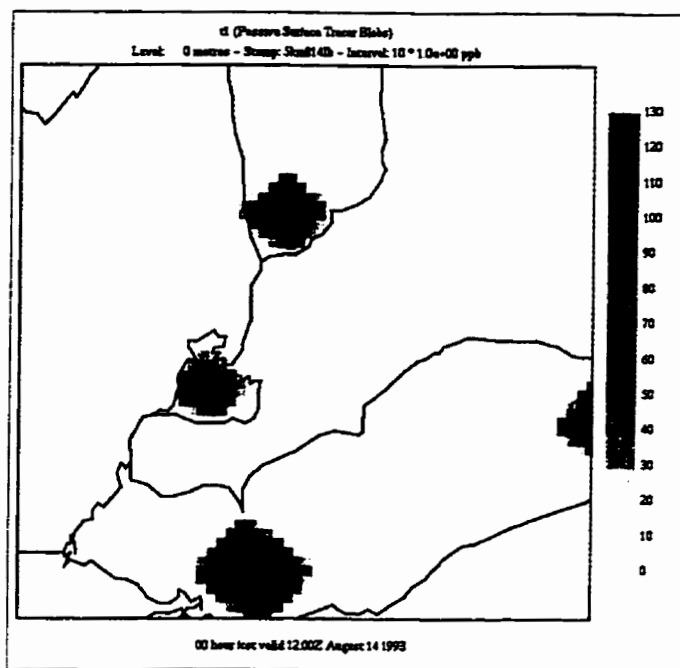


Figure 4.47. Idealized schematic diagrams illustrating the 'ozone at the surface' (a) and 'ozone aloft' (b) hypotheses. Areas of elevated ozone are hatched. It is assumed for (b) that the layer of ozone aloft was initially over land. The long-dashed line represents the outward extent of the lake breeze inflow layer while the short-dashed lines mark the top of the convective boundary layer. Arrows show the general air motions.

a)



b)

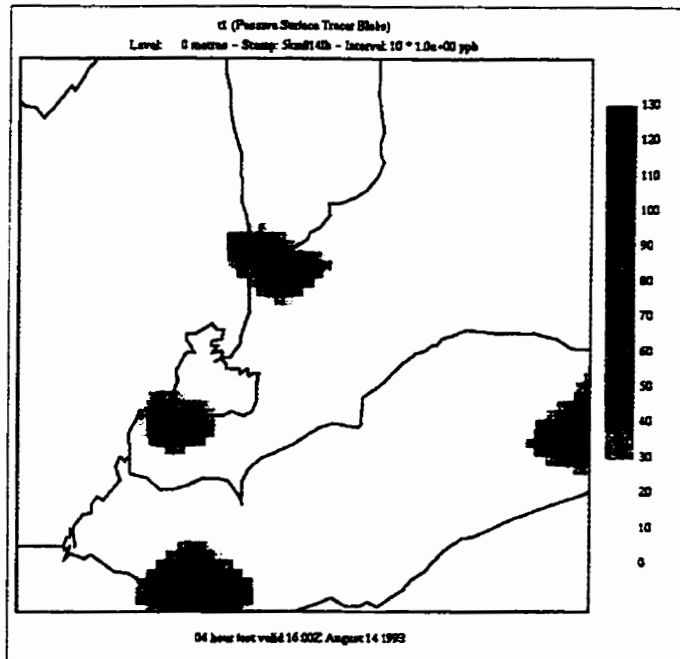
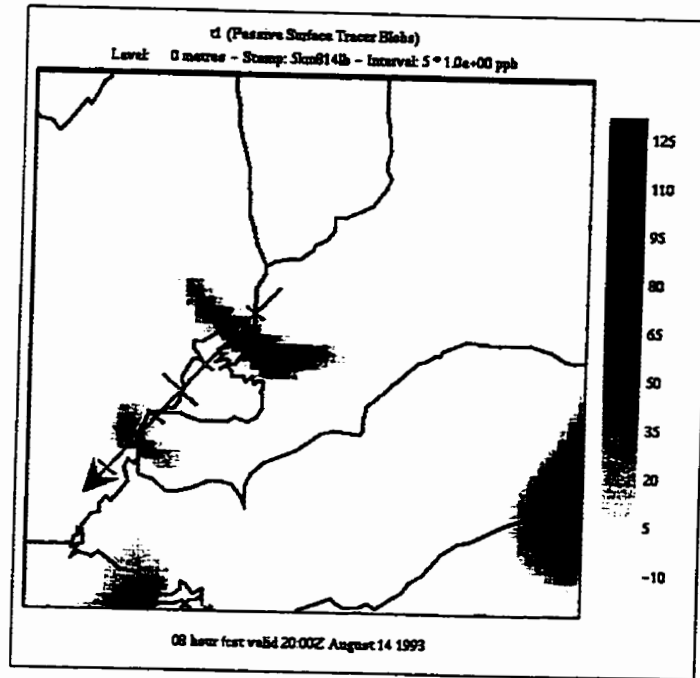


Figure 4.48. Plan views of surface tracer concentrations at 1200 UTC (a), 1600 UTC (b) and 2000 UTC (c) from the 5 km grid MC2 model run for August 14. A vertical cross-section through the tracer field (d) along the arrow shown in (c) is valid at 2000 UTC.
continued

c)



d)

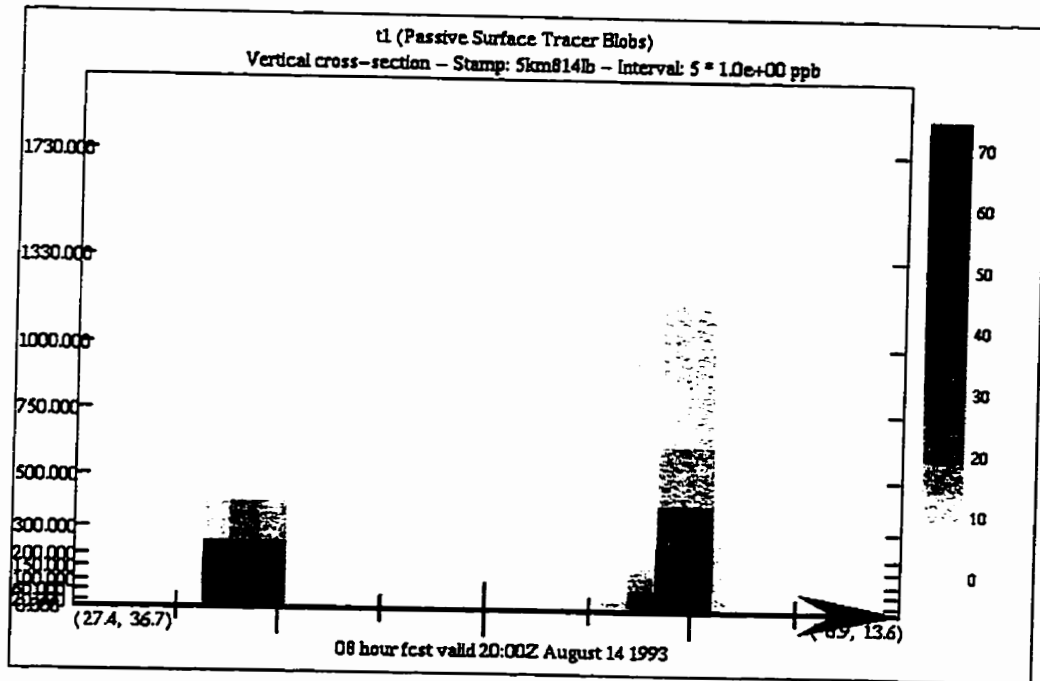


Figure 4.48, continued.

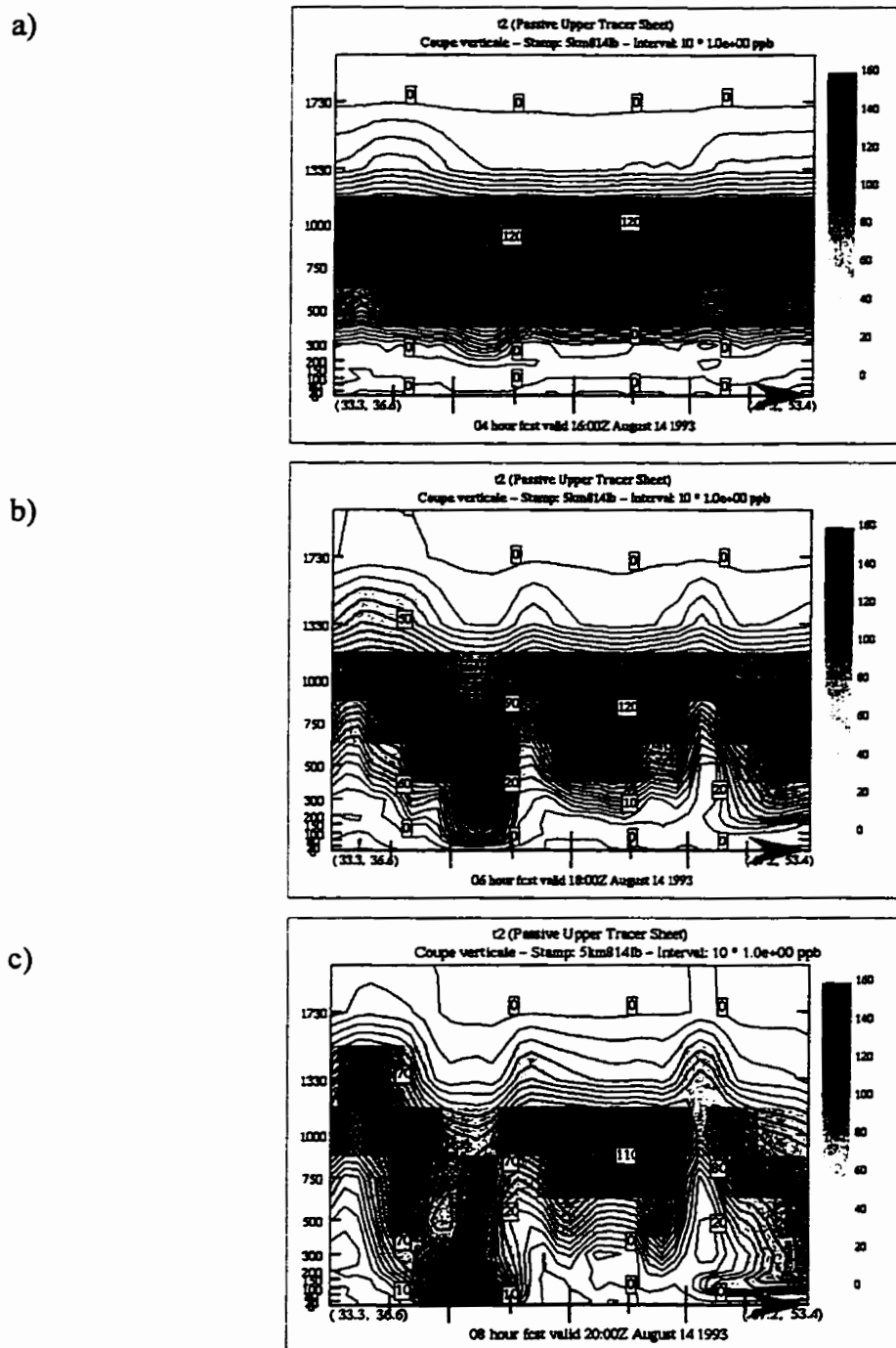
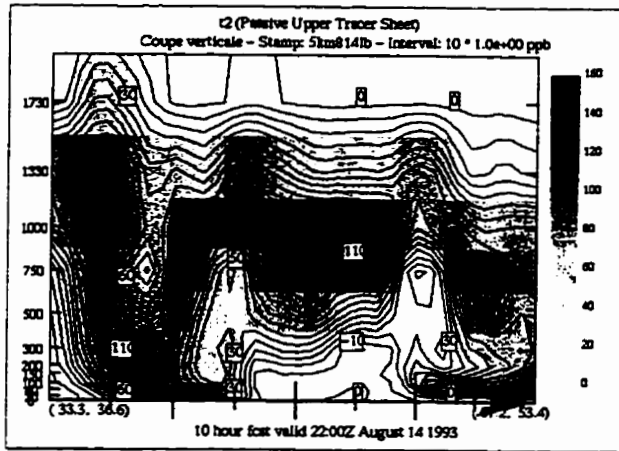
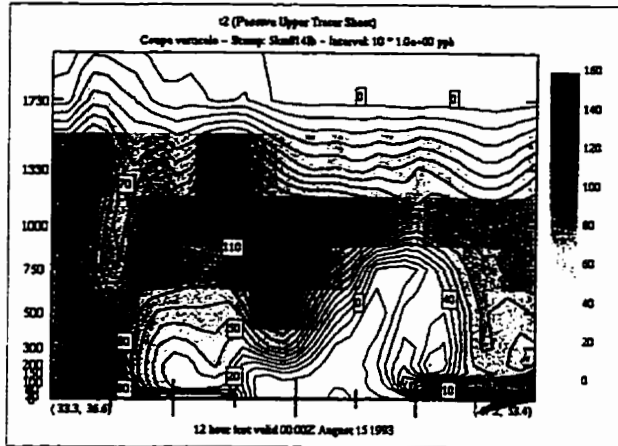


Figure 4.49. Vertical cross-sections through the tracer field at 1600 UTC (a), 1800 UTC (b), 2000 UTC (c) and 2200 UTC (d) on August 14 and 0000 UTC (e) on August 15. The vertical resolution of the shaded values is relatively coarse. However, smoothed concentrations have been contoured at 10 unit intervals. The cross-section arrow is shown with the plan view of 200 m tracer values at 2000 UTC on August 14 (f). *continued*

d)



e)



f)

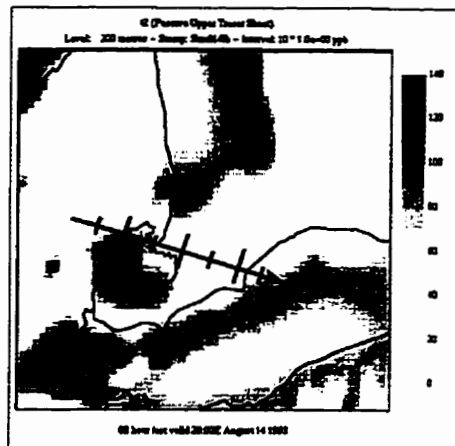


Figure 4.49, continued.

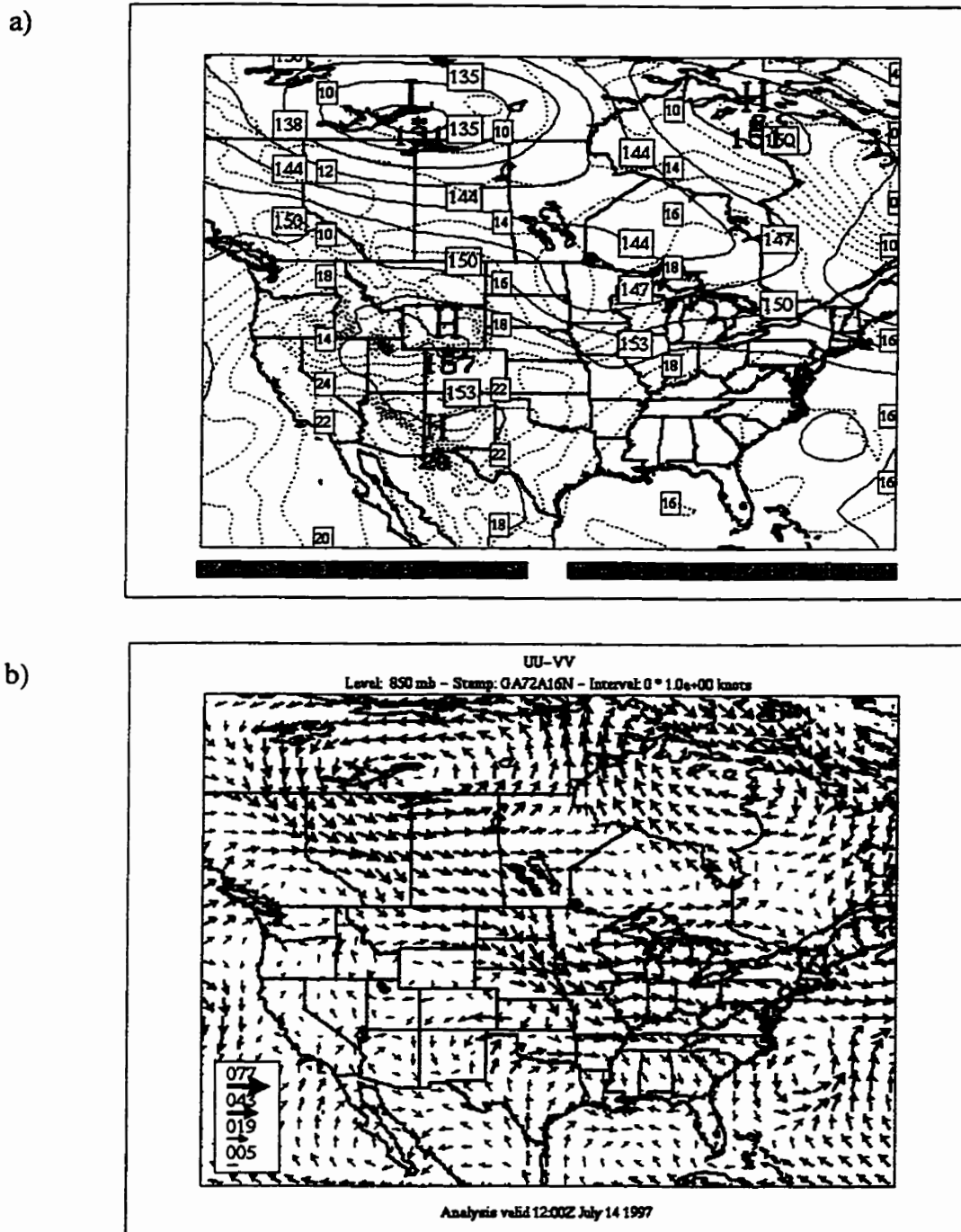


Figure 4.51. Analyzed 850 hPa geopotential and temperature contours (a) and winds (b) at 1200 UTC on July 14. Geopotential contours have an interval of 3 dam and the temperature contour used was 2°C. Winds are shown in knots.

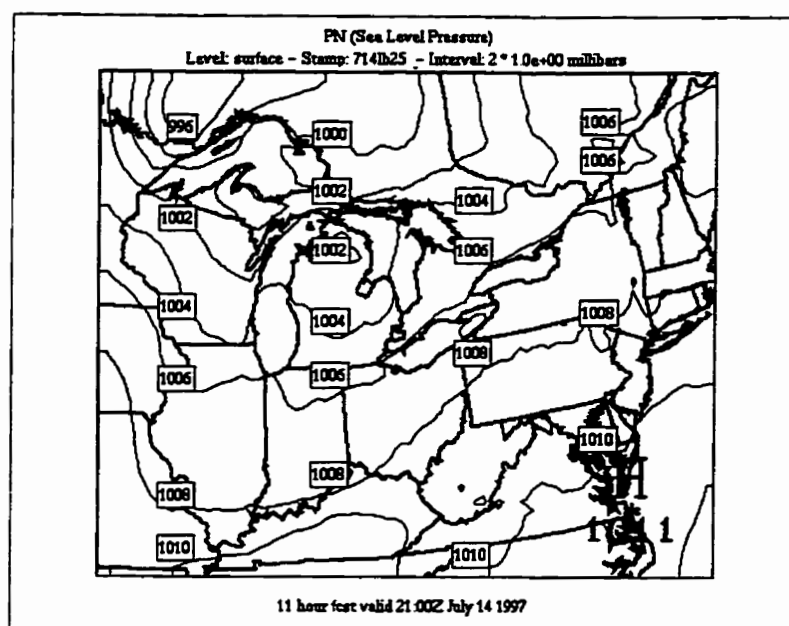


Figure 4.52. Sea level pressure at 2100 UTC on July 14 as predicted by the 25 km grid MC2 model run. The contours have a 2 hPa interval.

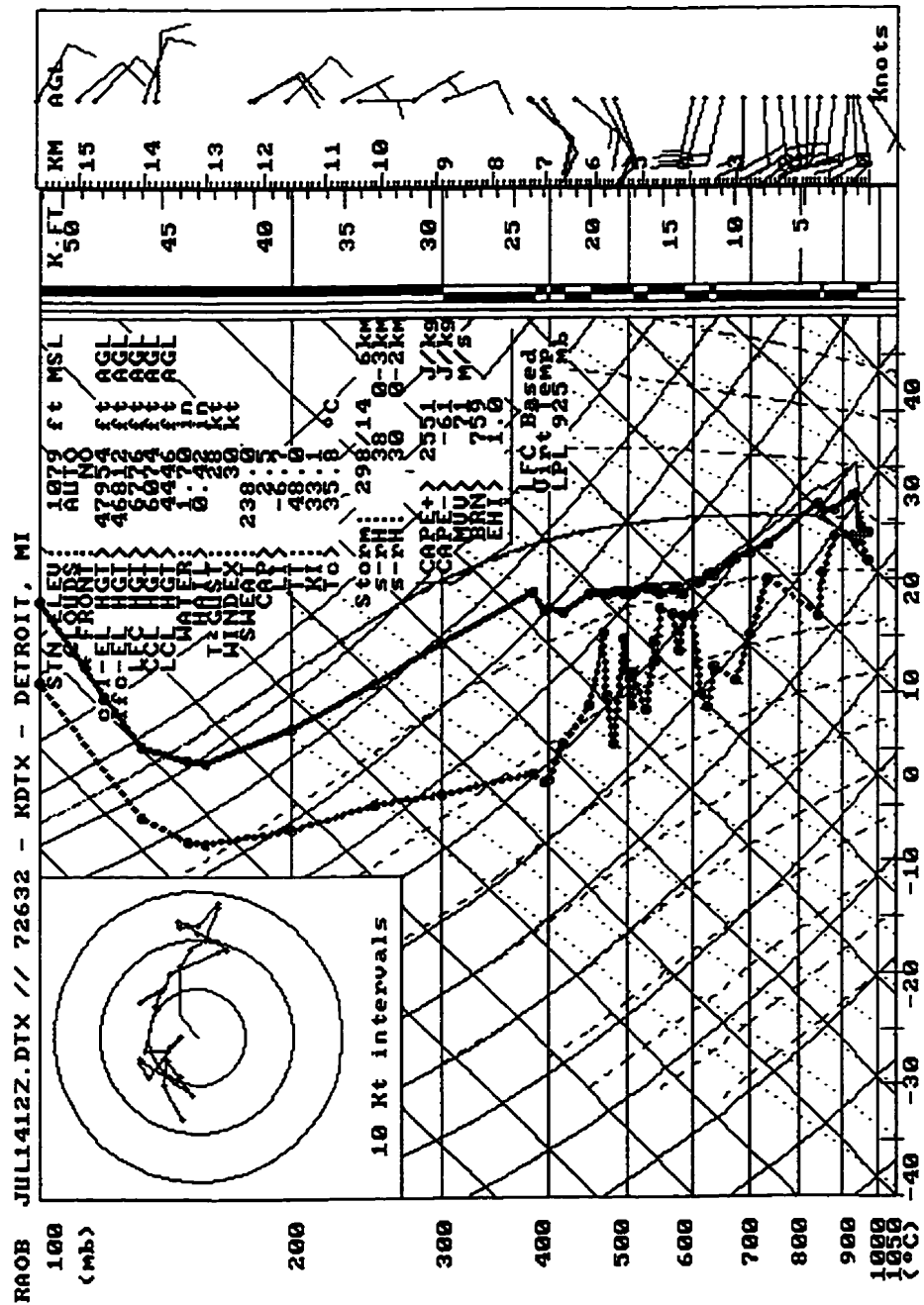


Figure 4.53. Radiosonde data from the DTX station northwest of Detroit at 1200 UTC on July 14. Data are plotted on a skew-T diagram using RAOB software. Winds at the right side are in knots. The solid line is the temperature profile and the broken line is the dew point profile. A supplementary hodograph is provided in the top left corner.

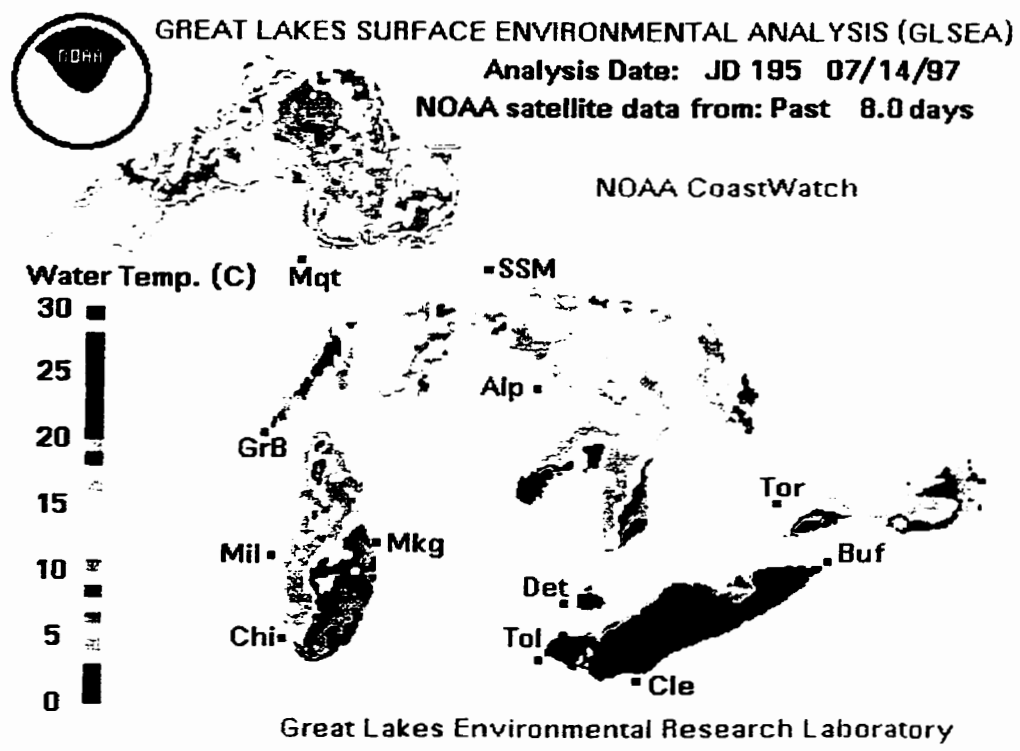


Figure 4.54. Lake surface temperatures as measured by a satellite-borne infrared sensor. Water temperatures are given in °C. Temperatures are valid for mid-afternoon on July 14. Courtesy of NOAA CoastWatch.

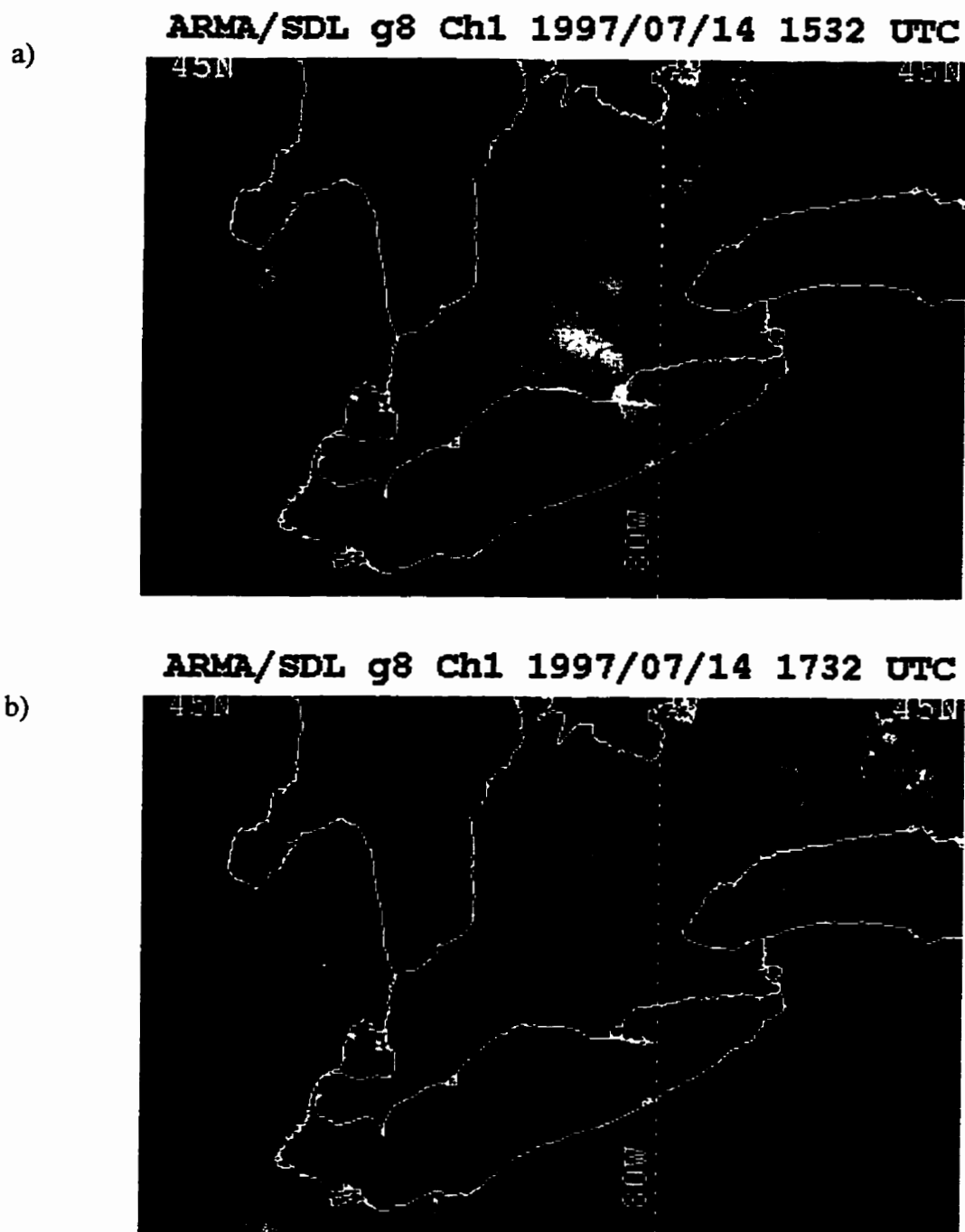


Figure 4.55. GOES-8 visible satellite images valid at 1532 UTC (a), 1732 UTC (b), 1902 UTC (c) and 2015 UTC (d). North is toward the top of the image. *continued*

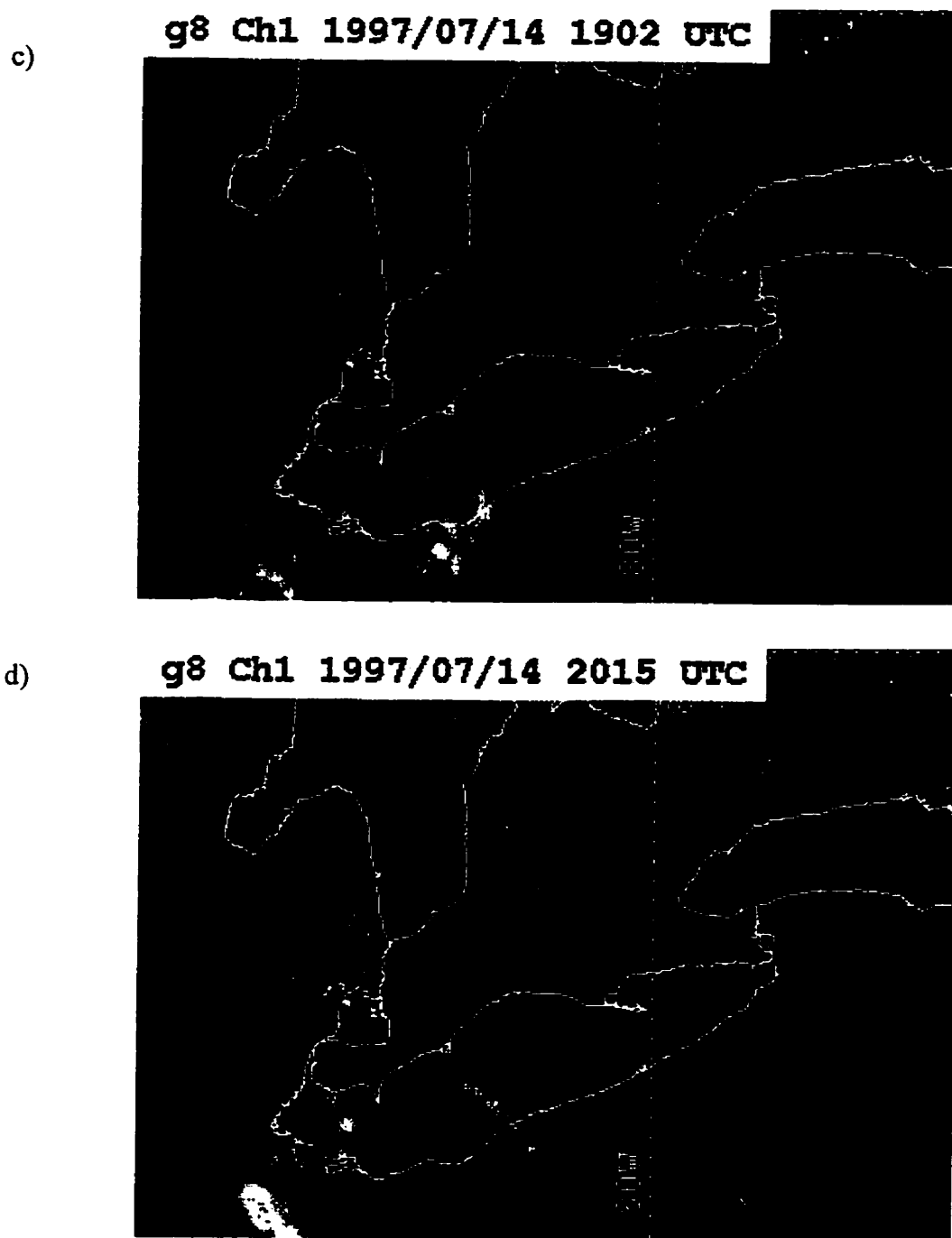


Figure 4.55, continued.

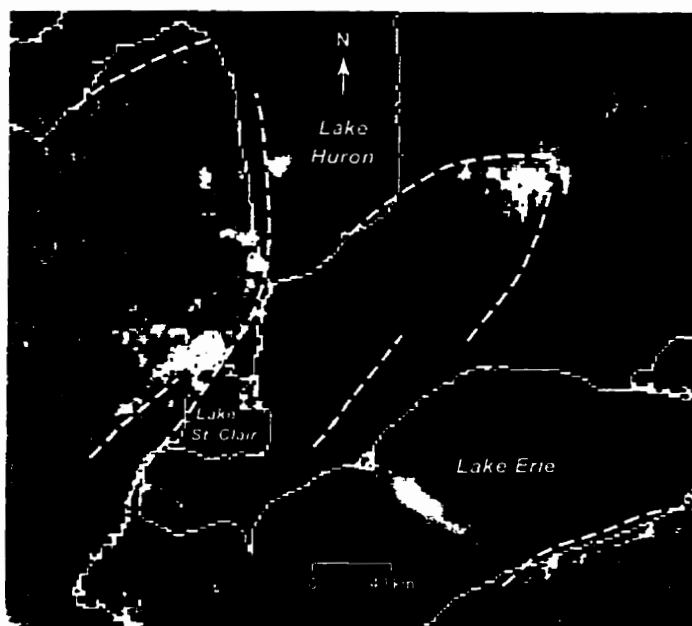


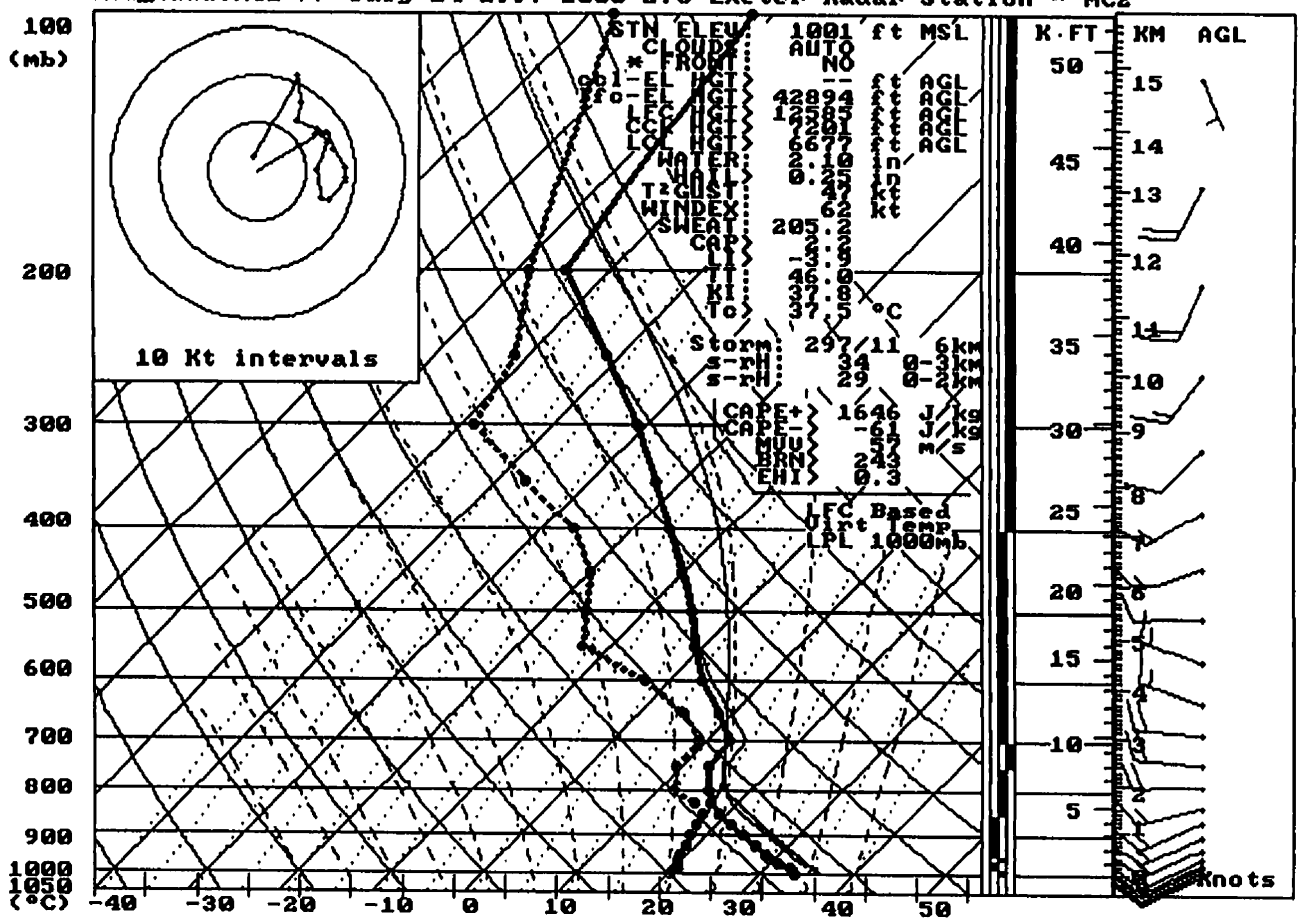
Figure 4.56. Visible GOES-8 satellite image valid at 1545 LST showing lake-induced cloud lines (indicated by dashed lines on the lakeward edges).



Figure 4.57. Close-up view of the visible satellite image at 1545 LST with station data at times with data available nearest 1545 LST (within 1 hour). The standard synoptic station format is used (small wind barb = 5 knots, temperatures in °C, pressure in tenths of hPa).

Figure 4.58, continued.

RAOB 714_2000.MC2 // July 14 1997 2000 UTC Exeter Radar Station - MC2



b)

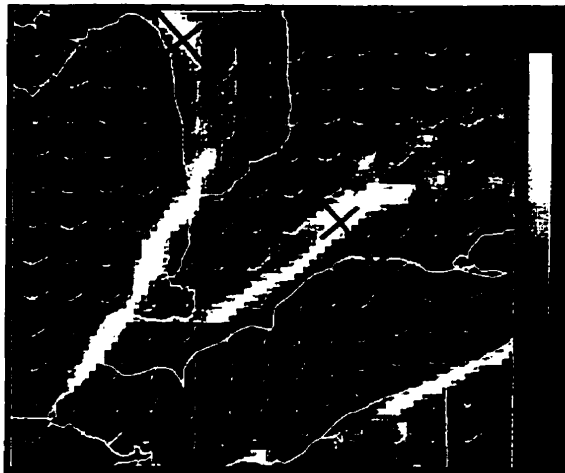


Figure 4.59. Vertical motion at 500 m and the 10 m wind field valid at 1600 LST on July 14 as output by the MC2 model on the 5 km grid. The shaded vertical motion scale at the right of the figure is in units of 10^{-1} m s^{-1} . Winds are in knots with a full barb equal to 10 knots. The arrow gives the location for the cross-section shown in Figure 4.60. Note that part of the arrow runs off the image.

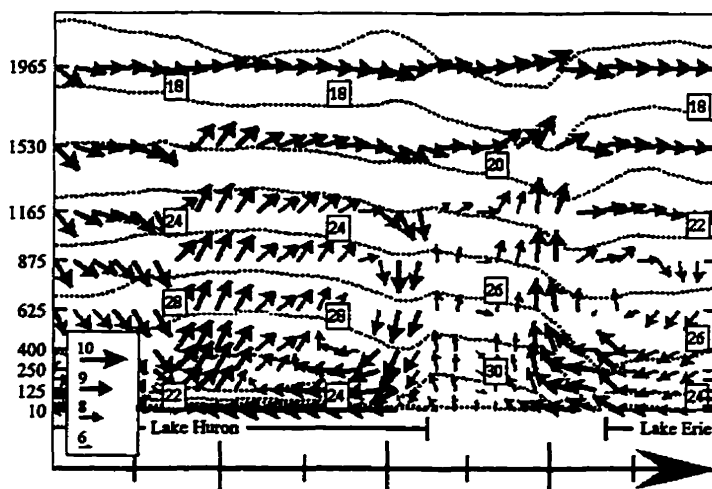


Figure 4.60. Vertical cross-sections through the combined horizontal and vertical wind fields and the air temperature field at 1600 LST along the arrow marked in Figure 4.59. Vertical levels at left are in metres. Winds are in knots with vertical winds multiplied by 50. Dotted lines are isotherms at 2°C intervals. The horizontal extents of Lakes Huron and Erie are indicated by the labelled lines near the bottom. The length of the arrow is approximately 300 km.

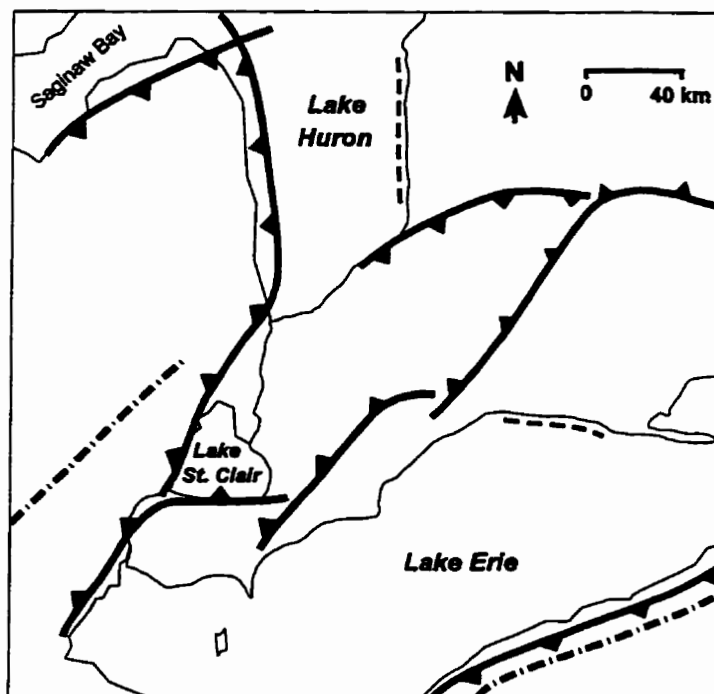
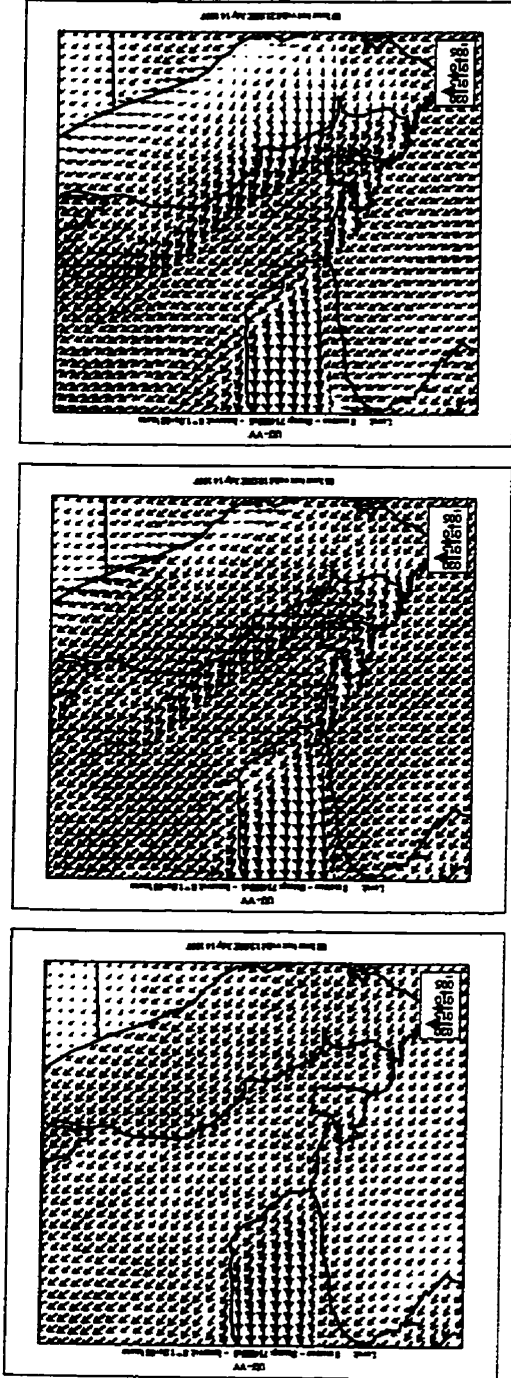


Figure 4.61. Map showing the suggested arrangement of lake breeze fronts (cold front symbol) and frictional (dashed line) and topographic (dash-dotted line) convergence zones at 1545 LST on July 14.

Figure 4.62. Modelled 10 m winds for 1500 UTC (a), 1800 UTC (b) and 2100 UTC (c) on July 14. Winds are in knots and north is toward the top of the image.



(c)

(b)

(a)

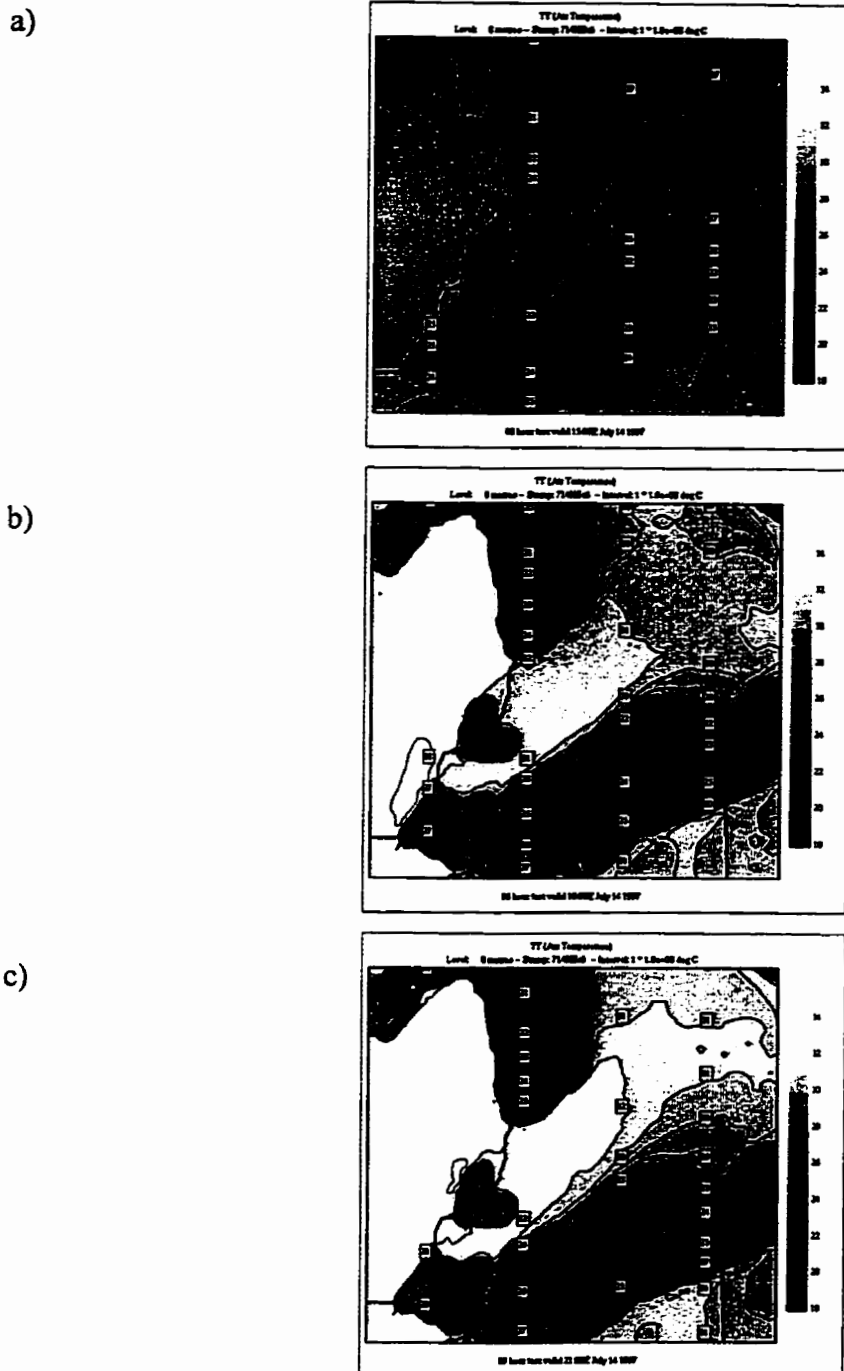


Figure 4.63. Modelled 1.5 m temperatures for 1500 UTC (a), 1800 UTC (b) and 2100 UTC (c) on July 14. A 1°C temperature contour interval is used.

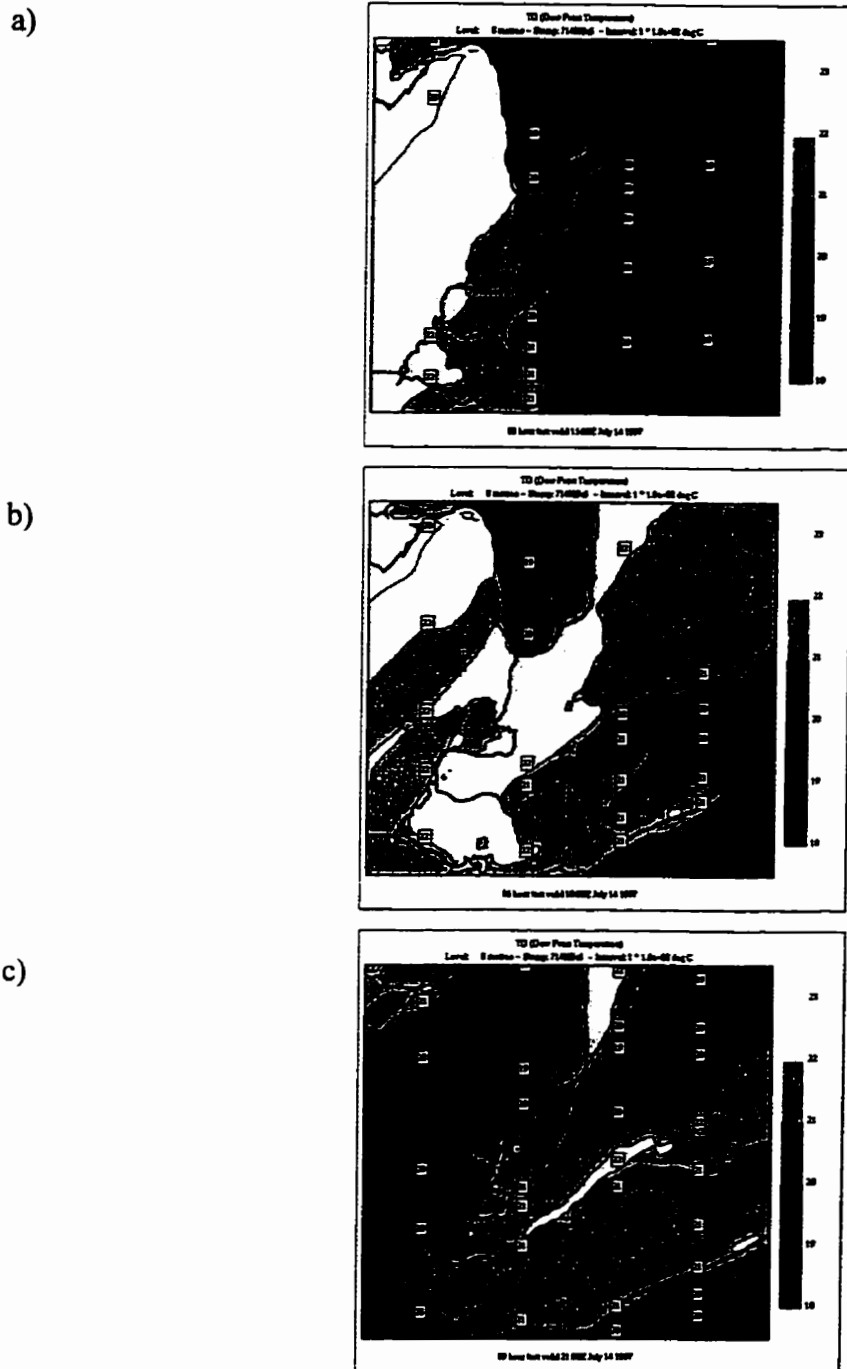


Figure 4.64. As in Figure 4.63, except values are 1.5 m dew point temperatures.

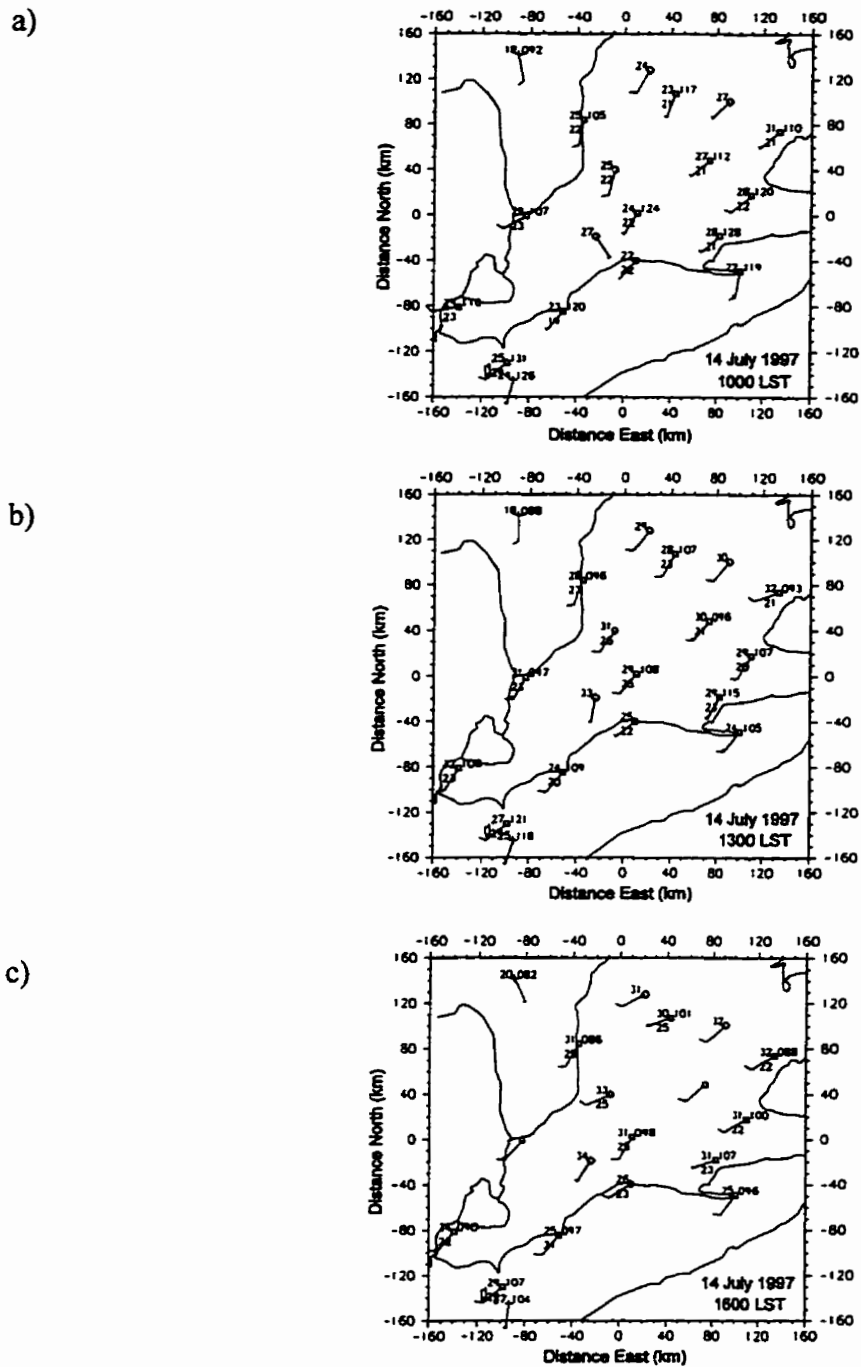


Figure 4.65. A sequence of mesonet station plots for 1000 LST (a), 1300 LST (b) and 1600 LST (c) on July 14. The standard synoptic plotting format is used (small wind barb = 5 knots, temperatures in $^{\circ}\text{C}$, pressure in tenths of a hPa).

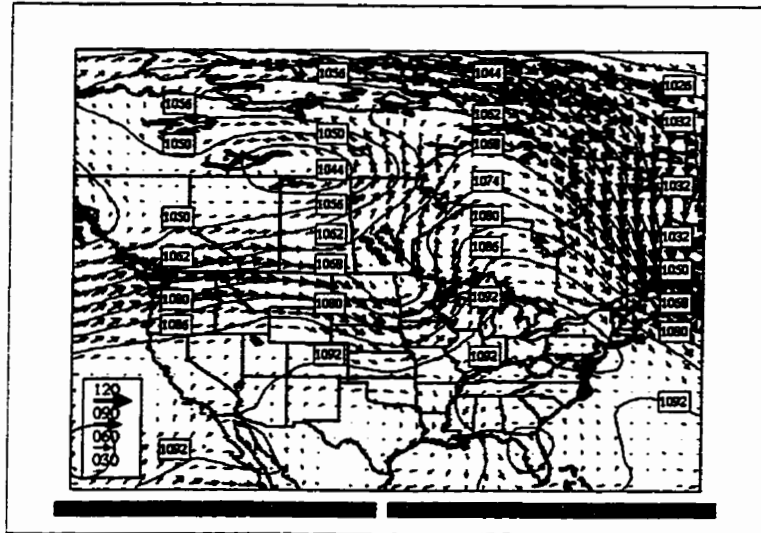


Figure 4.66. Analyzed 250 hPa chart valid for 1200 UTC on July 14. The geopotential height contour is 6 dam. Winds are given in knots.

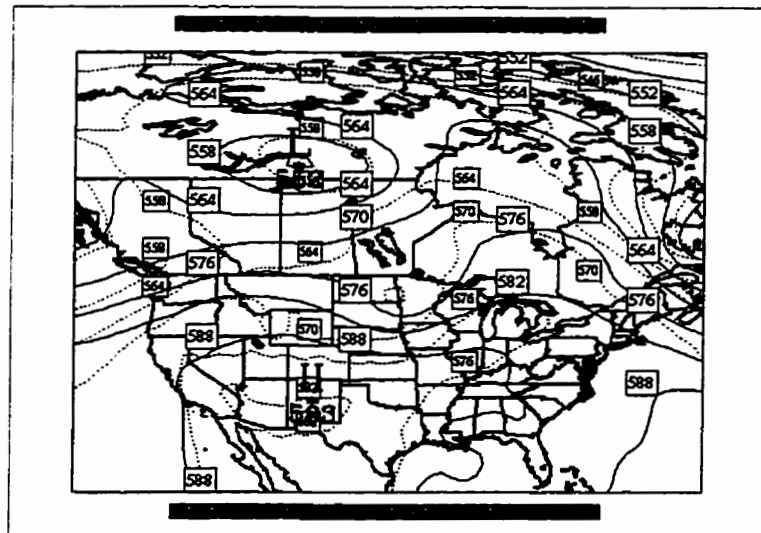
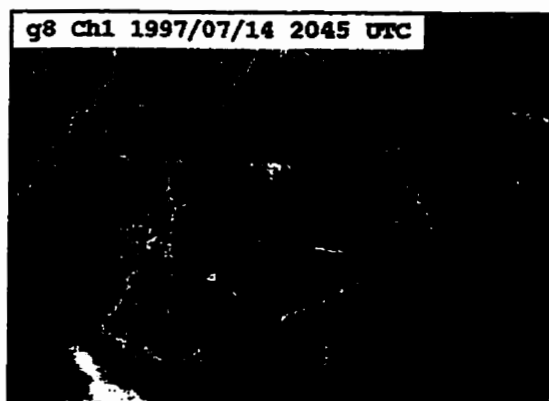
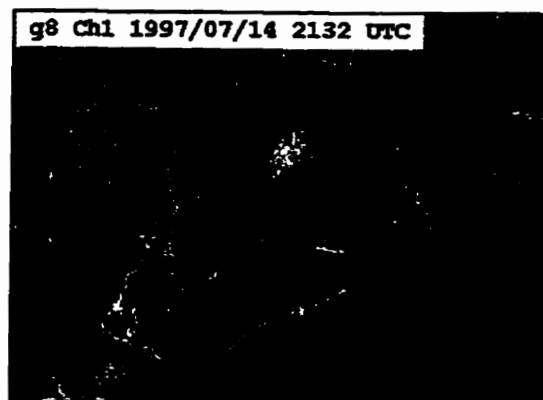


Figure 4.67. Analyzed 500 hPa chart for 1200 UTC on July 14 showing geopotential heights on the 500 hPa surface (solid line) with the 500-1000 hPa thickness pattern superimposed (broken line). Contour intervals are 6 dam.



a (above)



b (above)

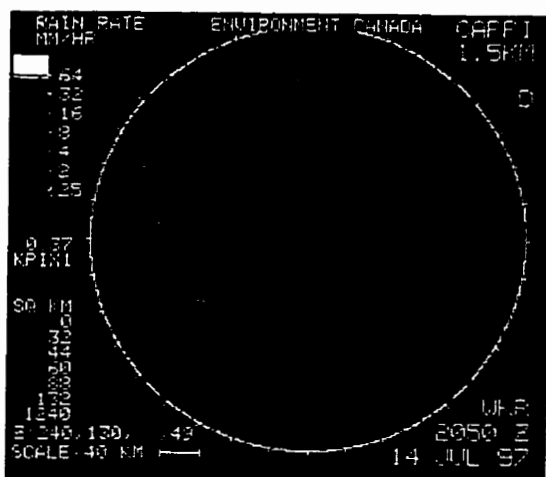


c (above)

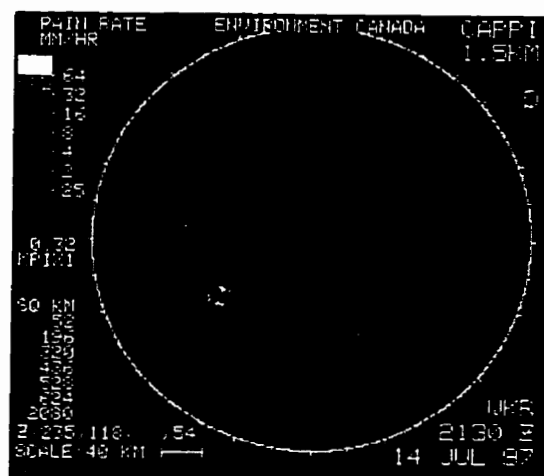


d (above)

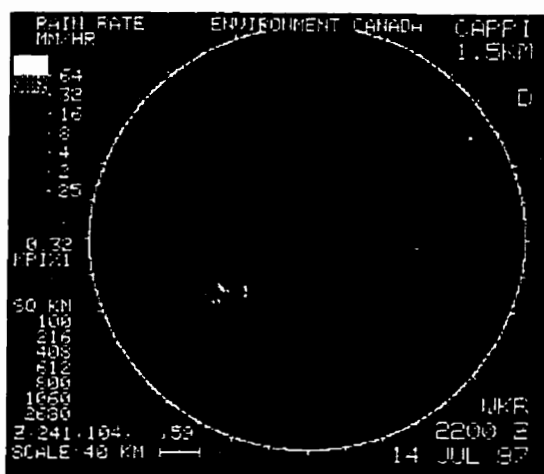
Figure 4.68. GOES-8 visible satellite images valid at 2045 UTC (a), 2132 UTC (b), 2202 UTC (c) and 2315 UTC (d) showing the development of a severe thunderstorm on July 14. North is toward the top of the image.



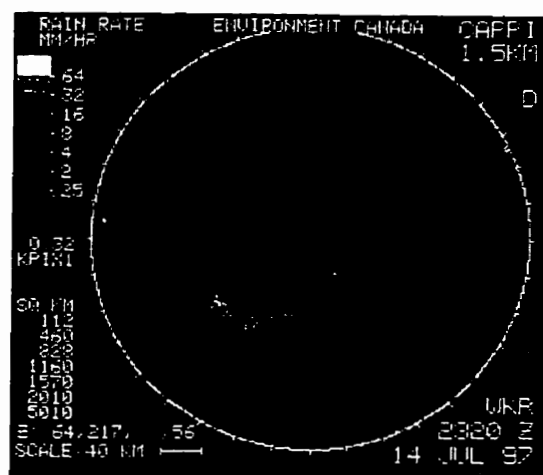
a (above)



b (above)



c (above)



d (above)

Figure 4.69. Constant altitude (1.5 km) radar data from the King City radar at 2050 UTC (a), 2130 UTC (b), 2200 UTC (c) and 2320 UTC (d) on July 14. The stationary radar echoes south of the radar site are due to ground clutter.

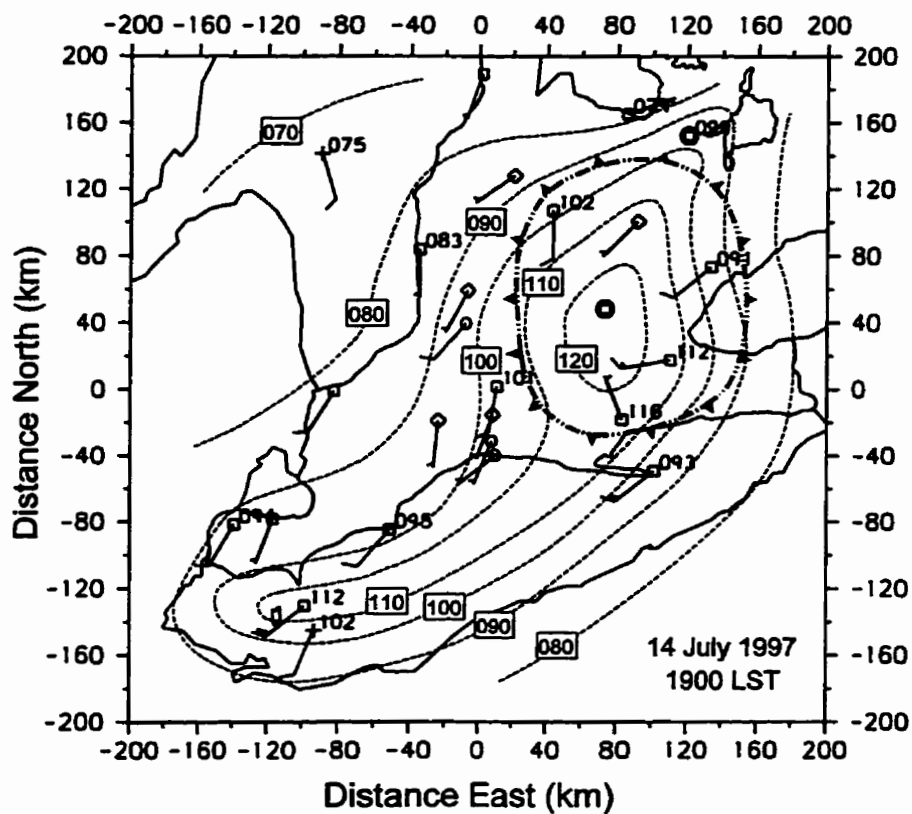


Figure 4.70. Map of the ELBOW study area showing station winds and sea level pressures (where available), a subjective isobaric analysis, and the estimated boundary of the thunderstorm outflow at 1900 LST on July 14. Wind are in knots (long barb = 10 knots), pressures are in tenths of hPa and the isobar interval is 1 hPa.

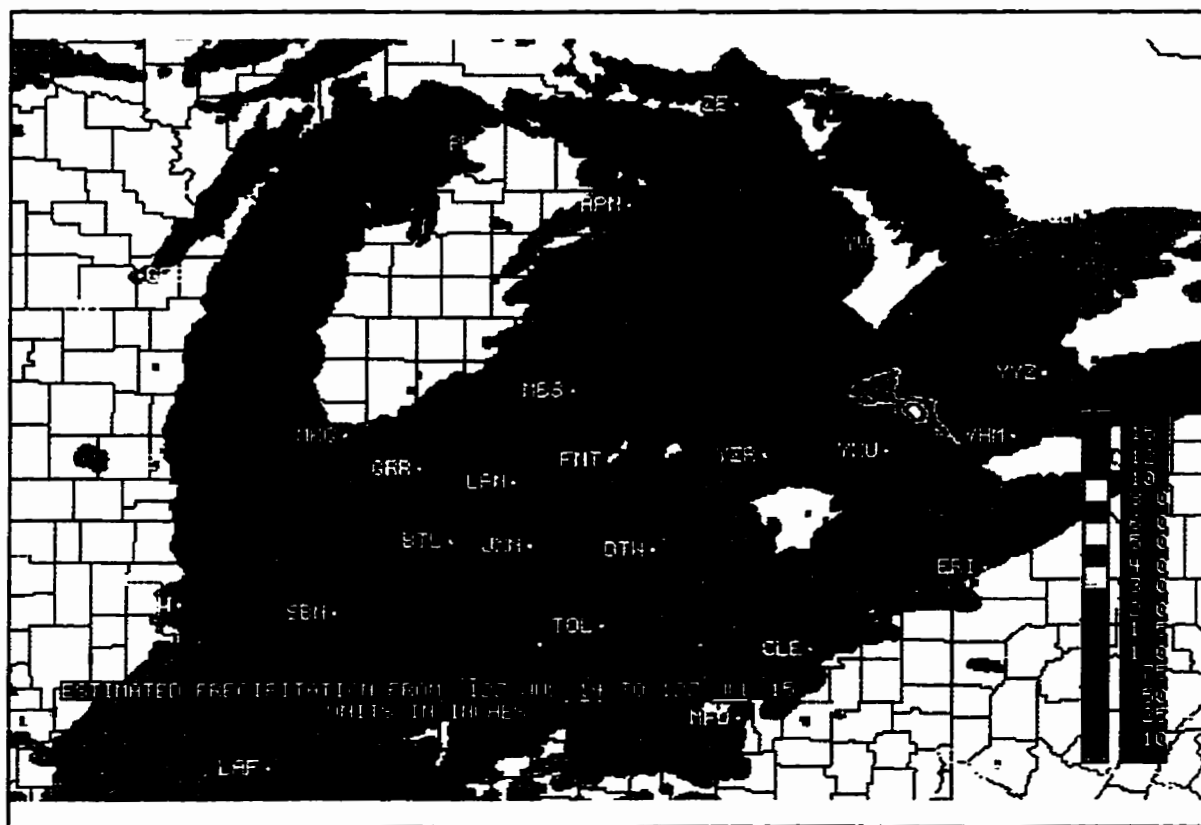


Figure 4.71. Map showing precipitation accumulation (inches) in the Great Lakes region between 1200 UTC on July 14 and 1200 UTC on July 15 as estimated by NEXRAD Doppler radars in the United States. Accumulations of 8-10 inches (roughly 200-250 mm) are estimated near the location of the Punkeydoodle's Corners storm. Image courtesy of WSI Corporation.

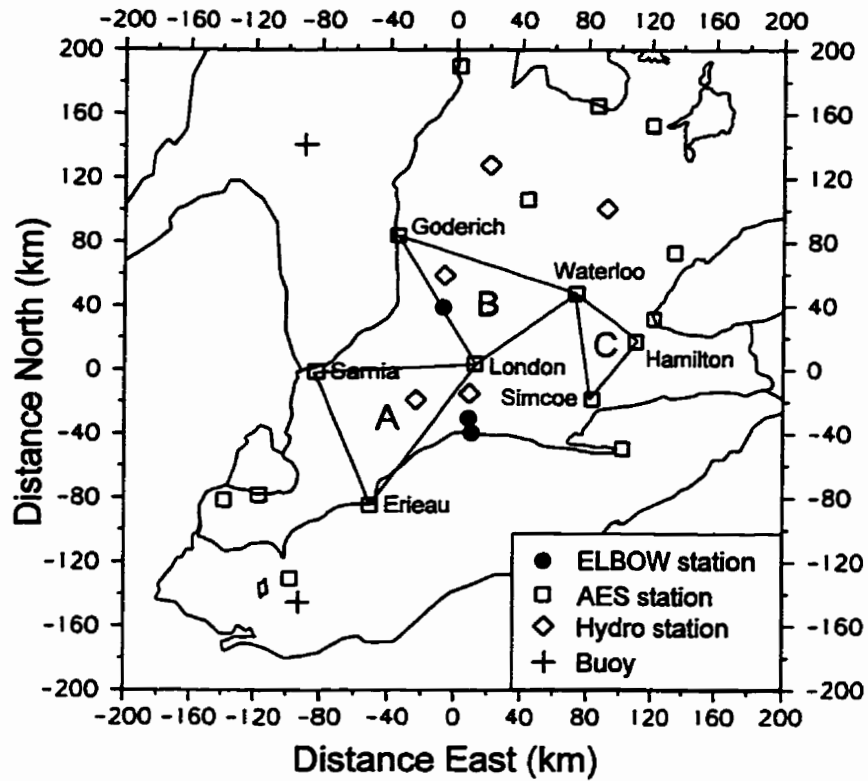


Figure 4.72. Map showing the locations of triangles A, B and C and their vertices used for divergence calculations. Divergence values from these triangle are shown in Figure 4.73.

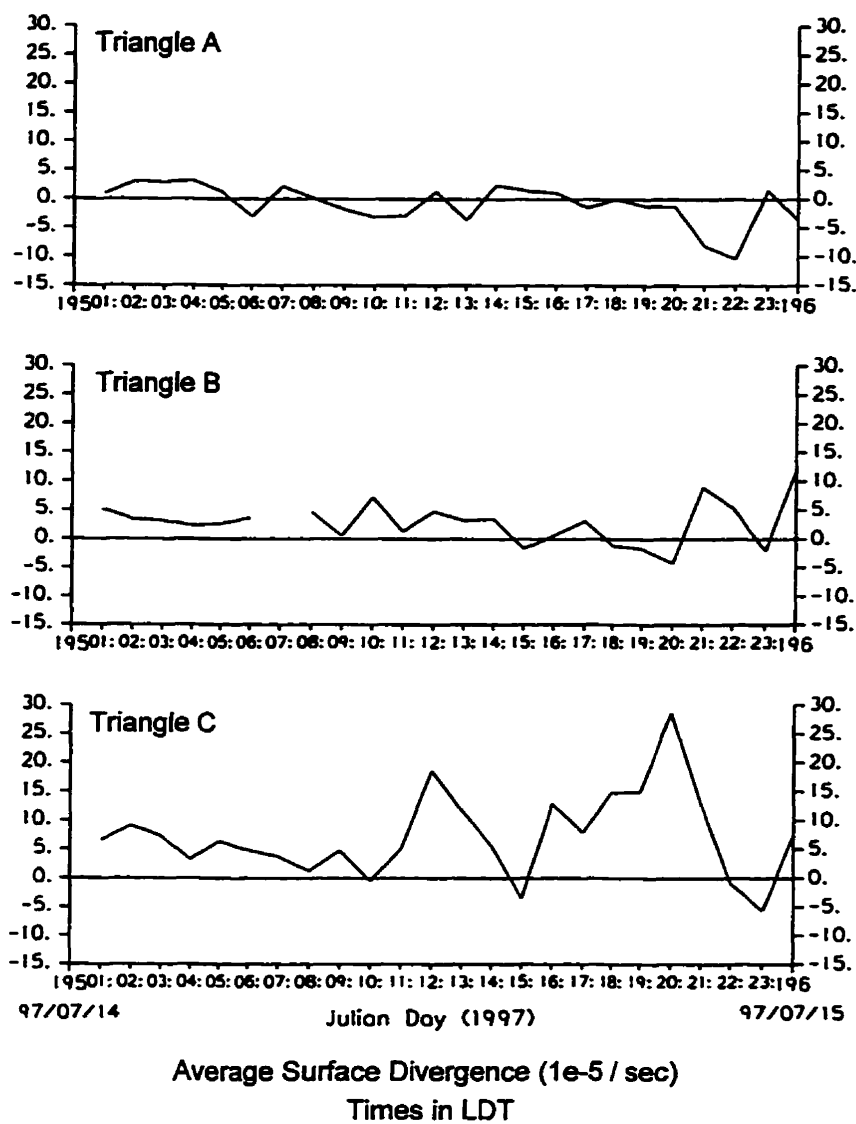


Figure 4.73. Divergence time series from Triangle A, B and C calculated using one-hour, 10 m wind data between 0000 LDT on July 14 and 0000 LDT on July 15 (between 2300 LST on July 13 and 2300 LST on July 14). The locations of the triangles from which the divergence is calculated are shown in Figure 4.72. Details of the divergence calculation are given in Appendix C.

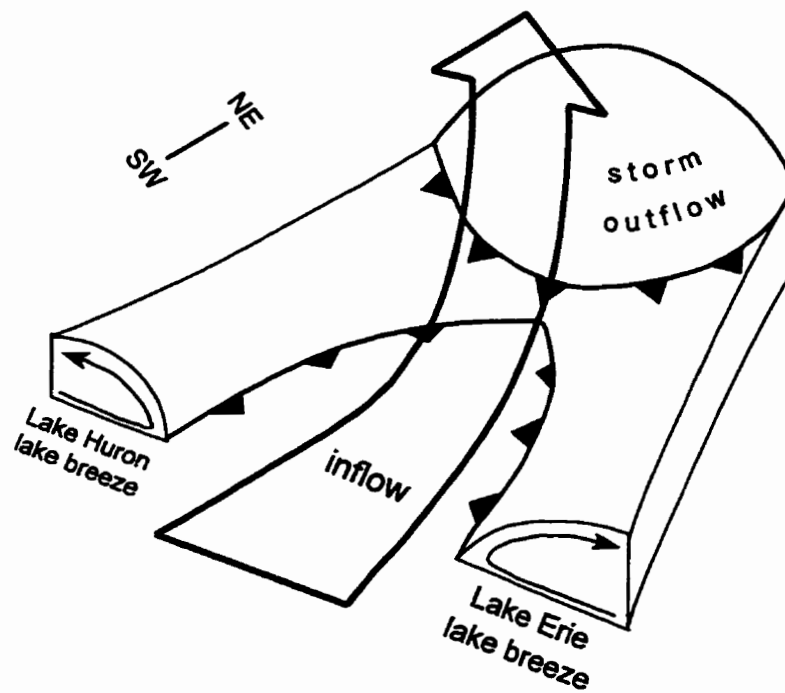


Figure 4.74. Schematic diagram showing the estimated positions of lake breeze fronts relative to the estimated position of the storm outflow boundary. In such as scenario, the flow may be forced up and over the quasi-stationary boundaries providing quasi-continuous inflow to the storm.

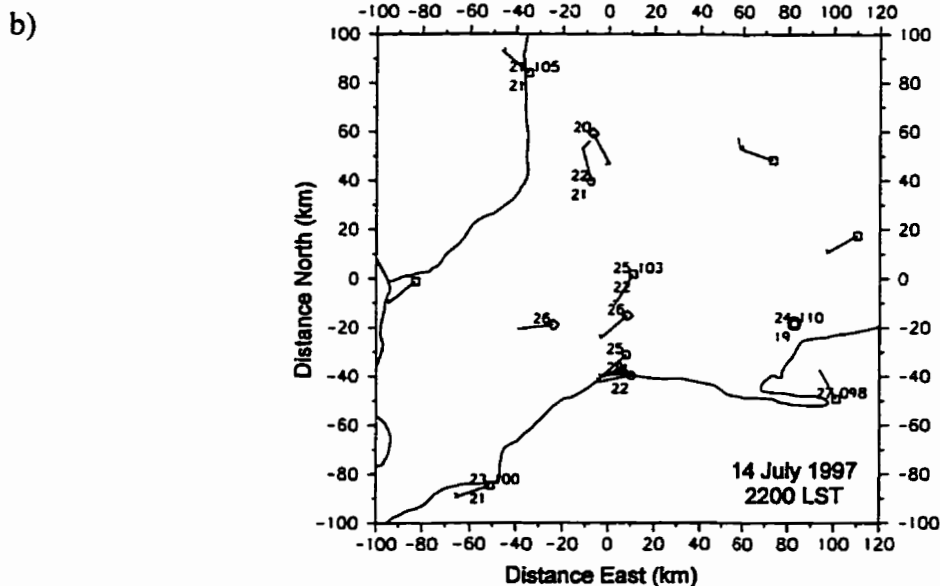
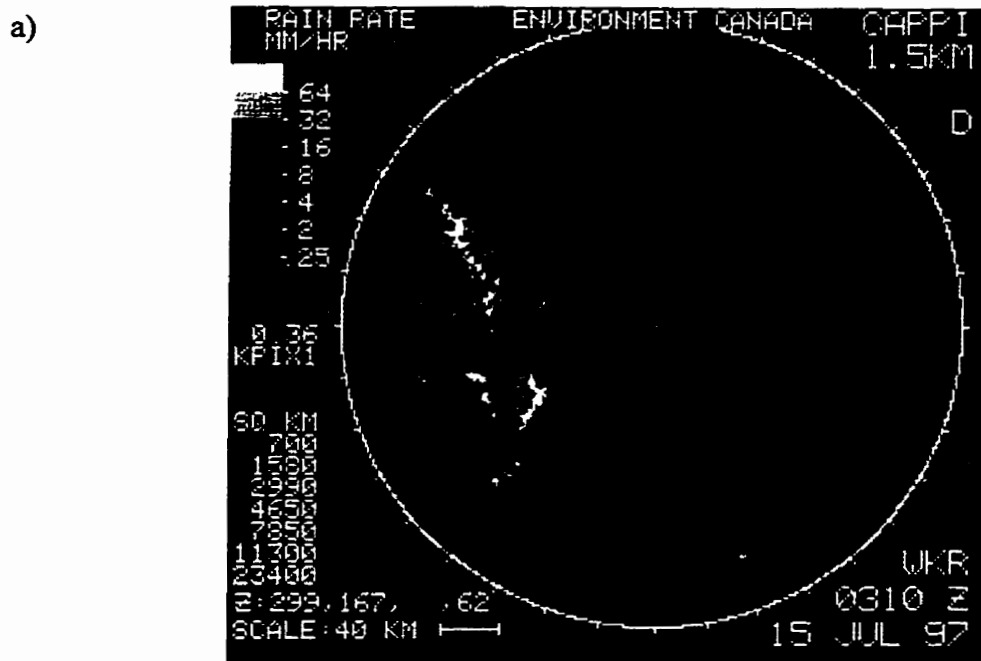


Figure 4.75. Constant altitude (1.5 km) radar data (a) from the King City radar at 0310 UTC on July 15. The radar echoes south of the radar site are due to ground clutter. Mesonet station data at 2200 LST on July 14 are shown in (b). The standard synoptic plotting format is used (small wind barb = 5 knots, temperatures in °C, pressure in tenths of a hPa).

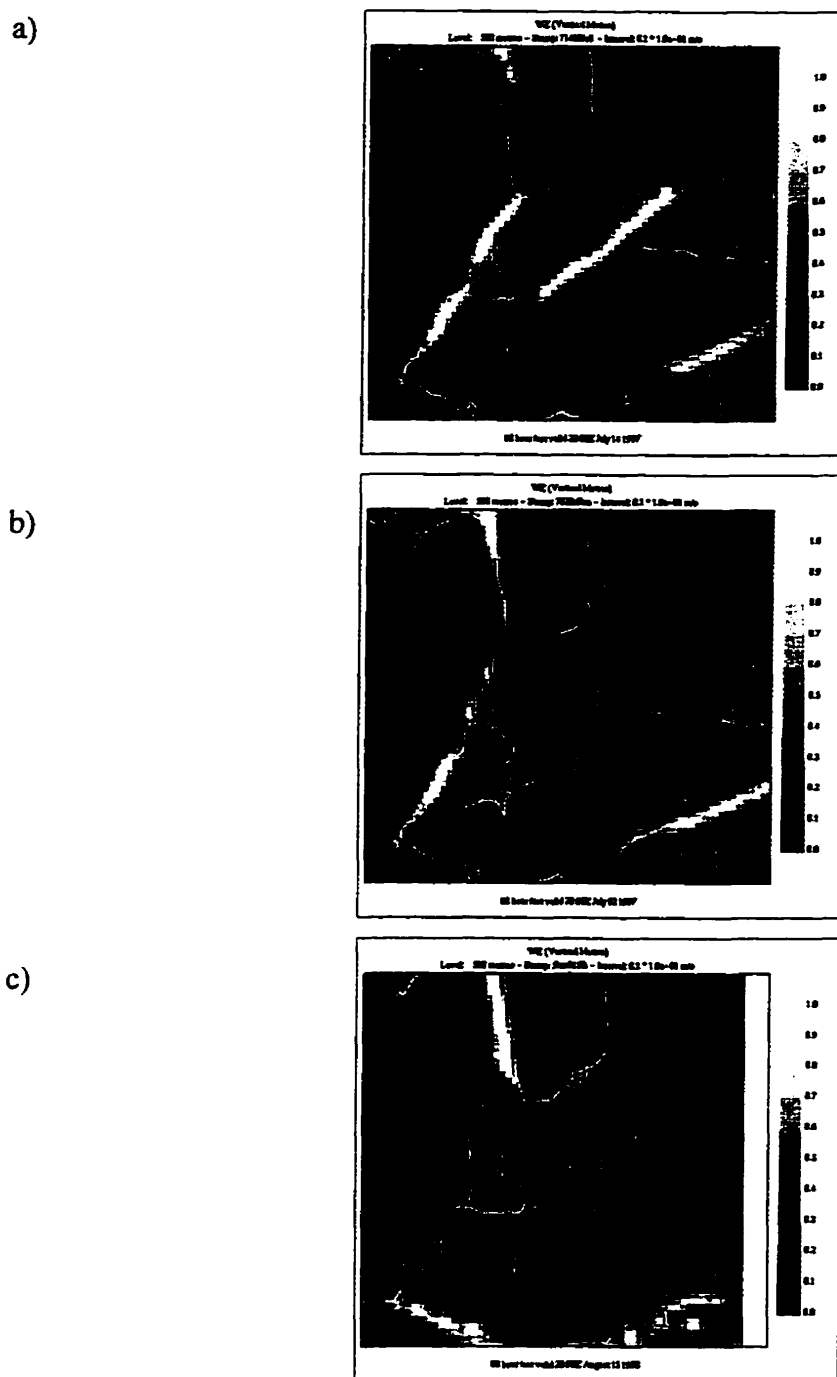


Figure 4.76. Plots of the modelled 625 m positive vertical motion field at 2000 UTC on 14 July 1997 (a), 2 July 1997 (b) and 15 August 1993 (c). The shaded vertical motion scale at the right of the figure is in units of 10^{-1} m s^{-1} .

CHAPTER 5 - DISCUSSION AND CONCLUSIONS

5.1 Introduction

The material that has been presented here comprises a broad investigation of lake and land breezes in southwestern Ontario and nearby portions of southeastern Michigan and their effects on processes such as thunderstorm initiation / maintenance and local / regional air pollution transport. Two different but related field projects conducted in conjunction with this study, SOMOS and ELBOW, generated a large volume of data collected over a combined duration of several months. These data have been analyzed to provide a preliminary characterization of lake and land breeze circulations and their effects in the study regions. In addition, a sophisticated mesoscale model has been employed to simulate meteorological conditions during lake and land breezes on selected days. The field observations were used to evaluate the model while model simulation data were used to provide four-dimensional insight on the mesoscale processes that occurred on case study days. In the following sections, the main results of the above efforts and their significance with respect to various fields of research will be discussed. In addition, several suggestions for future research investigations will be offered.

5.2 Regional Lake and Land Breeze Characteristics

5.2.1 The SOMOS Study

High quality, high density mesonet data were successfully collected during the SOMOS field project. These data, when combined with satellite, radar, and operational surface and

upper-air sounding data, provided a suitable database for studies of warm season mesoscale processes. The dataset was found to be seriously lacking only with regard to measurements in the vertical and over the lakes. Using these data and a modified version of Lyons' criteria for lake breeze identification (Lyons, 1972), a lake and land breeze occurrence record was established for southwestern Ontario and nearby areas of southeastern Michigan. To the author's knowledge, this record provides the first survey of lake and land breeze occurrence across this region. Since the sample size for this analysis was limited to two summer months, this survey can only be regarded as preliminary. However, it is expected that many of the characteristics described provide a good first-order approximation to the summer lake and land breeze climatology of the region.

One of the characteristics that is amenable to comparison with values from other studies is the lake and land breeze frequency for the study period. It was found that lake breezes occurred in the study region on 57% of study days. The shore of Lake Erie had the greatest lake breeze activity (54% of study days) and while the shore of Lake St. Clair had the least activity (46% of study days). A lake breeze was identified at the Lake Huron shore on 51% of study days. These values are significantly higher than those reported for lake breezes during the summer months in other locations around the Great Lakes such as Lake Michigan (25-45%; Lyons, 1972), Lake Ontario (30%; Comer and McKendry, 1993), and western Lake Erie (less than 25%; Biggs and Graves, 1962). It is believed that the disparity is due to the overly stringent identification criteria used by some of these

researchers and the slightly greater than normal frequency of lake breeze occurrence in the region during the study period.

Land breezes were found to occur in the study region on 58% of study nights. The Lake Erie shore had the greatest activity (56% of study nights) and the Lake St. Clair shore had the least activity (40% of study nights). A land breeze was identified at the Lake Huron shore on 50% of study nights. To the author's knowledge, these land breeze frequency statistics are the first of their kind in the Great Lakes region.

It was also found that lake and land breezes tended to occur in episodes, frequently of four or more days in length. During one extraordinary episode, lake breezes occurred on all lakeshores in the study region on eight consecutive days. Lake and land breezes were also observed to occur contiguously for periods of up to five days. The occurrence of lake breeze, land breeze and contiguous lake-land breeze episodes is strongly correlated with the light and variable gradient wind regime and can have serious consequences for the dispersion of air pollutants in the region.

Another unique aspect of this study was the spatial characterization of lake breeze occurrence frequency in the region. Frequency analyses by individual lake (see Figure 2.16) show that while Lake Erie and Lake St. Clair lake breezes commonly penetrated up to 30 km inland, Lake Huron lake breezes often affected locations up to 100 km from

shore. The lake breeze day analysis (see Figure 4.18) showed that lake breezes occurred most frequently near the lakeshores and elongated lake breeze day minima existed between the lakes. However, the observed frequencies within these minima ranged from 14% to 33% indicating that lake breezes were able to reach all inland areas of southwestern Ontario on a regular basis. Strong correlations were also found between the lake breeze day frequency pattern and occurrence patterns for severe weather elements and high ground-level ozone. Maxima in annually-averaged lightning flash, extreme rainfall and tornado occurrences were shown to be located in the vicinity of the elongated lake breeze day frequency minimum between Lakes Huron and Erie. It is believed that these correlations are due to a combination of convective enhancement associated with lift at the lake breeze front and convective suppression within the remainder of the lake breeze circulation. Convective enhancement may also occur with the collision of lake breeze fronts. The annually-averaged ozone exceedance frequency pattern is also well correlated with the lake breeze day frequency pattern. Exceedance values increase toward the shores of Lakes Huron and Erie where lake breezes and their detrimental effects on air quality are most often experienced.

Meteorological conditions on selected SOMOS days with 'classic' lake and land breezes (occurring under light to moderate gradient winds as is typical of those described in the literature) were analyzed and simulated using the MC2 mesoscale model.

5.2.2 The ELBOW Study

The main goals of the ELBOW field project were to investigate lake breezes effects on summer severe weather in southwestern Ontario and determine the nature of lake-induced cloud lines that are frequently observed on visible satellite imagery under moderate gradient wind regimes. Severe thunderstorms have been found to occasionally occur in association with these cloud lines (King, 1996). In these respects, the ELBOW project was a success. Measurements were made in the vicinity of lake breeze initiated storms on several occasions. One of these storms, severe in nature, appeared to be initiated at the point of merger of lake-induced cloud lines. Through observational analysis and numerical modelling of the conditions on this day, it was found that these lake-induced cloud lines were likely fronts associated with lake breeze circulations that were 'highly-perturbed' by the gradient wind. These highly-perturbed lake breezes appeared to have well-developed fronts near shoreline segments approximately aligned with the surface wind. Lake breeze fronts were weak or absent near lakeshore segments approximately perpendicular to the surface flow. The modelled updraft velocities of the lake breeze fronts aligned with the surface wind were similar to those of the 'classic' lake breeze fronts. This suggests that there may be a broad range of gradient wind intensities over which a lake breeze with well-developed fronts may exist. The upper limit of this range on a particular day would likely be directly correlated with the difference in vertically-integrated air temperatures over water and over land. To the author's knowledge, only Pielke (1974), in a modelling study of southern Florida sea breezes and the Lake

Okeechobee lake breeze, has simulated lake breezes showing highly-perturbed characteristics though Pielke makes no mention of their significance. Only in this study, and in observational studies by King (1996) and King *et al.* (1996) leading up to the ELBOW project, have highly-perturbed lake breezes been investigated directly.

5.3 The Role of Lake Breezes in Summer Severe Weather

It is well-known that lake breezes and sea breezes can have a controlling influence on deep, moist convection and are capable of initiating thunderstorms, including severe storms, if other storm ingredients such as abundant instability and low-level moisture are available (see Chapter 1). Results from the SOMOS project show that lake breezes were active on at least five of the six days on which severe or near-severe weather occurred during daylight hours. Strong links between lake breezes and the occurrence of severe or near-severe weather were apparent for four of these days and were demonstrated for two of these days - August 14 and 15, 1993 - in this study. Occurrences of lake breezes and severe or near-severe weather during ELBOW also appear to be closely related. This suggests that the majority of summer severe weather occurring during daylight hours in southwestern Ontario is influenced to some degree by these circulations. Indeed, in this region, lift at lake breeze fronts is occasionally the only mechanism available to initiate thunderstorms in the presence of other necessary storm ingredients. For the severe thunderstorm cases described in Chapter Four, synoptic-scale forcing appeared to be limited over the study regions and mesoscale dynamics, including enhanced vertical

motion at the lake breeze fronts, appeared to dominate. It is recognized, however, that this is not always the case and that interactions between synoptic-scale dynamics and mesoscale lake breeze dynamics may have combined effects.

It was also suggested in Chapter Four that the weak tornadoes produced by thunderstorms initiated at lake breeze fronts were of the 'landspout' variety described in Chapter One. Several other examples of apparent landspouts occurring in southern Ontario were cited in Chapter One. The prevalence of low-level boundaries in this region due to relatively frequent occurrences of both thunderstorms and multiple lake breezes suggests that southwestern Ontario may be a preferred region for the development of these vortices, much like parts of Colorado and the Florida Peninsula (Brady and Szoke, 1989).

Lastly, MC2 model simulations show a pattern of convergence lines and surface winds very similar to that predicted for July 14, 1997 on two other days, indicating that this highly-perturbed lake breeze configuration may not be an uncommon occurrence. This could have important implications for severe weather forecasting in the region since the synoptic-scale regime that is typically associated with this configuration is often conducive to the development of severe thunderstorms. In fact, severe summer weather occurred on each of the three days with this configuration.

5.4 The Role of Lake and Land Breezes in High Ozone Concentrations

Lake breezes, and land breezes to a lesser extent, appear to play a major role in the dispersion of pollutants including ozone in southwestern Ontario and nearby areas of southeastern Michigan. One-hour average ground-level ozone concentrations greater than 80 ppb (the Ontario one-hour ozone criterion) were recorded on 20 of the 63 days of the SOMOS study. Lake breezes occurred on 16 of these days. Also, the highest ozone concentrations during SOMOS were recorded within an 8-day episode of lake breezes on all lakes and a 5-day episode of contiguous lake and land breezes on all lakes. In this situation, the ability of lake and land breezes to continuously recirculate air within the region seriously impedes pollutant dispersion and thus may cause a severe erosion of air quality. The highest ozone concentrations during SOMOS were reported in the vicinity and downwind of the urban / industrial centres of Sarnia-Port Huron and Windsor-Detroit. Locations along the north shore of Lake Erie rarely exceeded the Ontario one-hour ozone criterion of 80 ppb. However, other studies have found much higher ozone concentrations north of Lake Erie, especially north of the eastern half of the lake (Chung, 1977; Mukammal *et al.*, 1982; Fuentes and Dann, 1994). This discrepancy is likely due to the small sample size used for the present analysis.

A detailed examination of the meteorology and air chemistry on August 14, 1993 was undertaken to elucidate the role of the lake breeze in delivering high concentrations of ozone at ground-level to locations near the lakes. Ozone concentrations up to 147 ppb

were recorded with the passage of the Lake Huron lake breeze near Sarnia-Port Huron on this day. Large increases were also observed as the Lake St. Clair lake breeze moved inland over the region north of Detroit. Passive tracers were used within the MC2 model to investigate possible mechanisms for ozone transport within the lake breeze circulation. One mechanism brought ozone onshore from over the lake within the inflow layer of the lake breeze. Several studies have explained ozone increases in the Great Lakes region using this type of mechanism (see Chapter Four). The tracer, initialized from the surface to 200 m in this simulation, moved inland with the lake breeze and was transported aloft at the front leaving no tracer at the surface by the end of the integration. Translocation of an entire plume of ozone initially located near the surface by a lake breeze has also been modelled by Lyons *et al.* (1995).

A second mechanism was tested that required tracer to be available in a layer between 500 m and 1000 m. Lake breeze circulations entrained tracer from this layer and advected it toward the surface behind the lake breeze front. By the end of the integration, much of the tracer that was initially aloft was located at levels near the surface. The author knows of no other study that has examined this particular lake breeze / ozone transport mechanism.

The results of both of these simulations indicate that the transport of ozone in the vicinity of a lake breeze circulation is a complex three-dimensional process and that the height at

which high concentrations of ozone are initially located is important to their subsequent location later in the day.

5.5 Skill and Utility of the MC2 Model

The MC2 mesoscale model that was used for simulations in this study was found to be a versatile, robust, and powerful tool. Evaluations of model results on the 100 km and 25 km grid meshes using CMC objective analyses showed skill in predicting conditions on the study days selected. The model had some difficulties with the calculation of the pressure field, especially on the 25 km grid. However, significant anomalies generally occurred outside of the area of interest for the case study days simulated. The model was able to produce lake breeze circulations on the 5 km grid mesh with considerable skill relative to the mesonet station data and upper-air soundings on case study days. Part of the reason for the model's success in the simulation of lake breezes is that the circulations are strongly forced by quasi-stationary surface perturbations. Thus, features entering and exiting through the lateral boundaries are less of a concern than for transient processes such as frontal precipitation and mesoscale convective systems. Many of the inaccuracies that were noted in the 5 km grid model results were due either to inaccurate nesting data from coarse grid model runs or geophysical data at inadequate resolution. MC2 model developers have recognized these short-comings and plan to address them for future versions of the model (Benoit *et al.*, 1997).

The MC2 model appeared to have difficulty with light surface flow situations and failed to predict the development of the August 14-15 1993 land breeze. It appears that the nocturnal radiational cooling at the surface was insufficient to decouple the near-surface winds from the gradient wind aloft. The warmer than observed temperatures over land also reduced the temperature difference between air over land and air over water that drives the land breeze circulation. It is thought that improved surface schemes such as those provided with the more recent versions of the model may remedy this problem.

The final grid spacing of 5 km used here for lake and land breeze simulations presented problems for the representation of deep convection. The 5 km grid size was found to be sufficient for the modelling of lake breezes and could be adequately handled by the computer hardware and software used. However, as mentioned in Chapter Three, convective parameterization for grid spacing near 5 km is quite difficult since physical processes at various scales are involved. Thus, no convective scheme adequate for simulations with 5 km horizontal grid size is provided with the MC2 model. This problem should begin to diminish as computing power and capacity continues to increase and explicit convection can be used with grid sizes ≤ 1 km.

Lastly, the use of passive tracers in the model successfully illustrated the movement of inert material within the lake breeze circulation. However, passive tracers can only crudely represent changes in absolute concentrations of reactive trace gases such as

ozone, as was discussed in Chapter Three. It would be beneficial to include at least the basic set of chemical reactions necessary for the production and destruction of ozone and processes by which ozone may be scavenged by dry and wet deposition. In fact, a group at York University has successfully added photochemistry, transport, emission and deposition modules to the MC2 model and has enabled these modules to run 'on-line' with the meteorology (Plummer *et al.*, 1996).

5.6 Directions for Future Research

Several facets of the work completed for this study may be extended through additional research investigations. A few suggestions for subsequent related research are given below:

- To assess the validity of the preliminary lake and land breeze climatology presented here, a much larger sample size is required. The method used here for lake breeze and land breeze identification is thorough but quite labour intensive. Biggs and Graves (1962) developed a lake breeze index for the purpose of lake breeze prediction. This index may also be used for hindcasting of lake and sea breeze occurrences and has been used to construct lake and sea breeze climatologies (see for example Comer and McKendry, 1993; Steyn and Faulkner, 1986). The author has noted deficiencies in the lake breeze index of Biggs and Graves and has modified the index to more accurately reflect the driving forces

behind the lake breeze. The index was also modified for use with land breezes. Perhaps an expanded study of the lake and land breeze climatology in this area can be conducted with the use of these revised indices.

- Some progress was made toward the understanding of the role of lake breezes in severe weather occurrence and ozone transport in southwestern Ontario. However, the observational data used here were insufficient to determine with confidence the exact processes at work in either case. In addition, the final model resolution was not fine enough to resolve the details of the lake breeze front that were most important to these processes - namely large updraft and downdraft velocities. Further research efforts might concentrate on the fine-scale features associated with the lake breeze front both observationally and through the use of very high resolution numerical modelling with a horizontal grid spacing sufficient to resolve the details of the lake breeze front.
- Finally, it may be a worthwhile exercise to run the MC2 model at high resolution (~ 5 km) in a real-time, forecast mode over southwestern Ontario to obtain a better understanding of the different lake breeze configurations that occur and their relative frequencies. A more formal evaluation of the model's capacity to predict these circulations may be possible using such data. To accomplish this task, MC2 would likely have to be initialized directly on the 5 km grid without self-nesting.

Currently, there is no appropriate data assimilation tool for such initialization and the development of such a tool would be necessary. Other obstacles that would have to be overcome are the lack of high-resolution geophysical data for model runs and the coarse resolution of surface and upper-air data needed for model verification.

REFERENCES

- ARRITT, R. W. 1987. The Effect of Water Surface Temperature on Lake Breezes and Thermal Internal Boundary Layers. *Boundary-Layer Meteorol.* **40**: 101-125.
- . 1993. Effects of the Large-Scale Flow on Characteristic Features of the Sea Breeze. *J. Appl. Meteorol.* **32**:116-125.
- ATKINSON, B. W. 1981. *Meso-scale Atmospheric Circulations*. Academic Press, London, 495 pp.
- ATMOSPHERIC ENVIRONMENT SERVICE OF ENVIRONMENT CANADA (AES).
1994a. *Annual Meteorological Summary for Windsor Airport, 1993*. Environment Canada. 10 pp.
- . 1994b. *Annual Meteorological Summary for London, 1993*. Environment Canada. 10 pp.
- BANFIELD, C.E. 1991. The Frequency and Surface Characteristics of Sea Breezes at St. John's, Newfoundland. *Climatol. Bull.* **25**: 3-20.
- BECHTOLD, P., J.P. PINTY and P. MASCART. 1991. A Numerical Investigation of the Influence of Large-Scale Winds on Sea-Breeze and Inland-Breeze-Type Circulations. *J. Appl. Meteorol.* **30**: 1268-1279.
- BENOIT, R.; M. DESGAGNÉ, P. PELLERIN, S. PELLERIN, Y. CHARTIER and S. DESJARDINS. 1997. The Canadian MC2: A Semi-Lagrangian, Semi-Implicit Wideband Atmospheric Model Suited for Finescale Process Studies and Simulation. *Mon. Wea. Rev.* **125**: 2382-2415.
- BERTOLONE, L. 1984. *The Metropolitan Toronto Tornado of August 14, 1984*. Atmos. Env. Serv. of Canada. Ont. Region. Tech. Note ORTN-84-9. 22 pp.
- BIGGS, W.G. and M.E. GRAVES. 1962. A Lake Breeze Index. *J. Appl. Meteorol.* **1**: 474-480.
- BLANCHARD, D.O. and R.E. LOPEZ. 1985. Spatial Patterns of Convection in South Florida. *Mon. Wea. Rev.* **113**: 1282-1299.

- BLUESTEIN, H.B. 1985. The Formation of a "Landspout" in a "Broken-Line" Squall Line in Oklahoma. Preprints. *14th Conf. On Severe Local Storms*. Baltimore, Amer. Meteorol. Soc. pp. 312-315.
- BRADY, R.H. and E.J. SZOKE. 1989. A Case Study of Nonmesocyclone Tornado Development in Northeast Colorado: Similarities to Waterspout Formation. *Mon. Wea. Rev.* **117**: 843-856.
- BROWN, D.M.; G.A. MCKAY and L.J. CHAPMAN. 1980. *The Climate of Southern Ontario*. Climatol. Study no 5. Atmos. Env. Serv. of Env. Canada, Toronto, 67 pp.
- BYERS, H.R. and H.R. RODEBUSH. 1948. Cause of Thunderstorms on the Florida Peninsula. *J. Meteor.* **5**: 275-280.
- CANADIAN COUNCIL OF MINISTERS OF THE ENVIRONMENT (CCME). 1990. *Management Plan for Nitrogen Oxides (NO_x) and Volatile Organic Compounds (VOCs). Phase I*. CCME.
- CARACENA, F., J. MCCARTHY and J.A. FLUECK. 1983. Forecasting the likelihood of microbursts along the front range of Colorado. *Proceedings. 13th Conference on Severe Local Storms*, Amer. Meteorol. Soc. , 261-264.
- CHANDIK, J.F. and W.A. LYONS. 1971. Thunderstorms and the Lake Breeze Front. *7th Conf. on Sev. Local Storms*. Amer. Meteorol. Soc. 218-225.
- CHADWICK, P. 1994. *Summer Severe Weather Season 1993*. AES Ontario Region Technical Note OTRN-94-1. 31 pp.
- CHUNG, Y.-S. 1977. Ground-level Ozone and Regional Transport of Air Pollution. *J. Appl. Meteorol.* **16**: 1127-1136.
- CLARKE, J.F. and J.K.S. CHING. 1983. Aircraft Observations of Regional Transport of Ozone in the Northeastern United States. *Atmos. Env.* **17**: 1703-1712.
- CLIMATE CHANGE DETECTION DIVISION. 1993. Summer 1993 - A National Summary. *Clim. Perspec.* **15**: 2.
- CLODMAN, S. and W. CHISHOLM. 1994. High Lightning Flash Density Storms in the Southern Great Lakes Region. *Nat. Wea. Digest.* **19**: 34-44.

- and ———. 1996. Lightning Flash Climatology in the Southern Great Lakes Region. *Atmos.-Ocean*. **34**: 345-377.
- COMER, N.T. and I.G. McKENDRY. 1993. Observations and Numerical Modelling of Lake Ontario Breezes. *Atmos.-Ocean*. **31**: 481-499.
- DAVIS, W.M.; L.G. SCHULTZ and R. DE C. WARD. 1890. An investigation of the sea-breeze. *Ann. Harv. Coll. Obs.* Cambridge, Mass. **21**: 215-263 (cited in Simpson, 1994).
- DEFANT, F. 1950. Theorie der Land und Seewinde. *Arch. Met. Geophys. Bioklim. A*, **2**: 404-425.
- ELLCOTT, A. 1799. Miscellaneous Observations Relative to the Western Parts of Pennsylvania, Particularly those in the Neighbourhood of Lake Erie. *Transactions of the American Philosophical Society*. **4**: 224-240. (cited in Lyons and Olsson, 1973).
- ESTOQUE, M.A. 1961. A theoretical investigation of the sea breeze. *Q. J. R. Meteorol. Soc.* **87**: 136-146.
- . 1962. The Sea Breeze as a Function of the Prevailing Synoptic Situation. *J. Atmos. Sci.* **19**: 244-250.
- and J.M. GROSS. 1981. Further Studies of a Lake Breeze Part II: Theoretical Study. *Mon. Wea. Rev.* **109**: 619-634.
- ; ——— and H.W. LAI. 1976. A Lake Breeze over Southern Lake Ontario. *Mon. Wea. Rev.* **104**: 386-396.
- FINKELE, K; J.M. HACKER, H. KRAUS and R.A.D. BYRON-SCOTT. 1995. A Complete Sea-Breeze Circulation Cell Derived from Aircraft Observations. *Boundary-Layer Meteorol.* **73**: 299-317.
- FISHER, E.L. 1961. A theoretical study of the sea breeze. *J. Meteorol.* **18**: 216-233.
- FORD, R.P. (Editor) 1995. *Summer Severe Weather: Distance Learning Course*, Training and Education Services Branch, National Weather Service Directorate, Downsview, Ontario, Canada.

- FUENTES, J.D. and T.F. DANN. 1994. Ground-Level Ozone in Eastern Canada: Seasonal Variations, Trends, and Occurrences of High Concentrations. *J. Air & Waste Manage. Assoc.* **44**: 1019-1026.
- FUJITA, T.T. 1981. Tornadoes and Downbursts in the Context of Generalized Planetary Scales. *J. Atmos. Sci.* **38**: 1511-1534.
- and R.M. WAKIMOTO. 1982. Anticyclonic Tornadoes in 1980-1981. Preprints. *12th Conf. on Sev. Local Storms*, Kansas City, Amer. Meteorol. Soc. 259-266.
- HASTIE, D.R.; J. NARAYAN, C. SCHILLER, H. NIKI, P.B. SHEPSON, D.M.L. SILLS, P.A. TAYLOR, WM.J. MOROZ, J.W. DRUMMOND, N. REID, R. TAYLOR, P.B. ROUSSEL and O.T. MELO. 1998. Observational Evidence for the Impact of the Lake Breeze Circulation on Ozone Concentration in Southern Ontario. *Atmos. Env.* (In press).
- HAURWITZ, B. 1947. Comments on the sea-breeze circulation. *J. Meteorol.* **4**: 1-8.
- HEIDORN, K.C. and D. YAP. 1986. A Synoptic Climatology for Surface Ozone Concentrations in Southern Ontario, 1976-1981. *Atmos. Env.* **20**: 695-703.
- HOGG, W.D. and D.A. CARR. 1985. *Rainfall Frequency Atlas for Canada*. Atmospheric Environment Service, Environment Canada, Ottawa, 89 pp.
- HOGUE, R; P. JOE and T. NICHOLS. 1989. *The 17 September 1988 Weak Tornadoic Storm in Metro Toronto*. Atmos. Env. Serv. of Env. Canada. Ont. Region. Tech. Note ORTN-89-2. 17 pp.
- IRBE, G.J. 1992. *Great Lakes Surface Water Temperature Climatology. Climatological Studies Number 43*. Atmospheric Environment Service. Environment Canada, Ottawa. 215 pp.
- JEFFREYS, H. 1922. On the dynamics of wind. *Q. J. R. Meteor. Soc.* **48**: 29-47.
- JOE, P.; C. CROZIER, N. DONALDSON, D. ETKIN, E. BRUN, S. CLODMAN, J. ABRAHAM, S. SIOK, H-P. BIRON, M. LEDUC, P. CHADWICK, S. KNOTT, J. ARCHIBALD, G. VICKERS, S. BLACKWELL, R. DROUILLARD, A. WHITMAN, H. BROOKS, N. KOUWEN, R. VERRET, G. FOURNIER, B. KOCHTUBAJDA. 1995. Recent Progress in the Operational Forecasting of Summer Severe Weather. *Atmos.-Ocean.* **33**: 249-302.

- KEEN, C.S. and W.A. LYONS. 1978. Lake/Land Breeze Circulations on the Western Shore of Lake Michigan. *J. Appl. Meteorol.* 17: 1843-1855.
- KELLY, N.A.; M.A. FERMAN and G.T. WOLFF. 1986. The Chemical and Meteorological Conditions Associated with High and Low Ozone Concentrations in Southeastern Michigan and Nearby Areas of Ontario. *J. Air Poll. Control Assoc.* 36: 150-158.
- KENDALL, G.R. and A.G. PETRIE. 1962. *The Frequency of Thunderstorms Days in Canada*. Canada Department of Transport, Meteorology Branch, Toronto. Climatol. Study no. 4. 18 pp.
- KING, P. 1996. A Long-lasting Squall Line Induced by Interacting Lake Breezes. *Preprints of the 18th Conference on Severe Local Storms*, Amer. Meteorol. Soc., February 19-23, San Francisco, CA, 764-767.
- ; M. LEDUC and B. MURPHY. 1996. The Climatology of Tornadoes in Southern Ontario: Possible Effects of Lake Breezes. *Preprints of the 18th Conference on Severe Local Storms*, Amer. Meteorol. Soc., February 19-23, San Francisco, CA, 627-630.
- ; D. SILLS, D. HUDAK, P. JOE, N. DONALDSON, P. TAYLOR, X. QIU, P. RODRIGUEZ, M. LEDUC, R. SYNERGY, P. STALKER. 1998. ELBOW: An Experiment to Study the Effects of Lake Breezes on Weather in Southern Ontario. Submitted to the *CMOS Bulletin*.
- LEE, B.D. and R.B. WILHELMSON. 1997. The Numerical Simulation of Nonsupercell Tornadogenesis. Part II: Evolution of a Family of Tornadoes along a Weak Outflow Boundary. *J. Atmos. Sci.* 54: 2387-2415.
- LU, R. and R.P. TURCO. 1995. Air Pollutant Transport in a Coastal Environment - II. Three-Dimensional Simulations over Los Angeles Basin. *Atmos. Env.* 29: 1499-1518.
- LYONS, W.A. 1972. The Climatology and Prediction of the Chicago Lake-breeze. *J. Appl. Meteorol.* 11: 1259-1270.
- and H.S. COLE. 1976. Photochemical Oxidant Transport: Mesoscale Lake Breeze and Synoptic-Scale Aspects. *J. Appl. Meteorol.* 15: 733-743.

- and —————. 1973. Fumigation and Plume Trapping on the Shores of Lake Michigan during Stable Onshore Flow. *J. Appl. Meteorol.* **12**: 494-510.
- and L.E. OLSSON. 1973. Detailed Mesometeorological Studies of Air Pollution Dispersion in the Chicago Lake Breeze. *Mon. Wea. Rev.* **101**: 387-403.
- , R.A. PIELKE, C.J. TREMBACK, R.L. WALKO, D.A. MOON, and C.S. KEEN. 1995. Modeling Impacts of Mesoscale Vertical Motions upon Coastal Zone Air Pollution Dispersion. *Atmos. Env.* **29**: 283-301.
- MAILHOT, J.; S BÉLAIR, R. BENOIT, B. BILODEAU, Y. DELAGE, L. FILLON, L. GARAND, C. GIRARD and A. TREMBLAY. 1998. *Scientific Description of RPN Physics Library. Version 3.6*. RPN-AES, Dorval, Quebec, Canada, pp. 188.
- McKENDRY, I.G.; D.G. STEYN, J. LUNDGREN, R.M. HOFF, W. STRAPP, K. ANLAUF, F. FROUDE, B.A. MARTIN, R.M. BANTA and L.D. OLIVIER. 1997. Elevated Ozone Layers and Vertical Down-Mixing Over the Lower Fraser Valley, B.C.. *Atmos. Env.* **31**:2135-2146.
- McPHERSON, R.D. 1970. A Numerical Study of the Effect of Coastal Irregularity on the Sea Breeze. *J. Appl. Meteorol.* **9**: 767-777.
- MEYER, J.H. 1971. Radar Observations of Land Breeze Fronts. *J. Appl. Meteorol.* **10**: 1224-1232.
- MOLINARI, J. 1993. An Overview of Cumulus Parameterization in Mesoscale Models. *Representation of Cumulus Convection in Numerical Models. Meteor. Monogr.*, No. 46, Amer. Meteorol. Soc., p. 155-158.
- MOROZ, W.J. 1967. A Lake Breeze on the Eastern Shore of Lake Michigan: Observation and Model. *J. Atmos. Sci.* **24**: 337-355.
- and E.W. HEWSON. 1966. The Mesoscale Interaction of a Lake Breeze and Low Level Outflow from a Thunderstorm. *J. Appl. Meteorol.* **5**: 148-155.
- MUKAMMAL, E.I.; H.H. NEUMANN and T.J. GILLESPIE. 1982. Meteorological Conditions Associated with Ozone in Southwestern Ontario, Canada. *Atmos. Env.* **16**: 2095-2106.

- ; ————— and T.R. NICHOLS. 1985. Some Features of the Ozone Climatology of Ontario, Canada and Possible Contributions of Stratospheric Ozone to Surface Concentrations. *Arch. Met. Geoph. Biocl.* **34**: 179.
- MUNN, R.R. and T.L. RICHARDS. 1964. The lake-breeze: a survey of the literature and some applications to the Great Lakes. *Proc. Seventh Conf. on Great Lakes Research. Pub. 11, Great Lakes Res. Div., Univ. of Mich.*, pp. 253-266.
- MURPHY, B.P. 1991. *Tornado and Flash Flood in Southwestern Ontario on 31 May, 1991*. Atmos. Env. Serv. of Env. Canada. Ont. Region. Tech. Note ORTN-91-3. 8 pp.
- NEU, U.; T. KUNZLE and H. WANNER. 1994. On the Relation Between Ozone Storage in the Residual Layer and Daily Variation in Near-Surface Ozone Concentration - A Case Study. *Bound.-Layer Meteorol.* **69**: 221-247.
- NEUMANN, J. 1951. Land Breezes and Nocturnal Thunderstorms. *J. Meteorol.* **8**: 60-67.
- NEWARK, M.J. 1984. Canadian Tornadoes, 1950-1979. *Atmos.-Ocean.* **22**: 343-353.
- PEARCE, R.P. 1955. The calculation of a sea breeze circulation in terms of the differential heating across the coast line. *Q. J. R. Meteorol. Soc.*, **81**: 351-381.
- PEARCE, R.P. 1956. Roy. Met. Soc. Discussion. *Q. J. R. Meteorol. Soc.*, **82**: 239.
- PHYSICK, W. 1976. A Numerical Model of Sea-Breeze Phenomenon over a Lake or Gulf. *J. Atmos. Sci.* **33**: 2107-2135.
- PIELKE, R.A. 1974. A Three-Dimensional Numerical Model of the Sea Breezes over South Florida. *Mon. Wea. Rev.* **102**: 115-139.
- . 1984. *Mesoscale Meteorological Modeling*. Academic Press, 612 pp.
- and M. SEGAL. 1986. Mesoscale Circulations Forced by Differential Terrain Heating. In *Mesoscale Meteorology and Forecasting* (P.S. Ray, Ed.), Amer. Meteorol. Soc. , 516-548.
- PLUMMER, D.A; L. NEARY, J.W. KAMINSKI, J.C. McCONNELL. 1996. Modeling the Role of Lake Breeze Transport on Ozone Concentrations in Southern Ontario. *Proceedings of the Quadrennial Ozone Symposium, L'Aquila, Italy*.

- REID, N.W.; H. NIKI, D. HASTIE, P. SHEPSON, P. ROUSSEL, O. MELO, G. MACKAY, J. DRUMMOND, H. SCHIFF, L. POISSANT and W. MOROZ. 1996. *Atmos. Env.* **30**: 2125-2132.
- RYZNAR, E. and J. S. TOUMA. 1981. Characteristics of True Lake Breezes along the Eastern Shore of Lake Michigan. *Atmos. Env.* **15**: 1201-1205.
- SAJECKI, P.J.F. 1988. *Mean Number of Days with Thunderstorms 1951-1980*. Report no. 88-4, Climatological Services Division, AES, Environment Canada, 13 pp.
- SAVIJARVI, H. and M. ALESTALO. 1988. The Sea Breeze over a Lake or Gulf as the Function of the Prevailing Flow. *Beitr. Phys. Atmosph.* **61**: 98-104.
- SCHMIDT, F.H. 1947. An elementary theory of the land- and sea-breeze circulation. *J. Meteorol.* **4**: 9-15.
- SEGAL, M.; R.W. ARRITT, J. SHEN, C. ANDERSON, and M. LEUTHOLD. 1997. On the Clearing of Cumulus Clouds Downwind from Lakes. *Mon. Wea. Rev.* **125**: 639-646.
- SEGAL, M.; M. LEUTHOLD, R.W. ARRITT, C. ANDERSON and J. SHEN. 1997. Small Lake Daytime Breezes: Some Observational and Conceptual Evaluations. *Bull. Amer. Meteorol. Soc.* **78**: 1135-1147.
- SILLS, D.M.L.; P.A. TAYLOR and J.R. SALMON. 1994. *Southern Ontario Oxidant Study- Meteorological Measurements. Final Data Report*. York University and Zephyr North. 87 pp.
- ; X. QIU and P. TAYLOR. 1997. *SOMOS II. Southern Ontario Oxidant Study - Meteorological Modelling. Final Report*. York University. 117 pp.
- SIMPSON, J.E. 1994. *Sea Breeze and Local Wind*. Cambridge University Press, 234 pp.
- ; D.A. MANSFIELD and J.R. MILFORD. 1977. Inland Penetration of Sea-Breeze Fronts. *Quart. J. R. Met. Soc.* **103**: 47-76.
- SORBJAN, Z. 1989. *Structure of the Atmospheric Boundary Layer*. Prentice Hall, New Jersey, U.S.A. Pg. 181.
- STEYN, D.G. and D.A. FAULKNER. 1986. The climatology of sea breezes in the lower Fraser Valley, B.C. *Climatol. Bull.* **20**: 21-39.

- STEYN, D.G. and G. KALLOS. 1992. A Study of the Dynamics of Hodograph Rotation in the Sea Breezes of Attica, Greece. *Bound.-Layer Meteorol.* **58**: 215-228.
- TANGUAY, M.; A. ROBERT and R. LAPRISE. 1990. A semi-implicit semi-Lagrangian fully compressible regional forecast model. *Mon. Wea. Rev.*, **118**: 1970-1980.
- VERSEGHY, D.L. 1991. CLASS - A Canadian Land Surface Scheme for GCMs. Part I: Soil model. *Int. J. Climatol.*, **11**: 111-133.
- ; N.A. MCFARLANE and M. LAZARE. 1993. CLASS - A Canadian Land Surface Scheme for GCMs. Part II: Vegetation model and coupled runs. *Int. J. Climatol.*, **13**: 347-370.
- WAKIMOTO, R.M. and J.W. WILSON. 1989. Non-supercell Tornadoes. *Mon. Wea. Rev.* **117**: 1113-1140.
- WATTS, A. 1955. Sea Breeze at Thorney Island. *Meteorol. Mag.* **84**: 42-8.
- WEXLER, R. 1946. Theory and observations of land and sea breezes. *Bull. Amer. Meteorol. Soc.* **27**: 272-287.
- WILSON, J.W. and D.L. MEGENHARDT. 1997. Thunderstorm Initiation, Organization and Lifetime Associated with Florida Boundary Layer Convergence Lines. *Mon. Wea. Rev.* **125**: 1507-1525.
- WOLFF, G.T. and P.E. KORSOG. 1996. Preliminary Results of the 1993 Southeast Michigan Ozone Study (SEMOS) Field Study. *Tropospheric Ozone: Critical Issues in the Regulatory Process. Proceedings of a Air and Waste Management Association Specialty Conference*, Orlando, Florida, May 11-13, 1994. Pages 151-161.
- , G.T.; P.J. LIOY, G.D. WIGHT, R.E. MEYERS and R.T. CEDERWALL. 1977. An Investigation of Long-range Transport of Ozone Across the Midwestern and Eastern United States. *Atmos. Env.* **11**: 797-802.
- YAP, D.; D.T. NING and W. DONG. 1988. An assessment of source contributions to the ozone concentrations in southern Ontario. 1979-1985. *Atmos. Env.* **22**: 1161-1168.

APPENDIX A

Lake and Land Breeze Occurrence Records

Lake and land breeze occurrences were catalogued for each day in the SOMOS study as discussed in Chapter Two. Lake breeze occurrences were recorded both by the shore on which they occurred and by individual stations. Since land breeze identification is inherently more difficult with this dataset, especially at inland locations, land breeze occurrences were recorded by shore only.

Table A.1 gives lake and land breeze occurrences grouped by the shore on which they occurred. Start and end times are also given for each occurrence. Land breezes are associated with the day on which they began. In some cases, two land breeze occurrences are associated with one day since both circulations began on the same '24 hour' day though they occurred on subsequent nights. In these cases, the second occurrence is shown in parentheses and start and end times for both occurrences are given (see, for example, August 2).

Table A.2 gives lake breeze occurrences by station for stations over land with continuous data through the SOMOS study period. In some cases, more than one lake breeze front reached a station in one day. These instances are shown separated by commas.

Table A.1. Lake and Land Breeze Occurrence Record for SOMOS 93								
E = Lake Erie			H = Lake Huron			S = Lake St. Clair		
Date mdd	Lake Breeze?	Lake Shores	Time Begin (LST)	Time End (LST)	Land Breeze?	Lake Shores	Time Begin (LST)	Time End (LST)
715	Yes	ALL	14:00	21:00	Yes	ALL	22:00	07:00
716	Yes	ALL	08:00	20:00	Yes	ALL	22:00	07:00
717	Yes	ALL	11:00	19:00	Yes	ALL	23:00	02:00
718	No				No			
719	Yes	ALL	14:00	19:00	No			
720	Yes	ALL	11:00	19:00	Yes	H,E	23:00	05:00
721	Yes	S,H	13:00	18:00	Yes	ALL	21:00	05:00
722	Yes	ALL	13:00	21:00	Yes	ALL	22:00	08:00
723	Yes	ALL	10:00	20:00	Yes	ALL	21:00	08:00
724	Yes	H,E	11:00	18:00	Yes	H,E	22:00	07:00
725	No				No			
726	No				No			
727	Yes	H,E	14:00	21:00	Yes	H,E	23:00	07:00
728	No				No			
729	No				No			
730	No				No			
731	Yes	ALL	11:00	20:00	Yes	E	20:00	01:00
801	No				No			
802	Yes	E	11:00	14:00	Yes	E,(E)	01: , 22:	06: , 05:
803	Yes	H	12:00	15:00	No			
804	No				Yes	H,E	23:00	08:00
805	Yes	ALL	11:00	19:00	Yes	E	21:00	03:00
806	Yes	E	11:00	19:00	No			
807	Yes	ALL	10:00	19:00	Yes	ALL,(ALL)	03: , 23:	08: , 09:
808	Yes	ALL	09:00	19:00	Yes	ALL	20:00	08:00
809	Yes	ALL	09:00	19:00	No			
810	No				No			
811	Yes	ALL	11:00	19:00	Yes	ALL	20:00	08:00
812	Yes	ALL	10:00	20:00	Yes	ALL	22:00	08:00
813	Yes	ALL	10:00	20:00	Yes	ALL	20:00	08:00
814	Yes	ALL	10:00	20:00	Yes	ALL	22:00	06:00
815	Yes	ALL	10:00	18:00	No			

Date mdd	Lake Breeze?	Lake Shores	Time Begin (LST)	Time End (LST)	Land Breeze?	Lake Shores	Time Begin (LST)	Time End (LST)
816	Yes	ALL	13:00	19:00	No			
817	Yes	ALL	11:00	19:00	Yes	H,E	23:00	08:00
818	Yes	ALL	10:00	20:00	Yes	ALL	20:00	08:00
819	No				No			
820	No				No			
821	Yes	ALL	11:00	20:00	Yes	ALL	21:00	09:00
822	Yes	ALL	10:00	18:00	Yes	ALL	20:00	08:00
823	No				No			
824	No				Yes	ALL	19:00	07:00
825	Yes	ALL	10:00	20:00	Yes	ALL	20:00	06:00
826	Yes	ALL	11:00	18:00	No			
827	Yes	H,E	10:00	19:00	No			
828	Yes	E	13:00	20:00	Yes	ALL	21:00	07:00
829	No				No			
830	Yes	E,S	12:00	19:00	No			
831	No				Yes	ALL	22:00	09:00
901	Yes	ALL	11:00	19:00	Yes	ALL	20:00	06:00
902	No				No			
903	No				No			
904	No				Yes	H,(E)	03: , (22:)	10: , (04:)
905	Yes	ALL	12:00	17:00	Yes	ALL	20:00	09:00
906	No				Yes	ALL	20:00	10:00
907	Yes	ALL	11:00	17:00	Yes	ALL	20:00	09:00
908	No				Yes	ALL	19:00	05:00
909	No				No			
910	No				No			
911	No				No			
912	No				No			
913	No				No			
914	No				No			
915	No				No			

Table A.2a. Lake Breeze Occurrence Record -											
E = Lake Erie		H = Lake Huron		S = Lake St. Clair		- = no lake breeze					
Date mdd	Willow Beach	Essex	Stoney Point	Wheatley	Morpeth	Port Talbot	Bentpath	Walnut	Fernhill	Cedar Point	Dashwood
715	E,H	S,H	S,H	H	H	H	H	H	H	H	H
716	E,H	S,H	S,H	H	H	H	H	H	H	H	H
717	E	E	S,E	E	E	E	H	H	H	H	H
718	-	-	-	-	-	-	-	-	-	-	-
719	E	-	S	-	-	-	-	-	-	H	H
720	-	-	S	-	-	-	-	-	H	H	H
721	-	S	S	-	-	-	H	H	H	H	H
722	E	E,H	S,H	H	H	H	H	H	H	H	H
723	E	E	S	E	E	E	H	H	H	H	H
724	-	-	-	E	E	E	-	-	-	H	H
725	-	-	-	-	-	-	-	-	-	-	-
726	-	-	-	-	-	-	-	-	-	-	-
727	-	-	-	-	-	-	-	-	-	H	H
728	-	-	-	-	-	-	-	-	-	-	-
729	-	-	-	-	-	-	-	-	-	-	-
730	-	-	-	-	-	-	-	-	-	-	-
731	E	E	S	E	E	E	S	H	H	H	H
801	-	-	-	-	-	-	-	-	-	-	-
802	-	-	-	-	-	E	-	-	-	-	-
803	-	-	-	-	-	-	-	-	-	-	H
804	-	-	-	-	-	-	-	-	-	-	-
805	E	E	S	E	E	E	S	H,S	H	H	H
806	-	-	-	E	E	E	-	-	-	-	-
807	E	-	S,H	E,H	E,H	E,H	H	H	H	H	H
808	E	E	S,E	E	E	E	S,E	H	H	H	H
809	E	E	E	E	E	E	E	E	E	E	H,E
810	-	-	-	-	-	-	-	-	-	-	-
811	E	E	S	E	E	E	H	H	H	H	H
812	E	-	S	E	E	E	-	-	-	H	H
813	E	E	S	E	E	E	S,H	H	H	H	H

APPENDIX B

Chronology of MC2 Model Revisions

The following is a list highlighting important changes to the MC2 model dynamics and physics between the version of the model described by Benoit et al. (1997) (Version 3.0) and the version used for this study (Version 3.4.3). Descriptions of changes have been gleaned from the MC2 model release notes.

Version 3.1 - improved automatic Gal-Chen level distribution
- physics package updated to v3.0

Version 3.2 - upgrade to a more accurate pressure solver
- new full dynamic allocation of the central memory
- introduction of the Sundqvist deep convection scheme

Version 3.3 - independent selection of condensation and convection schemes allowed
- greater flexibility in the distribution of vertical Gal-Chen Levels, especially with respect to the planetary boundary layer
- connection to physics package version 3.3 with several new convection schemes

Version 3.4 - the first thermodynamic level may be raised to improve physics feedback
- addition of passive tracer capability
- physics package upgraded to version 3.4

Version 3.4.1 - reformulation of the semi-Lagrangian interpolator
- modification of the vertical nesting routine so that the weighting function (\cos^2) used is the same as that for horizontal nesting

Version 3.4.2 - update to a faster dynamic kernel
- addition of an alternate pressure solver (fgmres)

Version 3.4.3 - first fully parallel MPI-based version of the MC2 dynamics
- physics package upgraded to version 3.4.3
- two new microphysics schemes for explicit condensation
- introduction of a Newtonian-type vertical sponge layer to control vertical reflection of gravity waves at the model lid
- new option to allow manual vertical level specification without having to change the source code
- option for vertical diffusion of vertical motion added
- option to include the water loading term in the vertical momentum equation

APPENDIX C

Surface Divergence Calculation Method

Divergence values at the 10 m level from mesonet station data were calculated using a simple algorithm suggested by Dr. Peter Taylor (supervisor). The algorithm uses 10 m wind data from stations at the vertices of a triangle to calculate a value for inflow into the triangle. A divergence value is found by dividing the inflow by the area of the triangle. The order of the vertices selected for the triangle is important. Vertices ordered in a clockwise orientation around the perimeter of the triangle will correctly give positive values of divergence when inflow into the triangle is occurring.

The inflow into the triangle is found by first calculating a vector average of the 10 m winds for a pair of vertices. The component of this average wind along the normal to the triangle side multiplied by the length of the side gives the flux into the triangle along that side (see Figure C.1). This calculation is performed for the other two sets of vertices and two triangle sides. The total flux into the triangle is the sum of the fluxes along the sides. Finally, the total flux is divided by the area of the triangle to find the divergence. A relatively small triangle with nearly equal sides works best with this algorithm.

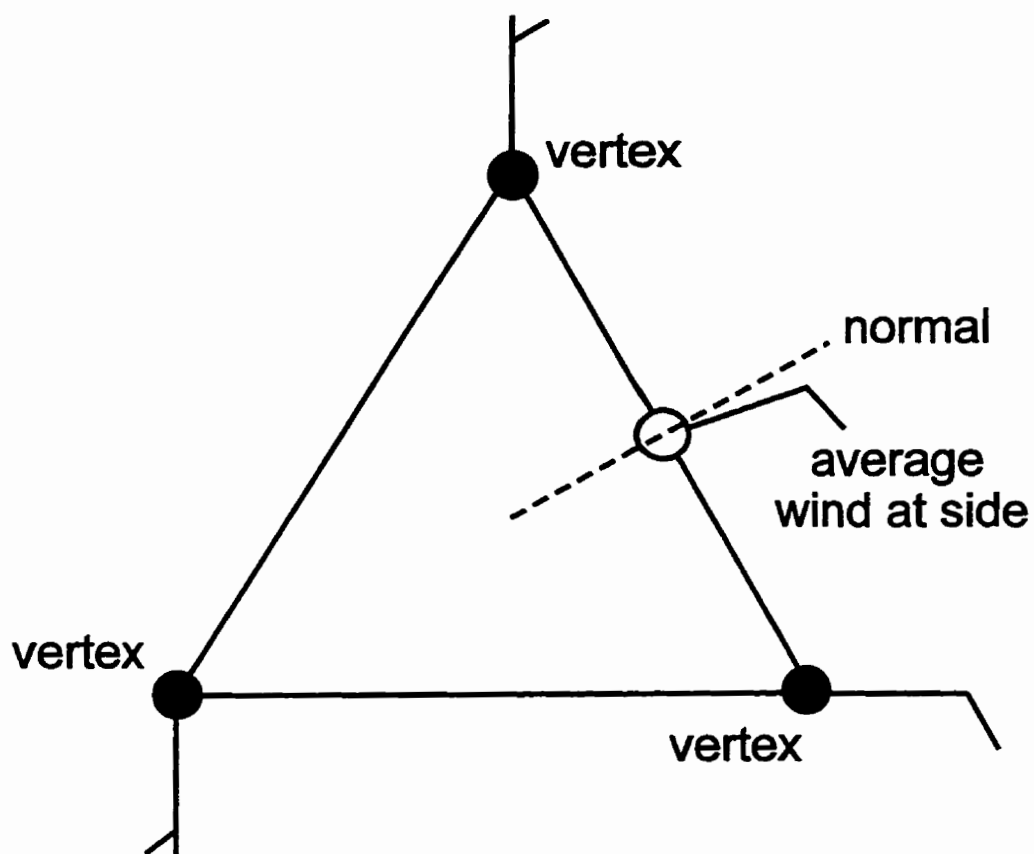


Figure C.1. Diagram showing triangle vertices and sides. The component of the vector average wind normal to the side is multiplied by the side length to get the flux at that side.

APPENDIX D

**Telephone Interviews with Witnesses to
the Tuppersville Tornado (August 14, 1993) and
the Tilbury Tornado (August 15, 1993)**

Interview with: Paul McFadden, son and former neighbour of deceased eyewitness
Tupperville, Ontario

Interviewer: David Sills

Date: July 17, 1996

Regarding: Tupperville Tornado
August 14, 1993

Question 1. Time Tornado First Sighted

Response - mid-afternoon

Question 2. General Description of Events

Response - funnel cloud was in distance then moved over house heading from
northeast to southwest, funnel cloud did not touch the ground
- lasted for more than one mile (between farms)

Question 3. Any Damage Sighted

Response - very localized damage - shingles off roof

Interview with: Gerry Harvieux
Tilbury, Ontario

Interviewer: David Sills

Date: July 17, 1996

Regarding: Tilbury Tornado
August 15, 1993

- Question 1
Response General Description of Events
- He first sighted the tornado just east of the corner of Rose Avenue and Laurentia Street. The tornado headed south across "98" [Kent County Road 8], then headed west from Kent County Road 1, to the south of the golf course, continued on for a concession or two.
- Question 2.
Response Number of Tornados Formed
- two tornados tried to form, only one did
- Question 3.
Response General Weather Conditions Prior to the Tornado
- hot and humid
 - not raining
- Question 4.
Response Any Damage Sighted
- crop damage south of golf course
- Question 5.
Response General Description of Area
- Rose Avenue backs onto an open field, farm fields over most of path
- Question 6.
Response Photographs or Video Taken
- some photographs, possibly some video footage

Interview with: Noah and Rose Reaume
Tilbury, Ontario

Interviewer: David Sills

Date: February 28, 1997

Regarding: Tilbury Tornado
August 15, 1993

- Question 1. Location of Reaume Household
Response - two miles south of "98" [Kent County road 8] on Kent County Road 1
- Question 2. Time Tornado was first Sighted
Response - between 2:30 pm and 3:00 pm
- Question 3. Direction Tornado Took
Response - from east to west
- Question 4. Direction of Rotation
Response - could not recall
- Question 5. Any Damage Sighted
Response - corn stalks lodged in car radiator, car "pushed" across road
- Question 6. Presence of Thunderstorm Before or After Tornado
Response - heavy rain encountered to south of area
- Question 7. Number and Description of Tornado(s)
Response - one

Interview with: Heather Tofflemire
Tilbury, Ontario

Interviewer: David Sills

Date: March 3, 1997

Regarding: Tilbury Tornado
August 15, 1993

- Question 1. Location of Ms. Tofflemire's House
Response - one mile past "98" on Kent County Road Number 5
- Question 2. Time Tornado First Sighted
Response - approximately 2:00 pm
- Question 3. Direction Tornado Took
Response - from west to east
- Ms. Tofflemire watched the tornado go towards the golf course
- tornado seemed to be from thunderstorm
- Question 4. Direction of Rotation
Response - could not recall
- Question 5. Any Damage Sighted
Response - none that Ms. Tofflemire saw
- Question 6. Presence of Thunderstorm Before or After Tornado
Response - no rain before the tornado, became dark and windy, sky turned "a funny colour"
- may have rained after the tornado passed
- Question 7. Number and Description of Tornado(s)
Response - tornado lifted up and then came down
- other funnel clouds in different locations

Interview with: Elaine Skinner
Tilbury, Ontario

Interviewer: David Sills

Date: March 3, 1997

Regarding: Tilbury Tornado
August 15, 1993

- Question 1. Location of Ms. Skinner's House
Response - Centennial Crescent [intersects with Rose Avenue]
- Question 2. Time Tornado First Sighted
Response - not sure, but some time later than 2:00 pm
- Question 3. Duration of Tornado
Response - lasted for a city block, 5 to 6 minutes
- Question 4. Direction Tornado Took
Response - started as a dust whirl off Park Lane, whirl increased in size, with erratic movement, moving from east to west
- Question 5. Direction of Rotation
Response - not sure, but believed rotation was clockwise
- Question 6. Any Damage Sighted
Response - minor damage to houses
- Question 7. Presence of Thunderstorm Before or After Tornado
Response - no rain or thunderstorms
- some sun
- "ordinary day"
- Question 8. Number and Description of Tornado(s)
Response - when the tornado ended, everything fell to the ground

Interview with: Fred Marchand
Tilbury, Ontario

Interviewer: David Sills

Date: March 3, 1997

Regarding: Tilbury Tornado
August 15, 1993

Question 1. Location of Mr. Marchand's House
Response

- two miles south of "98" [Kent County Road 8] on Kent County Road 1
- neighbour of Heather Tofflemire

Question 2. General Description of Events
Response

- Mr. Marchand saw two funnel clouds
- the first was a few miles away on the west-southwest side of his house, past Kent County Road 1, touched ground
- the second ran southwest of Mr. Marchand's house, moved down towards the ground, and lifted; funnel never touched ground, but came close
- both funnels came out of one cloud

Question 3. Direction Tornado Took
Response

- moved from golf course towards him

Question 4. Presence of Thunderstorm Before or After Tornado
Response

- no rain
- before tornado, windy with swirling clouds

Interview with: Brenda Mailloux
Tilbury, Ontario

Interviewer: David Sills

Date: March 13, 1997

Regarding: Tilbury Tornado
August 15, 1993

Question 1. Location of Ms. Mailloux's House

Response - 130 Queen Street

Question 2. General Description of Events

Response - Ms. Mailloux was at the park in Tilbury when she heard thunder and saw lightening, although there was no rain or wind
- trees about a block away started "swirling"
- saw a lot of minor wind damage
- clouds moving in swirling circles
- tornado made a "swishing" sound

Question 3. Direction Tornado Took

Response - moved from park south toward Lake Erie

Question 4. Time Tornado First Sighted

Response - 1:55 pm

Question 5. Direction of Rotation

Response - clockwise

Question 6. Presence of Thunderstorm Before or After Tornado

Response - thunderstorms 5-10 km south before funnel cloud
- no rain or wind, but cloudy before tornado

Question 7. Estimate of Cloud Base Height

Response - base height of regular cumulus clouds
- cloud base not especially dark

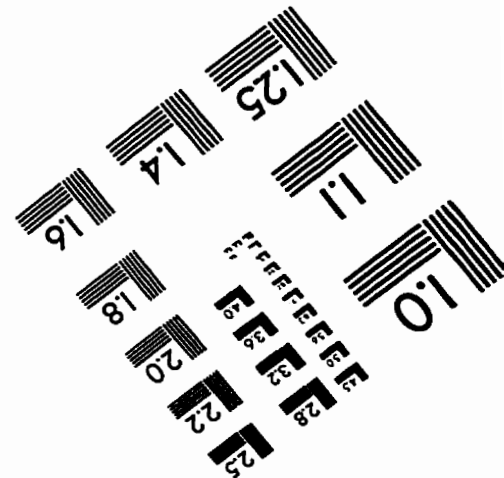
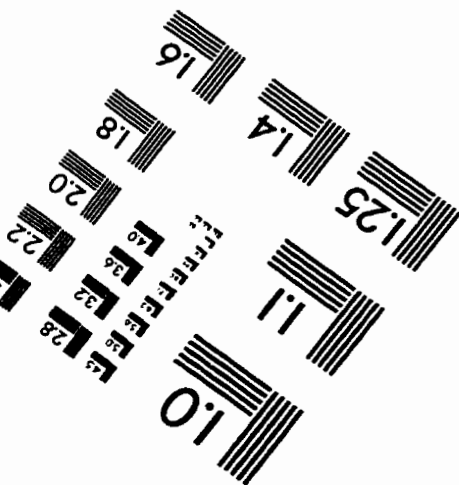
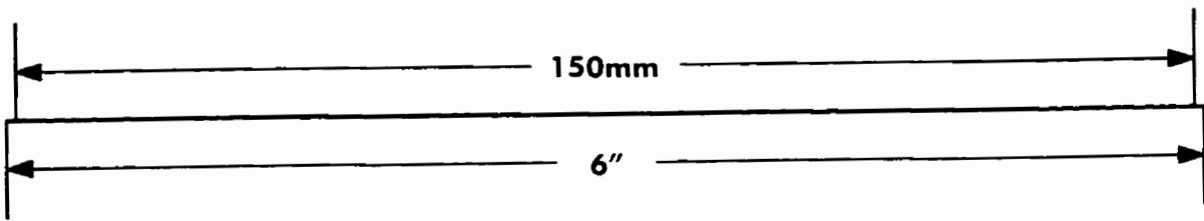
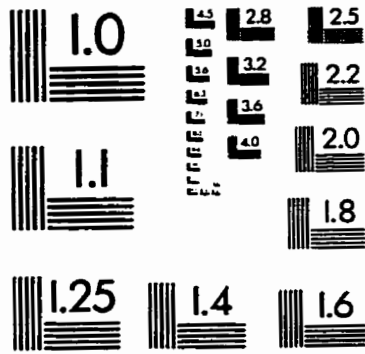
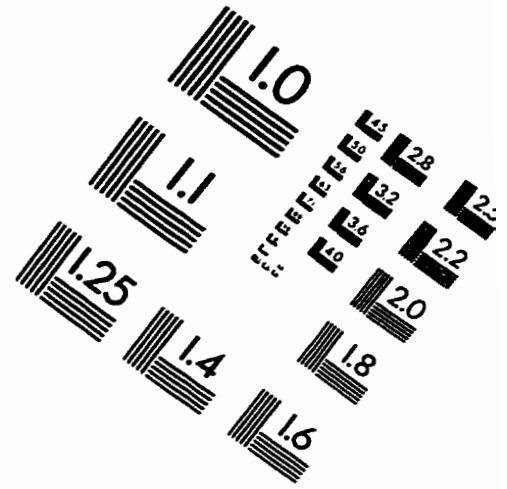
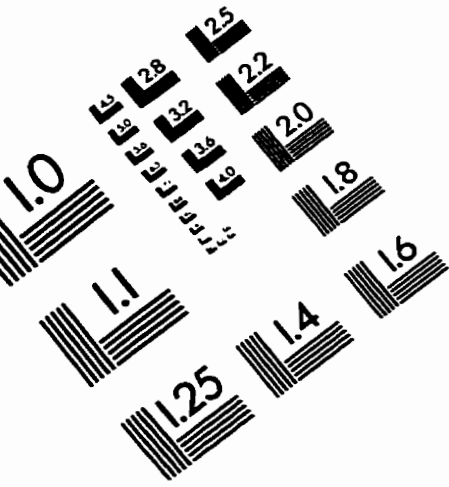
continued on next page

Interview with: Brenda Mailloux, continued

Question 8. Estimated Tornado Duration
Response - in sight for less than 5 minutes

Question 9. Any Damage Sighted
Response - shingles off roof
- motor home damaged
- damage on Park Lane

IMAGE EVALUATION TEST TARGET (QA-3)



APPLIED IMAGE, Inc
1653 East Main Street
Rochester, NY 14609 USA
Phone: 716/482-0300
Fax: 716/288-5989

© 1993, Applied Image, Inc., All Rights Reserved